ENERGY-EFFICIENT CONNECTED *k*-COVERAGE, DUTY-CYCLING, AND GEOGRAPHIC FORWARDING IN WIRELESS SENSOR NETWORKS

By

HABIB M. AMMARI

Presented to the Faculty of the Graduate School of

The University of Texas at Arlington in Partial Fulfillment

of the Requirements

for the Degree of

DOCTOR OF PHILOSOPHY

THE UNIVERSITY OF TEXAS AT ARLINGTON

May 2008

In the Name of Allah, the Most Gracious, the Most Merciful

“And of knowledge, you (mankind) have been given only a little.”

Al-Isra, 85

To my parents, Mbarka and Mokhtar

my wife, Fadhila, my kids, Leena, Muath, Mohamed-Eyed, Lama, and Maitham

my parents-in-law, Henia and Hedi

and to the memory of my grand-parents and uncle, Fatma, Abdelkarim, and Mahfoudh

ACKNOWLEDGMENTS

First of all, I would like to express my sincere gratitude to Allah – the Most Gracious, the Most Merciful for the wonderful opportunity He has given me to pursue and complete my Ph.D. in a very comfortable manner, and for His blessing by helping me work with very nice people to achieve this goal.

I would like to express my profound gratitude and special thanks to my Ph.D. advisor, Professor Sajal K. Das, for his exceptional guidance and consistent support. It has been a great pleasure working with him and constantly learning from him over these years. His breadth of knowledge and his enthusiasm for research make him an "Encyclopedia" in at least my research areas, and amaze and inspire me. Hopefully, I would be able to put into practice all what I have learned from him.

I would also like to express my very deep appreciation to all my committee members, Professors Gautam Das, Qilian Liang, Yonghe Liu, and Bob Weems, for their insightful comments and constructive feedback on my dissertation work and research directions, their kind flexibility, their concern, their always-willingness to help with job applications, and their valuable time. In particular, I am very grateful to Professor Yonghe Liu for his kind suggestion to work on solid, good, and fundamental problems in wireless sensor networks, such as the *k*-coverage problem.

I am also very grateful to all the CSE faculty members at UTA, and particularly, Professors Kalyan Basu, Bahram Khalili, Fillia Makedon, Lynn Peterson, Ramesh Yerraballi, Gergely Zaruba (UTA), as well as the CSE staff members, Camille Costabile, Will Griffith, Pam McBride, and Sherri Warwick, for their encouragements and kind support. My special thanks go to Professor Fillia Makedon, CSE Chairperson, for her continuous encouragements and kind support with my travel to Italy to attend EWSN'08 conference and participate in the Best Paper Award competition; Professor Lynn Peterson, Senior Associate Dean of the College of Engineering, for her constant encouragements and kind generosity with my travel to Hong Kong to attend IEEE PerCom'08 conference and participate in the Google Ph.D. Forum competition; and Professor Gergely Zaruba for his constant encouragements and kind support to attend IEEE PerCom'08 conference and participate in the Google Ph.D. Forum competition.

I would very much like to thank Professors Tom Chen, Maggie Dunham, and Dick Helgason at SMU, and Krish Pillai at LHUP, for their continuous support and invaluable time with job applications.

I would also like to express my gratitude to the library staff members at UTA, and particularly, those working in the Interlibrary Loan section, as well as the staff members at the Office of Graduate Studies at UTA for their great efforts and kind support.

I would like to thank all CReWMaN members, and particularly, Drs. Preetam Ghosh and Sumantra Kundu for the very fruitful conversations we had regarding my research work. I learned a lot from both.

I am very grateful to my brother, Dr. Nedal Nasser, for his kind support and encouragements since I joined UTA. He made my studies at UTA much easier than I thought.

Last but not least, my special thanks go to my first instructors, Mbarka and Mokhtar, my wonderful wife and very best friend, Fadhila, my lovely kids, Leena, Muath, Mohamed-Eyed, Lama, and Maitham, my very nice and thoughtful parents-in-law, Henia and Hedi, and my wonderful grand-parents and uncle, Fatma, Abdelkarim, and Mahfoudh. They all taught me the value of knowledge and the importance of family, and provided me with constant support, encouragements, and unconditional love. Thank you all very much!

This dissertation work was supported by the US National Science Foundation (NSF) under Awards IIS-0326505 and CNS-0721951 and Texas Advanced Research Program (ARP) under Award 14-748779.

April 21, 2008

ABSTRACT

ENERGY-EFFICIENT CONNECTED *k*-COVERAGE, DUTY-CYCLING, AND GEOGRAPHIC FORWARDING IN WIRELESS SENSOR NETWORKS

HABIB M. AMMARI, Ph.D.

The University of Texas at Arlington, 2008

Supervising Professor: Sajal K. Das

With the fast advances in inexpensive sensor technology and wireless communications, the design and development of large-scale *wireless sensor networks* has become cost-effective and viable enough to attract the attention of a wide range of civilian, natural, and military applications, such as health and environmental monitoring, seism monitoring, and battlefields surveillance. The main challenge in the design of wireless sensor networks is the limited battery power of the sensors and the difficulty of replacing and/or recharging these batteries due to the nature of the monitored field, such as hostile environments, and cost. Thus, it is necessary that the sensors be densely deployed and energy-efficient protocols be designed to maximize the network lifetime while meeting the specific application requirements in terms of coverage and connectivity. In this dissertation, we propose a continuum percolation-based approach to compute the critical sensor spatial density above which a field is *almost surely* covered and the network is *almost surely* connected. This approach helps network designers achieve full coverage of a field with a minimum number of connected sensors, thus maximizing the network lifetime. In order to support different applications and environments with diverse requirements in terms of coverage and connectivity, we extend our above analysis to *k*-coverage with $k \geq 3$ using a deterministic approach so the network self-configures to meet these requirements. More specifically, we

propose a unified, energy-efficient framework for connected *k*-coverage, duty-cycling, and geographic forwarding in wireless sensor networks. Our framework, called *Cover-Sense-Inform* (CSI), includes randomized centralized, pseudo-distributed, and distributed protocols for connected *k*-coverage along with geographic forwarding protocols in duty-cycled, *k*-covered wireless sensor networks. We prove that *k*-covered wireless sensor networks have connectivity that is higher than their degree of coverage *k*, thus providing architectures with high degree of fault-tolerance.

In the *centralized* connected *k*-coverage protocol, the sink is responsible for selecting a minimum number of active sensors to fully *k*-cover a field while maintaining connectivity between them. Both of the *pseudo-distributed* connected *k*-coverage protocols consider different levels of network clustering and are run under the control of a subset of sensors, called *cluster-heads*, which are selected by the sink in each scheduling round. Each cluster-head is responsible for selecting a subset of active neighboring sensors to *k*-cover its cluster while guaranteeing connectivity between all active sensors. In the *distributed* connected *k*-coverage protocol, all the sensors are required to coordinate among themselves to fully *k*-cover a field while ensuring network connectivity. Simulation results show that our protocols select a minimum number of sensors, thus maximizing energy saving.

Using a potential fields-based approach, we propose deterministic and hybrid geographic forwarding protocols for duty-cycled, *k*-covered wireless sensor networks with different levels of data aggregation. Simulation results show that CSI yields significant energy savings while guaranteeing high data delivery ratio. Besides, we extend CSI to address the stochastic connected *k*-coverage problem in wireless sensor networks using a more realistic sensing model that accounts for the stochastic properties of the sensors. We also extend CSI to three-dimensional wireless sensor networks and find that the extension of our analysis from two-dimensional to three-dimensional space is not straightforward. Finally, we propose a solution to the energy sink-hole problem, which is inherent to static wireless sensor networks, by exploiting energy heterogeneity, sink mobility, and energy aware Voronoi diagram. Simulation results show that our solution yields uniform energy consumption of all the sensors, thus extending the network lifetime.

TABLE OF CONTENTS

LIST OF ILLUSTRATIONS

LIST OF TABLES

CHAPTER 1

INTRODUCTION

Recent advances in miniaturization, low-cost and low-power circuit design, and wireless communications have led to the development of low-cost, low-power, and tiny communication devices, called *sensors*. Like nodes (or computers, laptops, etc) in traditional wireless networks, such as mobile ad hoc networks, the sensors have data storage, processing, and communication capabilities. Unlike those nodes, the sensors have an extra functionality related to their sensing capability. However, sensors suffer from severe limitations of their battery power (or *energy*) storage, processing, sensing, and communication resources compared to personal computers, for instance, with energy being the most crucial one. For an excellent survey on wireless sensor networks, the interested reader is referred to [6].

A *wireless sensor network* is composed of a large number of sensors that are densely deployed in a field of interest to monitor specific phenomena. Sensors can be engaged in a variety of sensing tasks, such as temperature, sound, vibration, light, humidity, etc. These sensors sense specific environment phenomenon and perform in-network processing on the sensed data before sending their results to a central gathering node, called the *sink*. In this type of network, sensors communicate with each other (possibly) through multi-hop communication links and forward sensed data on behalf of others so the sink can receive them on-time for further processing and analysis. Wireless sensor networks can be used for a wide variety of applications dealing with monitoring (health environments monitoring, seism monitoring, etc), control (object detection and tracking), and surveillance (battlefields surveillance).

Compared to traditional wireless networks, such as mobile ad hoc wireless networks, wireless sensor networks have several inherent characteristics. First, sensors are very tiny and hence more susceptible to hardware failure. It is worth mentioning that *battery power* (or *energy*) is the most crucial resource, and hence sensors can fail due to low energy. Second, sensors are deployed in a field with high density to extend the network lifetime. Indeed, using a large number of sensors facilitates multi-hop communication between them, and hence sensors can save their energy by transmitting or forwarding

their sensed data through short distances. Third, the network topology may change very frequently as sensors join and/or leave the network. Thus, protocols designed for wireless sensor networks should account for all these features so these networks stay operational as longer as possible.

The remainder of this chapter is organized as follows. Section 1.1 describes a sample of applications of wireless sensor networks while Section 1.2 gives the challenges that face their design. Section 1.3 presents the motivations of the work in this dissertation. Section 1.4 states the main problems that are addressed in this dissertation. Section 1.5 discusses the major contributions of this dissertation while Section 1.6 gives a summary of the chapters of this dissertation.

1.1 Wireless Sensor Network Applications

The design of wireless sensor networks should also be guided by the very specific requirements of the target applications. The knowledge gathered about the underlying application would help a network designer deploy more appropriate types of sensors and develop algorithms and protocols the meet the needs of the application. In this section, we describe some potential applications of wireless sensor networks spanning health, home, environmental, and military areas [6].

- Tracking and monitoring a hospital: Sensors may be attached to patients and doctors. For a patient, specific sensors are used to perform a particular task. For instance, to detect the heart rate, a special sensor needs to be used. Also, to detect the blood pressure, another specific type of sensor has to be used. For a doctor, sensors may be used to track their locations in the hospital to facilitate their mission.
- Smart environment: One of the home applications is the design and development of a smart home (or environment), where a wireless sensor network can be deployed to satisfy the specific needs of habitants. Sensors could be embedded anywhere in a room (or apartment) and communicate with each other to offer services desired by habitants. For instance, for saving energy, the light and temperature in a room could be controlled by sensors. In this case, the light is on only when the habitants are in the room and the temperature should be set to appropriate value depending on the time and season, for instance. The goal of this type of network is to provide habitants with the level of comfort they wish to have without any human intervention.

- Forest fire detection: Sensors could be randomly and densely deployed in a forest to detect the origin of a fire and report this information in a timely fashion to the end users to act accordingly before the fire spreads, and hence avoid catastrophic situations that may result. In this type of application, sensors may be used for a long period of time, and hence have to be equipped with continuous source of energy, such as solar cells. Furthermore, sensors need to collaborate with each other in their sensing activity to overcome several problems, such as obstacles. Also, sensors should be highly dense deployed for a quick and accurate detection.
- Intruder detection and tracking: Business stores, for instance, could be covered with special sensors to detect and track the motion of intruders. To achieve high accuracy of detection and tracking of an intruder, sensor redundancy is desirable and hence a dense network should be deployed. When an intruder is detected by some sensors, several other sensors become awake to cover the trajectories of the intruder. The collected information about an intruder is reported to end users for analysis and processing.
- Battlefield surveillance: A wireless sensor network can be deployed in a battlefield for performing detection and tracking of target objects, such as tanks and vehicles, and sending real-time information about the enemy mobility to a central control unit. Precisely, a network should be able to detect and classify multiple targets, such as vehicles and troop movements, using sensors that are capable of sensing acoustic and magnetic signals generated by different target objects.

1.2 Wireless Sensor Network Challenges

The design of network protocols for wireless sensor networks, including those for coverage configuration and data dissemination, is a challenging problem due to several constraints. Next, we describe these constraints that are imposed not only by the characteristics of the individual sensors, the behavior of the network, and the nature of physical environments (or *sensor fields*), but also by the requirements of the sensing applications in terms of some desirable metrics.

1.2.1 Sensor Characteristics

Because of their inherent characteristics, the design of wireless sensor networks for different applications running in different sensor fields is facing several challenges. First of all, energy efficiency is

the primary concern in the design of wireless sensor networks. Indeed, sensors forming a network suffer from the limitations of several resources, such as storage, CPU, bandwidth, communication, sensing, and battery power (or *energy*). In particular, energy is the most crucial resource as it determines the lifetime of the sensors and the lifetime of the entire network. Energy poses a serious problem for network designers especially in hostile environments, such as battle-field, where it is difficult or even impossible to access the sensors and recharge or renew their batteries. Furthermore, when the energy of the sensors reaches a certain threshold, they become unreliable (or *faulty*) and would not be able to function properly. As a consequence, the behavior of those faulty sensors will have a major impact on the network performance. Thus, network protocols and algorithms designed to be run by the sensors should be as energy-efficient as possible to extend their lifetime and hence prolong the network lifetime while guaranteeing good performance overall. Another challenge that faces the design of routing and data dissemination, and coverage and connectivity protocols is managing the locations of the sensors. Most of the routing and data dissemination protocols in wireless sensor networks assume that the sensors are equipped with *global positioning system* (GPS) receivers or use a localization technique [47], [96] to learn about their locations.

1.2.2 Field Nature

As mentioned earlier, a sensor field may cause a problem not only to access the sensors for replacing and/or recharging their batteries but also for their deployment. Thus, a deterministic sensor deployment strategy is not always possible. Such a strategy would help cover the field appropriately and minimize the total number of sensors required to achieve the specific needs of sensing applications in terms of their expected type of coverage. Indeed, an application may demand partial coverage where only a certain percentage of the field is covered; full coverage, where the entire field is covered; or redundant coverage, where every location in the field is covered by multiple sensors simultaneously. In the case where the sensors cannot be deployed deterministically because of the field nature, random deployment is the only remaining strategy. However, there is no guarantee that the coverage required by the application would be satisfied. There might be some areas that are not covered well or even not covered at all and this would lead to a problem, known as *coverage hole*. Moreover, all the deployed sensors are not guaranteed to be connected to each other or to the sink. This would lead to another problem, known as *connectivity hole*. These are two of the reasons why most of time wireless sensor networks are designed

with densely deployed sensors. Thus, the nature of the field has an influence on the network and this is a challenge for the designer and the investing party at least cost-wise. As will be discussed later, one of the most widely used assumption in the design of routing and data dissemination protocol is highly dense network. Although highly dense deployed wireless sensor networks involve more than necessary sensors, they help guarantee network connectivity and achieve the coverage demanded by the application.

1.2.3 Network Features

The topology of a wireless sensor network, which is defined by the sensors and communication links between them, changes frequently due to sensor addition and deletion. When new sensors decide to join the network, the neighbor set of some sensors have to be updated. Indeed, it may seem necessary to add more sensors to maintain certain properties of coverage of the sensor field and network connectivity. Similarly, when sensors deplete all their energy, they are considered faulty and no longer belong to the network. Thus, the neighbor sets of the fault sensors' neighbors should be updated. Also, in mobile wireless sensor networks, the network topology gets updated as sensors move in the sensor field. Consequently, any topology change in the network will have an impact on the communication paths (or routes) between the sensors in the network. Therefore, routing and data dissemination paths should consider network topology dynamics due to limited energy and mobility of the sensors as well as increasing the size of the network to maintain specific application needs in terms of coverage and connectivity. It is worth noting that connectivity to the sink is very important. In fact, coverage would be meaningless if the sensed data cannot reach the sink, i.e., there is no communication path between the source sensors (or data generators) and the sink. Thus, connectivity between all source sensors and the sink, either directly or indirectly, should be guaranteed for the correct operation of the network.

Another challenge is network scalability so routing and data dissemination protocols be able to scale with the network size. Also, the sensors may not necessarily have the same capabilities in terms of energy, processing, sensing, and particularly communication. Hence, communication links between the sensors may not be symmetric, i.e., a pair of sensors may not be able to have communication in both directions. This needs to be taken care of by the routing and data dissemination protocols.

1.2.4 Sensing Application Requirements

In most sensing applications, the sensed data should be as accurate as possible to assure better

decision making by the sink. Moreover, the sensed data needs to reach the sink in a timely manner. Thus, the *delay* metric should also be considered in the design process of wireless sensor networks; otherwise, the underlying network may not be useful. Also, for several sensing applications, data redundancy is desirable in that it increases data accuracy. For instance, in an intruder detection and tracking application, multiple sensors should be active at the same time to gather enough information about the intruder and track its motion accurately. Therefore, the design of routing and data dissemination, and coverage configuration protocols should guarantee data delivery and accuracy so the sink can gather the required knowledge about the physical phenomenon on time. Furthermore, sensors may deplete their energy before expected and become faulty. As discussed earlier, a sensor field may not be accessible and thus replacing those faulty sensors would be impossible. Hence, a wireless sensor network should tolerate the presence of faulty sensors and remain functional in spite of those failures. The degree of fault tolerance of a network depends on the underlying sensing application. Thus, routing and data dissemination, and coverage configuration protocols for wireless sensor networks should be fault-tolerant for this type of sensor failure. It is worth noting that link and sensing unit failures may also occur during the operation of a wireless sensor network. While sensing unit failure are due to imperfections in manufacturing or aging, link failure is caused by sensor mobility. In this thesis, however, we only consider sensor failure due to low battery.

1.3 Motivations of this Dissertation

There are several critical applications, such as intruder detection and tracking, where wireless sensor networks need to be deployed in a field in such a way that every point is sensed (or covered) by at least one sensor. In particular, it is sometimes desirable to deploy sensors to achieve redundant coverage of a field, where every point is guaranteed to be covered by at least k sensors simultaneously and we say that the network is configured to provide *k-coverage*. Indeed, there are at least three applications that require a degree of coverage at least equal to three, i.e., $k \geq 3$. First, in order to cope with the problem of sensor failures due their fragility, the design of sensor networks for planet exploration [151] should be as reliable as possible since failed sensors in space cannot be easily diagnosed and replaced. In [151], it was showed that k-cover deployment with $k \geq 3$ is necessary to guarantees data redundancy to improve data

reliability and fault tolerance of sensing applications. Second, multiple-sensor data fusion was found to be useful for at least a three-sensor system, i.e., system whose degree of coverage is $k \geq 3$ [102]. This helps detect, classify, and track the target objects. As at least all three sensors participate in the decision, it is unlikely that a false target would be detected as a true target [102]. Third, the design of triangulation-based positioning systems requires that each point in a target field be covered by at least three sensors to increase the position accuracy [134].

The design of network configuration protocols for wireless sensor networks faces a challenging problem, namely *energy conservation*, due to the constrained battery-power of the sensors. Several energy conservation protocols for wireless sensor networks have been proposed at the MAC and network layers [38], [50], [184], [185], and a variety of energy-efficient coverage configuration schemes have been suggested [166], [176]. In general, the sensors are deployed with high density, and hence the design of network configuration protocols should benefit from this fact to provide *k*-coverage. It is well known that the best approach to save the sensors' energy is *duty-cycling* so the sensors remain operational for as long as possible. Using a duty-cycling approach, the sensors can be turned *on* (i.e., active) or *off* (i.e., inactive) according to some sleep-wakeup scheduling protocol while guaranteeing *k*-coverage all the time. Achieving *k*-coverage becomes difficult especially in hostile environments, such as battle-fields, where access to the sensors is not feasible or even impossible. This implies that the sensors cannot be always-on but rather duty-cycled; otherwise, they will deplete their energy and die quickly. Also, *k*-coverage of a field should use as minimum number of active sensors as possible to extend the network lifetime.

The main goal of sensor deployment is to monitor a field and report data to the sink for further analysis and processing. Hence, the sensors should also be able forward data on behalf of each other. More importantly, the load of data forwarding should be evenly among all the active sensors, which currently *k*-cover the field, so all have the same chance to relay data for others. This implies that the network of active sensors should be connected; otherwise, sensed data will not reach the sink. Indeed, network connectivity is required for data routing and information dissemination. Thus, it is important that the network provide *k*-coverage while maintaining connectivity between *all* active sensors. It is well known that geographic forwarding, on the other hand, is an energy-efficient and practical scheme for wireless sensor networks in that the sensors are not required to maintain global and detailed information on the topology of the entire network. The sensors

need only maintain local knowledge on their one-hop neighbors. Therefore, for more effective sensor deployment, the load of *k*-coverage and data forwarding should be evenly distributed among all the sensors so that the network lifetime is maximized. These are the motivations of this dissertation research.

1.4 Contributions of this Dissertation

The contribution of this dissertation can be summarized as follows:

Problem 1 (*Almost Sure* Connected Coverage): What is the critical sensor spatial density above which a field (respectively, network) is *almost surely* covered (respectively, connected)?

We propose a continuum percolation-based approach to study phase transitions in coverage and connectivity in wireless sensor networks in an integrated fashion. Precisely, we propose a probabilistic approach to compute the critical sensor spatial density above which a field is almost surely covered and the network is almost surely connected. This approach helps network designers achieve full coverage of a field with a minimum number of connected, active sensors, thus maximizing the network lifetime.

Problem 2 (Connected *k*-Coverage): What is a sufficient condition of the sensor spatial density for full *k*-coverage of a two-dimensional (three-dimensional) field, where each point in a field is guaranteed to be covered by at least *k* sensors and what are the network connectivity and fault-tolerance of *k*-covered wireless sensor networks? How to design energy-efficient geographic forwarding protocols with and without data aggregation in duty-cycling, *k*-covered wireless sensor networks with $k \geq 3$? And how to extend these results to stochastic connected *k*-coverage and three-dimensional wireless sensor networks?

In order to solve this problem, thus supporting different applications and environments with diverse requirements in terms of coverage and connectivity, we extend our above analysis to *k*-coverage using a deterministic approach so the network self-configures to meet these requirements. More specifically, we design a unified framework, called Cover-Sense-Inform (CSI), for geographic forwarding in duty-cycled, *k*-covered wireless sensor networks. To this end, we compute the minimum active sensor spatial density that is necessary to achieve full *k*-coverage of a field while guaranteeing connectivity between all active sensors. Our analysis is based on Helly's Theorem [39] and the geometric properties of the Reuleaux triangle. Then, we design randomized centralized, pseudo-distributed, and distributed connected *k*-

coverage protocols for wireless sensor networks. We also compute the unconditional connectivity as well as the conditional connectivity of *k*-covered wireless sensor networks based on the concept of forbidden faulty set. The latter show shows that the classical connectivity used to capture network fault tolerance underestimates the resilience of large-scale networks, such as *k*-covered wireless sensor networks.

Using a potential fields-based approach, we propose three geographic forwarding protocols for duty-cycled, *k*-covered wireless sensor networks with different levels of data aggregation. We extend these results to address the problem of stochastic connected *k*-coverage in two-dimensional wireless sensor networks using a more realistic, stochastic sensing model instead of the deterministic one. We also study the connected *k*-coverage problem in three-dimensional wireless sensor networks. Surprisingly, we find that the extension of our analysis from two-dimensional to three-dimensional space is not straightforward due to the inherent properties of the Reuleaux tetrahedron. Thus, we propose a solution to this problem based on the "closest shape" to the Reuleaux tetrahedron.

Problem 3 (Energy sink-hole): How and to what extent can a uniform energy depletion of all the sensors be guaranteed so as to avoid the energy sink-hole problem in always-on, static wireless sensor networks, where the sensors nearer the sink are heavily used in forwarding data to the sink on behalf of all other sensors, thus depleting their energy very quickly compared to all other sensors in the network? And how can this problem in homogeneous, always-on wireless sensor networks be addressed?

We show that static wireless sensor networks suffer from the energy sink-hole problem regardless of how efficient a geographic forwarding protocol is. We propose a solution to this problem by enabling sensors to adjust their transmission range when sending/forwarding sensed data to the sink. However, we prove that this solution imposes a severe restriction on the size of the field. Thus, we propose an energy heterogeneity-based sensor deployment strategy so *all* the sensors in the network deplete their energy uniformly. When all the sensors have the same initial energy, we propose greedy, localized protocol, called energy aware Voronoi diagram-based data forwarding (EVEN), which exploits sink mobility and uses a new concept, called energy aware Voronoi diagram, where the locations of the sensors are time-varying and are locally and virtually computed based on their remaining energy.

1.5 Organization of this Dissertation

The remainder of this dissertation is organized as follows:

Chapter 2 presents the necessary definitions and fundamental concepts and models used throughout this dissertation. It also describes the network model used in the design and development of our protocols.

Chapter 3 reviews related work in coverage, connectivity, duty-cycling, and data forwarding in wireless sensor networks.

Chapter 4 computes the critical sensor spatial density above which a field is *almost surely* covered and the network is *almost surely* connected.

Chapter 5 computes the minimum sensor spatial density required to fully *k*-cover a field and describes our centralized, pseudo-distributed, and fully distributed connected *k*-coverage configuration protocols using the deterministic sensing model. These protocols form the basis of our CSI-Sensors framework. It also presents an extension of our protocols by considering a stochastic sensing model.

Chapter 6 presents our energy-efficient, unified CSI framework for geographic forwarding in duty-cycled, *k*-covered wireless sensor networks.

Chapter 7 extends CSI by considering a stochastic sensing model to solve the stochastic connected *k*-coverage problem in two-dimensional wireless sensor networks. It also extends CSI to three-dimensional wireless sensor networks.

Chapter 8 describes the energy sink-hole problem in always-on, static wireless sensor networks and presents our protocol EVEN to solve it by exploiting heterogeneity, mobility, and our new concept of energy-aware Voronoi diagram.

Chapter 9 computes the connectivity and fault-tolerance of *k*-covered wireless sensor networks.

Chapter 10 summarizes our main contributions and discusses future work of this dissertation.

CHAPTER 2

PRELIMINARIES AND NETWORK MODEL

In this dissertation, we use some terminology and different models, such as Voronoi diagram model, energy model, sensing model, and continuum percolation model, to describe our proposed approaches and protocols for connected k-coverage, duty-cycling, and geographic forwarding in wireless sensor networks. Furthermore, our work is based on a specific network model. The goal of this chapter is to present the different terms and models we use in this dissertation work.

The remainder of this chapter is organized as follows: Section 2.1 presents key definitions and fundamental concepts that are used in this dissertation. Section 2.2 presents deterministic and stochastic sensing models. Section 2.3 discusses different types of network connectivity. Section 2.4 describes the energy model while Section 2.5 presents the percolation model. Section 2.6 presents the network model that we used in the design of our energy-efficient framework for joint *k*-coverage, duty-cycling, and geographic forwarding in wireless sensor networks. Section 2.7 summarizes the chapter.

2.1 Basic Definitions

In this section, we give key definitions and describe some fundamental concepts used throughout this dissertation

The *sensing range* (or *detection range*) of a sensor s_i is a region where every event that takes place in this region can be detected by s_i. The *sensing neighbor set* $SN(s_i)$ of s_i is the set of all the sensors located in its sensing range.

The *communication range* of a sensor s_i is a region such that s_i can communicate with any sensor located in this region. The *communication neighbor set* $CN(s_i)$ of s_i is a set of all the sensors in its communication range.

A wireless sensor network is said to be *homogeneous* if all of it sensors have the same storage, processing, battery power, sensing, and communication capabilities. Otherwise, it is *heterogeneous*.

The *potential energy* of a sensor is equal to its remaining energy.

The *width* of a closed convex planar area is the maximum distance between parallel lines that bound it. The *breadth* of closed convex volume is the *maximum distance* between tangential planes on opposing faces or edges of the volume.

The *largest enclosed disk* (respectively, *sphere*) of closed convex region A is a disk (respectively, sphere) that lays inside A and whose diameter is equal to the minimum distance between any pair of points on $A's$ boundary.

Let $S = \{s_0,...,s_{n-1}\}$ be a finite set of n sites in the plane. The *Voronoi diagram* [33], also known as *Dirichlet tessellation*, represents one of the most fundamental data structures in computational geometry. It has interesting mathematical and algorithmic properties and potential applications. The Voronoi diagram of S, denoted by $Vor(S)$, is a subdivision of the plane containing S into n cells $VC(s_i)$, $1 \le i \le n$, such that each cell $VC(s_i)$ includes only one site s_i with the property that any point p located in $VC(s_i)$ is closer to s_i than any other site in S. The cell $VC(s_i)$ corresponding to site s_i is called the *Voronoi cell* of s_i, which is a (possibly unbounded) open convex polygonal region. The edges of a Voronoi cell are called *Voronoi edges* and its endpoints are called *Voronoi vertices*. The Voronoi diagram of S is the union of the Voronoi cells of all sites in S. The Delaunay triangulation, denoted by $DT(S)$, is the dual of the Voronoi diagram [33]. A $DT(S)$ graph has an edge between two sites if and only if their Voronoi cells share a common edge. Notice that $DT(S)$ is a planar graph whose edges are orthogonal to their corresponding Voronoi edges. Figure 2.1 shows a Voronoi diagram and its dual.

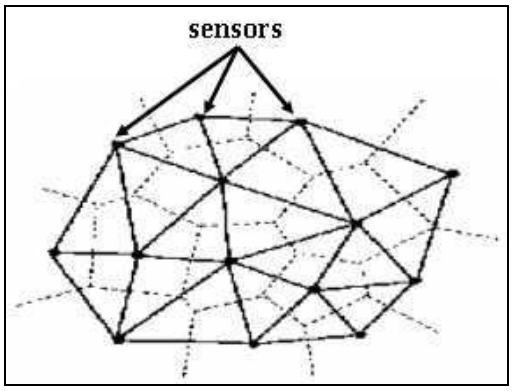

Figure 2.1 The Delaunay triangulation (bold lines) on top of the Voronoi diagram (dotted lines) of a wireless sensor network

2.2 Deterministic and Stochastic Sensing Models

In the *deterministic sensing model* (also known as *binary*), a point (or event) ξ in a field is sensed/covered (or detected) by a sensor s_i based on the Euclidean distance $\delta(\xi, s_i)$ between ξ and s_i. Throughout this chapter, we use "coverage of a point" and "detection of an event" interchangeably. Formally, the coverage $Cov(\xi, s_i)$ of a point ξ by a sensor s_i is defined as follows:

$$Cov(\xi, s_i) = \begin{cases} 1 & \text{if } \delta(\xi, s_i) \le r \\ 0 & \text{otherwise} \end{cases} \tag{2.1}$$

As can be seen, the deterministic sensing model considers the sensing range of a sensor as a *disk*, and hence all sensor readings are precise and have no uncertainty. However, it was found that the radios' communication range is highly probabilistic and irregular [182]. Thus, the deterministic sensing model does not reflect the real behavior of the sensing units of the sensors, which are irregular in nature. Hence, given the signal attenuation and the presence of noise associated with sensor readings, it is necessary to consider a more realistic sensing model by defining the coverage $Cov(\xi, s_i)$ using some probability function. In other words, the sensing capability of a sensor needs to be modeled as the probability of successful detection of an event. Specifically, the sensor's sensing capability should depend on the distance between it and the event as well as the type of propagation model being used (free-space vs. multi-path). Indeed, it has been showed that the probability that an event in a distributed detection application can be detected by an acoustic sensor depends on the distance between the event and sensor [64]. A realistic sensing model for passive infrared (PIR) sensors that reflects their non-isotropic range was presented in [48]. This sensing irregularity of PIR sensors was verified by simulations [48]. Thus, in a *stochastic sensing model*, the coverage $Cov(\xi, s_i)$ is defined as the *probability of detection* $p(\xi, s_i)$ of an event occurring at point ξ by sensor s_i as follows:

$$p(\xi, s_i) = \begin{cases} e^{-\beta \delta(\xi, s_i)^{\alpha}} & \text{if } \delta(\xi, s_i) \le r \\ 0 & \text{otherwise} \end{cases} \tag{2.2}$$

where β represents the physical characteristic of the sensors' sensing units and $2 \le \alpha \le 4$ is the path-loss exponent. Precisely, β measures the uncertainty introduced by the sensing unit of the sensors. Also, for the free-space model, we have $\alpha = 2$ and for the multi-path model, $2 < \alpha \le 4$. Our stochastic sensing

model is motivated by the one introduced by Elfes [66], where the sensing capability of a sonar sensor is modeled by a Gaussian probability density function. A probabilistic sensing model for coverage and target localization in wireless sensor networks was proposed in [187]. This sensing model is similar to ours except that it considers $\delta(\xi, s_i) - (r - r_e)$ instead of $\delta(\xi, s_i),$ where r is the detection range of the sensors and $r_e < r$ is a measure of uncertainty in sensor detection. Our stochastic sensing model is also similar to the one in [186], except that ours uses $\alpha,$ and reduces to the deterministic sensing model if we set $\beta = 0.$

Under the deterministic sensing model, a point ξ in a field is said to be *k-covered* if it belongs to the intersection of the sensing ranges of at least *k* sensors. Under the stochastic sensing model, a point ξ in a field is said to be *k-covered* if the detection probability of an event accruing at ξ by at least *k* sensors is at least equal to some *threshold probability* $0 < p_{th} < 1.$ For both sensing models, A region A is said to be *k-covered* if every point $\xi \in A$ is *k-covered*. A *k-covered* wireless sensor network is a network that fully *k*-covers a field. We call *degree of coverage* provided by a wireless sensor network the *maximum value* of *k* such that a field is fully *k*-covered.

2.3 Network Connectivity and Fault Tolerance

A *communication graph* of a homogeneous (*heterogeneous*) wireless sensor network is an undirected (*directed*) graph, $G = (S, E)$, where S is a set of sensors and E is a set of (*directed*) edges between them such that for all $s_i, s_j \in S$, $(s_i, s_j) \in E$ if $| \xi_i - \xi_j | \leq R_i,$ where ξ_i and R_i stands for the location and radius of the communication disk of sensor $s_i.$ The *vertex-connectivity* (or *connectivity*) of G is equal to K if and only if G can be disconnected by the removal (or failure) of at least K nodes. The *fault tolerance* of the underlying network is equal to $\mathrm{K} - 1.$

A *forbidden faulty set* of a graph $G = (S, E),$ is a set of nodes $F \subset S$ that cannot fail at the same time.

According to our conditional fault-tolerance model, a faulty sensor set F_{P} is given by $F_{\mathrm{P}} = \{U \subset S \mid \forall s_i \in S : CN(s_i) \not\subset U\},$ where $CN(s_i)$ is the communication neighbor set of sensor $s_i.$ Thus, the communication neighbor set of a sensor cannot fail simultaneously, and hence it is a forbidden faulty set.

Let P be "The faulty set cannot include the neighbor set of any sensor", $F_{\mathrm{P}} \subset S$ a faulty set satisfying property $\mathrm{P},$ and $G = (S, E)$ a communication graph representing a wireless sensor network. The

conditional connectivity of G with respect to P, denoted by $\kappa(G:\mathrm{P})$, is the minimum size of F_{P} such that the resulting graph $G_d = (S - F_{\mathrm{P}}, E_d)$ is disconnected into components each having property P. Another generalization of connectivity, called *restricted connectivity*, was proposed in [67] in which the restriction is on the faulty set (i.e., set of nodes that can fail). Restricted connectivity uses the concept of *forbidden faulty set* in which the entire neighbor set of a given node cannot be faulty at the same time. The *conditional fault-tolerance* of G with respect to P is given by $\eta(G:\mathrm{P}) = \kappa(G:\mathrm{P}) - 1.$

2.4 Energy Model

According to [88], the energy spent in transmitting one message of size κ bits from sensor s_i to sensor s_j is computed as $E_{tx}(s_i, s_j) = \kappa(E_{elec} + \varepsilon\, \delta^{\alpha}(s_i, s_j))$ and the energy spent in message reception is given by $E_{rx} = \kappa E_{elec}$, where E_{elec} represents the electronics energy, $\varepsilon \in \{\varepsilon_{fs}, \varepsilon_{mp}\}$ is the transmitter amplifier in the free-space (ε_{fs}) or the multi-path (ε_{mp}) model, $2 \le \alpha \le 4$ is the path-loss exponent, and $\delta(s_i, s_j)$ is the Euclidean distance between s_i to s_j. Thus, the total energy consumption for s_i when it receives a message and forwards it to s_j is given by $E_{tot}(s_i, s_j) = 2\,\kappa\, E_{elec} + \kappa\, \varepsilon\, \delta^{\alpha}(s_i, s_j).$ Moreover, the *energy consumption rate in transmitting* over a distance d is given by $ER_{tx}(d) = (\varepsilon\, d^{\alpha} + E_{elec})\, b$ and the *energy consumption rate in receiving* is given by $ER_{rx} = E_{elec}\, b,$ where b (in bits/sec) is the sensor's data rate. We assume all sensors have the same data rate. For a fixed message size, the energy consumed by the sensors depends on the transmission distance d and the path-loss exponent α, where $2 \le \alpha \le 4$.

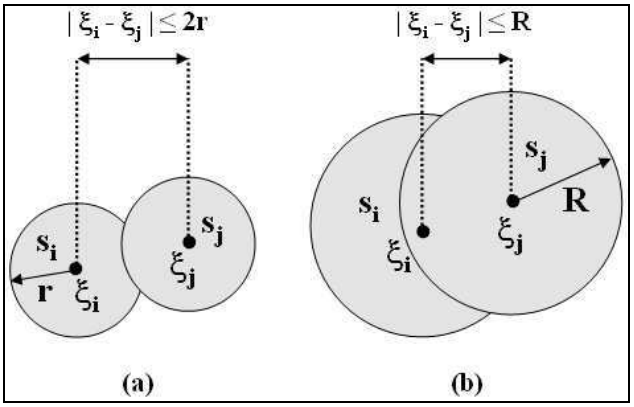

Figure 2.2 (a) Collaborating sensors s_i and s_j, and (b) communicating sensors s_i and s_j

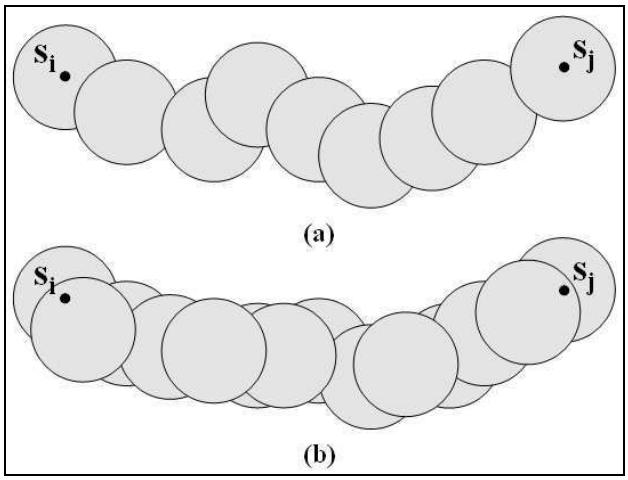

Figure 2.3 (a) collaboration path and (b) communication path between s_i and s_j

2.5 Percolation Model

Assume that the sensing and communication ranges of the sensors are represented by disks. Two sensors s_i and s_j are said to be *collaborating* if the Euclidean distance between the centers of their sensing disks satisfies $|\xi_i - \xi_j| \leq 2r$, where r is the radius of their sensing disks. Intuitively, the two sensing disks centered at ξ_i and ξ_j are either *tangential* or *overlapping* (see Figure 2.2a). The *collaborating set* of the sensor s_i, denoted by $Col(s_i)$, includes all the sensors it can collaborate with, i.e., $Col(s_i) = \{ s_j : |\xi_i - \xi_j| \leq 2r \}$. Two sensors s_i and s_j are said to be *communicating* if the Euclidean distance between the centers of their communication disks satisfies $|\xi_i - \xi_j| \leq R$, where R is the radius of the communication disks of the sensors (see Figure 2.2b). The *communicating set* of the sensor s_i is the set of sensors it can communicate with, i.e., $Com(s_i) = \{ s_j : |\xi_i - \xi_j| \leq R \}$.

A *collaboration path* between two sensors s_i and s_j, is a sequence of sensors s_i, $s_{i+1}, \ldots, s_{j-1}$, s_j, such that any pair of sensors s_l and s_{l+1}, , for $i \leq l \leq j-1$, are collaborating (see Figure 2.3a). Similarly, a *communication path* between two sensors, s_i and s_j, is a sequence of sensors, s_i, $s_{i+1}, \ldots, s_{j-1}$, s_j, such that any pair of sensors s_l and s_{l+1}, for $i \leq l \leq j-1$, are communicating (see Figure

2.3b). A wireless sensor network is said to be *connected* if there is a communication path between any pair of sensors.

Let $X_\lambda = \{\xi_i : i \geq 1\}$ be a two-dimensional homogeneous Poisson point process of density λ, where ξ_i represents the location of a sensor s_i. Let $X_\lambda(\mathrm{A})$ be a random variable representing the number of points in an area A. The probability that there are k points inside A is computed as

$$P(X_\lambda(\mathrm{A}) = k) = \frac{\lambda^k \mid \mathrm{A} \mid^k}{k!} e^{-\lambda|\mathrm{A}|} \tag{2.3}$$

for all $k \geq 0$, where $\mid \mathrm{A} \mid$ is the size of $\mathrm{A}'s$ area.

The *covered area fraction* of a Poisson Boolean model $(X_\lambda, \{D_i(r) : i \geq 1\})$ given by $A(r) = 1 - e^{-a\lambda}$ [86] is the mean fraction of area covered by the sensing disks $D_i(r)$, for $i \geq 1$, in a region of unit area, where $a = \pi r^2$ is the area of a sensing disk and λ is the density of the Poisson point process X_λ.

A set of sensing disks $\{D_i(r) : 1 \leq i \leq m\}$ is said to be a *covered component* if it is *maximal* (or not included in any other set except when it is equal to the original entire set of sensing disks) and there exists a collaboration path between any pair of sensors s_j and s_l, for all $1 \leq j, l \leq m$ and $j \neq l$. A *covered k-component*, denoted by CC_k, is a covered component having *k* sensing disks.

Assume that λ is not a constant as the sensors could appear and disappear independently of one another. We want to compute the density λ_c, called *critical percolation density* (or *critical density*) such that there exists an infinite covered component when $\lambda > \lambda_c$, and hence the Boolean model $(X_\lambda, \{D_i(r) : i \geq 1\})$ is said to be *percolating*. Otherwise, there is no infinite covered component and hence $(X_\lambda, \{D_i(r) : i \geq 1\})$ does not percolate.

The *critical covered area fraction* of $(X_\lambda, \{D_i(r) : i \geq 1\})$, computed as $A_c(r) = 1 - e^{-a\lambda_c}$, is the fraction of area covered at critical percolation, where λ_c is the associated density of X_λ.

A set of communication disks $\{D_i(R) : 1 \leq i \leq n\}$ is said to be a *connected component* if it is *maximal* (or not included in any other set except when it is equal to the original entire set of transmission disks) and

there exists a communication path between any pair of sensors s_j and s_l, for all $1 \le j, l \le n$ and $j \ne l$. A *connected k-component*, denoted by CC_k, is a connected component with k communication disks.

Percolation processes were introduced by Broadbent and Hammersley [46] to model the random flow of a fluid through a medium. Because of their simplicity of description and display of critical behavior, where a model's behavior changes abruptly (phenomenon known as phase transition) as a parameter value crosses a threshold, percolation models are attractive in several areas of mathematics, physical science, and engineering. A percolation model can be viewed as an ensemble of points distributed in space, where some pairs are adjacent (or connected) [69]. We consider a Boolean model [128] which is defined by two components, namely point process X_λ and connection function h. The set $X_\lambda = \{ \xi_i : i \ge 1 \}$ is a homogeneous Poisson point process of density λ in a 2-dimensional Euclidean plane IR^2, where the elements of X_λ are the locations of the sensors used to cover a field. The connection function h is defined such that two points ξ_i and ξ_j are adjacent independently of all other points with probability $h(\| \xi_i - \xi_j \|)$ given by

$$h(\| \xi_i - \xi_j \|) = \begin{cases} 1 & \text{if } \| \xi_i - \xi_j \| \le d \\ 0 & \text{otherwise} \end{cases}$$

where $\| \xi_i - \xi_j \|$ is the *Euclidean distance* between ξ_i and ξ_j.

Why a Continuum Percolation Model? We consider a *continuum* percolation model rather than a discrete percolation model for the following reason. In discrete percolation [81], also known as *lattice model*, the sites, which are randomly occupied in a discrete lattice, may have different configurations, namely square, triangle, honeycomb, etc. In continuum percolation [128], the positions of the sites are randomly distributed and thus there is no need to have different analysis for each of these regular lattices. Precisely, we consider a continuum percolation model, which consists of homogeneous disks whose centers (i.e., sensors' locations) are randomly distributed in IR^2 according to a spatial Poisson point process of density λ. In percolation theory, we are interested in the *critical density* λ_c above which an *infinite cluster of overlapping disks* first appears. The density λ_c is the critical value for the density λ such that there exists

no infinite cluster of overlapping disks *almost surely* when $\lambda < \lambda_c$, but there is an infinite cluster of overlapping disks *almost surely* when $\lambda > \lambda_c$ and we say that *percolation* occurs.

2.6 Network Model

In this section, we specify the network model used in this dissertation unless stated otherwise.

All the sensors are static and isotropic. In other words, all the sensors have the same sensing and communication ranges. Furthermore, the latter follow the *unit disk model*, i.e., they are modeled by disks (respectively, spheres) in two-dimensional (respectively, three-dimensional) wireless sensor networks, called *sensing* and *communication disks* (respectively, *spheres*) of radii r and R, respectively, centered at the locations of their corresponding sensors. Moreover, all the sensors are homogeneous and always-on, meaning that they constantly report their sensed data to a single static sink. Hence, the sensors cannot be turned off while monitoring a physical phenomenon. Each sensor has a unique *id* (an integer, for instance) and is aware of its own location information through GPS (Global Positioning System) or some localization technique [96]. The sensors advertise their location information only once when they start their sensing task. In addition, each sensor advertises its remaining energy by piggybacking it on the data sent to the sink. The sensors are randomly, uniformly deployed in a field whose size is much larger than that of the sensing and communication ranges of the sensors. Moreover, the sensors are supposed to be *densely* deployed. As indicated in Chapter 1, the limited battery power of the sensors and the difficulty of replacing and/or recharging batteries on the sensors in hostile environments require that the sensors be deployed with high density in order to extend the network lifetime. We also assume that each sensor has transmit-power control and hence can adjust its transmission distance so it can transmit its data over a distance that is less than or equal to the radius of its communication range. The communication links between the sensors are perfectly reliable while the sensors can fail or die independently due to low battery power.

We should mention that some of these assumptions will be further relaxed so as to promote the use of our proposed protocols in real-world sensing applications.

2.7 Summary

In this chapter, we described a few applications of wireless sensor networks and presented the main challenges that have to be dealt with in the design process. The inherent features of wireless sensor

networks, such as limited battery power, high magnitude, high density, failures, and dynamic topology, require that their design and development be tailored to make them more practical and very effective. In particular, any protocol designed for wireless sensor networks should meet the constraint imposed by the limited battery power of the sensors. Also, we defined useful terms that are used throughout this dissertation. Also, we described the energy and percolation models as well as our network model.

CHAPTER 3

RELATED WORK

With the fast advances in inexpensive sensor technology and wireless communications, the design and development of large-scale wireless sensor networks has become cost-effective and viable enough to attract the attention of several applications, such as health/environmental monitoring and battlefields surveillance. Two fundamental aspects in the design of wireless sensor networks are sensor deployment and data forwarding. In fact, the main function of a wireless sensor network is to monitor a field and report data to a central gathering node, called the *sink*, for further analysis and processing. The sensors, however, suffer from several scarce resources, such as battery power (or *energy*), storage, CPU, and bandwidth, to name a few, with energy being the most critical one.

Although several algorithms and protocols have been proposed for wireless mobile ad hoc networks, they cannot be directly applied to wireless sensor networks. This is mainly due to the inherent characteristics of the sensors, such as limited battery power, sensing, communication, processing, and storage; the number of sensors in a wireless sensor network is much higher than that of the nodes in an ad hoc network; the sensors are highly dense deployed due to their limited energy resources; the sensors are prone to failure due to their limited battery power; The topology of a wireless sensor network changes very frequently due to the limited energy of the sensors; the broadcast communication nature of wireless sensor networks; the sensors may not have global identification like nodes in a wireless mobile ad hoc network nodes due to their large number. Thus, protocols designed for wireless sensor networks, and particularly those for field coverage and data forwarding, should be as energy-efficient as possible to extend the operational network lifetime.

The remainder of this chapter is organized as follows: Section 3.1 reviews probabilistic approaches that compute the sensor density to achieve coverage of a field. Section 3.2 describes related work in coverage, connectivity, and duty-cycling approaches for wireless sensor networks. Section 3.3 presents approaches for data forwarding in wireless sensor networks. Section 3.4 describes approaches for joint

coverage and geographic forwarding in wireless sensor networks. Section 3.5 describes existing approaches using the notion of conditional connectivity. Section 3.6 reviews stochastic coverage approaches. Section 3.7 describes protocols for minimizing and balancing energy consumption. Section 3.8 discusses existing approaches for coverage and connectivity in three-dimensional wireless sensor networks. Section 3.9 presents percolation theory-based approaches for coverage and connectivity. Section 3.10 summarizes the chapter.

3.1 Computing the Sensor Density for Coverage

Adlakha and Srivastava [2] showed that the number of sensors required to cover an area of size A is in the order of $O(A/\hat{r}_2^2)$, where $\hat{r}_2$ is a good estimate of the radius r of the sensing disk of the sensors. Specifically, r lies between $\hat{r}_1$ and $\hat{r}_2$, where $\hat{r}_1$ overestimates the total number of sensor required to cover an area of size A, while $\hat{r}_2$ underestimates it. Our approach, however, gives an exact value of the minimum sensor spatial density required for *k*-coverage based on the exact value of the sensing range of the sensors. Franceschetti *et al.* [71] investigated the number of disks of given radius r, centered at the vertices of an infinite square grid, which are required to entirely cover an arbitrary disk of radius r placed on the plane. Their result depends on the ratio of r to the grid spacing.

Kumar *et al.* [108] proved that for random deployment with uniform distribution, if there exists a slowly growing function $\phi(np)$ such that $n\,p\pi r^2 \geq \log(np) + k\log\log(np) + \phi(np)$, then a square unit area is *k*-covered with high probability when n sensors are deployed in it, where p is the probability that a sensor is active. It is worth noting that n also represents the sensor spatial density given that the area of the square region is equal to 1. Hence, the above inequality can be written as $n\,p \geq \frac{\log(np) + k\log\log(np) + \phi(np)}{\pi r^2}$, which means that the minimum sensor density required for *k*-coverage of a unit square region is equal to $\frac{\log(np) + k\log\log(np) + \phi(np)}{\pi r^2}$. If we set $p = 1$ (i.e., every sensor is active), we obtain $\frac{\log(n) + k\log\log(n) + \phi(n)}{\pi r^2}$.

Recently, Balister *et al.* [35] computed the sensor density necessary to achieve both sensing coverage and network connectivity in finite region, such as thin strips (or annuli) whose lengths are finite. Balister *et al.* [35] applied this result to achieve barrier coverage [107] and connectivity in thin strips, where sensors

act as a barrier that ensures that any moving object or phenomenon that crosses the barrier of sensors will be detected.

Zhang and Hou [175], [177] proved that the required density for *k*-coverage of a square field, where sensors are distributed according to a Poisson point process and always active, depends on both the side length of the field and *k*. Precisely, Zhang and Hou [175], [177] found that a necessary and sufficient condition of complete *k*-coverage of a square field with side length l is that the sensor density is equal to $\lambda = \log l^2 + (k+1)\log\log l^2 + c(l),$ where $c(l) \to +\infty$ as $l \to \infty.$ In another paper, given a wireless sensor network deployed as a Poisson point process with density λ and every sensor is active, Zhang and Hou [174] provided a sufficient condition for *k*-coverage of a square region with area $A.$ Precisely, they proved that assuming $\lambda = \log A + 2k\log\log A + c(A),$ if $c(A) \to \infty$ as $A \to \infty,$ then the probability of *k*-coverage of the square region approaches 1. Zhang and Hou [174] provided the same result in the case where sensors are deployed according to a uniformly random distribution. Both results are based on the following statement: the square region is divided into square grids with side length $s = \frac{\sqrt{2}\,r}{\log A},$ where r stands for the radius of the sensing range of the sensors. For a grid i to be completely *k*-covered, it is sufficient that there are at least k sensors within a disk centered at the center of the grid and with radius $(1-u)\,r,$ denoted by $B_i((1-u)\,r),$ where $u = 1/\log A.$ Based on this characterization, we can claim that the spatial density of active sensors required for *k*-coverage of a square region with area $A.$ is equal to $\frac{k}{s^2} = \frac{k\log^2 A}{2r^2}.$

Wan and Yi [155] showed that with boundary effect, the asymptotic (*k+1*)-coverage of a square with area s by Poisson point process with unit-area coverage range requires that the sensor density be equal to $\log s + 2(k+1)\log\log s + \xi(s)$ with $\lim_{s\to\infty}\xi(s) = \infty.$ Without the boundary effect, however, the asymptotic (*k+1*)-coverage requires that the sensor density be computed as $\log s + (k+2)\log\log s + \xi(s)$ with $\lim_{s\to\infty}\xi(s) = \infty.$

It is easy to prove that $\lambda(r,k)$ is much less than its counterpart λ computed in [175], [177]. Furthermore, we always have $\lambda > 1$ when $\ell \geq 2.$ For a large square sensor field, the value of λ [175], [177] is high. However, our density measure $\lambda(r,k)$ depends on the radius r of the sensing disks of the sensors

and tends to decrease as r increases, thus reflecting a more expected behavior. Also, the density computed by Zhang and Hou [174] depends on the geometry of the sensor field and is much higher than $\lambda(r,k)$. Also, the sensor density for *k*-coverage computed by Kumar *et al.* [108] depends on the number of deployed sensors and is higher than our density $\lambda(r,k)$.

3.2 Coverage, Connectivity, and Scheduling Protocols

A variety of configuration protocols for coverage and connectivity in wireless sensor networks have been proposed in the literature with a goal to extend the network lifetime. In this section, we review a sample of these configuration protocols and summarize their shortcomings.

The issue of determining the required number of sensors to achieve full coverage of a desired region was addressed in [2]. Precisely, an exposure-based model was proposed to find the sensor density based on the physical characteristics of the sensors and the properties of the target. The minimum number of sensors needed to achieve *k*-coverage with high probability was showed in [108] to be approximately the same regardless of whether the sensors are deployed deterministically or randomly, if the sensors fail or sleep independently with equal probability. Necessary and sufficient conditions for 1-covered, 1-connected wireless sensor grid network were given in [146], [147]. Also, a variety of algorithms have been proposed to maintain connectivity and coverage in large wireless sensor networks [146], [147]. The problem of coverage and connectivity in three-dimensional networks were studied in [7]. Also, a placement strategy based on Voronoi tessellation of a three-dimensional space was proposed [7]. In [142], several fundamental characteristics of randomly deployed wireless sensor networks regarding communication and sensing range for connectivity and coverage in three-dimensional sensor networks were investigated.

An optimal deployment pattern for achieving *k*-barrier coverage was established, efficient global algorithms for checking *k*-barrier coverage of a given region were developed, and it was showed the non-existence of localized algorithms for testing the existence of global barrier coverage [107]. To address this limitation, localized algorithms so sensors can locally determine the existence of local barrier coverage were proposed in [54]. Moreover, optimal polynomial-time algorithms were proposed to solve the sleep-wakeup problem for the barrier coverage model using sensors with equal and unequal lifetimes [109].

A directional sensors-based approach for network coverage was proposed in [3], where the

coverage region of a sensor depends on its location and orientation. The coverage problem in heterogeneous sensor networks was discussed in [112], [113]. They formulated the coverage problem as a set intersection problem and derived analytical expressions, which quantify the coverage achieved by stochastic coverage. Efficient distributed algorithms to optimally solve the best-coverage problem with the least energy consumption were proposed in [119]. Optimal polynomial time worst and average case algorithms for coverage calculation based on the Voronoi diagram and graph search algorithms were proposed in [129], [131]. In [91], polynomial-time algorithms, in terms of the number of sensors, were presented for the coverage problem formulated as a decision problem. A distributed algorithm was proposed in [1] to partition a wireless sensor network into *k* covers, each of which contains a subset of sensors that is activated in a round-robin fashion such that as many areas are monitored as frequently as possible. Surveys of a variety of approaches on energy-efficient coverage problems are in [49], [76].

In [34], an optimal deployment strategy to achieve both full coverage and 2-connectivity regardless of the relationship between communication and sensing radii of the sensors was proposed. In [93], the relationship between coverage and connectivity of wireless sensor networks was studied and distributed protocols to guarantee both their coverage and connectivity were proposed. The problem of sensor selection to provide both sensing and connectivity was addressed in [106] and an approach for solving it based on the concept of connected dominating set was proposed. A joint scheduling scheme based on a randomized algorithm for providing statistical sensing coverage and guaranteed network connectivity was presented in [124]. A distributed algorithm to keep a small number of active sensors in a network regardless of the relationship between sensing and communication ranges was proposed in [176]. It was also proved that if the original network is connected and the identified active nodes can cover the same region as all the original nodes, then the network formed by the active nodes is connected when the communication range is at least twice the sensing range [152]. A probabilistic Markov model was proposed to solve the problem of minimizing power consumption in each sensor while ensuring coverage and connectivity [172].

In [83], centralized and distributed algorithms for connected sensor cover were proposed so the network can self-organize its topology in response to a query and activate the necessary sensors to process the query. Datta, *et al.* [61] proposed two self-stabilizing algorithms to the problem of minimal connected sensor cover [83]. In [180], a distributed and localized algorithm using the concept of the k^{th}-order Voronoi

diagram was proposed to provide fault tolerance and extend the network lifetime, while maintaining a required degree of coverage. Control and coordination algorithms were designed for a multi-vehicle network with limited sensing and communication capabilities [58]. Also, adaptive, distributed, and asynchronous coverage algorithms were proposed for mobile sensing networks. Indeed, it was proved that mobility can be used to improve coverage in wireless sensor networks [122]. A distributed algorithm was proposed in [1] in order to partition a WSN into *k* covers, each of which contains a subset of sensors that is activated in a round-robin fashion such that as many areas are monitored as frequently as possible.

The first combined study on *k*-coverage and connectivity was proposed in [166] and it was proved that if the radius of the communication ranges of sensors is double the radius of their sensing ranges, the network is connected provided that sensing coverage is guaranteed. In [166], the network connectivity was also computed based on whether the disconnected node is boundary or interior, and proposed a network configuration protocol based on the degree of coverage of the sensing application. The *k*-coverage set and the *k*-connected coverage set problems were formalized in terms of linear programming and two non-global solutions were proposed for them [167].

3.3 Data Forwarding Protocols

Xing, *et al.* [165] proposed a greedy geographic routing protocol, called Bounded Voronoi Greedy Forwarding (BVGF). The nodes eligible to act as the next hops are the ones whose Voronoi regions are traversed by the segment line joining the source and the destination. The BVGF protocol chooses as the next hop the neighbor that has the shortest Euclidean distance to the destination among all eligible neighbors. This protocol does not help the sensors deplete their battery power uniformly. Each sensor has, indeed, only one next hop to forward its data to the sink. Therefore, any data dissemination path between a source sensor and the sink will always have the same chain of next hops, which will severely suffer from battery power depletion. The greedy geographic routing protocol BVGF allows sensing-covered networks to achieve a lower routing path length compared to other existing protocols [60]. Bose and Morin [41] proposed a Voronoi routing for Delaunay triangulations that moves the data packet along the nodes whose Voronoi regions intersect the straight line between the sender and the receiver. The major problem of this algorithm is that it requires the construction of the Voronoi diagram and the

Delaunay triangulation of all the wireless nodes. This strategy is very expensive in distributed environments, such as sensor networks. Also, this protocol would consider the same path between the source and destination, and hence would deplete the battery power of the sensors very quickly. Karp and Kung [100] proposed a Greedy Perimeter Stateless Routing (GPSR) protocol for mobile wireless ad hoc networks. The GPSR protocol forwards data packets through long distances and hence consumes much energy. Our protocol, however, forwards sensed data through short Delaunay edges and hence achieves significant energy savings. Li *et al.* [115] studied different routing algorithms, such as compass routing [104], random compass routing [104], greedy routing [42], and most forwarding routing [150] on different graphs. Wang *et al.* [157] proposed a proxy-based sensor deployment protocol for mobile wireless sensor networks. A proxy sensor is a static sensor that is closest to the logical position of its delegated mobile sensor. As can be seen, checkpoints in our protocol differ from proxy sensors in Wang *et al.*'s protocol [157]. However, both of them are used for energy efficiency purpose. Proxy sensors are introduced to help mobile sensors move only when needed so that they save their energy, while our checkpoints are introduced to shorten data dissemination paths between source sensors and the sink, and hence minimize the total energy consumption. Choi and Das [55] proposed an applicative indirect routing (AIR) protocol for ad hoc wireless networks using the notion of proxy candidates. These proxies are defined as the neighbors that are shared by the sender and the receiver and are introduced to cope with unreliable links in the original path. Zhang *et al.* [173] proposed a dynamic proxy tree-based data dissemination framework for mobile wireless sensor networks. Mobile sources and mobile sinks are associated with stationary source proxies and sink proxies, respectively, and proxies related to the same source form a proxy tree. The latter is used to multicast data from the source proxy to the sink proxies. When the distance between sources or sinks and their proxies do not change beyond the threshold distance, the sources and sinks will keep the same proxies. This situation could lead to a battery power depletion of the associated proxies. In our protocol, checkpoints dynamically change based on both their closeness to the shortest path between the senders and receivers and their remaining energy. Zhang *et al.* [173] protocol introduces an overhead in reconfiguring the proxy tree due to source and sink mobility. The overhead introduced by our protocol is due to the construction of localized Delaunay triangulation which occurs only once as the network is static, thus yielding little overhead. Luo *et al.* [126] and Ye *et al.* [170] proposed a

scalable and efficient data delivery to multiple mobile sinks using two-tier data dissemination (TTDD) model. Ammari and Das [29] proposed an information theory-based approach for data dissemination in wireless sensor networks with a mobile sink. Also, Ammari and Das [18] formulated the energy-delay tradeoff for geographic forwarding in wireless sensor networks as a multi-objective optimization problem and solved it using an approach that is simpler than genetic algorithms [70].

Yang and Vaidya [168] proposed a wakeup scheme, called Pipelined Tone Wakeup (PTW), which achieves a balance between energy saving and end-to-end delay. The PTW scheme is based on an asynchronous wakeup pipeline that overlaps the wakeup procedures with the packet transmissions. It uses wakeup tones which allow a large value of duty cycle ratio without causing a large wakeup delay at each hop. Miller *et al.* [132] studied the trade-off between energy, latency and reliability. They presented a Probability-Based Broadcast Forwarding (PBBF) scheme which minimizes energy usage and optimizes latency and reliability. Bandyppadhyay and Coyle [36] proposed a transmission scheduling scheme using a collision-free protocol for gathering sensor data. They also studied many trade-offs between energy usage, sensor density, temporal and spatial sampling rates. Sohrabi *et al.* [149] proposed a sequential assignment routing (SAR) protocol which is used by sensors to select a path among multiple ones to the sink node. The SAR protocol selects a path based on the energy resources and the priority level of a packet. Lindsey *et al.* [121] presented a scheme, called PEGASIS (Power-Efficient Gathering in Sensor Information Systems), where each node can receive from and send to close neighbors. The data gathered by nodes in each round has to be collected and transmitted to the base station by only one designated node to reduce energy consumption and extend the life of the network. The PEGASIS considered $energy \times delay$ as an optimization metric per round of data gathering in wireless sensor networks and showed that it outperforms the LEACH protocol [88]. Krishnamachari *et al.* [105] surprisingly showed by well-selected examples that when robustness and energy efficiency are the main concern, single-path routing outperforms multipath routing under the assumption of perfectly reliable source and destination sensors. Choi and Das [56] proposed a data gathering scheme which trades off coverage and data reporting latency while enhancing energy conservation. Kim *et al.* [101] proposed a Scalable Energy-efficient Asynchronous Dissemination (SEAD) protocol for wireless sensor networks, which is based on dissemination trees that are built to disseminate data to mobile sinks. Every mobile sink is supported by a

special node, called access node, which acts as the relay between the mobile sink and source sensors. Boukerche *et al.* [45] proposed a novel protocol, called *energy-aware data-centric* (EAD), which builds a virtual backbone composed of active sensors that are responsible for in-network data processing and traffic relaying. EAD attempts to construct a broadcast tree that approximates an optimal spanning tree with a maximum number of leaves, thus reducing the size of the backbone formed by active sensors. Luo and Hubaux [125] discussed an energy efficient routing protocol for wireless sensor networks which exploits base station mobility and multi-hop routing. Different mobility strategies of a mobile station have been studied to identify the optimum one in terms of balanced load distribution. Intanagonwiwat *et al.* [94] proposed a data-centric paradigm for sensor query dissemination and processing in static wireless sensor networks, called directed diffusion (DD), which uses attribute-based naming to match data to sensors. The DD paradigm provides robust multi-path delivery and achieves energy saving when intermediate nodes aggregate responses to queries. When a data source detects a stimulus, it builds a data dissemination grid structure over the sensor field and sets up the forwarding information at sensors closest to grid points. For a more comprehensive survey on routing and data dissemination protocols in wireless sensor networks along with their taxonomy, the interested reader is referred to [60].

3.4 Joint Coverage and Geographic Forwarding Protocols

The study of joint coverage and geographic forwarding, however, has received little attention. In particular, a few works addressed the problem of geographic forwarding on duty-cycled wireless sensor networks [38], [133], [184]. While Biswas and Morris [38] and Zorzi and Rao [184] assumed duty-cycling at the MAC layer, Nath and Gibson [133] considered both routing and duty-cycling at the routing layer. In traditional routing, a sender chooses the next forwarder before transmitting its data. However, when the link quality is poor, the probability that the selected forwarder receives the data is low. In contrast, using *opportunistic routing*, *any* node that overhears the transmission and is closer to the destination can participate in forwarding the packet. The packet duplication problem is solved using a scheme for contention among receivers. Zorzi and Rao [184] also gave a detailed description of a MAC protocol and an evaluation of the latency and energy performance. Zorzi and Rao [184] proposed an opportunistic data transmission scheme for wireless sensor networks, called *geographic random forwarding* (GeRaF), which

uses geographic routing where a sensor acting as relay is not known *a priori* by a sender. In other words, relay nodes are decided only after the transmission has started. Thus, GeRaF does not guarantee that a sender will always be able to forward a message towards the sink, and hence GeRaF is said to be *best-effort* forwarding scheme. Biswas and Morris [38] proposed an integrated routing and MAC protocol, called ExOR, to enhance throughput in multi-hop wireless networks, where a source sends a batch of packets destined to the same destination. ExOR is also an opportunistic routing protocol that determines the next forwarder of a packet after the transmission of the packet. The node closest to the destination among all the candidate forwarders that receive the packet is selected in each hop. Nath and Gibbons [133] presented the first analysis of the performance of geographic routing on duty-cycled wireless sensor networks, where every sensor has *k* awake neighbors. They also proposed a sleep-wakeup scheduling protocol for opportunistic geographic routing.

3.5 Network Connectivity Measures

The concept of conditional connectivity [87] has been investigated in several research works. Esfahanian [67] presented a new fault-tolerance analysis for the *n*-cube networks based on the concept of forbidden faulty set. Latifi *et al.* [111] introduced a new measure of conditional connectivity for the *n*-dimensional cube, where every node is required to have at least *g* good neighbors. Wu and Guo [164] computed the fault tolerance of the *m*-ary *n*-dimensional hypercubes using forbidden faulty sets. Also, Chen *et al.* [53] proposed a probabilistic approach for computing the fault tolerance of hypercube network using forbidden faulty sets. Malde and Oellermann [127] introduced the notion of *F*-connectivity as the smallest number of vertices of G whose removal produces a trivial graph or a disconnected graph with each component a subgraph of *F*, where *F* is an induced subgraph of G. Oellermann [135] proposed the P-connectivity of a graph G with respect to hereditary properties, where every induced subgraph F of a graph G having property P also has property P. Ammari and Das [26] proposed measures of conditional fault-tolerance of *k*-covered wireless sensor networks but considered connectivity from graph theory perspective, which is quite different from connectivity with the sink. Indeed, network connectivity is not necessarily a condition for the network to operate whereas connectivity to the sink is. Thus, more realistic measures of fault tolerance should be defined with respect to the sink.

Existing works on coverage and connectivity in wireless sensor networks assumed the concept of traditional connectivity. Our proposed approach [26], however, considers both concepts of traditional and conditional connectivity. The latter is based on the concept of forbidden faulty sensor set that includes subsets of sensors that cannot be faulty at the same time. Furthermore, our measures of connectivity and fault tolerance for *k*-covered wireless sensor networks take into consideration their morphology, where the sink is the most crucial node.

3.6 Stochastic Coverage Approaches

An exposure-based model to find the sensor density to achieve full coverage of a desired region based on the physical characteristics of the sensors and the properties of the target was proposed in [2]. In [108], it was showed that the minimum number of sensors needed to achieve *k*-coverage with high probability is approximately the same regardless of whether the sensors are deployed deterministically or randomly. The coverage problem in heterogeneous wireless sensor networks was formulated in [113] as a set intersection problem and analytical expressions, which quantify the coverage achieved by stochastic coverage, were derived. Necessary and sufficient conditions for 1-covered, 1-connected wireless sensor grid network were given in [146] and a variety of algorithms have been proposed to maintain connectivity and coverage in large wireless sensor networks [146]. The exposure in wireless sensor networks, which is related to the quality of coverage provided by these networks, was studied in [130] based on a general sensing model, where the sensing signal of a sensor at an arbitrary point by a function that is inversely proportional to the distance between the sensor and point. Three coverage measures, namely area coverage, node coverage, and detectability were studied in [123] using the general sensing model defined in [130].

A joint scheduling scheme based on a randomized algorithm for providing statistical sensing coverage and guaranteed network connectivity was presented in [124]. This scheme does not make any assumption on the relationship between sensing and transmission ranges, and works without the availability of per-node location information. A distributed approach for the selection of active sensors to fully cover a field based on the concept of connected dominating set was proposed in [186]. This approach is based on a probabilistic sensing model, where the probability of the existence of a target is defined by an exponential function that represents the confidence level the received sensing signal.

Solutions to the *k*-coverage sensor deployment problem using both deterministic and probabilistic sensing models were proposed in [159]. These solutions compute the minimum number of sensors required to *k*-cover a field as well as their locations, and schedule the sensors to move to these locations. In the first solution, the sink computes those locations and the sensors bid for their closest locations. The second solution enables the sensors to derive the target locations by themselves. The CCP protocol [166] was extended to provide probabilistic coverage guarantee based on a probabilistic coverage model, where the sensors may have non-uniform and irregular communication and sensing regions. According to this model, a point in a convex coverage area is guaranteed to be *k*-covered with a probability no lower than β. CCP provides probabilistic coverage via a mapping of the (k,β)-coverage requirement to a *pseudo coverage degree* k', which is computed analytically.

3.7 Minimizing Energy Consumption vs. Balancing Energy Consumption

Data forwarding protocols for wireless sensor networks can be categorized into two main classes. The first one consists of protocols that attempt to minimize the energy consumption of sensors. Unfortunately, these protocols do not consider some particular regions in the network whose sensors are heavily used compared to others, and hence deplete their initial energy very quickly. This behavior may result in network disconnections although most of the rest of sensors have enough amount of energy to work correctly. The second class includes protocols that attempt to balance the energy consumption among all sensors in the network. The next two paragraphs review protocols for both classes.

Chang and Tassiulas [51] proposed different approaches for maximizing the network lifetime based on finding the best link cost function. Boukerche *et al*. [44] proposed power-efficient data dissemination protocols that combine sleep/awake and probabilistic forwarding techniques. Boukerche *et al*. [45] also proposed a protocol, called *energy-aware data-centric* (EAD), which constructs a broadcast tree rooted at the sink. Gao and Zhang [75] proposed greedy forwarding algorithms for load-balanced routing in wireless networks when nodes lie either on a line or in a narrow strip. Sankar and Liu [144] proposed a distributed routing algorithm that checks whether it is possible to route flow in the network while satisfying all the demands in terms of total energy consumed by all nodes before threshold for lifetime expires. Zhou *et al*. [183] investigated the problem of finding energy-efficient paths to the sink using the notion of transmitter

power control. Shah *et al.* [145] proposed a three-tier architecture for data dissemination in sparse wireless sensor networks using the concept of MULES. Wang *et al.* [156] proposed distributed self-deployment protocols to discover coverage holes and cover those using mobile sensors.

The *energy sink-hole* problem in wireless sensor networks has gained relatively less attention in the literature. This problem was originally addressed by Guo *et al*. [82]. They proposed an energy-balanced transmission scheme that adjusts the ratio between direct transmission to the sink and next-hop transmission. Precisely, sensors far away from the sink send larger percent of data to the next hop, while sensors near the sink send more data directly to the sink. Zhang *et al*. [178] also exploited this combination of hop-by-hop transmission and direct transmission to find a trade-off between them. Efthymiou *et al*. [65] proposed a probabilistic data propagation algorithm for balancing energy consumption among all sensors. Antoniou *et al.* [32] and Boukerche *et al*. [43] proposed a protocol, called *Variable Transmission Range Protocol* (VTRP). VTRP contributes to solve the energy sink-hole problem by varying the transmission range of sensors in order to bypass sensors lying close to the static sink and avoid their overuse. Powell *et al*. [141] used the probabilistic data propagation algorithm in [65] and proved that there is a relationship between energy balancing and lifespan maximization [95]. Leone *et al*. [114] considered non-uniform sensor distribution and proposed a *blind* algorithm that computes a solution to the energy-balancing problem on-line without prior knowledge on the occurrences of the events. Li and Mohapatra [117], [118] characterized the energy hole around the sink with an analytical model and investigated the effectiveness of a few approaches for mitigating the energy hole problem. Olariu and Stojmenovic [136] proved that energy-efficient routing can be guaranteed when the coronas of a circular field have the same width, but this would lead to uneven energy depletion of sensors. Hence, they computed the widths of coronas and their number to achieve even energy depletion of sensors. They also proved that uneven energy depletion is unavoidable for the free space model but can be prevented for the multi-path model. Lian *et al.* [120] showed that up to 90% of the total initial energy is unused due to the static network model with uniformly distributed homogenous sensors and a stationary sink. They also proposed a non-uniform sensor distribution-based deployment strategy. Non-uniform node distribution was also considered in [162], [163] to achieve balanced energy depletion. Luo and Hubaux [125] proposed a data collection protocol for wireless sensor networks that makes use of multi-hop routing and base station mobility to solve the energy-sink-hole problem.

3.8 Three-Dimensional Coverage and Connectivity

The study of coverage, connectivity, and routing in three-dimensional wireless sensor networks, such as underwater sensor networks [4], has gained relatively less attention in the literature compared to that of two-dimensional wireless sensor networks. Alam and Haas [7] proposed a placement strategy based on Voronoi tessellation of a three-dimensional space, which creates truncated octahedral cells. Huang *et al* [92] proposed a polynomial-time algorithm to solve the α-Ball-Coverage (α-BC) problem whose goal is to check α-coverage of a three-dimensional region. Pompili *et al.* [140] proposed a deployment strategy for three-dimensional communication architecture for underwater acoustic sensor networks, where sensors float at different depths of the ocean to cover the entire three-dimensional region. Poduri *et al* [138] discussed some difficulties encountered in the design of three-dimensional wireless sensor networks, such as ensuring networ*k* connectivity in the case of uniform random deployment and restrictions imposed by the environment structure on sensor deployment. In [142], Ravelomanana investigated fundamental properties of randomly deployed three-dimensional wireless sensor networks for connectivity and coverage, such as the required sensing range to guarantee certain degree of coverage of a region, the minimum and maximum network degrees for a given communication range, and the network hop-diameter. Kao *et al*. [99] proposed a heuristic for routing in three-dimensional space using the two-dimensional face routing algorithm. Pompili *et al.* [139] proposed different routing algorithms for applications in underwater sensor networks depending on whether delay is sensitive or not.

3.9 Percolation

The concept of *continuum percolation* originally due to Gilbert [77], is to find the critical density of a Poisson point process at which an unbounded connected component *almost surely* appears so the network can provide long-distance multi-hop communication. For random plane networks, Gilbert claimed that the filling factor, representing the critical value of the expected number of points in a circle of radius R, should be around 3.2. Since then, Gilbert's model has become the basis for studying continuum percolation in wireless networks. Booth *et al.* [40] discussed different classes of covering algorithms and determined the critical density of a Poisson point process (centers of disks of radius r) above which an unbounded connected component arises. They also discussed the almost sure existence of an

unbounded connected component based on the ratio of the connectivity range of the base stations to the connectivity range of the clients. Bertin *et al.* [37] proved the existence of site percolation and bond percolation in the Gabriel graph [73] for both Poisson and hard-core stationary point processes. The critical bounds corresponding to the existence of a path of open sites and a path of open bonds were found by simulation. Glauche *et al.* [78] proposed a distributed protocol, which guarantees strong connectivity *almost surely* of ad hoc nodes. They translated the problem of finding the critical transmission range of mobile devices to that of determining the critical node neighborhood degree above which an ad hoc network graph is *almost surely* connected. To achieve a little above this degree, each node needs to adjust its transmission power locally. Jiang and Bruck [97] proposed the concept of monotone percolation based on the local adjustment of the transmission radii of the nodes for efficient topology control of the network. Their proposed algorithms guarantee the existence of relatively short paths between any pair of source and destination nodes, which makes monotonic progress. Liu and Towsley [123] considered both Boolean and general sensing models, each with a variety of network scenarios, to characterize fundamental coverage properties of large-scale sensor networks, namely area coverage, node coverage, and detectability. According to their simulation setting, the critical sensor density is about 3.53×10^{-3}.

3.10 Summary

In this chapter, we described a variety of approaches that compute the sensor spatial density that is needed to guarantee some degree of coverage of a field. However, all the proposed bounds for the sensor spatial density are asymptotic and depend on the geometry of the field and its size. We believe that the sensor spatial density to achieve (redundant) coverage should depend only on the sensing range of the sensors and the degree of coverage dictated by the underlying application. Hence, new approaches are required to provide more accurate bounds on the sensor spatial density. Furthermore, we presented different approaches for coverage, connectivity, duty-cycling, and data forwarding in wireless sensor networks. However, due to their dependency, a few protocols that combine some of them have been proposed. We believe that a more energy-efficient and unified framework should be proposed in which coverage, connectivity, duty-cycling, and geographic forwarding are jointly considered.

CHAPTER 4

PHASE TRANSITIONS IN COVERAGE AND CONNECTIVITY

In wireless sensor networks, *sensing coverage* reflects the surveillance quality provided by active sensors in a field, while *network connectivity* enables active sensors to communicate with each other in data forwarding to a central gathering node, called the *sink*. For the correct operation of the network, it is necessary that both sensing coverage and network connectivity be maintained. Assuming perfectly reliable wireless links, both sensing coverage and network connectivity are affected by the sensor spatial density.

Given a field that is initially uncovered, as more and more sensors are continuously added to the network, the size of the partial covered areas increases. At some point, the situation abruptly changes from small fragmented covered areas to a single large covered area in the field. We call this abrupt change as the *sensing-coverage phase transition* (SCPT) [11]. The SCPT problem can be stated as follows:

Given a field that is initially uncovered, what is the sensor spatial density corresponding to the first appearance of a single large covered component that spans the entire network?

Likewise, given a network that is originally disconnected, the number of connected components changes with the addition of sensors such that the network suddenly becomes connected at some point. We call this sudden change in the network topology as the *network-connectivity phase transition* (NCPT) [11]. The NCPT problem can be expressed as follows:

Given a network that is initially disconnected, what is the sensor spatial density corresponding to the first appearance of a single large connected component that spans the entire network?

The nature of such phase transitions is a central topic in percolation theory of Boolean models. The process of the *ground getting wet* during a period of rain [128] gives us a better analogy with the SCPT and NCPT problems. A circular wet patch forms whenever a point of the ground is hit by a raindrop. At the start of the rain, one can see a small wet area within a large dry area. After some time and as many raindrops continue to hit the ground, the situation suddenly changes and one can see a small dry area within a large

wet area. This phase transition phenomenon occurs at a given density of the raindrops. This example helps us approach the SCPT and NCPT problems from a perspective of continuum percolation. In this chapter, we propose a probabilistic approach to compute the *covered area fraction* at critical percolation for both of the SCPT and NCPT problems. In [13], we proposed a different percolation theory-based approach for three-dimensional wireless sensor networks.

As will be discussed later, the specific connection function used in NCPT problem has not been studied before and hence no bound on the critical covered area fraction is known. Furthermore, given that sensing coverage and network connectivity are not totally orthogonal [27], [166] (see Chapter 3), we propose a new model for percolation in wireless sensor networks, called *correlated disk model*, which allows network connectivity and sensing coverage to be studied together in an integrated fashion. We show that the SCPT and NCPT problems have the same solution (i.e., same critical covered area fraction). Precisely, we solve the SCPT and NCPT problems together, where the radii of the sensing disks (r) of the sensors and the radii of their transmission disks (R) are related by $R = \alpha r,$ where $\alpha \geq 1.$ We show that NCPT occurs provided that SCPT arises and the ratio R/r has certain value. It is worth noting that the exact value of the critical density at which an infinite (or single large) cluster of overlapping disks first appears is still an open problem, and its approximation is either predicted by simulations [137], [143], [154] or computed analytically [72]. From now on, "infinite" means "single large".

The remainder of this chapter is organized as follows. Section 4.1 solves the SCPT problem. Section 4.2 solves the NCPT problem. Section 4.3 discusses our results. Section 4.4 concludes the chapter.

4.1 Phase Transition in Sensing Coverage

This section discusses the *sensing-coverage phase transition* (SCPT) problem and solves it using a percolation-theoretic approach.

Let $X_\lambda = \{ \xi_i : i \geq 1 \}$ be a two-dimensional homogeneous Poisson point process of density $\lambda,$ where ξ_i represents a sensor $s_i.$ Given an initially uncovered field, the SCPT problem is to compute the probability of the first appearance of an *infinite (or single large) covered component* that spans the entire network. In particular, we are interested in the limiting case of an infinite field, where there exist no collaboration paths for sufficiently small density λ and they suddenly appear at a *critical percolation density* $\lambda_c.$

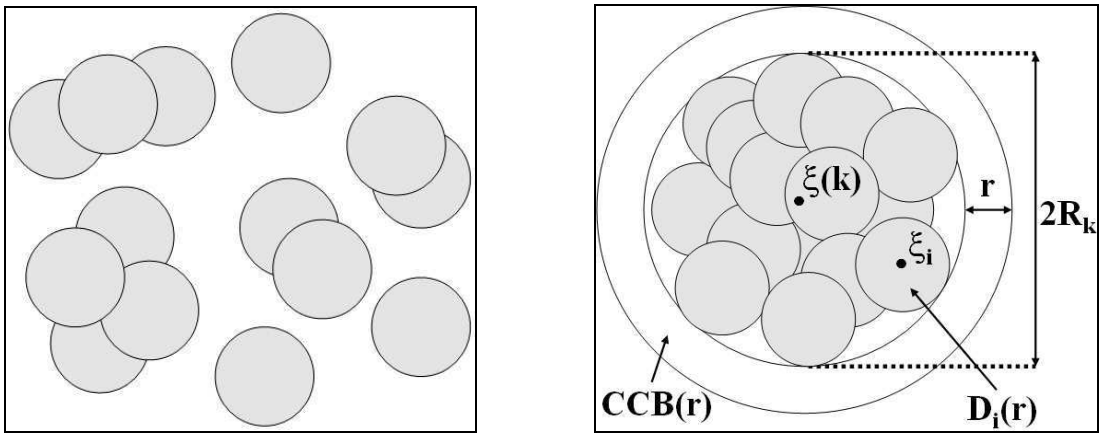

(a) (b)

Figure 4.1 (a) Schematic of overlapping disks (three covered components of size 1, two of size 2, one of size 3, and one of size 4) (b) Shape of a covered component

4.1.1 Estimation of the Shape of Covered Components

Each *k*-covered component CC_k is characterized by a reference point, called *center* and denoted by $\xi(k)$. Figure 4.1a shows various covered components of different sizes. Using the Poissonness argument stated in [68] (pages 200-202), as the centers $\{\xi_i : i \geq 1\}$ form a Poisson process with density λ, the centers of all *k*-covered components also form a Poisson process with density $\lambda(k)$. In other words, the covered components are randomly and independently distributed according to a Poisson process with a density of $\lambda(k)$ centers per unit area. We want to determine the smallest shape enclosing a *k*-covered component. In fact, the shape of the covered components varies depending on the number of its overlapping sensing disks. For tractability of the problem, we assume that the geometric form that encloses a *k*-covered component is a circle (Figure 4.1b), which tends to minimize the area of uncovered region around the covered component. Indeed, the circle is the most compressed shape. Let R_k be the radius of a circle, denoted by $C(R_k, k)$, which encloses a *k*-covered component. Thus, there is no other sensing disk that could overlap with the boundary of the circle. That is, the concentric circular band of width r, denoted by $CCB(r)$ and which surrounds the circle, should not include any other sensing disk. Hence, the annulus between radii R_k and $R_k + r$ around the center $\xi(k)$ must be empty.

Let $\mathrm{P}(k)$ be the conditional probability that the circle encloses only one *k*-covered component. This probability is given by

$$\mathrm{P}(k) = \mathrm{Prob}[\, C(R_k, k) \mid CCB(r) \text{ is empty }]$$

By definition, this probability is computed as

$$\mathrm{P}(k) = \frac{\mathrm{Prob}[\, C(R_k, k) \wedge CCB(r) \text{ empty }]}{\mathrm{Prob}[\, CCB(r) \text{ empty }]} \tag{4.1}$$

where $\mathrm{Prob}[\, C(R_k, k) \wedge CCB(r) \text{ empty }]$ can be interpreted as the probability that the circle of radius $R_k + r$ encloses only one *k*-covered component. Thus,

$$\mathrm{Prob}[\, C(R_k, k) \wedge CCB(r) \text{ empty }] = \mathrm{Prob}[\, C(R_k + r, k) \,]$$

Using equation (2.3) (see Chapter 2), we obtain the following results:

$$\mathrm{Prob}[\, C(R_k + r, k) \,] = \frac{(\lambda \pi (R_k + r)^2)^k}{k!} e^{-\lambda \pi (R_k + r)^2}$$

$$\mathrm{Prob}[\, CCB(r) \text{ empty }] = e^{-\lambda \pi ((R_k + r)^2 - r^2)}$$

Therefore, equation (4.1) becomes

$$\mathrm{P}(k) = \frac{(\lambda \pi (R_k + r)^2)^k}{k!} e^{-\lambda \pi R_k^2} \tag{4.2}$$

It is worth mentioning that the analysis of SCPT and NCPT problems will be based on the form of conditional probability given in (4.2).

4.1.2 Critical Density of Covered Components

Although there exist a few definitions of the average distance between clusters (i.e., covered components), one of them is more appropriate. It is defined as the average of the minimum distance between all pairs of sensing disks, each from one covered component. Indeed, two covered components could be merged together into a single one if and only if there is at least a pair of sensing disks, one from each covered component, such that the distance between their centers is at most equal to $2r$. Lemma 4.1 computes the mean distance between neighboring *k*-covered components at critical percolation.

Lemma 4.1: Let $\{CC_k\}$ be a set of *k*-covered components with density $\lambda(k)$ and Y a random variable representing distances between them. The mean distance d_{avg}^1 between two neighboring covered components at critical percolation is given by

$$d_{avg}^1 = \frac{1}{2\sqrt{\lambda_c(k)}} \tag{4.3}$$

where $\lambda_c(k)$ is the density of $\{CC_k\}$ at critical percolation.

Proof: Let ω_k be the mean number of *k*-covered components in a circular field of radius $\Re$. Denote by $p(\sigma)$ the probability that there is a covered component whose center is located at a distance upper bounded by σ from the center, say $\xi(k)$, of a given covered component. We denote by $P(\sigma)d\sigma$ the probability that a nearest center of a covered component to a given center $\xi(k)$ is located at a distance between σ and $\sigma + d\sigma$. Hence, $P(\sigma)d\sigma$ can be viewed as the probability that there exists one of the $\omega_k - 1$ covered components at a distance between σ and $\sigma + d\sigma$ from the center $\xi(k)$ and the other $\omega_k - 2$ covered components are at a distance larger than σ from $\xi(k)$. Thus,

$$\begin{aligned} P(\sigma)\, d\sigma &= \binom{\omega_k - 1}{1} \frac{\partial\, p(\sigma)}{\partial\, \sigma} d\sigma \left(1 - p(\sigma)\right)^{(\omega_k - 2)} \\ &= (\omega_k - 1) \frac{\partial p(\sigma)}{\partial \sigma} d\sigma \left(1 - p(\sigma)\right)^{(\omega_k - 2)} \end{aligned} \tag{4.4}$$

where $\frac{\partial\, p(\sigma)}{\partial\, \sigma} d\sigma$ stands for the probability that there is a covered component whose center lies within a circular band located at a distance σ from the center $\xi(k)$ and whose width is $d\sigma$. Notice that $p(\sigma)$ can be computed as the ratio of the number of covered components within the circle of radius σ to the total number of covered components within the field. Thus, we obtain:

$$p\,(\sigma) = \frac{\lambda_k\, \pi\, \sigma^2}{\lambda_k\, \pi\, \Re^2} = \frac{\sigma^2}{\Re^2}$$

and

$$\frac{\partial\, p\,(\sigma)}{\partial\, \sigma} = \frac{2\,\sigma}{\Re^2} \tag{4.5}$$

Substituting equation (4.3) in equation (4.4) gives

$$P(\sigma)\,d\sigma = (\omega_k - 1)\frac{2\sigma}{\Re^2}\,d\sigma\left(1-\frac{\sigma^2}{\Re^2}\right)^{(\omega_k-2)}$$

where $\omega_k = \lambda_k\,\pi\,\Re^2$. We assume that the circular field contains all covered components. Now, the mean distance between two *k*-covered components can be computed as

$$\begin{aligned}\mathrm{E}[Y] &= \int_0^{\Re} \sigma\,P(\sigma)\,d\sigma \\ &= \frac{2(\omega_k-1)}{\Re^2}\int_0^{\Re}\sigma^2\left(1-\frac{\sigma^2}{\Re^2}\right)^{(\omega_k-2)} d\sigma\end{aligned}$$

Using the variable change $T = \dfrac{\sigma^2}{\Re^2}$, we obtain

$$\mathrm{E}[Y] = (\omega_k - 1)\,\Re\int_0^1 \sqrt{T}\,(1-T)^{(\omega_k-2)}\,dT$$

Recall that the beta function [190] is defined by

$$B(\mathrm{m},\mathrm{n}) = \int_0^1 u^{m-1}\,(1-u)^{n-1}\,du$$

Thus,

$$\mathrm{E}[Y] = (\omega_k - 1)\,\Re\,B(3/2, \omega_k\text{ -}1) \tag{4.6}$$

where

$$B(\mathrm{m},\mathrm{n}) = \frac{\Gamma(\mathrm{m})\,\Gamma(\mathrm{n})}{\Gamma(\mathrm{m}+\mathrm{n})}$$

$$\Gamma(m) = (m\text{ -}1)\Gamma(m\text{ -}1) = (\mathrm{m}\text{ -}1)!$$

Hence, equation (4.6) becomes

$$\mathrm{E}[Y] = (\omega_k - 1)\,\Re\,\frac{\Gamma(3/2)\,\Gamma(\omega_k\text{ -}1)}{\Gamma(\omega_k + 1/2)} = \Re\,\frac{\Gamma(3/2)\,\Gamma(\omega_k)}{\Gamma(\omega_k + 1/2)}$$

However, Graham, *et al.* [80] proved that

$$\frac{\Gamma(\mathrm{x}+1/2)}{\Gamma(\mathrm{x})} = \sqrt{x}\left(1-\frac{1}{8x}+\frac{1}{128x^2}+\frac{5}{1024x^3}-\frac{21}{32768x^4}+\ldots\right)$$

Thus,

$$\lim_{x\to\infty} \frac{\Gamma(x+1/2)}{\Gamma(x)} = \sqrt{x}$$

Notice that at critical percolation, the value of ω_k should be *large enough* $(\omega_k \to \infty)$ so an infinite covered component spanning the network could form. Since $\Gamma(3/2) = \frac{\sqrt{\pi}}{2}$ and $\omega_k = \lambda_k \pi \Re^2$, the mean distance d_{avg}^1 between two neighboring *k*-covered components at critical percolation is given by

$$d_{avg}^1 = \lim_{\omega_k \to \infty} \mathrm{E}[Y] = \Re\, \Gamma(3/2) \frac{1}{\sqrt{\omega_k}} = \frac{1}{2\sqrt{\lambda_c(k)}}$$

where $\lambda_c(k)$ is the critical density of *k*-covered components. □

Lemma 4.2 computes the average distance between neighboring *k*-covered components at critical percolation using another approach. As can be seen later, Lemma 4.2 will help us compute the density of *k*-covered components at critical percolation.

Lemma 4.2: Let $\{CC_k\}$ be a set of *k*-covered components with density $\lambda(k)$, and Y a random variable associated with the distances between them. The mean distance d_{avg}^2 between two neighboring covered components at critical percolation is computed as

$$d_{avg}^2 = \frac{erf(2\sqrt{\lambda_c\, \pi}\, r) - 4\sqrt{\lambda_c}\, r\, e^{-4\lambda_c \pi r^2}}{2\sqrt{\lambda_c}} \tag{4.7}$$

where λ_c is the density of a set of sensing disks $\{D_i(r) : i \geq 1\}$ at critical percolation.

Proof: For a homogeneous Poisson point process, the probability that there is no neighbor within distance σ of an arbitrary point is given by $e^{-\lambda \pi \sigma^2}$ [59]. Therefore, the probability that the distance between a point and its neighbor is less than or equal to σ is equal to

$$\mathrm{P}[Y \leq \sigma] = 1 - e^{-\lambda \pi \sigma^2}$$

Hence, the corresponding probability density function is given by

$$f(Y \mid Y \leq \sigma) = 2\lambda \pi \sigma\, e^{-\lambda \pi \sigma^2}$$

The mean distance d_{avg}^2 between two neighboring *k*-covered components of $\{CC_k\}$ at critical percolation is obtained when the distance σ between two sensing disks, say $D_i(r)$ and $D_j(r)$, each from one covered component, belongs to the interval $[0,2r]$. Therefore,

$$d_{avg}^2 = \mathrm{E}[Y \mid Y \le 2r] = \int_0^{2r} \sigma \times f(Y \mid Y \le \sigma) d\sigma = \frac{erf(2\sqrt{\lambda_c \pi}\, r) - 4\sqrt{\lambda_c}\, re^{-4\lambda_c \pi r^2}}{2\sqrt{\lambda_c}}$$

where $erf(x)$ is the error function [191]. □

Lemma 4.3, which follows from Lemmas 4.1 and 4.2, computes the density of *k*-covered components at critical percolation.

Lemma 4.3: The critical density of a set of *k*-covered components $\{CC_k\}$ is given by

$$\lambda_c(k) = \frac{\lambda_c}{\left(erf(2\sqrt{\lambda_c\, \pi}\, r) - 4\sqrt{\lambda_c}\, r\, e^{-4\lambda_c \pi r^2}\right)^2} \tag{4.8}$$

where λ_c is the density of sensing disks at critical percolation and $erf(x)$ is the error function [191].

Proof: From Lemma 4.1 (equation 4.3) and Lemma 4.2 (equation 4.7), the mean distance between two *k*-covered components at critical percolation should verify the following equality $d_{avg}^1 = d_{avg}^2$, which implies that the density of *k*-covered components at critical percolation $\lambda_c(k)$ is given by

$$\lambda_c(k) = \frac{\lambda_c}{\left(erf(2\sqrt{\lambda_c\, \pi}\, r) - 4\sqrt{\lambda_c}\, r\, e^{-4\lambda_c \pi r^2}\right)^2}$$ □

4.1.3 Critical Radius of Covered Components

There is a particular value of the radius R_k of the circular shape enclosing a covered component that *almost surely* guarantees the formation of special class of *k*-covered components, called *critical k-covered components*. Any non-empty circle of radius $2r$ should enclose a *k*-covered component. In other words, regardless of the number of sensing disks of radius r located in a circle of radius $2r$, these sensing disks should definitely form a *k*-covered component. Moreover, this *k*-covered component is a *complete graph* in that each pair of sensors, say s_i and s_j, whose sensing disks are included in this

circle of radius $2r$ are collaborating given that $|\xi_i - \xi_j|_{\max} \le 2r$. Lemma 4.4 computes the density of critical *k*-covered components at critical percolation.

Lemma 4.4: At critical percolation, the density of *k*-covered components, which are enclosed in circles whose radii is equal to $2r,$ is given by

$$\lambda_c(k) = \lambda_c \frac{(9\lambda_c \pi r^2)^k}{k!} e^{-4\lambda_c \pi r^2} \tag{4.9}$$

where λ_c and $\lambda_c(k)$ are the densities of sensing disks and *k*-covered components, respectively, at critical percolation.

Proof: Let N be the total number of sensing disks that are randomly deployed on a circular field of radius $\Re$ according to a spatial Poisson process with density equal to

$$\lambda = \frac{\mathrm{N}}{\pi \Re^2} \tag{4.10}$$

Using $\omega_k = \lambda(k) \pi \Re^2,$ which represents the mean number of *k*-covered components in the circular field, and equation (4.10) leads to

$$\lambda(k) = \lambda \frac{\omega_k}{\mathrm{N}} \tag{4.11}$$

We can approximate $\frac{\omega_k}{\mathrm{N}}$ by the probability $\mathrm{P}[rad(CC_k) = 2r]$ of finding a *k*-covered component whose radius is equal to $2r.$ Hence, we have

$$\mathrm{P}[rad(CC_k) = 2r] = \frac{\omega_k}{\mathrm{N}} \tag{4.12}$$

Substituting equation (4.12) in equation (4.11) gives

$$\lambda(k) = \lambda \, \mathrm{P}[rad(CC_k) = 2r] \tag{4.13}$$

Following the same reasoning as in Section 4.1.1, $\mathrm{P}[rad(CC_k) = 2r]$ is the conditional probability of finding k sensing disks enclosed in a circle with radius $2r$ and centered at $\xi(k)$ such that the annulus between circles of radii $2r$ and $2r + r$ around the center $\xi(k)$ is empty. Substituting $R_k = 2r$ into equation (4.2) gives

$$\mathrm{P}(k) = \frac{(9\lambda \pi r^2)^k}{k!} e^{-4\lambda \pi \mathrm{r}^2}$$

and hence equation (4.13) becomes

$$\lambda_c(k) = \lambda_c \frac{(9\lambda_c \pi r^2)^k}{k!} e^{-4\lambda_c \pi r^2}$$

where λ_c and $\lambda_c(k)$ are the critical densities of sensing disks and *k*-covered components, respectively. □

4.1.4 Characterization of Critical Percolation

Now, we generate an equation that characterizes a set of *k*-covered components at critical percolation. By equating equations (4.8) and (4.9), we obtain a new equation $g_1(\lambda_c, r, k) = 0,$ where

$$\begin{aligned} g_1(\lambda_c, r, k) = (erf(2\sqrt{\lambda_c \pi}\, r) - 4\sqrt{\lambda_c}\, r\, e^{-4\lambda_c \pi r^2})^2 \\ \times \frac{(9\lambda_c \pi r^2)^k}{k!} e^{-4\lambda_c \pi r^2} - 1 \end{aligned} \tag{4.14}$$

Instead of focusing on finding the critical value of the density λ_c of sensing disks at which an infinite covered component first appears, we consider a dimensionless metric, i.e., the *covered area fraction* at critical percolation given by

$$A_c(r) = 1 - e^{-\lambda_c \pi r^2}$$

The benefits of using $A_c(r)$ instead of λ_c are two-fold: first the number of unknown parameters is reduced to two, namely $A_c(r)$ and $k,$ thus removing any direct dependency of $g_1(\lambda_c, r, k)$ on $r.$ Hence, the parameter r will not have any direct impact on the critical percolation density. Second, we know the exact domain of $A_c(r)$ is $[0,1],$ which helps us study exactly the entire behavior of the function $g_1(\lambda_c, r, k) = 0$ for all values of $A_c(r).$ Substituting $A_c(r)$ into equation (4.14) and let $\mu = -\log(1 - A_c(r))$ gives a new function $g_1(A_c(r), k)$ given by

$$\begin{aligned} g_1(A_c(r), k) = \left(erf(2\sqrt{\mu}) - \frac{4\sqrt{\mu} e^{-4\mu}}{\sqrt{\pi}} \right)^2 \\ \times \frac{(9\mu)^k}{k!} e^{-4\mu} - 1 \end{aligned} \tag{4.15}$$

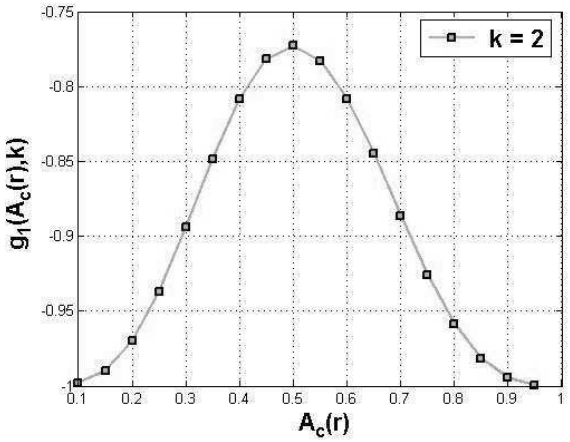

(a)

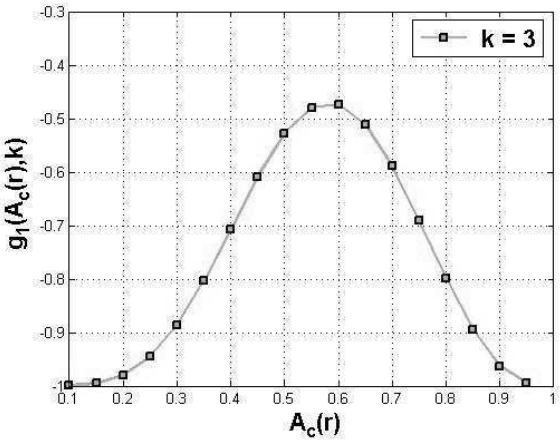

(b)

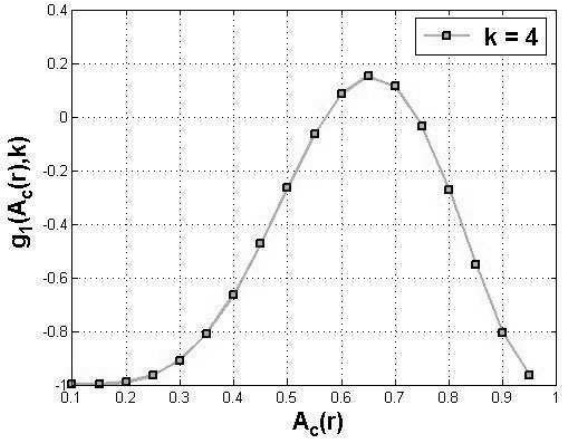

(c)

Figure 4.2 No critical percolation at (a) $k = 2$ and (b) $k = 3$. (c) Critical percolation at $k = 4$ and $A_c(r) = 0.575$

4.1.5 Numerical Results

Figure 4.2 plots the function $g_1(A_c(r), k)$ given in Equation (4.15) with respect to different values of k and $A_c(r)$. Notice that for $k < 4$, the function $g_1(A_c(r), k)$ cannot be equal to zero (Figures 4.2a and 4.2b). Thus, percolation first occurs at $k = 4$ and $A_c(r) = 0.575$ (Figure 4.2c), which is a bit smaller than the values 0.688 of Vicsek and Kertesz [154], 0.68 of Pike and Seager [137], and 0.62 of Roberts [143] (all predicted by Monte Carlo experiments), and the value 0.67 as calculated by Fremlin [72] for studying the percolation of overlapping homogeneous disks. Thus, when the number of collaborating sensors of a

sensor is larger than four $(k \geq 5)$, it is *almost surely* that an infinite covered component that spans the entire network will appear for the first time.

4.2 Phase Transition in Network Connectivity

Let $X_\lambda = \{\xi_i : i \geq 1\}$ be a two-dimensional homogeneous Poisson point process of density λ, where ξ_i represents the location of sensor s_i. Given a network that is originally disconnected, the *network-connectivity phase transition* (NCPT) problem is to compute the sensor spatial density corresponding to the first appearance of an *infinite (or single large) connected component* that spans the network.

Notice that both of the SCPT and NCPT problems have similar structure although the difference of the concepts of collaboration (SCPT) and communication (NCPT) between the sensors in the SCPT and SCPT problems, respectively, as stated earlier in Section 2.5 (see Chapter 2). While in the SCPT problem, two sensing disks belong to the same covered component if the distance between them is at most equal to one diameter $(2r)$, the NCPT problem requires that two communication disks be at a distance of at most half the diameter (R) from each other so they belong to the same connected component, where r and R stand for the radii of the sensing and communication disks of the sensors, respectively. To our knowledge, the connection function of the NCPT problem has not been studied previously in the literature.

Some sensing applications require that every location in the field be covered by at least one sensor and that the active sensors be also able to communicate with each other so the sensed data could reach the sink. Indeed, sensed data would be meaningless if connectivity between the sensors is not maintained. Thus, we are mainly interested in the formation of an *infinite* (or single large) *connected covered component* that spans the entire network. Next, we study the SCPT and NCPT problems *together* using percolation theory.

4.2.1 Integrated Sensing Coverage and Network Connectivity

We propose a new model for percolation in wireless sensor networks, called *correlated disk model*. Each sensor is associated with two concentric disks of radii r and R representing the radii of its sensing and communication disks, respectively. This kind of structure reveals a double behavior of the sensors that can be described by their *collaboration* and *communication*. The collaboration between sensors depends on the relationship between the radii of their sensing disks, whereas communication is related to

the relationship between the radii of their communication disks. Previous studies by Wang, *et al.* [160] and Ammari and Das [27] showed the existence of certain dependency between the concepts of sensing coverage and network connectivity. Our proposed correlated disk model allows us to study these two concepts together from a percolation-theoretic viewpoint to account for their correlation. This problem can be viewed as a *correlated continuum percolation* problem. Next, we study the simultaneous percolation of the sensing and communication disks of the sensors based on the ratio R/r.

4.2.1.1 Simultaneous Phase Transitions When $R \geq 2r$

As mentioned earlier in Chapter 3, Wang, *et al.* [160] proved that if a wireless sensor network is configured to be covered and the radius R of the communication disk of the sensors is at least double the radius r of their sensing disk, then the network is guaranteed to be connected. Ammari and Das [27] provided a tighter relationship between R and r, while achieving network connectivity provided that sensing coverage is guaranteed. In fact, the "worst-case" behavior is when the sensing disks of the sensors are tangential, i.e., the distance between their corresponding centers is equal to $2r$. Hence, when $R \geq 2r$, there is a dependency between sensing coverage and network connectivity in that the former implies the latter. In other words, collaboration between the sensors will lead to their communication. In this case, the SCPT and NCPT problems are equivalent, and thus have the same critical covered area fraction. Thus, a set of communication disks percolates at $k = 4$ with a covered area fraction $A_c(R) = 0.575$ at critical percolation. Therefore, when the number of communicating sensors of a given sensor is larger than four $(k = 4)$, an infinite connected component spanning the network will *almost surely* form.

4.2.1.2 Simultaneous Phase Transitions When $r \leq R < 2r$

The interesting case is when the radii of the sensing and communication disks of the sensors are related by $R = \alpha r$, where $1 \leq \alpha < 2$. Precisely, we focus on the study of the percolation of the sensing disks of the sensors, where two sensors collaborate if and only if the distance between the centers of their sensing disks is equal to αr, where $1 \leq \alpha < 2$. The communication disks of the sensors will also percolate given that $R = \alpha r$. Thus, our goal is to compute the critical covered area fraction above which both the

sensing and communication disks of the sensors percolate when $r \le R < 2r$. It is a valid assumption that the radius of the communication disks of the sensors cannot be less than the radius of their sensing disks as shown in Tables 2 and 3 [176] for a wide spectrum of sensor devices.

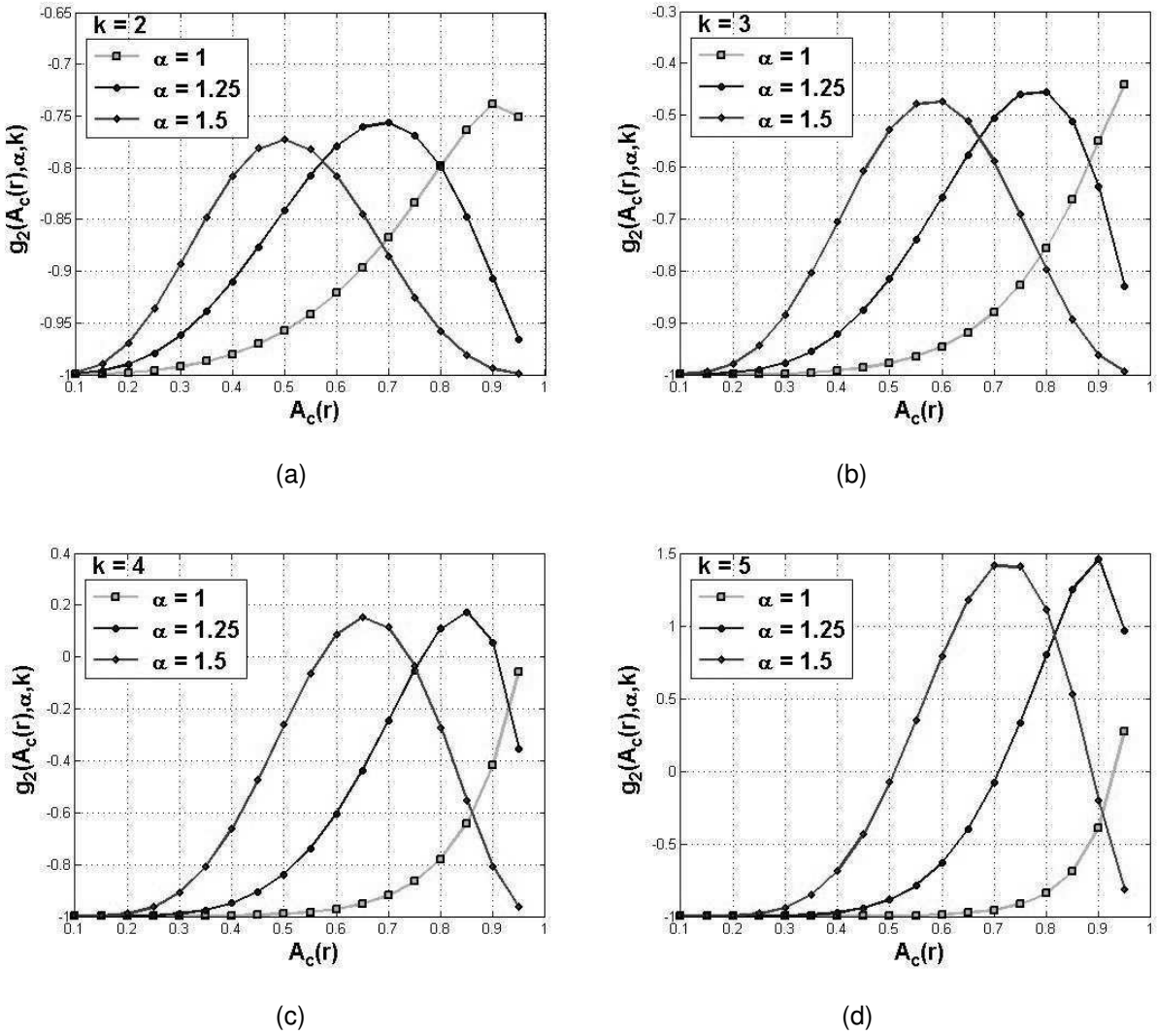

Figure 4.3 Plot of the function $g_2(A_c(r), \alpha, k)$ for different values of k $(2 \le k \le 5)$ and α $(1 \le \alpha < 2)$. No critical percolation occurs at $k = 2$ (a) and $k = 3$ (b). For $k = 4$ (c) and $k = 5$ (d), critical percolation depends on the value of α

We consider the previous analysis in Section 4.1, where we replace $2r$ by αr, with $1 \le \alpha < 2$. Without repeating those details, we obtain a new equation that characterizes the set of *k*-covered components at critical percolation, which is given by $g_2(\lambda_c, r, \alpha, k) = 0$, where

$$g_2(\lambda_c, r, \alpha, k) = (erf(\sqrt{\lambda_c \pi}\, \alpha r) - \sqrt{\lambda_c}\, \alpha^2 r\, e^{-\lambda_c \pi \alpha^2 r^2})^2 \times \frac{(9\lambda_c \pi \alpha^2 r^2/4)^k}{k!} e^{-\lambda_c \pi \alpha^2 r^2} - 1$$

Let $\mu = -\log(1 - A_c(r))$. We substitute $A_c(r)$ in $g_2(\lambda_c, r, \alpha, k)$ to obtain a new function $g_2(A_c(r), \alpha, k)$ given by

$$g_2(A_c(r), \alpha, k) = \left(erf(\alpha\sqrt{\mu}) - \frac{\alpha^2 \sqrt{\mu} e^{-\alpha^2 \mu}}{\sqrt{\pi}} \right)^2 \times \frac{(9\alpha^2 \mu/4)^k}{k!} e^{-\alpha^2 \mu} - 1 \quad (4.16)$$

Figure 4.3 shows the plots of the function $g_2(A_c(r), \alpha, k)$ given in Equation (4.16) for different values of k and α, where $2 \le k \le 5$ and $1 \le \alpha < 2$. As can be seen from Figures 4.3a and 4.3b, the function $g_2(A_c(r), \alpha, k)$ cannot be equal to zero for $k < 4$, regardless of the value of α. Furthermore, a set of sensing disks percolates (which occurs when $g_2(A_c(r), \alpha, k) = 0$) faster for large values of α. For instance, when $\alpha = 1$ (which corresponds to $R = r$), critical percolation occurs at $k = 5$ and $A_c(r) = 0.925$ (Figure 4.3d). Thus, when $\alpha = 1$, it is *almost surely* that an infinite covered component spanning the entire network will appear when the number of collaborating sensors of a sensor is larger than five $(k \ge 6)$. However, when $\alpha = 1.5$ (i.e., $R = 1.5r$), critical percolation occurs at $k = 4$ and $A_c(r) = 0.580$ (Figure 4.3c). Finally, for $\alpha = 1.25$ (i.e., $R = 1.25r$), critical percolation occurs at $k = 4$ and $A_c(r) = 0.760$ (Figure 4.3c). For the last two cases $(\alpha = 1.25$ and $\alpha = 1.5)$, it is *almost surely* that an infinite covered component that spans the entire network will appear when the number of collaborating sensors of a sensor is larger than four $(k \ge 5)$. Given the connection function defined for the collaboration between the sensing disks, percolation should be quicker for large disks than for smaller ones. In all cases, the value of the corresponding *critical covered area fraction* will *almost surely* guarantee the appearance of an infinite connected component that spans the underlying network provided that an infinite covered component arises and spans the entire network. Moreover, the value of *critical covered area fraction* depends on the ratio R/r.

4.3 Discussion

It is worth noting that both values of critical covered area fractions for sensing coverage and network connectivity represent only lower bounds. In other words, if the actual covered area fraction is higher than $A_c(r)$, it is *almost surely* that there exists an infinite (or single large) covered component that spans the entire network. That is, a large portion of the sensor field is guaranteed to be covered. Otherwise, there are only a few small fragmented regions of the field that are covered. However, there is no guarantee on the size of the region of the field being covered. Similarly, if the actual covered area fraction is higher than $A_c(R)$, it is *almost surely* that there exists an infinite connected component that spans the entire network. Otherwise, it is *almost surely* that the network is disconnected. However, there is no guarantee neither on the number of nodes being connected in this infinite component nor whether the sink belongs to the infinite connected component.

There appears to be little disagreement between our theoretical calculation of the critical covered area fraction $(A_c(r) = 0.575)$ compared to the values previously obtained by approximate calculation and Monte Carlo simulation (between 0.62 and 0.688). Our analysis of phase transitions in both sensing coverage (respectively network connectivity) is mainly based on an estimation of the smallest shape enclosing a *k*-covered (respectively *k*-connected) component. We have assumed that this shape is a circle. Although it may not be always true that a circle is the smallest shape enclosing *k*-covered (and *k*-connected) component, we have used it to simplify the analysis enough and make it mathematically tractable. We have also considered this shape as an ellipse with minor axis a_k and major axis b_k. Maximizing $\mathrm{P}(k) = \frac{(\lambda \pi (a_k + r)(b_k + r))^k}{k!} e^{-\lambda \pi a_k b_k}$, the probability that an ellipse encloses a *k*-covered component, leads however to a unique solution $a_k = b_k$ representing a degenerate ellipse or *circle*.

4.4 Summary

In this chapter, we have investigated two phase transition problems for *sensing-coverage* and *network-connectivity* in wireless sensor networks using a probabilistic approach [11]. Our goal is to determine when an infinite covered component (SCPT problem) and an infinite connected component (NCPT problem) could form for the first time. To achieve this objective, we have computed the covered

area fraction for SCPT and NCPT problems at critical percolation. The problem of overlapping disks has been studied extensively in percolation theory and is similar to the SCPT problem. We have found that the value of the covered area fraction is close to the one found by Monte Carlo simulations. The specific connection function of the Boolean model associated with the NCPT problem, however, has not been studied before and hence no bound exists in the literature. We have proposed a *correlated disk model* in order to study SCPT and NCPT problems in an integrated way from a continuum percolation perspective. Precisely, we have considered the physical correlation between them, which is based on the ratio of the radius of the communication disks of the sensors to the radius of their sensing disks. Thus, when an infinite covered component arises for the first time, an infinite connected component will *almost surely* appear based on the ratio $\alpha = R / r$.

CHAPTER 5

MINIMUM-ENERGY CONNECTED *k*-COVERAGE CONFIGURATIONS

Sensing coverage is an essential functionality of wireless sensor networks. However, it is also well-known that coverage alone in wireless sensor networks is not sufficient because data originated from *source sensors* are not guaranteed to reach the *sink* for further analysis. Thus, *network connectivity* should also be considered for a network to function correctly. In wireless sensor networks, *coverage* and *connectivity* have been jointly addressed in an integrated framework. While coverage is a metric that measures the quality of surveillance provided by a network, connectivity provides a means to the *source sensors* to report their sensed data to the *sink*. Some real-world applications, such as intrusion detection, may require high degree of coverage (or redundant coverage), and hence large number of sensors to enable accurate tracking of intruders. For such highly dense deployed and energy-constrained sensors, it is necessary to duty-cycle them to save energy. Thus, the design of coverage configuration protocols for wireless sensor networks should minimize the number of *active sensors* to guarantee the degree of coverage of a field required by an application while maintaining connectivity between all active sensors. Hence, the first challenge is the determination of the number of sensors required to remain active to *k*-cover a sensor field. Given that sensors have limited battery power and wireless sensor networks are generally randomly and hence highly dense deployed, the second challenge is the design of an efficient scheduling protocol that decides which sensors to turn *on* (active) or *off* (inactive) for *k*-coverage of a field.

In this chapter, we study *duty-cycling* to achieve both *k*-coverage and connectivity in highly dense deployed wireless sensor networks [16], where each location in a *convex sensor field* (or simply *field*) is *covered* by at least $k \geq 3$ active sensors while maintaining connectivity between *all* active sensors. Indeed, the limited battery power of the sensors and the difficulty of replacing and/or recharging batteries on the sensors in hostile environments require that the sensors be deployed with high density [148] in order to extend the network lifetime. Also, the sensed data originated from *source sensors* (or simply *sources*)

should be able to reach a central gathering node, called the *sink*, for further analysis and processing. Thus, network connectivity should be guaranteed so sources can be connected to the sink via multiple communication paths. Finally, wireless sensor networks suffer from scarce energy resources. A more practical deployment strategy requires that all the sensors be duty-cycled to save energy. With duty-cycling, sensors can be turned *on* or *off* according to some scheduling protocol, thus reducing the number of active sensors required for *k*-coverage and helping all sensors deplete their energy as slowly and uniformly as possible.

An important problem in the design of such network configurations is computing the *minimum active sensor spatial density* required to guarantee *k*-coverage of a field. For tractability of the problem, first we analyze the intersection of k sensing disks so we can characterize *k*-coverage provided by a wireless sensor network regardless of whether the sensors have identical sensing ranges and whether the sensing range of each sensor follows the *unit disk model*. Based on this analysis, we derive a tight sufficient condition of the spatial density of active sensors to achieve complete *k*-coverage of a field. Although the problem of *k*-coverage has been well-studied in the literature, only a few elegant approaches characterized *k*-coverage of a field [166], [176]. However, none of them guarantees the deployment of a minimum number of sensors to achieve *k*-coverage of a field and hence they would result in shorter operational network lifetime. Previous works [166], [176] only characterized *k*-coverage. According to [166], a field is *k*-covered if all *intersection points* between the boundaries of sensing ranges of the sensors and all those between the boundaries of sensing ranges of the sensors and the boundary of a field are *k*-covered. This is a generalization of the result for 1-coverage [86]. Thus, if two sensing ranges intersect, one more is needed to cover their intersection point. A point in a field that coincides with an intersection point would be 3-covered instead of 1-covered. Hence, more than enough sensors are required to *k*-cover a field. However, our approach for characterizing *k*-coverage of a field is different from the ones proposed in [166], [176]. Precisely, our approach is able to quantify the minimum spatial density of active sensors to fully *k*-cover a field, thus computing the corresponding minimum number of sensors.

The remainder of this chapter is organized as follows. Section 5.1 discusses the connected *k*-coverage problem in wireless sensor networks and shows how to solve it. Sections 5.2, 5.3, and 5.4

present our connected *k*-coverage configuration protocols. Section 5.5 enhances the applicability of these protocols by relaxing some widely used assumptions in coverage protocols. Section 5.6 presents simulation results of our protocols and compares them with another existing protocol for connected *k*-coverage in wireless sensor networks. Section 5.7 concludes the chapter.

5.1 Achieving Connected *k*-Coverage

In this section, we propose our approach for obtaining connected *k*-coverage configurations in wireless sensor networks. First, we model the connected *k*-coverage problem in wireless sensor networks. Then, we derive a necessary and sufficient condition of the active sensor spatial density such that a field is *k*-covered all the time during the operational lifetime of a network while all active sensors are being connected to each other. In Sections 5.2, 5.3, and 5.4, we propose four protocols for generating connected *k*-coverage configuration in wireless sensor networks based on the results of this section.

5.1.1 Connected *k*-Coverage Problem Modeling

Solving the connected *k*-coverage problem in wireless sensor networks requires finding a sensor deployment strategy such that each location in a field is covered by at least k active sensors while *all* active sensors are connected. Our approach solution to the connected *k*-coverage problem in wireless sensor networks consists of decomposing it into two sub-problems, namely *sensor field slicing* and *sensor selection*, and solving them. The *sensor field slicing* problem is to slice a field into small regions of particular shape (to be defined later), each of which is guaranteed to be *k*-covered provided that at least k sensors are randomly deployed in it. The *sensor selection* problem is to select a minimum subset of sensors to remain active and connected such that each location in a field is guaranteed to be *k*-covered. Besides selecting a *minimum* number of active sensors, all selected sensors should have the *maximum* remaining energy. Hence, our *min-max connected k-coverage* problem can be formulated as follows:

Definition 5.1 (min-max Connected *k*-Coverage Problem): Given a field, a set S of sensors, and a positive integer k, select a minimum subset $S_{\min} \subset S$ of sensors such that each point in the field is *k*-covered, all sensors in $S_{\min}$ are connected, and $\sum_{s_i \in S_{\min}} E_{\text{rem}}(s_i)$ is maximized, where $E_{\text{rem}}(s_i)$ is the remaining energy of sensor s_i. □

Because the problem of selecting a minimum subset of sensors to *k*-cover a field is NP-hard [181], we propose efficient centralized, clustered, and distributed approximation algorithms to solve the *min-max* connected *k*-coverage problem.

5.1.2 Sufficient Condition to Ensure *k*-Coverage

We want to compute the *minimum active sensor spatial density* required to *k*-cover a field. To do so, we should compute the maximum size of a convex area *A* of a field so that *A* is *k*-covered with exactly *k* sensors. Intuitively, the distance between any point in *A* and each of the *k* sensors should be at most equal to the radius of their sensing disks. Lemma 5.1 gives an upper bound on the *width* of such a convex area.

Lemma 5.1: Let r be the radius of the sensing disks of the sensors and $k \geq 3.$ A convex area A is guaranteed to be *k*-covered when exactly k homogeneous sensors are deployed in it, if the width of A does not exceed $r.$ □

Now, we present *Helly's Theorem* [39] (page 90), a fundamental result of convexity theory, which characterizes the intersection of convex sets.

Helly's Theorem [39]: Let E be a family of convex sets in IR^n such that for $m \geq n+1$ any m members of E have a non-empty intersection. Then, the intersection of all members of E is non-empty. □

Theorem 5.1, which is an instance of Helly's Theorem [39], will help us compute the minimum sensor spatial density required to *k*-cover a field. More specifically, Helly's Theorem [39] together with a geometric structure, called *Reuleaux triangle* [188], will be used to characterize *k*-covered wireless sensor networks.

Theorem 5.1: Let $k \geq 3.$ The intersection of k sensing disks is not empty if and only if the intersection of any three of those k sensing disks is not empty. □

Following Theorem 5.1, Lemma 5.2 states a *sufficient condition* for complete *k*-coverage of a field.

Lemma 5.2: Let r be the radius of the sensing disks of the sensors and $k \geq 3.$ A field is *k*-covered if any Reuleaux triangle region of width r in a field contains at least k active sensors.

Proof: First, we compute the maximum area that is *k*-covered with exactly k sensors. Let *A* be the

intersection area of the sensing disks of k sensors. From Lemma 5.1, the width of *A* should be upper-bounded by r so that any point in *A* is *k*-covered by these k sensors. Let us first consider the case of three sensors. Using the Venn diagram given in Figure 5.1a, the maximum size of the intersection area of the sensing disks of the sensors s_1, s_2, and s_3, so that the distance between any pair of sensors is at most equal to r, is obtained when s_1, s_2, and s_3 are symmetrically located from each other. This area, called *Reuleaux triangle* [188], is denoted by $RT(r)$ and has a constant width equal to r (see Figure 5.1b). Given that the intersection area of k sensing disks is at most equal to that of three sensing disks such that the maximum distance between any pair of sensors is at most equal to r, the maximum size of *A* is equal to the area of $RT(r)$, which we call *slice* (see Figure 5.2). Thus, any point in *A* is *k*-covered with exactly k active sensors deployed in *A*. Since this applies to any $RT(r)$ region (or *slice*) in a field, it is guaranteed that the field is *k*-covered. □

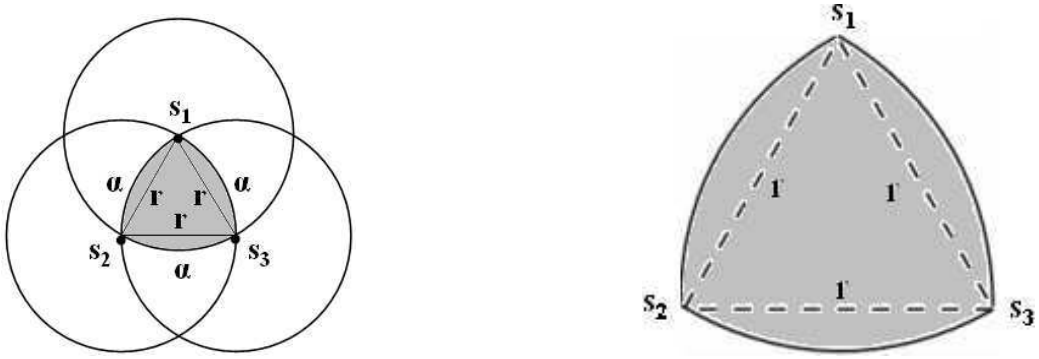

(a) (b)

Figure 5.1 (a) Intersection of three sensing disks and (b) their Reuleaux triangle

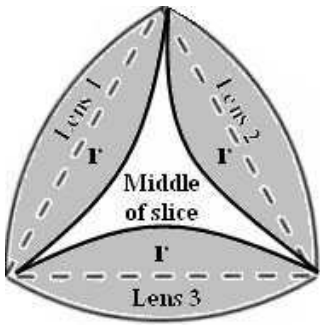

Figure 5.2 Three lenses of a slice.

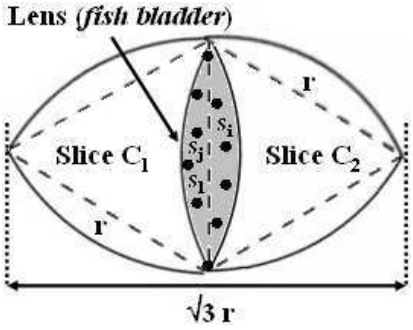

Figure 5.3 Adjacent slices.

As will be discussed in Section 5.2, our sensor selection scheme exploits the overlap between

adjacent slices in a field to select a minimum number of active sensors for full *k*-coverage of the field. Precisely, two adjacent slices intersect in a region shaped as a *lens* (also known as the *fish bladder*) so that the sides of their associated regular triangles fully coincide (Figure 5.3). Note that k sensors located in the lens of two adjacent slices, say C_1 and C_2, *k*-cover the area associated with their union. Indeed, the distance between any of these k sensors located in the lens and any point in the area of the union of both C_1 and C_2 is at most equal to r. Lemma 5.3 states this result.

Lemma 5.3: k active sensors located in the lens of two adjacent slices *surely k*-cover both slices. □

Theorem 5.2, which exploits the results of Lemma 5.3, refines the result of Lemma 5.2 by stating a *tighter sufficient condition* for complete *k*-coverage of a field.

Theorem 5.2: Let $k \geq 3$. A field is guaranteed to be *k*-covered if for any slice in a field, there is at least one adjacent slice such that their lens contains at least k active sensors. □

Theorem 5.3, which exploits the result of Theorem 2, computes the minimum sensor spatial density required for complete *k*-coverage of a field.

Theorem 5.3: Let $k \geq 3$. The *minimum active sensor spatial density* required to guarantee *k*-coverage of a field is given by

$$\lambda(r,k) = \frac{6k}{(4\pi - 3\sqrt{3})\, r^2}$$

where r is the radius of the sensing disks of the sensors.

Proof: It is easy to check that the area $\| Area(r) \|$ of the union of two adjacent slices is computed as

$$\| Area(r) \| = 2A_1 + 4A_2 = (4\pi - 3\sqrt{3})\, r^2 / 6$$

where $A_1 = \sqrt{3}\, r^2/4$ is the area of the central equilateral triangle of side r and $A_2 = (\pi/6 - \sqrt{3}/4)\, r^2$ is the area of each of the three curved regions α (Figure 5.1a). By Theorem 5.2, k sensors should be deployed in the lens of two adjacent slices to *k*-cover both of them. Thus, the *minimum sensor spatial density* that guarantees *k*-coverage of a field is equal to

$$\lambda(r,k) = k / \| Area(r) \| = 6k / (4\pi - 3\sqrt{3})\, r^2$$ □

It is worth noting that Adlakha and Srivastava [2] showed that the number of sensors required to

cover an area of size A is in the order of $O(A/\hat{r}_2{}^2)$, where $\hat{r}_2$ is a good estimate of the radius r of the sensing disks of the sensors. Precisely, r lies between $\hat{r}_1$ and $\hat{r}_2$; $\hat{r}_1$ overestimates the number of sensors required to cover A, while $\hat{r}_2$ underestimates it.

One may suggest that the *maximum area* that is guaranteed to be *k*-covered with exactly k sensors is a circle of radius $r/2$. Fortunately, it is easy to check that our density $\lambda(r,k)$ is smaller than the one corresponding to the configuration where k active sensors are deployed in a circle of radius $r/2$. In other words, $\lambda(r,k) = 6k/(4\pi - 3\sqrt{3})r^2 < 4k/\pi r^2$.

Using the *Reuleaux Triangle* model described earlier, we prove that *k*-coverage with $k \geq 3$ implies connectivity when $R \geq r$. Theorem 5.4 states this result.

Theorem 5.4: *Let* $k \geq 3$. A *k*-covered wireless sensor network is guaranteed to be connected if the radius R of the communication disks of the sensors is at least equal to the radius r of their sensing disks. □

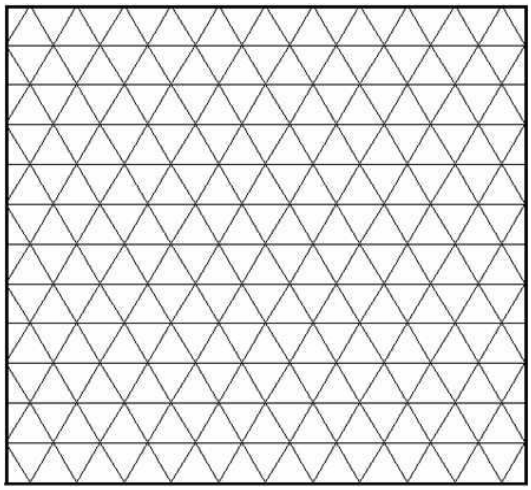

Figure 5.4 Slicing grid of a square field.

5.2 Centralized *k*-Coverage Protocol

In this section, we present our *centralized randomized connected k-coverage* (CERACC$_k$) protocol to fully *k*-cover a field while maintaining connectivity between active sensors.

According to the *min-max* connected *k*-coverage model mentioned in Section 5.1.1, the protocol has two main steps. First, we slice a field into regions whose shape helps characterize the *k*-coverage property

of the field, and thus leads to compute the corresponding minimum number of active sensors. Then, we select an appropriate subset of sensors to guarantee *k*-coverage of each slice, and hence *k*-cover the entire field based on the geometric characteristics of those regions.

Algorithm: CERACC$_k$
  Procedure Process_Slice $(i, k, S_{\min})$
  Begin
    1. $j = 1$
    2. $CovD = 0$
    3. While $j \le 3$ Do
      Begin
        3.1. Randomly select a subset S' of $k/3$
          sensors from j^{th} lens
        3.2. $CovD = CovD + \min\{k/3, |lens(j)|\}$
        3.3. $j = j + 1$
        3.4. $Update\_CovD(slice\_adj(j))$
        3.5. $S_{\min} = S_{\min} \cup S'$
      End
    4. If $CovD < k$ Then
      Begin
    4.1. Randomly select a subset of sensors S'
      of $k - CovD$ from middle area of the cell
    4.2. $CovD = CovD + \min\{k - CovD, |mid\_slice(j)|\}$
    4.3. $S_{\min} = S_{\min} \cup S'$
    4.4. If $CovD < k$ Then
        4.3.1. Return (*k*-coverage cannot be provided)
      End
  End
Begin
  1. Randomly slice a field into regular triangles of side r
  2. Randomly pick a slice (or Reuleaux triangle) i
  3. Call a Breadth-First-Search procedure to *k*-cover slice i
End

Figure 5.5 Sensor selection for *k*-coverage of a field.

5.2.1 Sensor Field Slicing

This section provides a solution to the sensor field slicing problem, where all sensors have the same sensing and communication disks whose radii are r and R, respectively.

Let us consider a square field and $k \ge 3$. Based on the result of Theorem 5.2, it is easy to check whether a given network can *k*-cover the field. For this purpose, we propose a *slicing* scheme of a field by dividing it into overlapping Reuleaux triangles of width r, called *slices* as shown in Figure 5.2, such that two

adjacent slices intersect in a region shaped as a *lens* (also known as the *fish bladder* – see Figure 5.3). This implies that the field is sliced into regular triangles of side r. The result of this slicing operation is called *slicing grid*. Figure 5.4 shows a slicing grid of a field.

5.2.2 Sensor Selection

In this section, we propose a centralized algorithm to select a minimum subset of active sensors that *k*-covers a field. We assume that the sink is responsible for this selection process.

The selection algorithm (Figure 5.5) exploits the overlap between slices to select a minimum number of sensors to be active in a given round. As can be observed, sensors located in the lens of two adjacent slices participate in *k*-covering the area associated with their union (Figure 5.3). Lemma 5.4 states this result.

Lemma 5.4: Sensors located in the lens of two adjacent slices participate in *k*-covering their union area. □

Using Lemma 5.4, we start first by selecting sensors located in the three lenses of a given slice as shown in Figure 5.2 (a slice overlaps with at most three other slices). At every selection, we check whether we have already selected k sensors to *k*-cover the underlying slice. At the same time, we update the degree of coverage of the other adjacent slices. We repeat this process until we visit all slices in a field. We assume that each slice has a unique *id*, such as an integer.

Theorem 5.5 refines the result of Theorem 1 and exploits the claim of Lemma 5.4.

Theorem 5.5: Let $k \geq 3$. A field is guaranteed to be *k*-covered with a minimum number of sensors if all sensors are selected from lenses of adjacent slices. □

The order in which the slices are treated is critical. It can be easily shown at the end of the sensor selection phase that if the slices are processed randomly, there is no guarantee that each slice is *k*-covered with a minimum number of sensors. Thus, the entire field is not guaranteed to be *k*-covered using a minimum total number of sensors. In order to avoid this problem, it is imperative that slices of a slicing grid be processed in a particular order. Assume that we have initially picked slice C_i for processing and let C_{i1}, C_{i2}, and C_{i3} be its adjacent slices. We use a FIFO (First-In-First-Out) data structure, called *NYP* (Not Yet Processed), to keep track of the slices whose degrees of coverage have been updated but not yet processed. Hence, when we process slice C_i, we store the id's i_1, i_2, and i_3 in NYP. When slice C_i has been processed, we consider slice C_{i1} as the next one to be processed. After that, we pick C_{i2} followed by

C_{i3} followed by the slices adjacent to C_{i1} and so on. The sensor selection algorithm for *k*-coverage of a field is given in Figure 5.5.

The sensor selection algorithm described earlier generates only one subset of active sensors to *k*-cover a field. If this algorithm is executed in each round for the same slicing pattern of the field, sensors located in the lenses will be suffering from a severe battery power depletion problem. Hence, those sensors will die very quickly and possibly disconnect the network. Recall that the sensors have several limited resources with energy being the most critical one. Thus, it would be more efficient if in each round a different subset of sensors is selected for *k*-coverage of the field so all the sensors are given the same chance to be active. Our objective is to balance the load of *k*-coverage on all sensors so they deplete their energy uniformly. Next, we describe an approach to achieve this goal.

5.2.3 Slicing Grid Dynamics

Our goal is to select different subsets of sensors $S_i,\ i \geq 1$ such that each subset S_i is selected to remain active in the i^{th} round to *k*-cover a field. Notice that to achieve a better load balancing among sensors, we could add a restriction so that selected subsets of sensors are *mutually disjoint*, i.e., $S_i \cap S_j = \varnothing,\ \forall\, i \neq j.$ However, the disjointness constraint yields a *small number* of mutually disjoint minimum subsets of sensors. Thus, we only require *partially disjoint* subsets of sensors. Given that our selection criterion is based on the remaining energy of sensors, it is guaranteed that sensors with low energy level would be avoided. Furthermore, it is rarely that the same sensors participate in several successive rounds to *k*-cover a field. The question that we want to address now is: *How would minimum subsets of sensors be selected, each of which k-covers a field*?

To address this question, we consider the *dynamics of slicing grid* from one round to another. Recall that the result of slicing a field into slices is called *slicing grid*. The selection of different minimum subsets of active sensors will be determined based on the obtained slicing grids. Since our scheme for selecting active sensors highly prioritizes the ones located in lenses of all slices, it is important that those lenses be able to scan the entire field, and hence include distinct subsets of sensors in different rounds. Thus, it is necessary that the sink be able to generate a slicing grid randomly at each round. Our objective is to obtain as (partially) disjoint minimum subsets of selected sensors as possible. For each obtained slicing grid, the sink applies the

selection algorithm in Figure 5.5. Thus, the slicing grid undergoes some dynamics to achieve balanced load of *k*-coverage among all sensors during the operation of CERACC$_k$. The question that we want to address now is: *How would a slicing grid of a field be randomly generated in each round?*

First, we randomly generate one point p_1 in the field as shown in Figure 5.6. Point p_1 is temporarily considered as the center of the Euclidean plane. To randomly determine a second point p_2, we generate a random angle $0 \le \theta \le 2\pi$ so that the line segment $\overline{p_1 p_2}$ forms an angle θ with the *x*-axis centered at p_1 and the distance between p_1 and p_2 is equal to r. Then, we deterministically find the third point p_3 to form the first regular triangle (p_1, p_2, p_3), called *reference triangle*, as shown in Figure 5.6. As its name indicates, the rest of regular triangles of the slicing grid will be computed based on this reference triangle. Figure 5.6 shows two randomly generated slicing grids.

Theorem 5.6 states that CERACC$_k$ is a minimum-energy connected *k*-coverage configuration protocol that guarantees maximum network lifetime.

Theorem 5.6: CERACC$_k$ fully *k*-covers a field with a minimum number of sensors in each round and maintains connectivity between them. Hence, it consumes minimum energy.

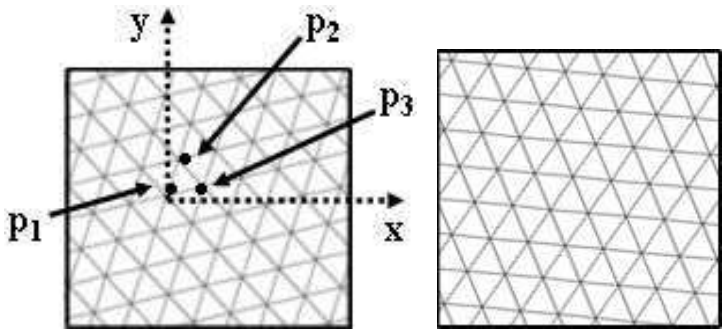

Figure 5.6 Random slicing grids with different orientations.

Proof: The sink guarantees that each slice of a field is covered by exactly k sensors. Therefore, by Theorem 5.2, each slice of the field is *k*-covered, and hence the entire field is fully covered. Moreover, sensors are selected from lenses so all adjacent slices are *k*-covered with a minimum number of active sensors. Thus, by Theorem 5.4, CERACC$_k$ guarantees that a field is *k*-covered using a minimum total number of active sensors in each round, and hence, it consumes a minimum amount of energy in each round. By Theorem 5.4, a *k*-covered wireless sensor network is connected, assuming that $R \ge r$. Given

that CERACC$_k$ prioritizes sensors with the highest remaining energy to remain active in each round, and given that it is based on the dynamics of slicing grid, necessarily all sensors deplete their energy slowly and uniformly, thus leading to a maximum network lifetime.

In general, the sink is connected to an infinite source of energy, such as a wall outlet, and thus can be viewed as a *line-powered* node [169] that has no energy constraint. Hence, if node failure is due only to low battery power, the problem of single-point failure does not arise at all in this type of centralized wireless sensor network architecture. Also, under the centralized control of the sink, no coordination between sensors is required to select a minimum number of active sensors to *k*-cover a field. Given that sensors have limited energy, this approach would save them energy. Indeed, a schedule that determines which sensors should remain active in each round to *k*-cover a field is computed by the sink and forwarded to the selected ones. Thus, such a centralized approach is intended to gain insight into a lower bound on the number of sensors required for complete *k*-coverage of a field, and hence an upper bound on the network lifetime. In Section 5.5, we will show how to relax the centralized approach to implement CERACC$_k$ in a fully distributed manner.

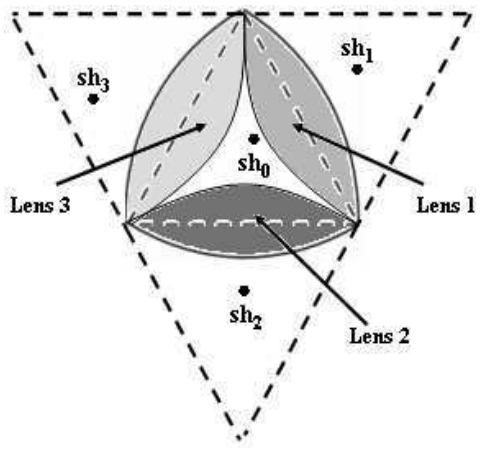

Figure 5.7 Adjacent cluster-heads.

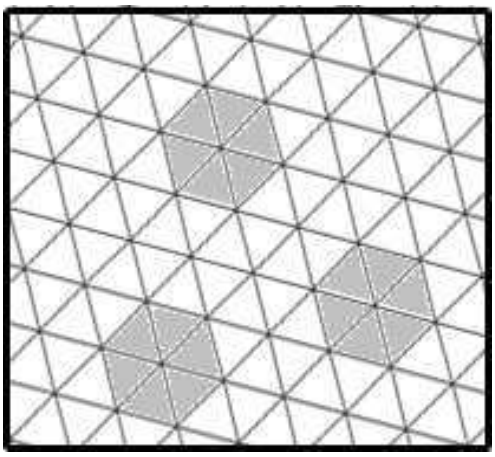

Figure 5.8 Clustering for D-CRACC$_k$.

5.3 Clustered *k*-Coverage Protocol

In this section, we propose a family of clustered *k*-coverage protocols, called *clustered randomized connected k-coverage* (CRACC$_k$), in which part of the duties of the sink in the centralized protocol

CERACC$_k$ is delegated to a subset of sensors, called *cluster-heads*. These protocols differ by their degree of granularity of network clustering, and hence produce clusters of different shapes and sizes.

5.3.1 Cluster-Head Selection and Attributed Roles

As in the centralized protocol CERACC$_k$, the family of protocols CRACC$_k$ allows the sink to randomly generate in each round a slicing grid, which consists of adjacent overlapping Reuleaux triangles. In contrast with CERACC$_k$, the sink randomly designates for each cluster a particular sensor, called *cluster-head*, which is responsible for *k*-coverage of its assigned cluster during a given round. Precisely, each cluster-head is located within the cluster it is in charge of selecting some of its sensing neighbors to *k*-cover it. The sink advertises a packet, called *ClusterHeadList*, including all sensors' ids that have been selected as cluster-heads. When a sensor receives *ClusterHeadList*, it checks whether its id is included. If so, it removes its id from the list and forwards the updated *ClusterHeadList* packet. Otherwise, it just forwards the original packet it has received. The CRACC$_k$ family of protocols requires that each cluster-head coordinates its activity with its adjacent cluster-heads to *k*-cover its cluster, and hence select a total minimum number of sensors to *k*-cover a field. To achieve this goal, sensors that would remain active in each round to *k*-cover a cluster should be selected from lenses (i.e., intersection areas of adjacent Reuleaux triangles). For a better balance, a cluster-head attempts to select $k/3$ sensors from each lens so any Reuleaux triangle in a cluster contains exactly k sensors as per Theorem 5.2. The size of a cluster and the number of its adjacent ones depend on the type of clustering being used. As can be seen, the protocols of the CRACC$_k$ family are pseudo-distributed in the sense that the selection of active sensors for complete *k*-coverage of a field is not under the control of the sink. Next, we describe two protocols of the CRACC$_k$ family, namely T-CRACC$_k$ and D-CRACC$_k$, for connected *k*-coverage in wireless sensor networks based on their degree of clustering.

5.3.2 The T-CRACC$_k$ Protocol

In T-CRACC$_k$ ("T" for Reuleaux *triangle*), a cluster is a *slice* in the obtained slicing grid and a cluster-head is called *slice-head*. In each round, the sink is responsible for randomly generating a slicing grid of a field. Given that each slice has at most three adjacent slices (Figure 5.2), the T-CRACC$_k$ protocol requires that each slice-head coordinates its activity with its adjacent slice-heads to select a minimum total number

of sensors to *k*-cover a field. Figure 5.7 shows slice-head sh_0 sharing three lenses with slice-heads sh_1, sh_2, and sh_3. For instance, sh_0 could *k*-cover its slice by selecting sensors located in its three lenses. Then, it communicates the numbers n_1, n_2, and n_3 of sensors selected from lenses $Lens\,1$, $Lens\,2$, and $Lens\,3$, respectively, to its adjacent slice-heads sh_1, sh_2, and sh_3, respectively. Slice-head sh_1 would need to select $k - n_1$ more sensors from its lenses to *k*-cover its slice. It would definitely coordinate with its adjacent slice-heads to *k*-cover its slice and so does each slice-head.

Theorem 5.7 states that T-CRACC$_k$ yields minimum-energy connected *k*-coverage.

Theorem 5.7: The T-CRACC$_k$ protocol fully *k*-covers a field. It also is a minimum-energy connected *k*-coverage protocol.

Proof: Each slice-head ensures that each slice of a field is *k*-covered by exactly k sensors by coordinating with each of its three adjacent slice-heads. Also, the sink assigns a slice-head to each slice in a field. Thus, by Theorem 5.2, the entire field is fully *k*-covered. Moreover, active sensors are selected only from lenses. Therefore, by Theorem 5.5, T-CRACC$_k$ guarantees that a field is *k*-covered with a minimum number of active sensors, and hence consumes a minimum amount of energy in each round. By Theorem 5.4, a *k*-covered wireless sensor network is connected, assuming that $R \geq r$. Given that T-CRACC$_k$ favors sensors with highest remaining energy in each round and benefits from slicing grid dynamics, all sensors are equally likely to be selected for *k*-coverage of a field in each round. Thus, all sensors deplete their energy slowly and uniformly, thus leading to a maximum network lifetime. □

5.3.3 The D-CRACC$_k$ Protocol

The D-CRACC$_k$ ("D" for Disk) protocol has a higher network clustering granularity than T-CRACC$_k$. Precisely, each cluster consists of six adjacent slices forming a disk (Figure 5.8). Notice that for ease of representation, Figure 5.8 represents each cluster by only six regular triangles instead of six Reuleaux triangles. In each round, the sink selects for each cluster a sensor, called *disk-head*, which is located nearer the center of its corresponding disk to *k*-cover it. Similarly, each disk-head needs to coordinate with at most six adjacent disk-heads to *k*-cover its disk with a minimum number of sensors so a field is guaranteed to be *k*-covered efficiently. First, we define the notions of *interior* and *boundary lenses*.

Definition 5.2 (Interior and boundary lenses): An *interior lens* of a disk is a lens that is shared with no other adjacent disk and a *boundary lens* is shared by two adjacent disks. □

In order to *k*-cover its disk, each disk-head manages at most six *interior lenses* and six *boundary lenses*. Hence, a disk-head should select sensors from its interior lenses by itself with no coordination with any other disk-head but needs to coordinate with its adjacent disk-heads for selecting sensors from its boundary lenses. Thus, each disk-head applies the result of Theorem 5.2 so that each slice is *k*-covered by exactly k sensors.

Theorem 5.8 states that D-CRACC$_k$ yields minimum-energy connected *k*-coverage.

Theorem 5.8: The D-CRACC$_k$ protocol fully *k*-covers a field. It also is a minimum-energy connected *k*-coverage protocol.

Proof: In each round, each disk-head uses exactly k sensors to *k*-cover each of its six slices by coordinating with its six adjacent disk-heads. Also, the sink guarantees that each disk is under the responsibility of a disk-head. Thus, by Theorem 5.2, the whole field is *k*-covered. Moreover, each disk-head *k*-covers its disk with sensors selected only from interior and boundary lenses. Therefore, by Theorem 43.5, D-CRACC$_k$ uses a minimum total number of active sensors in each round such that a field is guaranteed to be *k*-covered. Thus, D-CRACC$_k$ consumes a minimum amount of energy in each round. By Theorem 5.4, a *k*-covered wireless sensor network is connected, assuming that $R \geq r.$ Moreover, D-CRACC$_k$ selects sensors with maximum remaining energy, thus helping all sensors deplete their energy slowly and uniformly. Hence, D-CRACC$_k$ guarantees maximum network lifetime. □

Notice that T-CRACC$_k$ requires more coordination between cluster-heads than D-CRACC$_k$ and hence has more overhead to *k*-cover a field. This is due to the difference of their cluster sizes. Thus, D-CRACC$_k$ is more energy-efficient than T-CRACC$_k$.

5.4 Distributed *k*-Coverage Protocol

In this section, we propose a fully distributed *k*-coverage protocol, called *distributed randomized connected k-coverage* (DIRACC$_k$). The centralized protocol CERACC$_k$ presented in Section 5.2 does not rely heavily on global information. Thus, it can be redesigned in a fully distributed fashion based on the local information sensors have about their one-hop neighbors with regard to their physical locations and

remaining energy. Also, DIRACC$_k$ design requires coordination among sensors to achieve *k*-coverage of a field. Next, we describe DIRACC$_k$.

5.4.1 *k*-Coverage Checking Algorithm

A sensor runs a *k-coverage checking* algorithm to find out whether its sensing disk is *k*-covered. To do so, each sensor slices it sensing disk into six overlapping slices as shown in Figure 5.9 such that two adjacent slices intersect in a lens. Thus, the *slicing grid* in DIRACC$_k$ consists of exactly six complete slices. Similarly, the *k*-coverage checking algorithm exploits the overlap between adjacent slices as in the case of centralized protocol CERACC$_k$.

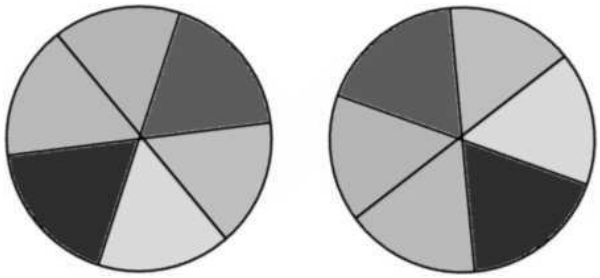

Figure 5.9 Slicing grids of the sensing disk of a sensor.

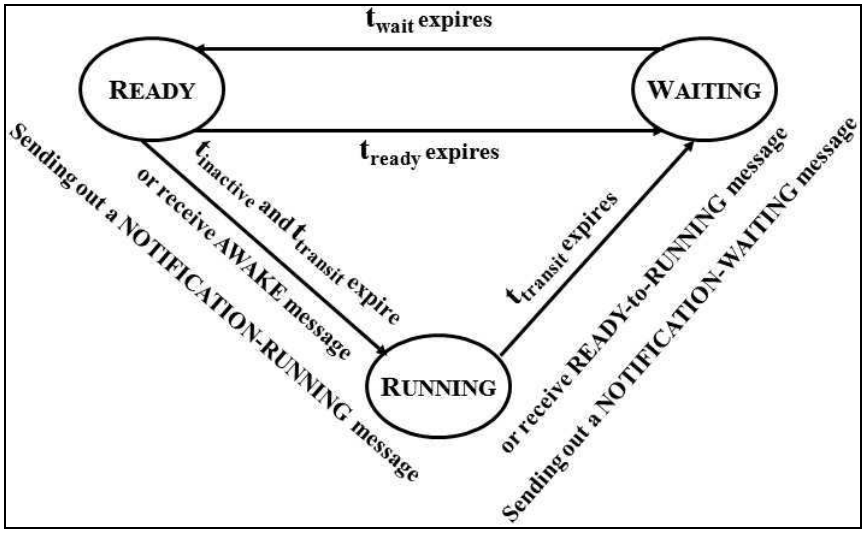

Figure 5.10 State diagram of DIRACC$_k$.

Using Lemma 5.4, each sensor checks whether each of the six slices forming its sensing disk is *k*-covered. For each slice, a sensor checks whether the number of active sensors in the three lenses (Figure 5.2) including itself is equal to k. Otherwise, it checks whether the number of active sensors located the

entire slice, i.e., three lenses and middle of the slice (Figure 5.2), is equal to k. For each slice, a sensor computes its degree of coverage and save the result in an array variable $CovDegSlices$. Based on the content of $CovDegSlices$, a sensor activates a necessary number of its sensing neighbors to *k*-cover its sensing disk.

If a sensor is unable to *k*-cover its sensing area when it runs the *k-coverage checking algorithm*, this means that the minimum sensor density required for *k*-coverage is not satisfied, and hence the field cannot be fully k-covered.

5.4.2 State Transition Diagram of DIRACC$_k$

At any time, a sensor can be in one of the three states: READY, WAITING, or RUNNING. A *state transition diagram* associated with DIRACC$_k$ and indicating the three possible states of a sensor and transitions between them is shown in Figure 5.10.

- In the READY state, a sensor is only listening to AWAKE messages and thus is ready to switch to the RUNNING state.
- In the WAITING state, a sensor is neither communicating with other sensors nor sensing a field, and thus its radio is turned off. However, after some fixed time interval, it switches to the READY state to receive AWAKE messages if its neighbors decide to do so for achieving *k*-coverage of their sensing areas.
- In the RUNNING state, a sensor can communicate with other sensors and sense the environment.
- At the start of the monitoring task, *all* sensors are in the READY state *except one* that is in the RUNNING state. The single sensor in the RUNNING state is one of the communication neighbors of the sink that is chosen randomly by the sink to activate some of its sensing neighbors to achieve *k*-coverage of its sensing area. Those selected sensors will in turn use the same approach to *k*-cover their sensing areas. This chain of sensor activations continues until the entire field is *k*-covered. As mentioned earlier, when a given sensor is selected by any other sensor to become active, it sends out a NOTIFICATION-RUNNING message to inform all its neighbors. While in the READY state, a sensor keeps track of its sensing neighbors that are in the RUNNING state. If it finds out that its sensing area is *k*-covered, it will switch to the WAITING state. It is not cost-effective to

guarantee that a sensor is not selected more than once during one round. Indeed, guaranteeing disjoint subsets of selected sensors requires much coordination between the sensors, thus introducing unnecessary overhead. Hence, to use its remaining energy efficiently, a sensor may wish to switch from the RUNNING state to the WAITING state. For this purpose, a sensor broadcasts a RUNNING-to-WAITING message and waits for some transit time $t_{transit}$. If $t_{transit}$ expires and it has not received any RUNNING-to-WAITING message, it switches to the WAITING state and sends a NOTIFICATION-WAITING message, where it can stay there for t_{wait} time. When t_{wait} expires, it switches to the READY state, where it can stay for t_{ready} time. When a sensor (in the READY state) receives a RUNNING-to-WAITING message from its sensing neighbor, it either switches to the RUNNING state or sends an AWAKE message to one of its sensing neighbors. If a sensor finds out that it has not been awaken by its neighbors to be active within some $t_{inactive}$ time, it will broadcast a READY-to-RUNNING message and wait for some $t_{transit}$ time before switching to the RUNNING state. If $t_{transit}$ expires without receiving any other READY-to-RUNNING message from its sensing neighbors, it will send out a NOTIFICATION-RUNNING message and switch to the RUNNING state. Otherwise, it stays in the READY state.

Theorem 5.9 states that DIRACC$_k$ is a minimum-energy distributed connected *k*-coverage protocol.

Theorem 5.9: The DIRACC$_k$ protocol fully *k*-covers a field. It also is as minimum-energy protocol as D-CRACC$_k$.

Proof: We proceed by contradiction. Assume that the total area A of a field is not fully *k*-covered by active sensors. Hence, A can be decomposed into a *k*-covered area A_c and a non-*k*-covered area A_{nc}, i.e., $A = A_c \cup A_{nc}$. Thus, there is at least one sensor s_i whose sensing disk intersects the area A_{nc}, i.e., $SD(\xi_i, r_i) \cap A_{nc} \neq \emptyset$. In particular, the sensing disk of s_i is not fully *k*-covered. Hence, sensor s_i is not active. Precisely, s_i is in the WAITING state. According to DIRACC$_k$, however, sensor s_i must be in the RUNNING state (i.e., active) given that its sensing disk is not fully *k*-covered. This contradicts our assumption. Thus, the total area A of a field is fully *k*-covered by active sensors. Let us now show that DIRACC$_k$ uses as minimum number of active sensors as D-CRACC$_k$ to *k*-cover a field. Using DIRACC$_k$, each sensor checks

whether its sensing area is *k*-covered. In order to *k*-cover each of its six slices, each sensor makes sure that there are exactly k active within its sensing disk. Each sensor favors active sensors that are located in the interior and boundary lenses of its sensing disk. Given that there is no pre-slicing of the entire field into adjacent slices as is the case with the three other protocols, there is no guarantee that all active sensors belongs to the lenses of each sensor. Therefore, it may happen that active sensors located in some lenses of the sensing disk of a sensor are located in the lenses and/or the middle of slices of other sensors. Definitely, these sensors will consider those active sensors located in the middle of their slices so they *k*-cover their sensing disks with as minimum number of active sensors as possible. By Theorem 5.2, it follows that DIRACC$_k$ could use a little more sensors than D-CRACC$_k$ to achieve complete *k*-coverage of a field. Hence, Thus, DIRACC$_k$ consumes as minimum amount of energy as D-CRACC$_k$ during the operational network lifetime. Similarly, DIRACC$_k$ selects sensors with highest remaining energy to remain active, thus helping all sensors deplete their energy as slowly and uniformly as possible, thus extending the network lifetime. By Theorem 5.4, a *k*-covered wireless sensor network is connected if $R \geq r$. □

5.5 Relaxation of Assumptions

The design of our connected *k*-coverage protocols are based on the *unit disk model* and *homogeneous sensor model*. Although these assumptions are the basis for most of coverage and connectivity protocols in wireless sensor networks, they may not be valid in real-world wireless sensor network platforms. In this section, we relax these assumptions to promote the use of our protocols in real-world applications.

5.5.1 Relaxing the Unit Disk Model

It was found that the communication range of MICA motes is asymmetric and depends on the environments [179] and that the communication range of radios is highly probabilistic and irregular [182]. For problem tractability, we consider a *convex model*, where the communication and sensing ranges of sensors are homogeneous and *convex* but not necessarily circular.

Lemmas 5.5 and 5.6 correspond to Lemma 5.1 and Theorem 5.2, respectively. Their proof is literally the same as that in Section 5.1.2 by using the notion of largest enclosed disk.

Let r_{led} be the radius of the largest enclosed disk of the sensing range of sensors.

Lemma 5.5: Let $k \geq 3$. A convex area A is guaranteed to be *k*-covered when exactly k homogeneous sensors whose sensing ranges are convex are deployed in it, if the width of A does not exceed r_{led}. □

Lemma 5.6: Let $k \geq 3$. A field is guaranteed to be *k*-covered if for any slice of width r_{led} in a field, there is at least one adjacent slice of width r_{led} such that their lens contains at least k active sensors. □

Now, we discuss how CERACC$_k$, T-CRACC$_k$, D-CRACC$_k$, and DIRACC$_k$ can be implemented using the convex sensing model. The unit of slicing, i.e., Reuleaux triangle, has a width equal to r_{led}. Any other processing remains the same for each of those four protocols. Hence, the assumption of the unit disk model can be easily relaxed with the help of the notion of the largest enclosed disk of the sensing range of the sensors.

5.5.2 Relaxing the Sensor Homogeneity Model

Real-world sensing applications [90] may require heterogeneous sensors in terms of their sensing and communication capabilities to enhance the reliability of the network and extend its lifetime [169]. Even sensors equipped with identical hardware may not always have the same sensing model. In this section, we consider heterogeneous sensors with different yet convex sensing and communication ranges.

Lemmas 5.7 and 5.8 correspond to Lemma 5.1 and Theorem 5.2, respectively.

Lemma 5.7: Let $k \geq 3$. A convex area A is guaranteed to be *k*-covered when exactly k heterogeneous sensors whose sensing ranges are convex but not necessarily circular are deployed in it, if the width of A does not exceed $r_{led}^{\min}$, the smallest radius of the largest enclosed disks of the sensors' sensing ranges. □

Lemma 5.8: Let $k \geq 3$. A field is guaranteed to be *k*-covered if for any slice of width $r_{led}^{\min}$ in a field, there is at least one adjacent slice of width $r_{led}^{\min}$ such that their lens contains at least k active sensors. □

In the case of CERACC$_k$, T-CRACC$_k$, and D-CRACC$_k$, the sink has to slice a field into slices of width $r_{led}^{\min}$ and apply the same processing as in Section 5.1.2. For DIRACC$_k$, each sensor needs to consider its largest enclosed disk and run the same steps as in Section 5.1.2. Thus, the assumption of homogeneous sensors can also be relaxed with slight updates to our protocols.

5.6 Performance Evaluation

In this section, we present the simulation results of our protocols using a high-level simulator written in the C programming language. First, we specify the simulation environment as well as the energy consumption model that we use. Then, we present the simulation results with respect to several parameters.

5.6.1 Simulation Settings

We consider a square field of side length $1000\,\mathrm{m}$. We use the energy model given in [171], where the sensor energy consumption in transmission, reception, idle, and sleep modes are 60 mW, 12 mW, 12 mW, and 0.03 mW, respectively. Following [176], the energy required for a sensor to stay idle for 1 second is equivalent to *one unit of energy*. We assume that the initial energy of each sensor is 60 Joules enabling a sensor to operate about 5000 seconds in reception/idle modes [171]. All simulations are repeated 20 times and the results are averaged.

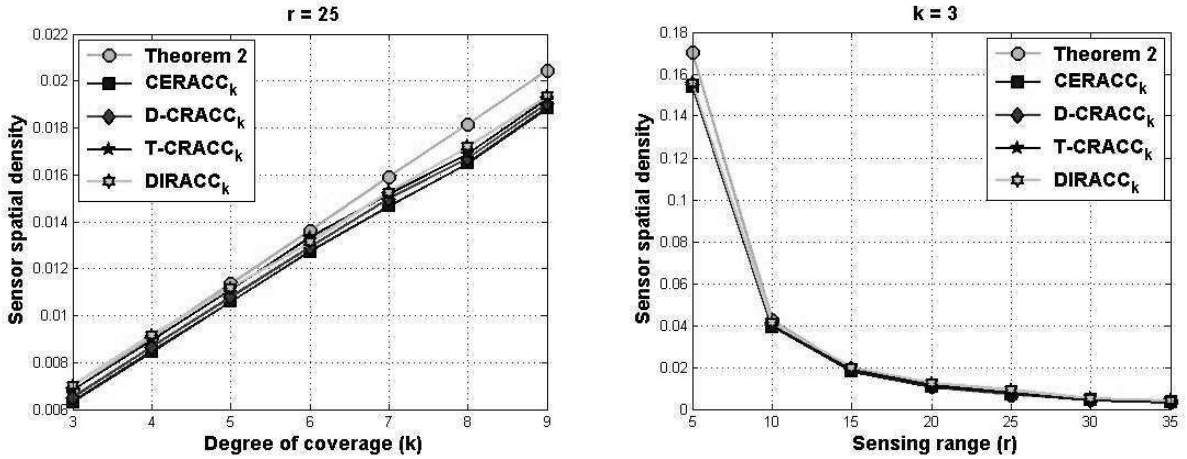

(a) (b)

Figure 5.11 $\lambda(r,k)$ vs. (a) k and (b) r.

5.6.2 Simulation Results

In this section, we present the simulation results of our protocols. Figure 5.11a shows the sensor density versus the coverage degree k, where the radius r of the sensing range of sensors is fixed to $r = 25\,\mathrm{m}$. The sensor density increases with k for a fixed r, as expected. As can be seen, the four protocols yield a sensor density less than the one given in Theorem 5.3. Also, CERACC$_k$ outperforms all

other protocols while DIRACC$_k$ uses more sensors than these protocols due to its distributed nature. Figure 5.11b plots the sensor density versus r with $k = 3$. We observe that the sensor density decreases with r for a fixed k, Likewise, the four protocols require a smaller sensor density than the one computed in Theorem 5.3.

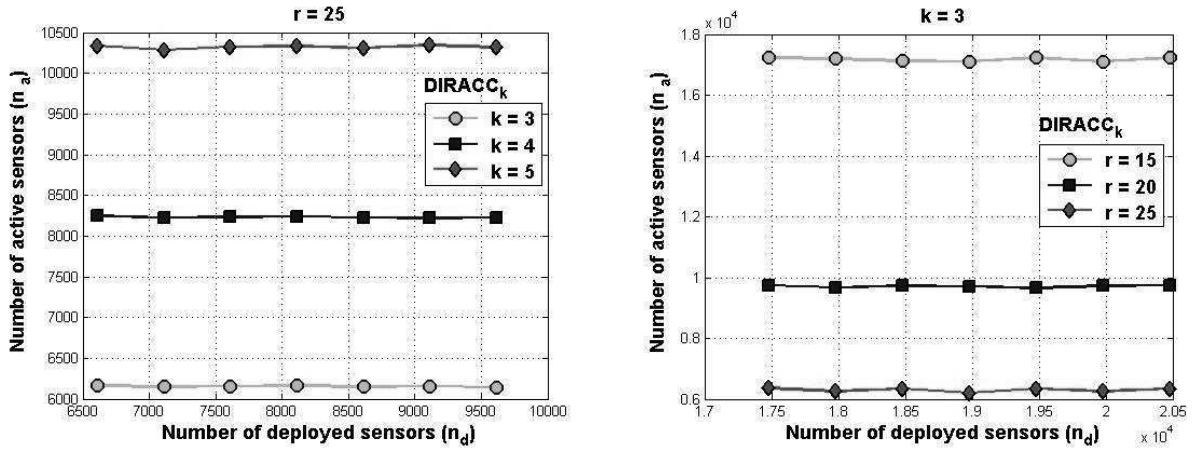

(a) (b)

Figure 5.12 Number of active sensors vs. number of deployed sensors while varying (a) k and (b) r.

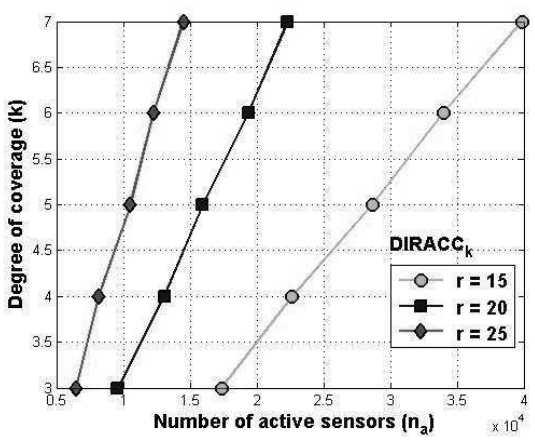

Figure 5.13 k vs. number n_a of active sensors.

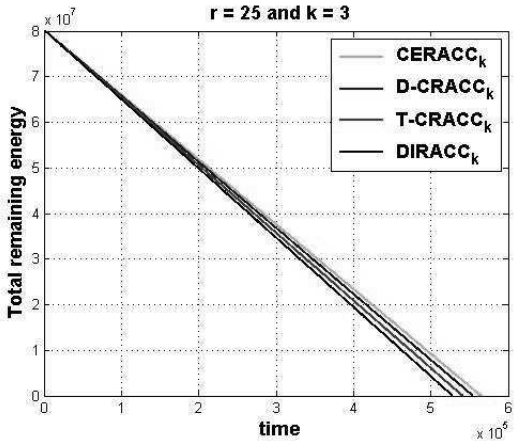

Figure 5.14 Remaining energy vs. time.

Figure 5.12 shows the number of active sensors versus the total number of deployed sensors for DIRACC$_k$. In Figure 5.12a, we consider different values of k, while in Figure 5.12b, we consider different values of r. For higher values of k, more sensors need to be active to achieve the required coverage.

However, for higher values of r, less number of sensors is needed to *k*-cover a field. In both experiments, the number of active sensors does not depend on the number of deployed sensors but only on k and r.

Figure 5.13 shows the degree k of coverage versus the total number n_a of active sensors for DIRACC$_k$. Notice that k increases with n_a. Also, for the same n_a, k increases quickly as r increases as a larger region of the field would be covered.

Figure 5.14 shows that the total remaining energy of the sensors in the four protocols decreases smoothly (in this experiment, the number of deployed sensors is 16,000). Notice that the centralized protocol CERACC$_k$ consumes less energy than all other protocols while the distributed protocol for DIRACC$_k$ consumes the highest amount of energy. Thus, CERACC$_k$ yields longer network lifetime than DIRACC$_k$. This shows the advantage of our centralized protocol (CERACC$_k$) over the distributed one (DIRACC$_k$). Indeed, the number of messages needed by CERACC$_k$ to distribute the optimal schedule to the selected sensors may be less than that required by DIRACC$_k$ due to the periodic messages exchanged by sensors to coordinate their mission for *k*-coverage of a field.

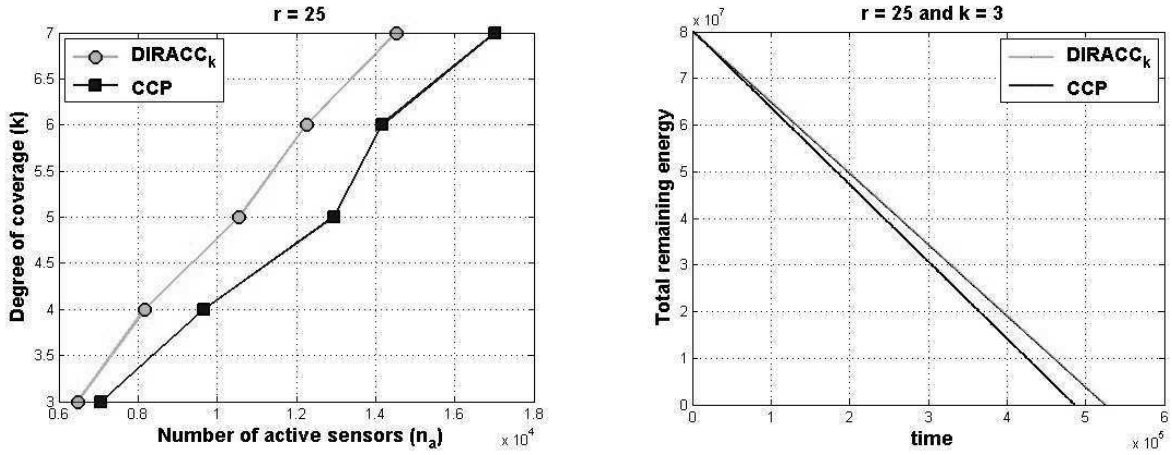

(a) (b)

Figure 5.15 DIRACC$_k$ compared to CCP (a) k vs. n_a and (b) remaining energy vs. time.

5.6.3 Comparison of DIRACC$_k$ with CCP

In this section, we compare DIRACC$_k$ with CCP [166]. The CCP protocol provides different degrees of full coverage of a convex region. CCP was the first protocol that discussed *k*-coverage and connectivity within a unified framework. It was proved that coverage implies connectivity when $R \geq 2r$ [166]. Hence, no

other mechanism would be necessary to guarantee connectivity. However, CCP was integrated with a topology maintenance protocol, called SPAN [52], to provide both coverage and connectivity guarantees when $R < 2r$. Recall that a convex region A is *k*-covered in CCP if all intersection points between sensing disks of sensors and between sensing disks of sensors and $A's$ boundary are at least *k*-covered.

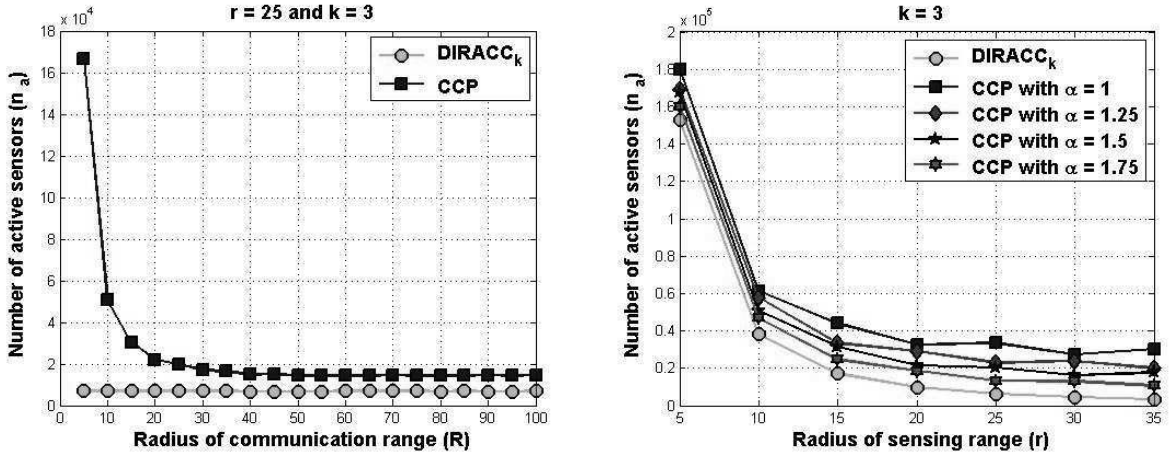

(a) (b)

Figure 5.16 DIRACC$_k$ compared to CCP (a) n_a vs. R and (b) n_a vs. r.

Figure 5.15a plots the degree k of coverage versus the number n_a of active sensors for DIRACC$_k$ as compared to CCP. It shows that DIRACC$_k$ requires less active sensors than CCP to achieve the same degree of coverage, thus yielding significant energy savings. This is due not only to a higher number of active sensors required by CCP, and hence an additional energy spent in sensing, but also to the communication overhead caused by the exchange of messages between active sensors running CCP to coordinate among themselves and provide the requested *k*-coverage service. Thus, CCP consumes more energy than DIRACC$_k$ as shown in Figure 5.15b. Note that while CCP requires SPAN to provide connectivity between active sensors when $R < 2r,$ DIRACC$_k$ does not need such a topology maintenance protocol as all it requires is $R \geq r,$ thus providing connectivity when *k*-coverage is guaranteed. Indeed, DIRACC$_k$ is based on the analysis of sensors' sensing range to provide *k*-coverage.

Figure 5.16a plots n_a versus R with $r = 30\,\mathrm{m},$ while Figure 5.16b plots n_a versus r for different ratios $\alpha = R / r,$ where $\alpha \geq 1.$ In both cases, we fix $k = 3.$ Given that $\alpha \geq 1,$ any increase in the communication range of sensors would not have any impact on the performance of DIRACC$_k$. It would,

however, affect the performance of CCP. As can be observed, n_a decreases as R increases. Indeed, SPAN would require less number of sensors to maintain connectivity between active sensors as R increases. However, at some point, (surprisingly enough, this point corresponds to $R \geq 2r$), the number n_a of active sensors required for *k*-coverage does not decrease any further. Indeed, when $R \geq 2r$, SPAN is not needed at all as both *k*-coverage and $R \geq 2r$ would guarantee connectivity. Similarly, the performance of CCP improves as the ratio α increases (Figure 5.16b), i.e., R increases. That is, less number of active sensors is needed to provide *k*-coverage and connectivity.

5.7 Summary

In this chapter, we have studied the problem of connected *k*-coverage in wireless sensor networks, where each location in a field is *covered* by at least k active sensors while *all* active sensors are being *connected* [16], [20]. First, we have characterized *k*-coverage of a field based on a geometric analysis of the intersection of sensing disks of k sensors. We have proved that *k*-coverage implies connectivity between active sensors when the communication range of the sensors is at least equal to their sensing range. By looking at real sensor node platforms, it is always the case that the communication range of the sensors is higher than their sensing range, and hence our argument is always valid. Indeed, Tables I and II given in [176] show the communication range of Berkeley motes is much higher than the sensing range of several typical sensors, that and hence support our argument. We have also proved that a sufficient condition of *k*-coverage of a field is that the minimum sensor spatial density depends only on k and the sensing range of the sensors. Moreover, we have proposed centralized (CERACC$_k$), pseudo-distributed (T-CRACC$_k$ and D-CRACC$_k$), and fully distributed (DIRACC$_k$) protocols to solve the connected *k*-coverage problem in wireless sensor networks. We have also extended our analysis by relaxing several widely used assumptions in *k*-coverage configuration in wireless sensor networks. We have also extended our analysis by relaxing the assumptions of the unit sensing disk model and homogeneous sensor. These relaxations have helped us handle the convex sensing model and heterogeneous wireless sensor networks, and hence promote the use of our protocols in real-world applications. Our simulation results show that DIRACC$_k$ is more energy-efficient than CCP [166], with respect to the number of active sensors required for *k*-coverage and network operational lifetime.

CHAPTER 6

GEOGRAPHIC FORWARDING ON DUTY-CYCLED SENSORS

The design of protocols for wireless sensor networks is challenging due to the scarce battery power of the sensors. It is well known that sensor *duty-cycling* is an important mechanism that helps densely deployed wireless sensor networks save energy so the sensors remain operational for as long as possible. Geographic forwarding, on the other hand, is an energy-efficient and practical scheme for wireless sensor networks in that the sensors are not required to maintain global and detailed information on the topology of the entire network. The sensors need only maintain local knowledge on their one-hop neighbors with respect to their geographic location information. Although there is a dependency between sensor duty-cycling and data forwarding in the sense that data should be forwarded to a central gathering point, known as the *sink*, via active sensors, only a few works jointly consider them. Indeed, most of geographic forwarding protocols assume that *all* sensors are *always on* during forwarding. However, such an assumption is not realistic in densely deployed wireless sensor networks [148], where sensors are *duty-cycled*, i.e., switched *on* or *off* to save energy. While most efforts focused on only single aspect of the problem (coverage, duty-cycling, routing), this chapter offers clarity into the issues that must be addressed for joint protocol development, where *k*-coverage, duty-cycling, and geographic forwarding are discussed in a unified framework.

In this chapter, we study the problem of joint *k*-coverage, duty-cycling, and forwarding in wireless sensor networks. Specifically, we focus on geographic forwarding in a duty-cycled, *k*-covered wireless sensor network, where each point in a field is *covered* by at least $k \geq 3$ active sensors while *all* active sensors are *connected*. Geographic forwarding in *k*-covered wireless sensor networks, however, faces three major challenges. The first challenge is *how to determine the number of active sensors required to fully k-cover a field*. As of writing this chapter, there is no exact bound on the sensor spatial density for *k*-coverage of a field. Besides *k*-coverage characterization, our approach *quantifies* the required minimum sensor spatial density. The second challenge is *how to design a minimum-energy duty-cycling protocol for*

a k-covered wireless sensor network that deploys as minimum number of active sensors as possible so all sensors deplete their energy slowly and uniformly. Our goal is to prolong the lifetime of the sensors in order to extend the network lifetime. Although several *k*-coverage protocols for wireless sensor networks have been proposed, none of them provided a guarantee of using a minimum number of active sensors. The third challenge is *how to design energy-efficient geographic forwarding protocols running on top of a duty-cycled k-covered wireless sensor network with a specific requirement in terms of data aggregation*. A few works on joint duty-cycling and forwarding exist in the literature [38], [133], [184]. The work in [133] jointly considers duty-cycling and opportunistic routing at the network layer. Our joint protocols are complementary to [133] and are more general in that they jointly consider geographic forwarding on a duty-cycled *k*-covered wireless sensor network along with different data aggregation levels [21], [22].

Although several elegant protocols have been proposed to solve the problem of *k*-coverage in wireless sensor networks as discussed earlier, the problem of routing on duty-cycled wireless sensor networks has received little attention in the literature. In particular, joint coverage and geographic forwarding in wireless sensor networks has been overlooked intentionally. This is due to the fact that *all* sensors are assumed to be always *on* during data forwarding. However, this assumption is not valid in real-world applications, where all sensors should not stay *on* all the times to save energy. This work is an effort complementing previous ones [38], [184], and particularly the one by Nath and Gibbons [133]. Precisely, we focus on the design of energy-efficient geographic forwarding on a minimum-energy duty cycled *k*-covered wireless sensor network, where every point in a field is covered by at least *k* sensors. Similar to [133], our joint sleep-wakeup scheduling and geographic forwarding in a *k*-covered wireless sensor network is done at the network layer. We believe that our joint protocols could be useful for several applications and particularly those requiring data aggregation at intermediate sensors along paths to the sink. To the best of our knowledge, this is the first study of geographic forwarding on a duty-cycled *k*-covered wireless sensor network.

The remainder of this chapter is organized as follows: Section 6.1 presents our sleep-wakeup scheduling protocol for full *k*-coverage of a field. Section 6.2 presents our geographic forwarding protocols for a duty-cycled *k*-covered wireless sensor network. Section 6.3 proposes relaxation of several

assumptions to generalize our protocols. Section 6.4 presents simulation results of our protocols. Section 6.5 concludes the chapter.

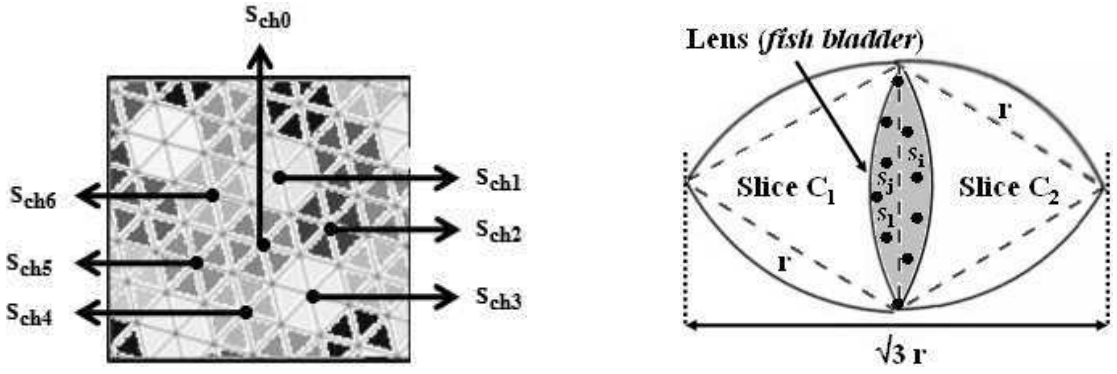

(a) (b)

Figure 6.1 (a) Randomly generated clustered sensor field and (b) intersection of adjacent slices.

6.1. Sensor Selection to Achieve *k*-Coverage: Revisited

First, we summarize the operation of field slicing and clustering. Then, we describe the coordination that is required between the cluster-heads to achieve *k*-coverage with a minimum number of sensors.

6.1.1 Sensor Field Clustering

In addition to slicing a field, we assume that the sink is also responsible for forming *clusters of slices* from the randomly obtained slicing grid. Precisely, each cluster consists of *at most* six adjacent slices forming a *disk*. Because of the random generation of slicing grids and the geometry of a field, some clusters consist of an entire disk, and hence called *interior clusters*, while others are formed by a portion of a disk, and hence called *boundary clusters*. Figure 6.1a shows a randomly generated clustered sensor field. Moreover, for each cluster, the sink selects a sensor, called *cluster-head*, which is located as near as possible to the center of its cluster. The random generation of slicing grid ensures that *all* sensors are *equally likely* to act as cluster-heads in each round. Each cluster is defined by one point, i.e., (x,y) coordinates, representing its center and at most six other points defining its slices (or slice portions for a non-complete cluster). These seven points define the *slicing information* of a cluster, which the sink would broadcast to its corresponding cluster-head. Next, we define *interior*/*boundary lenses* and *potential energy*.

Definition 6.1 (Interior and boundary lenses): An *interior lens* of a cluster is not shared with any of its

adjacent clusters while a *boundary lens* is shared by two adjacent clusters.

Notice that each cluster overlaps with at most six others as shown in Figure 1a. As discussed in Chapter 5, sensors located in the boundary lenses of a given cluster should be selected first in order to minimize the necessary total number of active sensors to achieve full *k*-coverage of a field. However, this would require certain *coordination* between cluster-heads.

ALGORITHM 1: *k*-COVERAGE-SLEEP-WAKEUP (CSW$_k$)
(* This code is run in each round *)
/* The following code is run by the sink */
1. Slice randomly a field into adjacent slices
2. Select a set *CH* of cluster-heads for all clusters in such a way they are located as close as possible to clusters' centers
3. Broadcast the selected set *CH* with all *slicing information*

/* The following code is run by each cluster-head */
4. Select sensors from its cluster (high priority to boundary lenses) and coordinate with all adjacent cluster-heads to *k*-cover a cluster based on the potential energy of sensors
5. Return

Figure 6.2 Sleep-wakeup scheduling for *k*-coverage.

6.1.2 Cluster-Heads Coordination and Sensor Selection

Each cluster-head is in charge of selecting some of its sensing neighbors to *k*-cover its cluster based on its *slicing information*. Precisely, each cluster-head exploits the overlap between the slices of its cluster as well as the overlap between its slices and those of its adjacent cluster-heads to select a minimum number of its sensing neighbors to *k*-cover its cluster. We assume that each sensor advertises its potential energy to its sensing neighbors at the start of a round when it turns itself *on*. Each cluster-head s_{ch_i} maintains a list of potential energy of its sensing neighbors, $\Pi(s_{ch_i}) = [\pi(s_j) : s_j \in SN(s_{ch_i})]$, where $\pi(s_i)$ is the potential energy of sensor s_i. It uses this list to select the ones with high potential energy to stay active by sending a *SELECT* message including the cluster-head's *id* as well as the *id*'s of all selected sensors. This would avoid those ones with low potential energy and help the sensors deplete their energy as slowly and uniformly as possible. We assume that at the beginning of each round, *all* the sensors are active. Those ones which are selected by their corresponding cluster-heads would remain active during the underlying round, while the others turn themselves *off* (or go to sleep). For the sensor selection, each cluster-head assigns *priorities* to sensors located in boundary lenses, interior lenses, and middle of slices in

descending order. In other words, sensors located in boundary lenses have high priority to be selected. Given that each cluster has at most six slices, each cluster-head manages at most six interior lenses and at most six boundary lenses. On the one hand, each cluster-head is responsible for selecting sensors from its interior lenses without any coordination with its adjacent cluster-heads. On the other hand, each cluster-head coordinates with at most six adjacent cluster-heads to select sensors from its boundary lenses in order to *k*-cover its cluster with a minimum number of sensors. For instance, in the case of a disk, its cluster-head, say s_{ch_0} (Figure 6.1a), would advertize the subsets $S_1, S_2, S_3, S_4, S_5, S_6$ of sensors selected from its six boundary lenses to its adjacent cluster-heads $s_{ch_1}, s_{ch_2}, s_{ch_3}, s_{ch_4}, s_{ch_5}, s_{ch_6}$, respectively.

The pseudo-code of our sleep-wakeup scheduling protocol (CSW$_k$) for ensuring *k*-coverage of a field is given in Figure 6.2.

6.2. Geographic Forwarding in a Duty-Cycled *k*-Covered Wireless Sensor Networks

In this section, we present our first *potential field* [89] based solution for geographic forwarding on a duty-cycled *k*-covered wireless sensor network, called *Geographic Forwarding through Fish Bladders* (GEFIB), where data is forwarded through *fish bladders* (or *lenses*). Precisely, we discuss three geographic forwarding protocols with different levels of data aggregation.

Assumption 6.1 (Data traffic model): We assume that in each round, every active sensor has data to report to the sink. Also, only sensors selected to *k*-cover a field act as *relays*. □

6.2.1 Potential Fields Based Modeling Approach

Sensors can be viewed as *particles*, and hence are subject to *virtual forces*, which attract sensors to each other. These virtual attractive forces are due to the *potential energy* of the sensors and their *geographic locations*. Indeed, the sensors with highest potential energy are preferred to act as relays in order to avoid *energy holes* (i.e., regions whose sensors have depleted their energy) that may disconnect the network. Also, as the energy spent in data transmission is proportional to the transmission distance [88], the sensors prefer closer ones to act as relays, thus forwarding data over short distances.

Using potential field terminology, each active sensor is subject to at least one *attractive force*, called *energy-location based force* and denoted by F_{el}, which is exerted by some active sensor and defined as the gradient of a unique scalar potential field, called *energy-location based potential field* and denoted by

U_{el}, i.e., $F_{el} = -\nabla U_{el}$. We should mention that this notion of attractive force is *symmetric*. That is, if a sensor s_i exerts a force on sensor s_j, the latter also exerts on the former a force with the same magnitude. Also, only active sensors can exert forces on each other. Our approach to modeling the resultant force that a sensor s_i exerts on its sensing neighbor s_j is borrowed from electromagnetism theory [153]. Using Coulomb's law [153], the magnitude of the electrostatic force $F(i,j)$ between two points electric charges q_i and q_j depends on their magnitudes and the Euclidean distance $d(i,j)$ between them and the permittivity ε_0 of free space, and is computed as

$$F(i,j) = -\nabla U(i,j) = \frac{1}{4\pi\varepsilon_0}\frac{|q_i||q_j|}{d^2(i,j)}$$

In our model, the charge of a sensor is its *potential energy* and permittivity is the *transmitter amplifier* [88] in the free-space (ε_{fs}) model $(\alpha = 2)$ or the multi-path (ε_{mp}) model $(2 < \alpha \leq 4)$, where α is the path-loss exponent. Thus, the magnitude of the force $F_{el}(i,j)$ that a sensor s_i exerts on its sensing neighbor s_j is proportional to the product of their potential energy, $\pi(s_i)$ and $\pi(s_j)$, and inversely proportional to the Euclidean distance $d(i,j)$ between them. Moreover, it is important that $F_{el}(i,j)$ account for the type of model being used, i.e., free-space model $(\varepsilon = \varepsilon_{fs})$ vs. multi-path model $(\varepsilon = \varepsilon_{mp})$. Therefore, the attractive force $F_{el}(i,j)$ is computed as

$$F_{el}(i,j) = -\nabla U_{el}(i,j) = \frac{1}{4\pi\varepsilon}\frac{\pi(s_i)\pi(s_j)}{d^{\alpha}(i,j)}$$

Similarly, there is an interaction between one sensor and a set of sensors. Precisely, the resultant force exerted by sensor s_i on a set of sensors S is given by

$$F_{el}(i,S) = \sum_{s_j \in S} F_{el}(i,j) = -\sum_{s_j \in S} \nabla U_{el}(i,j)$$

Next, we present three geographic data forwarding protocols for a duty-cycled *k*-covered wireless sensor network based on potential fields.

6.2.2 Potential Fields Based Data Forwarding without Aggregation

In this section, we propose a simple approach for geographic forwarding without data aggregation on a duty-cycled *k*-covered wireless sensor network based on artificial potential fields that were described

in Section 6.2.1. Let us first define the notion of *best relay* of a sensor.

Definition 6.2 (Best relay of a sensor): A *best relay* of a sensor s_i is a sensing neighbor s_l of s_i located between it and the sink such that $F_{el}(i,b)$ is the maximum over all resultant forces exerted by s_i on its sensing neighbors, i.e., $F_{el}(i,l) = \max\{F_{el}(i,j) : s_j \in SN(s_i)\}$. □

When a sensor receives data for which it is its *relay*, it selects a best relay from its sensing neighbor set and forwards the data to it. Otherwise, it just ignores it. This process repeats until the sink receives the data. The pseudo-code of our geographic forwarding without data aggregation on a duty-cycled *k*-covered wireless sensor network, called GEFIB-1, is given in Figure 6.3.

ALGORITHM 2: JOINT-*k*-COVERAGE-FORWARDING (GEFIB-1)
(* This code is run in each round. It is called by every sensor s_i holding data to be forwarded to the sink. It is assumed that CSW$_k$ has been already called to *k*-cover a field *)

1. Sort all active sensing neighbors in a list, *LIST*, based on their resultant forces $F_{el}(i,j)$ where $s_j \in SN(s_i)$
2. Select a best relay s_l from the sorted list, *LIST*
3. Forward sensed data to s_l
4. Return

Figure 6.3 Joint *k*-coverage and forwarding (GEFIB-1).

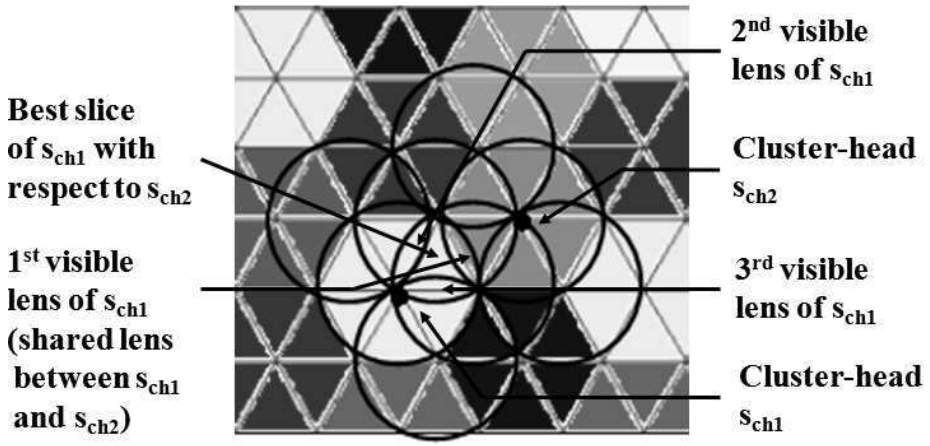

Figure 6.4 Communication between adjacent cluster-heads.

6.2.3 Potential Fields Based Data Forwarding with Aggregation

In this section, we present two geographic forwarding protocols with data aggregation on a duty-cycled *k*-covered wireless sensor network.

All data originated from sensors in a cluster are received by their corresponding cluster-head, which

aggregates them with its own data into only one single data. Precisely, each sensor sends its data directly to its cluster-head, where data is aggregated. We distinguish two types of aggregation. In the first scenario, referred to as *local data aggregation*, aggregation occurs only within clusters and all data aggregated by cluster-heads are forwarded to the sink without further aggregation. Thus, the sink receives data from each cluster-head in each round. In the second scenario, referred to as *global data aggregation*, the sink receives only *one* data packet in each round that represents the aggregation of *all* data aggregated by cluster heads. Precisely, each cluster-head also aggregates its own aggregated data with the aggregated data it has received from a cluster-head and forwards the result to another cluster-head. Before we discuss our geographic data forwarding protocol with data aggregation on a duty-cycled *k*-covered wireless sensor network, namely GEFIB-2 (Section 6.2.3.1) and GEFIB-3 (Section 6.2.3.2), we define *best slice*, *best lens*, and *best relay* of a cluster-head with respect to a destination.

ALGORITHM 3: JOINT-*k*-COVERAGE-FORWARDING (GEFIB-2)

(* This code is run in each round. It is called by every sensor s_i holding data to be forwarded to the sink. It is assumed that CSW$_k$ has been already called to *k*-cover a field. We assume that each sensor already sent its sensed data directly to its cluster-head *)

Procedure Identify_Best_Relay (*id1*, *id2*, *id3*: integer)

1. Determine a best slice of s_{id1} with respect to s_{id2}
2. Sort the three lenses L_1, L_2, L_3 of this slice based on the resultant forces $F_{el}(id1, L_j)$ of their sensors $(1 \le j \le 3)$
3. Select a best lens $L_b, 1 \le b \le 3$
4. Select a best relay $s_{id3} \in L_b$
5. Return(*id3*)

EndProcedure

/* The following code is run by a best relay */

1. If s_i is a relay Then /* *i* is the *id* of s_i */

1.1. Forward sensed data to the closest cluster-head

2. Else /* The following code is run by a cluster-head */

2.1. Identify_Best_Relay(*i*,*m*,*id*) /* *m* is the sink's *id* */

2.2. Forward sensed data to s_{id} /* *id* is a best relay's *id* */

EndIf

3. Return

Figure 6.5 Joint *k*-coverage and forwarding (GEFIB-2).

Definition 6.3 (Best slice, visible lens, best lens, and best relay of a cluster-head): A *best slice* of a cluster-head s_{ch} with respect to a destination $Dest$, which could be a cluster-head or the sink, is a slice that is

crossed by a line segment connecting s_{ch} and $Dest$ (Figure 6.4). A *visible lens* $L_v(i,Dest)$ of s_{ch} with respect to $Dest$, is a lens that belongs to the best slice of s_{ch} with respect to $Dest$, where $1 \le v \le 3$ (Figure 6.4). A *best lens* $L_b(i,Dest)$ of s_{ch} with respect to $Dest$, is a visible lens such that $F_{el}(i,L_b(i,Dest))$ is the maximum over all resultant forces exerted by s_{ch} on all its visible lenses $L_v(i,Dest)$, where $1 \le b,v \le 3$. A *best relay* s_l of a cluster-head s_{ch} with respect to a destination $Dest$, is a sensing neighbor of s_{ch} selected from a best lens $L_b(i,Dest)$ such that $F_{el}(i,l)$ is the maximum over all resultant forces exerted by s_i on its neighbors located in $L_b(i,Dest)$. That is, $F_{el}(i,L_b(i,Dest)) = \max\{F_{el}(i,L_v(i,Dest)) : 1 \le v \le 3\}$ and $F_{el}(i,l) = \max\{F_{el}(i,j) : s_j \in L_b(i,Dest)\}$. □

ALGORITHM 4: DAT-CONSTRUCTION (DAT-C)

(* This code is run in each round by the sink and cluster-heads *)

/* The sink initiates the DAT construction process */

1. Randomly select one cluster-head as *ring aggregator* and two adjacent cluster-heads as *aggregation initiators*
2. The sink assign a *ring_id* to the first ring (*ring_id* = 1) and advertizes it to its ring aggregator and aggregation initiators
3. The sink designates one of the aggregation initiators as an *Aggregation proxy* to designate two of its adjacent cluster-heads as *aggregation* initiators for the next ring
4. The aggregation proxy advertizes *ring_id* clockwise while the other aggregation initiator advertizes it counter-clockwise

/* Ring aggregators and aggregation initiators build the DAT */

5. *ring_id* = *ring_id* + 1
6. While (all cluster-heads are not being considered) Do
7. A ring aggregator selects one of its adjacent cluster-heads as a ring aggregator for the next ring whose id is *ring_id*
8. An aggregation proxy selects two of its adjacent cluster-heads as aggregation initiators for the next ring whose id is *ring_id*. One of these cluster-heads is designated as an aggregation proxy
9. An aggregation proxy advertizes *ring_id* clockwise while an aggregation initiator advertizes it counter-clockwise
10. *ring_id* = *ring_id* + 1

EndWhile

11. Return

Figure 6.6 DAT construction algorithm (DAT-C).

6.2.3.1 Locally Aggregated Data Forwarding

First, each sensor sends its data *directly* to its cluster head without relaying them through other intermediate sensors. When a cluster head s_i receives data from all sensors belonging to its cluster, it

aggregates them with its own data and forwards the result, called *locally aggregated data* (LAD), toward the sink. In each round, the sink receives as many *LAD* packets as cluster-heads. Indeed, when a cluster-head receives *LAD* packets initiated from other cluster-heads, it just forwards them without any update. Precisely, a cluster-head finds the best slice with respect to the sink (Definition 6.4) and chooses the best lens in terms of attractive force out of the three visible lenses (Figure 6.4). From this lens, it selects the best relay based on the potential field-based force and forwards data to it. However, when a relay receives the data, it forwards it directly to the closest cluster-head. This forwarding process between cluster-heads using relays takes place through fish bladders (or lenses) and repeats until data arrives at the sink. All cluster-heads and relays apply the algorithm GEFIB-2 whose pseudo-code is given in Figure 6.5.

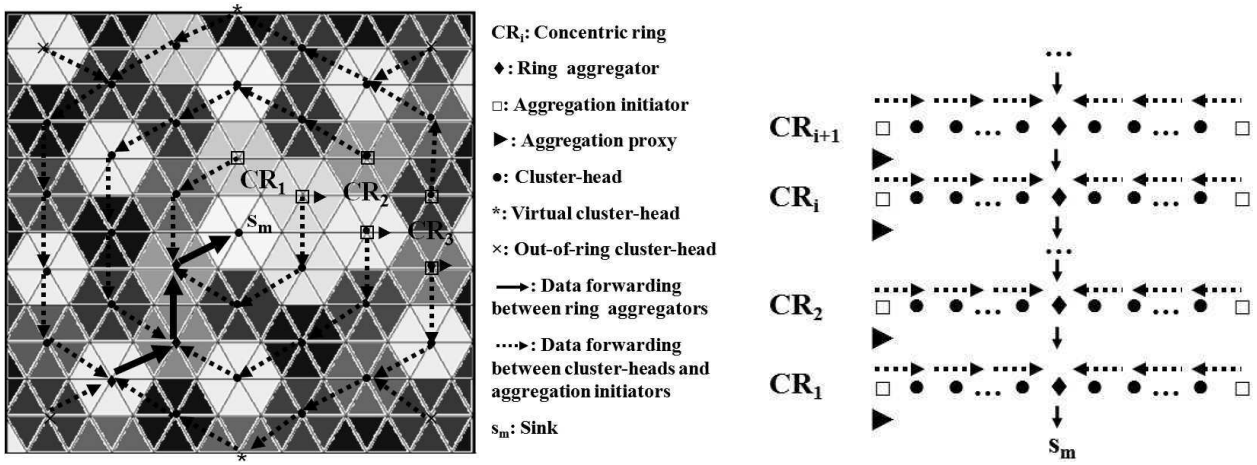

(a) (b)

Figure 6.7 (a) Data forwarding on a random data aggregation tree and (b) its linear representation.

6.2.3.2 Globally Aggregated Data Forwarding

In each round, the sink would receive only one data, called *globally aggregated data* (GAD), which represents the result of aggregation of all locally aggregated data generated by their cluster-heads. This implies that at the end of each round, only one cluster-head would forward the data aggregated by all other cluster-heads after it has been aggregated with its own data. Therefore, it is necessary that all cluster-heads participate in the data forwarding process. It follows that each cluster-head would act as a relay on behalf of other cluster-heads until a *GAD* packet reaches the sink. Precisely, at any time, there is only one aggregated data packet that is forwarded by cluster-heads until it reaches the sink.

ALGORITHM 5: JOINT-*k*-COVERAGE-FORWARDING (GEFIB-3)

(* This code is run in each round by a cluster-head or a relay s_i. It is assumed that CSW$_k$ has been already called to *k*-cover a field and that each sensor already sent its data to its cluster-head *)

/* Run the first step at the start of each round. The sink and Cluster-heads participate in the DAT construction */

1. Call to DAT-Construction algorithm (ALGORITHM 4)

/* All aggregation initiators initiate the data forwarding process on their corresponding ring in parallel */

2. If s_i is an aggregation proxy Then

2.1. Identify_Best_Relay(*i*,*j*,*id*) /* s_{id} is a best relay */

2.2. Forward data clockwise to the immediate successor cluster-head s_j in the corresponding ring via the relay s_{id}

(the destinations s_{id} and s_j are inserted in the data packet)

3. Else /* The other aggregation initiator */

3.1. Identify_Best_Relay(*i*,*j*,*id*)

3.2. Forward data counter-clockwise to the immediate successor cluster-head s_j in the corresponding ring via the relay s_{id}

(the destinations s_{id} and s_j are inserted in the data packet)

EndIf

/* Code is run by a best relay or a virtual cluster-head */

4. If s_i is a best relay or a virtual cluster-head Then

4.1. Forward data to the next cluster-head s_j

5. Else /* Cluster-heads and ring aggregators */

5.1. If s_i is a cluster-head Then /* Cluster-heads */

5.1.1. Identify_Best_Relay(*i*,*j*,*id*) /* s_{id} is a best relay */

5.1.2. Aggregate the received data with its own data

5.1.3. Forward data to the immediate successor cluster-head s_j in the corresponding ring via the relay s_{id}

(s_{id} and s_j are inserted in the data packet)

5.2. Else /* Ring aggregator */

5.2.1. If s_i is a ring aggregator Then

5.2.1.1. Identify_Best_Relay(*i*,*j*,*id*) /* s_{id} is a best relay */

/* s_j is a successor ring aggregator or the sink */

5.2.1.2. Wait until receipt of aggregated data from the immediate predecessor ring aggregator

5.2.1.3. Aggregate the received data from both neighboring cluster-heads in its ring and the one received from a predecessor ring aggregator with its own data

5.2.1.4. Forward data to s_j via the relay s_{id}

(s_{id} and s_j are inserted in the data packet)

EndIf

EndIf

EndIf

6. Return

Figure 6.8 Joint *k*-coverage and forwarding (GEFIB-3).

Notice that we could enable forwarding of *GAD* packets only through cluster-heads. However, this solution would be very costly for cluster-heads [84], [85] as the energy spent in data transmission is proportional to the transmission distance, which would be around the nominal transmission range of the sensors. It is easy to check that the distance between the centers of two adjacent clusters is equal to $\sqrt{3}\,r$ (Figure 6.1b), where r is the radius of the sensors' sensing disks. Also, if the radius R of the communication disks of the sensors does not satisfy $R \geq \sqrt{3}\,r,$ then cluster-heads cannot directly communicate with each other, and hence other relays should forward aggregated data between adjacent cluster-heads. On the other hand, inserting several relays between two adjacent cluster-heads would incur high delay [28].

We believe that a more balanced approach should be used to account for both energy and delay. First, we show how to construct a data aggregation tree to enable data aggregation at cluster-heads.

Data Aggregation Tree (DAT) Construction: The process of forming a binary tree of cluster-heads rooted at the sink for data aggregation benefits from the distribution of cluster-heads in a field. The sink is supposed to be located at its optimum position in terms of energy efficient data gathering, which corresponds to the center of a field [125]. Recall that cluster-heads are selected to be as close as possible to the centers of their clusters. The algorithm is initiated by the sink (Figure 6.6). The sink starts by randomly selecting three cluster-heads: two of them, called *aggregation initiators*, are adjacent to each other and constitute the extreme points of an open ring that initiate data aggregation on the ring itself, while the third one, called *ring aggregator*, is located somewhere on the open ring and is responsible for the aggregated data on its ring. Each ring is associated with an *identification number*, called *ring_id*, which will be used by the cluster-heads to forward their aggregated data toward their corresponding ring aggregator. Furthermore, one of the aggregation initiators is designated as an *aggregation proxy*, which will select the aggregation initiators for the next ring and advertize the value of *ring_id* for this next ring. The first ring is the one whose center is the closest one to the location of the sink (i.e., center of a field) and has *ring_id* = 1. The value of *ring_id* is incremented by 1 from the sink out by aggregation proxies. Each cluster-head belongs to only one ring. While an aggregation proxy advertizes the value of *ring_id* clockwise to the cluster-heads members of its ring, the other aggregation initiator advertizes it counter-

clockwise so all the cluster-heads that belong to the same ring receive the same value of *ring_id*. After the data aggregation tree construction, each cluster-head knows its immediate predecessor and successor cluster-head in its corresponding ring. Also, each ring aggregator knows its immediate predecessor and successor ring aggregators. Because of the boundary effect, the sink may designate a few sensors as *virtual cluster-heads* for clusters that are not complete (i.e., a portion of a disk) and which can be *k*-covered by adjacent cluster-heads provided that they select sensors to remain active from their boundary lenses, which they share with these non-complete clusters. Precisely, these virtual cluster-heads will not play the role of cluster-heads but will simply act just as relays between non-neighboring cluster-heads on the same ring on the boundary of a field. Also, some cluster-heads located on the boundary of a field do not belong to any ring. They are called *out-of-ring cluster-heads*, which *connect* to the closest ring via their neighboring cluster-heads to which they forward their data to be aggregated with theirs. Figure 6.7 shows a data aggregation tree and its components, where Figure 6.7a is a linear representation of Figure 6.7b.

Data Forwarding: We assume that the concentric rings are numbered $CR_1, CR_2, CR_3, \ldots$ from the sink out. For a given ring CR_i, while the aggregation proxy initiates data aggregation in one direction of the ring, the other one initiates data aggregation in the other direction of the ring. The ring aggregator of CR_i receives aggregated data originated from both of aggregation initiators of CR_i, and aggregated data from a ring aggregator of an outer adjacent ring CR_{i+1}. At the end, the ring aggregator of CR_1 aggregates its own data with those originated from both of the aggregation initiators of its ring and the one received from the ring aggregator of CR_2 and forward the *GAD* toward the sink. Specifically, when a cluster-head receives data from its predecessor cluster-head, it aggregates with its own data and forwards it to its successor cluster-head until it reaches the ring aggregator. Each ring aggregator would wait until it receives aggregated data from its immediate predecessor ring aggregator. Those out-of-ring cluster-heads would simply forward their data to the cluster-heads they registered with. Note that communication between adjacent cluster-heads follows the same scheme shown in Figure 6.4. The pseudo-code of GEFIB-3 is given in Figure 6.8.

6.3. Generalizability of GEFIB

The design of GEFIB framework for joint *k*-coverage, duty-cycling, and forwarding is based on the sensing and communication *disk,* and sensor *homogeneity* models. Although these assumptions are the

basis for most of coverage and forwarding protocols, they may not be valid in practice. In this section, we show how to relax them to promote the use of our protocols in real-world applications.

6.3.1 Convex Sensing and Communication Model

As mentioned earlier in Chapter 5, the communication range of MICA motes was found to be asymmetric and environment-dependent [179]. Furthermore, the communication range of radios was found to be highly probabilistic and irregular [182]. In this section, for problem tractability, we consider convex sensing and communication models, where sensors have the same *convex* sensing and communication ranges but not necessarily circular. Precisely, we consider the *largest enclosed disk* of the sensing range of the sensors whose radius is equal to r_{led}. In this case, the sink slices a field into overlapping Reuleaux triangles of width r_{led}. However, all other processing remains the same for all the protocols, namely GEFIB-1, GEFIB-2, and GEFIB-3.

6.3.2 Sensor Heterogeneity Model

It has been found that heterogeneity enhances reliability of the network and extends its lifetime [169]. In this section, we consider heterogeneous sensors with different yet convex sensing and communication ranges. Based on the notion of the largest enclosed disk of the sensing range of the sensors, the sink slices a field into overlapping Reuleaux triangles of width $r_{led}^{\min}$, the minimum radius of the largest enclosed disks of the sensing ranges of the sensors. However, a very small $r_{led}^{\min}$ could overestimate the required sensor density in the network. Indeed, with a single sensor with a very small radius, the network would be required to have a large sensor density. We believe that a more adaptive approach could be used to adapt the sensor density to the sensing ranges of the sensors in the area.

6.4. Performance Evaluation

In this section, we evaluate GEFIB performance using a high-level simulator written in the C programming language. We consider a square sensor field of side length 1000m where 16000 sensors are randomly and uniformly deployed. We use the energy model given in [171], where energy consumption in transmission, reception, idle, and sleep modes are 60 mW, 12 mW, 12 mW, and 0.03 mW, respectively. Following [176], we define *one unit of energy* as the energy required for a sensor to stay idle for 1 second. We assume that the initial energy of each sensor is 60 Joules enabling a sensor to

operate about 5000 seconds in reception/idle modes [171]. All simulations are repeated 20 times and the results are averaged.

First, we compare our *k*-coverage protocol CSW$_k$ with the Coverage Configuration Protocol (CCP) [166]. When the communication range of sensors is at least double their sensing range, Xing *et al.* [166] showed that full coverage implies network connectivity, and hence no other mechanism to guarantee connectivity is necessary. Otherwise, Xing *et al.* [166] integrated CCP with a topology maintenance protocol (SPAN) [52] to guarantee both coverage and connectivity.

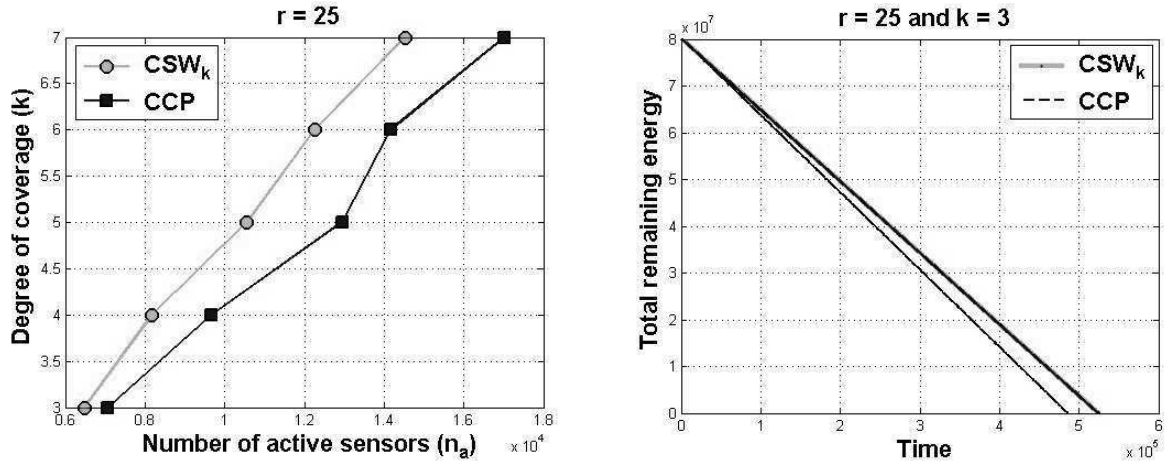

(a) (b)

Figure 6.9 CSW$_k$ compared to CCP (a) k vs. n_a and (b) total remaining energy vs. time.

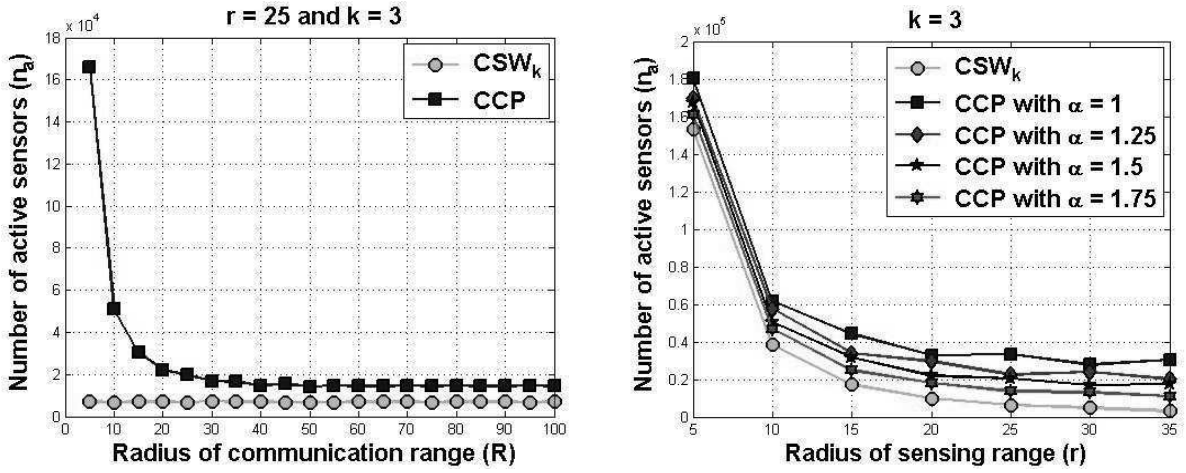

(a) (b)

Figure 6.10 CSW$_k$ compared to CCP (a) n_a vs. R and (b) r.

In all simulations, we consider $r = 25\,\mathrm{m}$ and $k = 3$ unless specified otherwise. Also, the energy consumption is due to all activities of each sensor necessary to achieve *k*-coverage as well as to forward and/or send control information. Figure 6.9a plots the degree k of coverage versus the number n_a of active sensors for CSW_k as compared to CCP. It shows that CSW_k requires less active sensors than CCP to achieve the same coverage degree, thus yielding significant energy savings. This is due not only to a higher number of active sensors required by CCP, but also to the communication overhead caused by the exchange of messages between active sensors running CCP to coordinate among themselves and provide the requested *k*-coverage service. Thus, CCP consumes more energy than CSW_k as shown in Figure 6.9b. While CCP requires SPAN to provide connectivity between active sensors when $R < 2r$, CSW_k does not need such a topology maintenance protocol as all it requires is that $R \geq r$, thus providing connectivity when *k*-coverage is guaranteed.

Figure 6.10a plots n_a versus R while Figure 6.10b plots n_a versus r for different ratios $\alpha = R / r$. Given the result reported in [176] with respect to the relationship between r and R for real-world sensor platforms $(R \geq r)$, we consider only the case $\alpha \geq 1$. Given that $\alpha \geq 1$, any increase in the communication range of sensors would not have any impact on the performance of CSW_k. It would, however, affect the performance of CCP. As can be observed, n_a decreases as R increases. Indeed, SPAN would require less number of sensors to maintain connectivity between active sensors as R increases. However, at some point, (surprisingly enough, this point corresponds to $R \geq 2r$), the number n_a of active sensors required for *k*-coverage does not decrease any further. Indeed, when $R \geq 2r$, SPAN is not needed at all as both *k*-coverage and $R \geq 2r$ guarantee connectivity. Similarly, the performance of CCP improves as the ratio α increases, i.e., R increases (Figure 6.10b). That is, less number of sensors is needed to provide *k*-coverage and connectivity.

Second, we compare between GEFIB-1, GEFIB-2, and GEFIB-3. We assume that the energy consumption in data transmission and reception follows the model given in [88]. Recall that GEFIB-1, GEFIB-2, and GEFIB-3 use CSW_k but *different* data collection protocols. Figure 6.11 shows that GEFIB-3 outperforms GEFIB-1 and GEFIB-2 with respect to energy consumption and delay (i.e., average time for

data sent by sensors to reach the sink). As expected, data aggregation yields significant energy savings in CSW_k as it reduces the amount of data communication in the network. Also, data aggregation improves on delay as relay forward data as they arrive without causing much delay overhead.

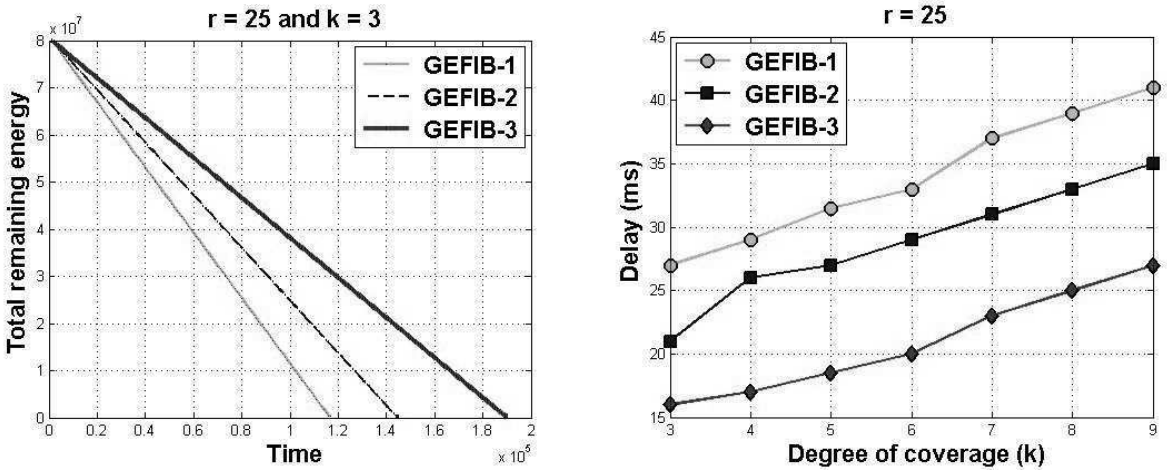

(a) (b)

Figure 6.11 GEFIB-1 vs. GEFIB-2 (a) total remaining energy vs. time and (b) average delay vs. k.

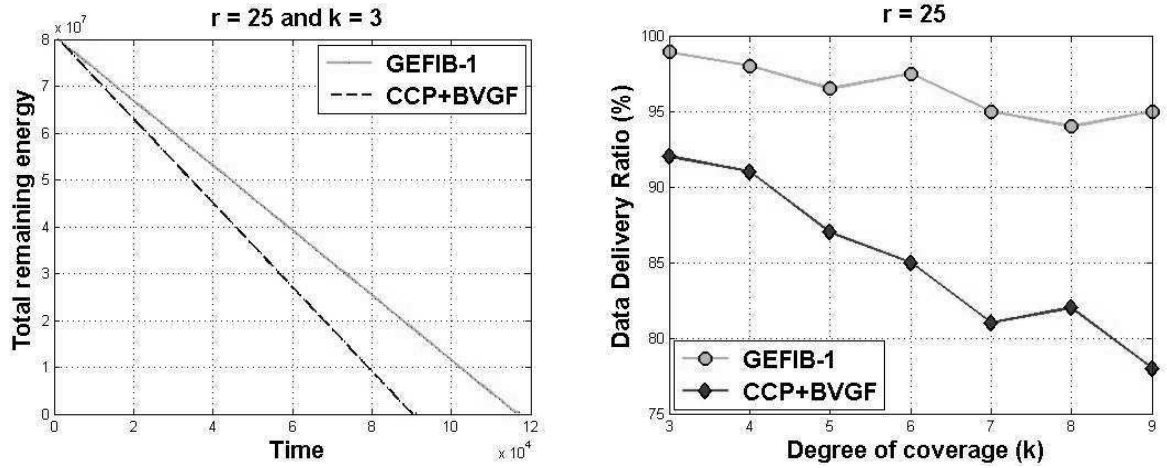

(a) (b)

Figure 6.12 GEFIB-1 vs. CCP+BVGF (a) total remaining energy vs. time and (b) data delivery rate vs. k.

Third, we consider CCP [166] with a geographic forwarding protocol, such as BVGF [165], on top of it, denoted by CCP+BVGF, and compare it to GEFIB-1. We have slightly updated BVGF to consider potential energy of the sensors that are candidate for data forwarding for a fair comparison. Here, the energy consumption is due to all activities of each sensor necessary to achieve *k*-coverage and to forward

and/or send sensed data as well as control information. Figure 6.12 shows that GEFIB-1 yields less average energy consumption and higher percentage of data delivery (i.e., success rate) than CCP+BVGF. This is due in part to CCP, which uses higher number of active sensors for *k*-coverage than CSW_k. Also, BVGF forwards data over long distances. Hence, it consumes considerable energy. Those selected sensors would deplete their energy very quickly and die before expected, thus disconnecting the network. Moreover, data may reach sensors whose remaining energy is not enough to progress data towards the sink, which causes data to be dropped. Our potential field-based forwarding protocol, however, selects next forwarders based on their remaining energy and location, and hence all neighbors of a sensor are equally likely to be selected as next forwarders.

6.5. Summary

In this chapter, we have also proposed energy-efficient geographic forwarding protocols on duty-cycled *k*-covered wireless sensor networks, where sensed data is forwarded to the sink through fish bladders (or lenses) [21], [22]. Our joint *k*-coverage and geographic forwarding (GEFIB) framework can be used for applications that demand high coverage degree, such as intruder detection and tracking. It is also useful for applications that require data aggregation and those where *all* data originated from sources should reach the sink.

CHAPTER 7

STOCHASTIC CONNECTED *k*–COVERAGE AND THREE-DIMENSIONAL DEPLOYMENT

The problem of coverage (and in particular *k*-coverage) has been well-studied in the literature [34], [107], [108], [119]. Also, the problem of coverage-preserving scheduling (or duty-cycling) has gained considerable attention [83], [93], [166], [176]. Several existing works on *k*-coverage in wireless sensor networks assumed a perfect sensing model (also known as *deterministic sensing model*), where a point in a field is guaranteed to be covered by a sensor provided that this point is within the sensor's sensing range [176]. While some approaches focused on coverage only [2], others considered both coverage and connectivity in an integrated framework to ensure the correct operation of the network [166], [176]. Indeed, coverage deals with all locations in a field, and hence informs how well a phenomenon in the field is monitored, whereas connectivity is related to the locations of the sensors, and hence quantifies how well the active sensors communicate with each other and forward sensed data on behalf of each other to the sink. We have addressed this problem in Chapter 5, where centralized, pseudo-distributed, and distributed protocols are proposed. A few works, however, considered a more realistic sensing model (also known as *stochastic sensing model*) in the design of sensor scheduling protocols while preserving either full coverage [103], [123], [130], [186] or *k*-coverage of a field [159], [166], [186], where a point is covered by a sensor with some probability.

As discussed in Section 3.8 of Chapter 3, three-dimensional settings reflect more accurately network design for real-world applications than their more traditional, two-dimensional counterparts. As of writing this dissertation, the assumption of two-dimensional space is well accepted by the sensor network community while that of three-dimensional space has been receiving little attention due to the challenges imposed by the design of three-dimensional wireless sensor networks [5]. Indeed, most (if not all) of the works on the design of protocols for wireless sensor networks, and particularly, those on deployment, have focused on two-dimensional space, where the sensors are deployed in a planar field. As mentioned by Poduri *et. al* [138], there is a tendency of ignoring the extension of protocols initially designed for two-

dimensional to three-dimensional wireless sensor networks either because it is simple or straightforward. Furthermore, Poduri *et. al* [138] showed that there are a few properties in two-dimensional wireless sensor networks that cannot generalize at all to three-dimensional wireless sensor networks. In general, the design of connected *k*-coverage configuration protocols for wireless sensor networks in three-dimensional space is more challenging than their counterparts in two-dimensional space.

In this chapter, we consider two fundamental problems in two-dimensional and three-dimensional wireless sensor networks, respectively. First, we focus on the design of stochastic connected *k*-coverage configuration protocols for two-dimensional wireless sensor networks [23]. More specifically, we decompose this problem into two sub-problems: *stochastic k-coverage characterization problem* and *stochastic k-coverage-preserving scheduling problem*. Specifically, the first problem is to find a sufficient condition so that every point in the field is covered by at least k sensors with a probability no less than p_{th}, called *threshold probability*, under our stochastic sensing model (see Chapter 2) and compute the corresponding minimum number of sensors. Second, we address the problem of connected *k*-coverage in three-dimensional wireless sensor networks using a deterministic sensing model of the sensors, and focus on the problem of sensor scheduling for *k*-coverage of a three-dimensional space [19], where $k > 1.$ Moreover, we focus on the problem of data forwarding on duty-cycled sensors in three-dimensional connected *k*-covered wireless sensor networks. Not surprisingly, we show that the extension of our analysis of two-dimensional wireless sensor networks is really not straightforward for three-dimensional wireless sensor networks due to the non-preserving nature of some of the properties for two-dimensional space when we consider three-dimensional space.

The remainder of this chapter is organized as follows. Section 7.1 discusses the problem of stochastic connected *k*-coverage in two-dimensional wireless sensor networks under a more realistic stochastic sensing model, which is described in Chapter 2. It also presents simulation results of our proposed protocol. Section 7.2 presents a solution to the problem of connected *k*-coverage in three-dimensional wireless sensor networks. It also describes a hybrid geographic forwarding protocol for duty-cycled *k*-covered three-dimensional wireless sensor networks and presents simulation results of our proposed protocols. Section 7.3 concludes the chapter.

7.1 Two-Dimensional Stochastic Connected *k*-Coverage

Although the approach on *k*-coverage in wireless sensor networks proposed in [166] is elegant and considers both deterministic and probabilistic sensing models, it does not provide any proof on whether its *k*-coverage eligibility algorithm would yield a minimum number of selected sensors to *k*-cover a field.

In this section, we propose a solution to the stochastic connected *k*-coverage problem stated earlier using our *stochastic sensing model*, which reflects the real behavior of the sensing units of the sensors that are irregular in nature.

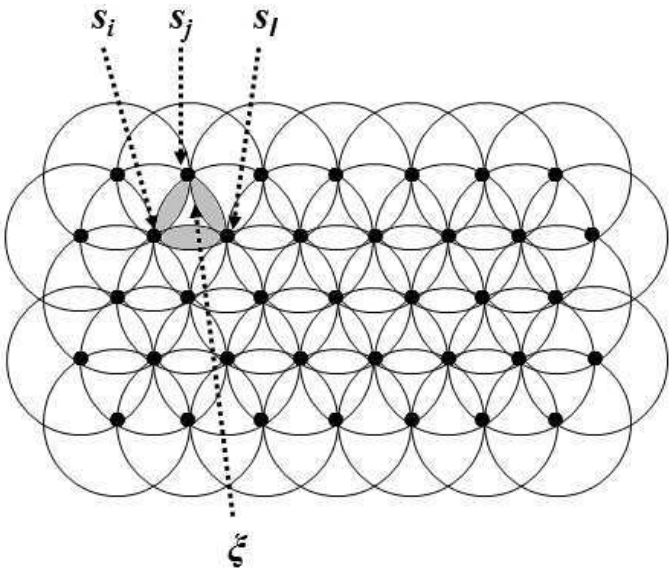

(a)

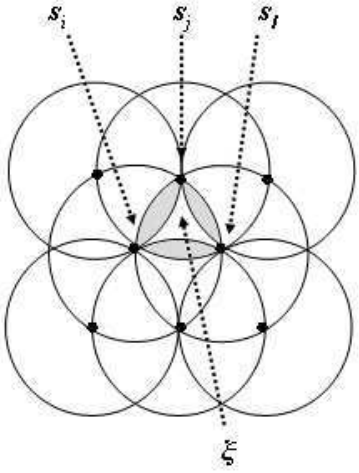

(b)

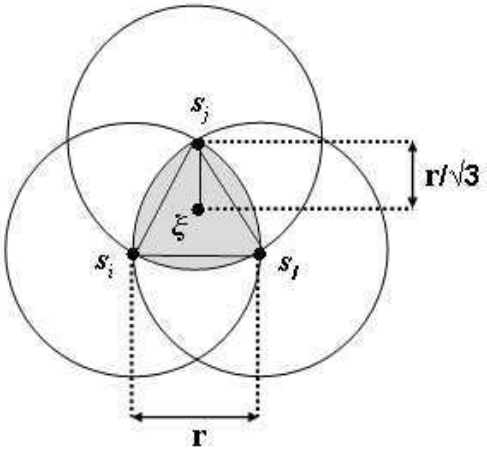

(c)

Figure 7.1 (a-b) Reuleaux triangle and (c) location of a least *k*-covered point.

7.1.1 Stochastic *k*-Coverage Characterization

In this section, we exploit the results of Section 5.1 of Chapter 5 in order to characterize *k*-coverage in wireless sensor networks based on the stochastic sensing model described earlier. It is also similar to the stochastic sensing model in [186], except that ours accounts for the type of propagation model, i.e., $2 < \alpha \leq 4.$ Precisely, we use the Reuleaux triangle model to compute the *minimum k-coverage probability*, denoted by $p_{k,\min}$, such that every point in a field is *k*-covered. Theorem 7.1 computes $p_{k,\min}$.

Theorem 7.1: Let r be the radius of the nominal sensing range of the sensors and $k \geq 3.$ The minimum *k*-coverage probability $p_{k,\min}$ so that each point in a field is probabilistically *k*-covered by at least k sensors under the stochastic sensing model defined in Equation (2.2) (Chapter 2) is approximately computed as

$$p_{k,\min} \approx 1 - \left(1 - e^{-\beta\left(\frac{r}{\sqrt{3}}\right)^{\alpha}}\right)^{k} \tag{7.1}$$

Proof: First, we identify the *least k*-covered point in a field so we can compute $p_{k,\min}.$ By looking at the Reuleaux triangle corresponding to three sensors and given in Figure 7.1a-b, it is easy to check that the center ξ of the Reuleaux triangle is the least 3-covered point. Indeed, ξ is located close to the boundaries of the sensing ranges of the sensors s_i, s_j, and $s_l.$ By Lemma 5.2 (see Chapter 5), k sensors should be deployed in each Reuleaux triangle regions of a field to achieve *k*-coverage with a minimum number of sensors. Thus, on the average, we can claim that the center ξ is also the least *k*-covered point in a field. Note that ξ is equidistant from the sensors s_i, s_j, and $s_l.$ Using the configuration in Figure 7.1c, a little algebra shows that the distance between ξ and each of these three sensors is equal to $r/\sqrt{3}.$ Let $S_k = \{s_1,...,s_k\} \subseteq S$ be a set of sensors that *k*-cover $\xi.$ As per the above observation, we can approximate the distance between any sensor in S_k and ξ by $r/\sqrt{3}$, i.e., $\delta(s_i,\xi) \approx r/\sqrt{3}$, for each sensor $s_i \in S_k.$ Therefore, the minimum *k*-coverage probability (or detection probability) for the least *k*-covered point ξ by exactly k sensors $(s_1,..,s_k)$ under our stochastic sensing model is given by

$$p_{k,\min} = 1 - \prod_{i=1}^{k} (1 - p(\xi, s_i)) \approx 1 - \left(1 - e^{-\beta \left(\frac{r}{\sqrt{3}} \right)^{\alpha}} \right)^{k}$$ □

The stochastic *k*-coverage problem is to select a minimum subset $S_{\min} \subseteq S$ of sensors such that each point in a field is *k*-covered by at least k sensors and that the minimum *k*-coverage probability of each point is at least equal to some given threshold probability p_{th}, where $0 < p_{th} < 1$. This helps us compute the sensing range r_s, which provide full *k*-coverage of a field with a probability no less than p_{th} :

$$p_{k,\min} \geq p_{th} \Rightarrow r_s \leq \sqrt{3} \left(-\frac{1}{\beta} \log (1 - (1 - p_{th})^{1/k}) \right)^{1/\alpha}$$

Lemma 7.1 computes the value of the *stochastic sensing range* of the sensors. Lemma 7.2 states a sufficient condition for full *k*-coverage of a field while Lemma 7.3 states a sufficient condition to guarantee connectivity between sensors under our stochastic sensing model when both p_{th} and k are known.

Lemma 7.1: Let $k \geq 3$. The *stochastic sensing range* r_s of the sensors that is necessary to fully *k*-cover a field with a minimum number of sensors and with a probability no lower than $0 < p_{th} < 1$ is given by

$$r_s = \sqrt{3} \left(-\frac{1}{\beta} \log (1 - (1 - p_{th})^{1/k}) \right)^{1/\alpha} \quad (7.2)$$

where β is the physical characteristic of the sensors' sensing units and $2 \leq \alpha \leq 4$ is the path-loss exponent, which depends on the propagation model (free space model versus multi-path model). □

The upper bound on the stochastic sensing range r_s of the sensors computed in Equation (7.2) will be used as one of the input parameters to the *k-coverage candidacy* algorithm, which will be presented in Section 7.1.2. Figure 7.2 shows r_s for different values of p_{th} and k while considering the free-space model $(\alpha = 2)$ (Figure 7.2a) and the multi-path model $(\alpha = 3,4)$ (Figure 7.2b-c). As can be seen, r_s decreases as p_{th} and α increase. However, it increases with k. Indeed, to achieve higher degree of coverage, the stochastic sensing range of the sensors should increase.

Lemma 7.2: Let $k \geq 3$. A field is probabilistically fully *k*-covered with a probability no lower than $0 < p_{th} < 1$ if any Reuleaux triangle region of width r_s in the field contains at least k sensors. □

Lemma 7.3: Let $k \geq 3$. The sensors that are selected to *k*-cover a field with a probability no less than $0 < p_{th} < 1$ under our stochastic sensing model defined in Chapter 2 are guaranteed to be connected if the radius of their communication range is at least equal to r_s, the sensors' stochastic sensing range. □

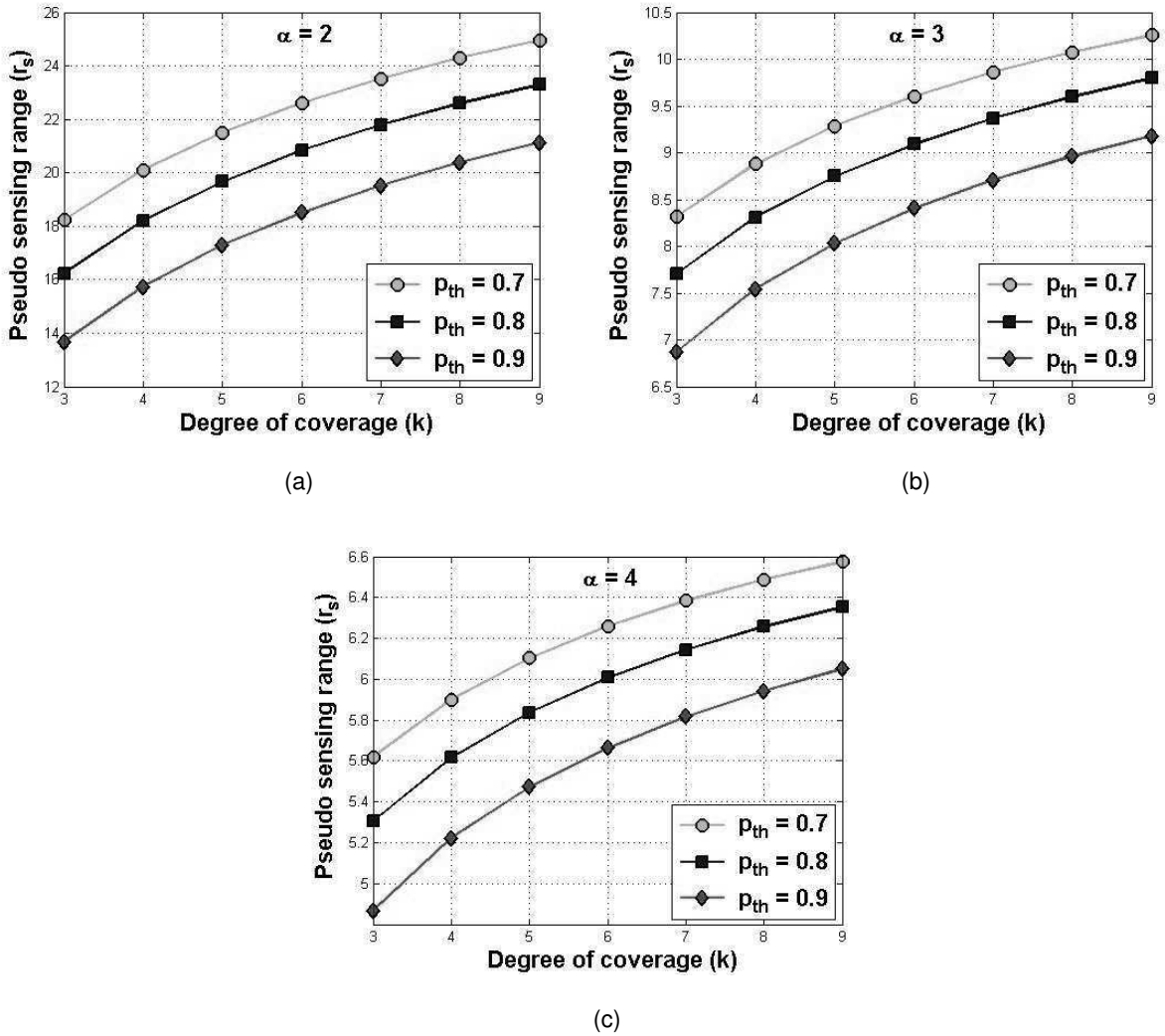

Figure 7.2: Upper bound of r_s vs. k for (a) α = 2, (b) α = 3, and (c) α = 4.

7.1.2 Stochastic *k*-Coverage-Preserving Scheduling

In this section, we focus on the design of a distributed sleep-wakeup scheduling protocol for stochastic *k*-coverage (SCP$_k$) of a field. The same approach could be applied for *k*-coverage under the deterministic sensing model by replacing r_s by r. We exploit the results of Chapter 5 to present a distributed approach for the selection of a minimum number of active sensors to *k*-cover a field under the

stochastic sensing model defined in Equation (2.2) of Chapter 2. This approach is different from the one presented in Chapter 5 in the sense that each sensor decides whether it is eligible to turn itself active. This decision is based on the degree of coverage of its sensing range. More specifically, each sensor runs our *k-coverage candidacy algorithm*, which is given in Figure 7.3, before it takes this decision.

```
ALGORITHM 1: k-COVERAGE-CANDIDACY(r_s,k)
(* This code is run by each sensor *)
Begin
/* Sensing range slicing */
1.  Randomly decompose sensing range into six
    overlapping Reuleaux triangles RT(r_s)_i, 1≤ i ≤ 6
/* Localized k-coverage candidacy checking */
2.  For each Reuleaux triangle RT(r_s)_i Do
3.    If RT(r_s)_i contains k active sensors Then
4.      Skip /* i.e., do nothing */
5.    Else
6.      Return ("candidate")
7.    End
8.  End
9.  Return ("non-candidate")
End
```

Figure 7.3 *k*-Coverage candidacy algorithm.

k-Coverage Candidacy Algorithm: A sensor turns active if its sensing disk is not *k*-covered. Precisely, a sensor randomly slices its sensing range into six overlapping Reuleaux triangle of width r_s and checks whether each one of them contains at least k sensors. Each sensor should know the status of its sensing neighbors only to decide whether it is candidate to turn active or not. If any of the six overlapping Reuleaux triangles of width r_s of the sensing range of a sensor s_i does not have k active sensors, the sensor s_i is a candidate to become active. Figure 7.3 shows the pseudo-code of our *k-coverage candidacy* algorithm.

State Transition of SCP_k: Figure 7.4 shows a state transition diagram associated with our *stochastic k-coverage protocol* (SCP_k). Likewise, the state transition diagram of is a bit similar to the one given in of Chapter 5 by replacing r with r_s. In this case, however, each sensor decides whether to turn itself on by running the *k-coverage candidacy* algorithm given in Figure 7.3.

At any time, a sensor can be in one of three states: READY, WAITING, and RUNNING.

- READY state: A sensor listens to messages and checks its candidacy to switch to the RUNNING state.

- RUNNING state: A sensor is active and can communicate with other sensors and sense the environment.
- WAITING state: A sensor is neither communicating with other sensors nor sensing a field, and thus its radio is turned *off*. However, after some fixed time interval, it switches to the READY state to check its candidacy for *k*-coverage (Figure 7.3) and receives messages.
- At the beginning of their monitoring task, all sensors are in the RUNNING state. Moreover, each sensor chooses randomly and independently of all other sensors a value t_{check} between 0 and t_{check_max} after which it runs the *k*-coverage candidacy algorithm (Figure 7.3) to check whether it stays active or not (i.e., switch to the WAITING state). Our intuition behind this random selection of t_{check} is to avoid as much as possible higher or lower coverage of any region in a field.
- When a sensor runs the *k*-coverage candidacy algorithm and finds out that it is a candidate, it sends out a NOTIFICATION-RUNNING message to inform all its neighbors. While in the READY state, a sensor keeps track of its sensing neighbors that are in the RUNNING state. If it finds out that its sensing area is *k*-covered, it will switch to the WAITING state.
- For energy efficiency purposes, a sensor may wish to switch from RUNNING state to WAITING state. For this purpose, a sensor broadcasts a RUNNING-to-WAITING message and waits for some transit time $t_{transit}$. If $t_{transit}$ expires and it has not received any RUNNING-to-WAITING message, it switches to the WAITING state and sends a NOTIFICATION-WAITING message, where it can stay there for t_{wait} time. When t_{wait} expires, it switches to the READY state, where it can stay for t_{ready} time. When a sensor in the READY state receives a RUNNING-to-WAITING message from its sensing neighbor, it runs the *k*-coverage candidacy algorithm to check whether it needs to turn active.

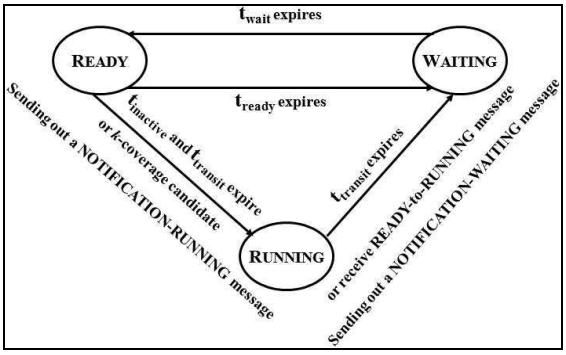

Figure 7.4 State transition diagram of SCP_k.

- If a sensor in the READY state finds out that it has not been active for some $t_{inactive}$ time, it will broadcast a READY-to-RUNNING message and wait for some $t_{transit}$ time. If $t_{transit}$ expires without receiving any other READY-to-RUNNING, it will send out a NOTIFICATION-RUNNING message and switch to the RUNNING state. Otherwise, it stays in the READY state. A sensor in the READY state would also apply the same process if it finds out that it has not heard from one of its sensing neighbors within some t_{alive} time. This means that this sensing neighbor has entirely depleted its energy and died. To this end, each sensor in the RUNNING state should broadcast an ALIVE message after each t_{active} time. We assume that each sensor stays active for at least t_{active} time.

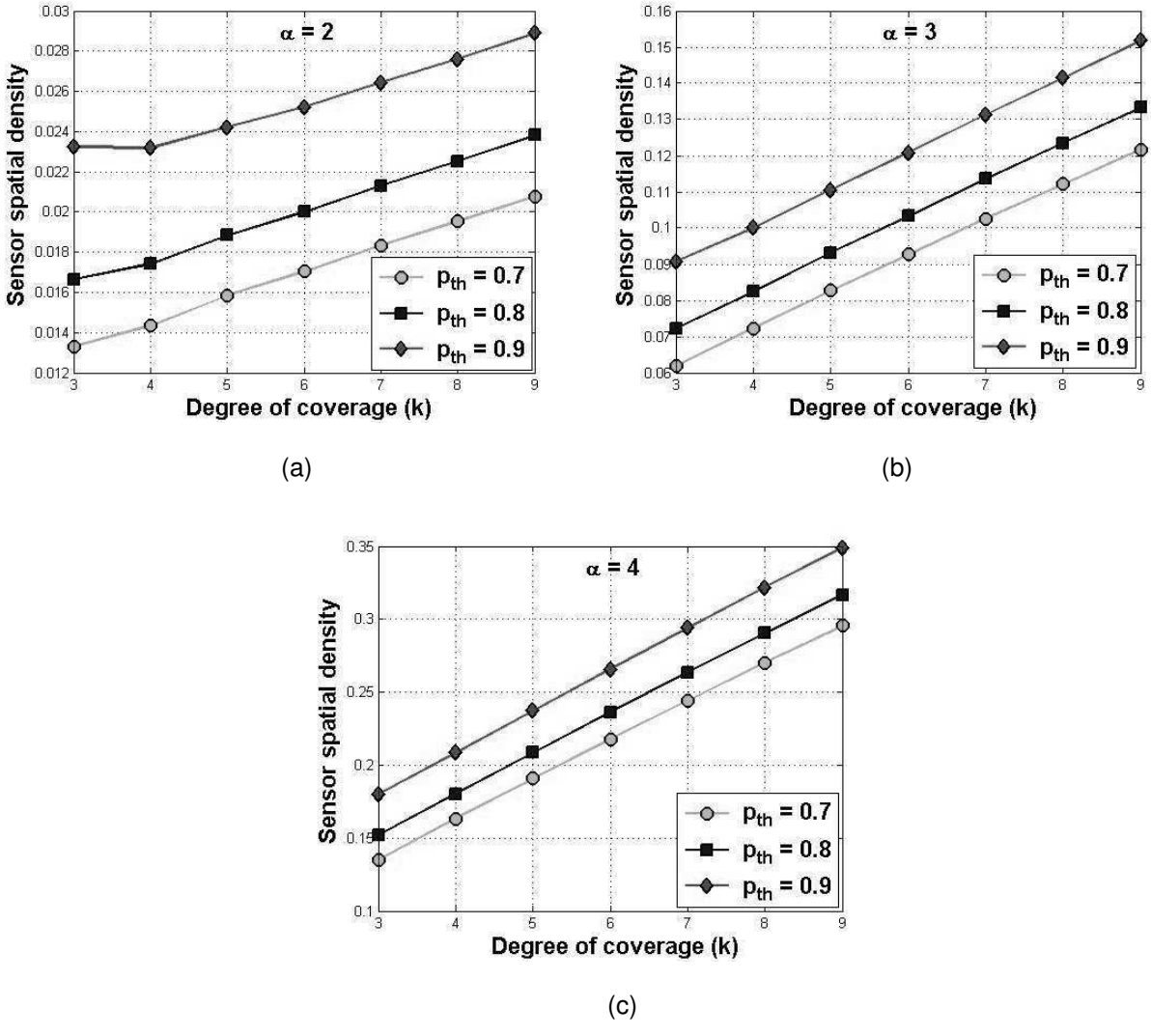

Figure 7.5 Sensor spatial density vs. degree of coverage k for (a) $\alpha = 2$, (b) $\alpha = 3$, and (c) $\alpha = 4$.

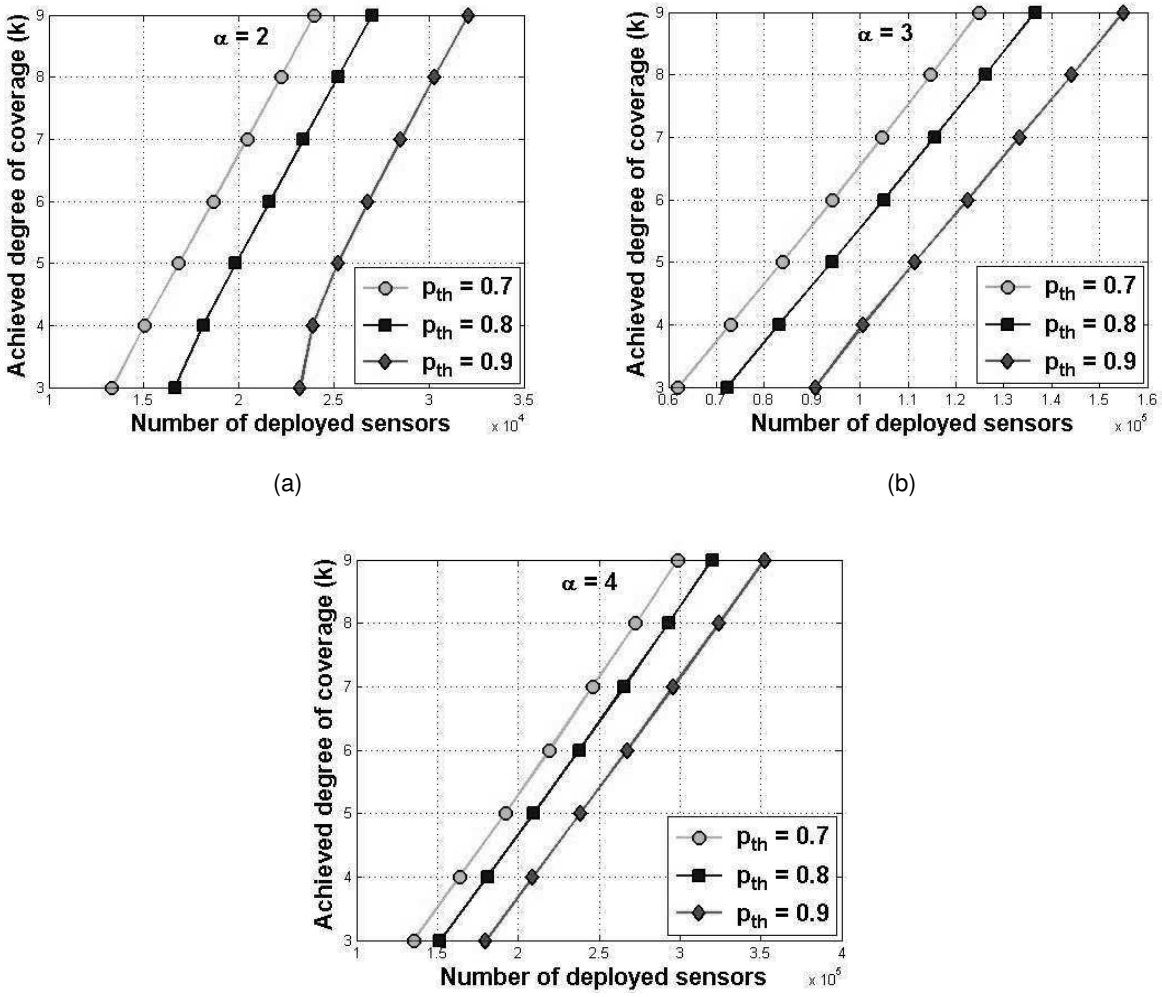

Figure 7.6 Degree of coverage k vs. number of deployed sensors for (a) $\alpha = 2$, (b) $\alpha = 3$, and (c) $\alpha = 4$.

7.1.3 Simulation Results

In this section, we present the simulation results of SCP_k using a high-level simulator written in the C programming language. We consider a square field of side length $1000\,\text{m}$. We use the energy model given in [171], where the sensor energy consumption in transmission, reception, idle, and sleep modes are 60 mW, 12 mW, 12 mW, and 0.03 mW, respectively. Following [176], the energy required for a sensor to stay idle for 1 second is equivalent to *one unit of energy*. We assume that the initial energy of each sensor is 60 Joules enabling a sensor to operate about 5000 seconds in reception/idle modes [171]. All simulations are repeated 20 times and the results are averaged.

In Figure 7.5, we plot the sensor spatial density as a function of the degree of coverage k for different values of the threshold probability p_{th} and path-loss exponent α. As expected, the density increases with p_{th} and α. Indeed, as we increase p_{th}, more sensors would be needed to achieve the same degree of coverage k. Recall that the width of the Reuleaux triangle that is guaranteed to be covered with exactly k sensors is equal to the stochastic sensing range of the sensors given in Equation (7.2) and hence decreases as p_{th} and α increase. On the other hand, the sensor density required for full *k*-coverage of a field is inversely proportional to the area of this Reuleaux triangle as stated in Lemma 7.2.

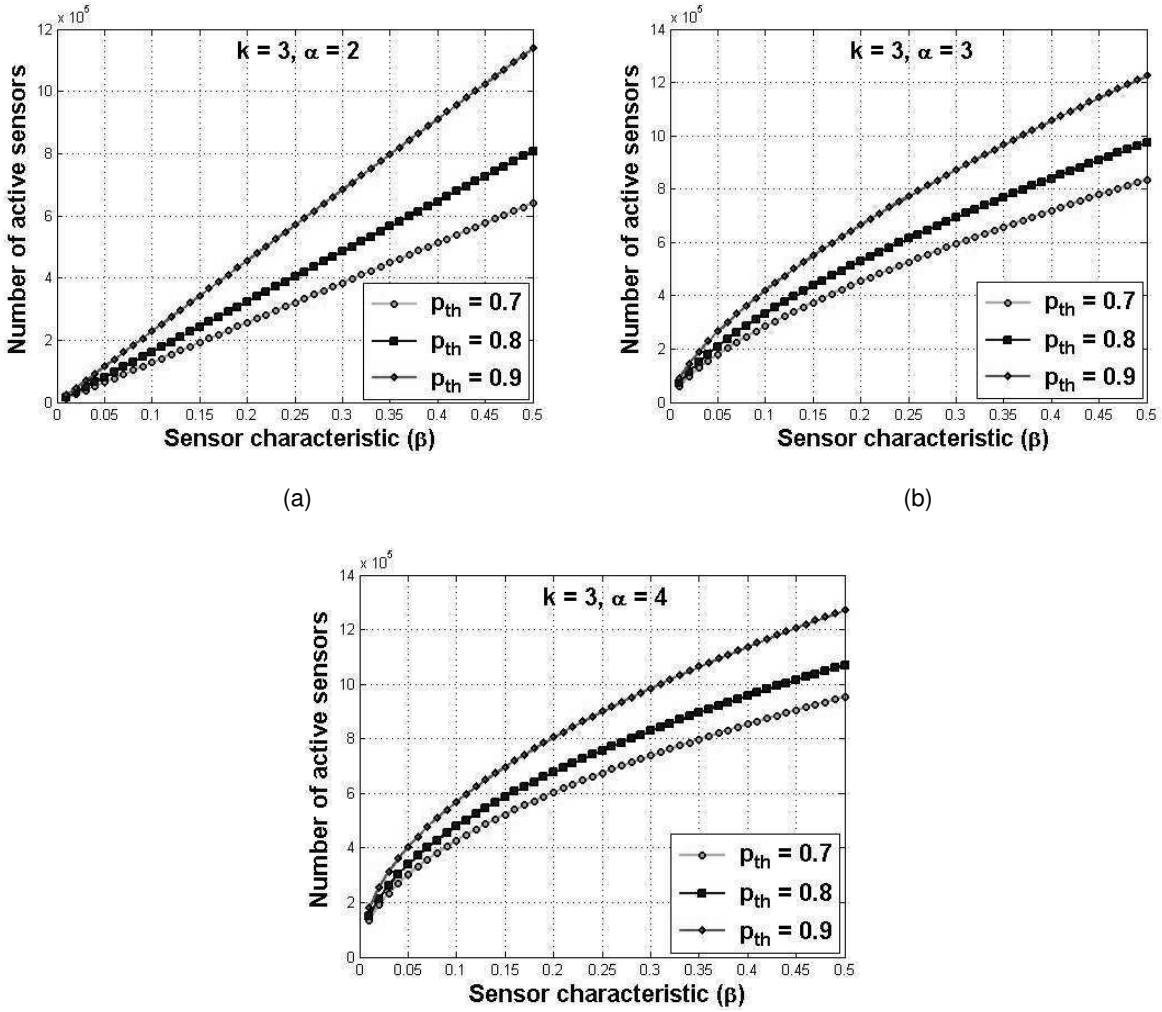

Figure 7.7 Number n_a of active sensors vs. number n_d of deployed sensors for $k = 3$ and (a) $\alpha = 2$, (b) $\alpha = 3$, and (c) $\alpha = 4$.

Figure 7.6 plots the achieved degree of coverage k versus the total number of deployed sensors. Moreover, we vary both p_{th} and α. Definitely, higher number of deployed sensors would yield higher coverage degree. Here also, any increase in p_{th} and α would require a larger number of deployed sensors to provide the same degree of coverage. Both experiments show a good match between simulation and analytical results. Figure 7.7 shows that the number of active sensors required to provide 3- coverage increases with the characteristic of the sensors β used in the definition of our stochastic sensing model presented in Chapter 2. Recall that β measures the uncertainty of the sensing units of the sensors. This result is expected given the definition of the stochastic sensing range in Equation (7.2).

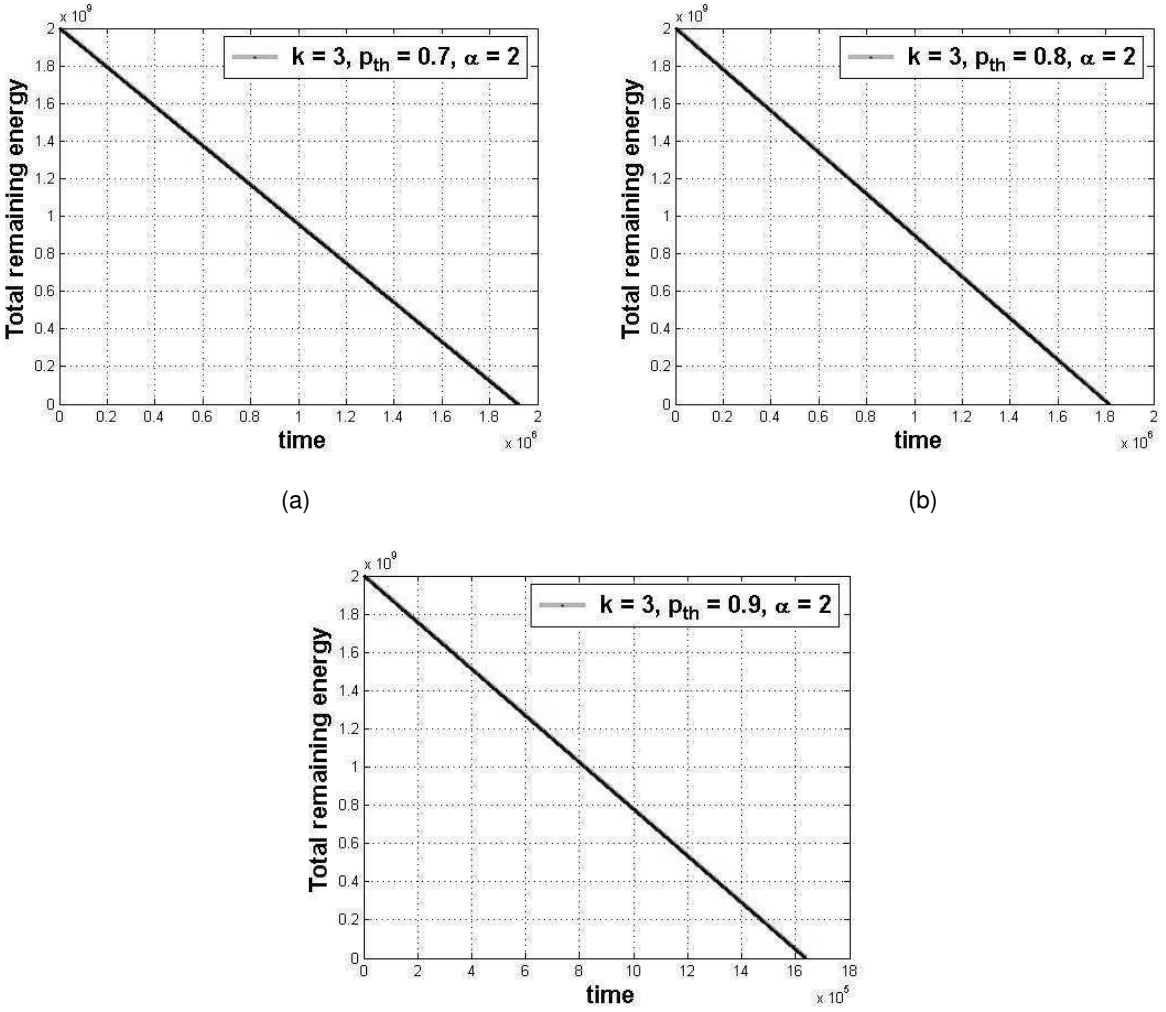

Figure 7.8 Total remaining energy vs. time for different $k = 3$, $\alpha = 2$, and (a) $p_{th} = 0.7$, (b) $p_{th} = 0.8$, and (c) $p_{th} = 0.9$.

Figure 7.8 shows the impact of p_{th} on the operational lifetime of the network to provide 3- coverage. As mentioned earlier, higher values of p_{th} require larger numbers of active sensors, and hence more energy consumption. To the best of our knowledge, the work in [166] is the only one on probabilistic *k*-coverage. However, the probabilistic sensing model used in [166] is totally different from ours. While our stochastic sensing model quantifies the detection probability of a sensor by an exponential function, the one in [166] only assigns it a constant value. Therefore, it is impossible to provide a fair quantitative comparison between our SCP_k protocol and the one in *et al.* [166]. Next, we focus on connected *k*-coverage and geographic forwarding in three-dimensional wireless sensor networks.

7.2 Three-Dimensional Connected *k*-Coverage and Geographic Forwarding

While coverage and geographic forwarding in two-dimensional wireless sensor networks have been well studied, three-dimensional wireless sensor networks have gained relatively less attention in the literature. In this section, we focus on the problem of forwarding in duty-cycled three-dimensional *k*-covered wireless sensor networks, where both *k*-coverage and data forwarding are discussed and addressed in a novel joint framework. We propose the first solution to the problem of geographic forwarding in duty-cycled three-dimensional *k*-covered wireless sensor networks. First, we analyze the *k*-coverage problem in three-dimensional wireless sensor networks and propose a distributed *k*-coverage protocol for three-dimensional wireless sensor networks. Second, we design a hybrid forwarding protocol for duty-cycled three-dimensional *k*-covered wireless sensor networks, which benefits from the advantages of both deterministic and opportunistic forwarding. Third, we relax some widely used assumptions to promote the use of our joint *k*-coverage and hybrid forwarding protocol in real-world scenarios. Finally, we evaluate the performance of our joint protocol. Our work is complementary to existing ones, especially those few works which dealt with three-dimensional wireless sensor networks. First, we propose a minimum-energy *k*-coverage protocol for three-dimensional wireless sensor networks. Indeed, Alam and Haas [7] considered only 1-coverage and proposed deterministic sensor placement strategies to achieve full coverage of a three-dimensional space. However, 1-coverage is not always enough given that sensors are not highly reliable and some applications, such intruder detection and tracking, require high coverage of a target field. Moreover, Kao *et al*. [99] did not consider duty-cycling in

three-dimensional wireless sensor networks. Thus, no other existing work addressed the problem of forwarding in duty-cycled three-dimensional *k*-covered wireless sensor networks, where uncertainty caused by duty-cycling is a true challenge. Our work proposes a solution to this problem.

7.2.1 Three-Dimensional Connected *k*-Coverage

First, we show the problem that we encounter when we attempt to extend our analysis of connected *k*-coverage in two-dimensional to three-dimensional wireless sensor networks. We refer to this problem as the *curse of dimensionality*, which is due to the fact that some properties that are valid for two-dimensional space cannot hold for three-dimensional space. Then, we propose an energy-efficient connected *k*-coverage protocol for three-dimensional wireless sensor networks.

7.2.1.1 Problem Analysis: The Curse of Dimensionality

In this section, we analyze the above problem from the perspective of the shape of a three-dimensional region C in a three-dimensional field corresponding to minimum *k*-coverage. In other words, we want to determine the shape of C so that it is guaranteed to be *k*-covered when exactly k sensors are deployed in it. Clearly, the *breadth* of C should be less than or equal to the radius r of the sensing spheres of sensors so that each location in C is within the sensing spheres of these k sensors. Since our goal is to achieve *k*-coverage of a three-dimensional field with a minimum number of sensors, the volume of C should be maximum, and hence the breadth of C must be equal to r. Therefore, our problem reduces to the problem of finding the shape of this three-dimensional region C that has a constant breadth equal to r.

In order to solve this problem, we consider *Helly's Theorem* [39] and apply the same analysis as in the case of two-dimensional space, which was described in Chapter 5. Thus, from Helly's Theorem, we infer that a three-dimensional $(n = 3)$ convex region C is *k*-covered by exactly k sensors $(|E| = k)$ if and only if C is 4-covered by any four $(m = 4)$ of those k sensors, where $k \geq 4$. Now, let us identify the shape of a three-dimensional convex region C whose breadth is constant and equal to the radius r of the sensing spheres of sensors, and hence has a maximum volume. More importantly, this region C should be guaranteed to be fully *k*-covered when *exactly* k sensors are deployed in it.

Let C_k be the intersection of k sensing spheres. Using Helly's Theorem [39], the maximum volume of the intersection of these k sensing spheres is equal to that of four spheres since $k \geq 4$. However, the maximum intersection (or overlap) volume of four sensing spheres such that the maximum distance between any pair of sensors is equal to r, corresponds to the configuration where the center of each sensing sphere is at distance r from the centers of all other three ones. In this configuration, the edges between the centers of these four spheres form a *regular tetrahedron* and the shape of their intersection volume is known as the *Reuleaux tetrahedron* [189] (Figure 7.9).

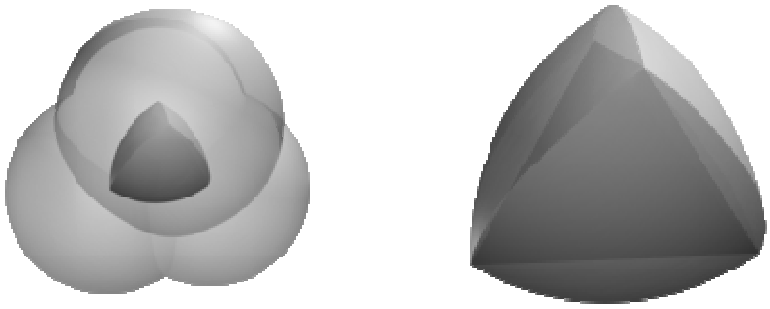

(a) (b)

Figure 7.9 (a) Intersection of four symmetric spheres and (b) their Reuleaux tetrahedron.

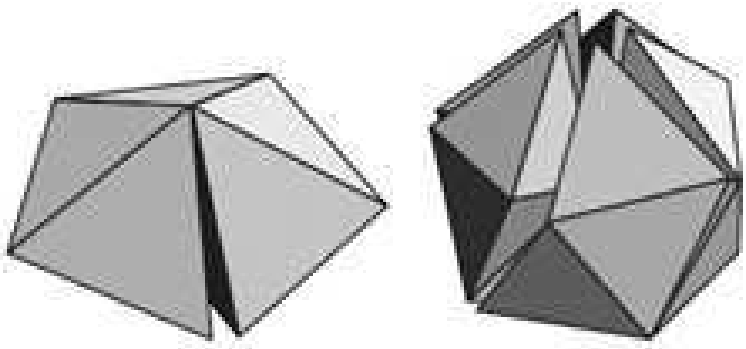

(a) (b)

Figure 7.10 (a) Five regular tetrahedra about a common edge and (b) twenty regular tetrahedra about a shared vertex [57].

In [16], [20], we used Helly's Theorem [39] in our analysis of the *k*-coverage problem and exploited the geometric properties of the Reuleaux triangle to derive a sufficient condition to fully *k*-cover a two-dimensional field. Note that the Reuleaux triangle of side r, which represents the intersection of three symmetric, congruent disks of radius r, consists of a central regular triangle of side r and three curved

regions. More importantly, it has a constant width equal to r [188]. We found that a Reuleaux triangle region of width r of a two-dimensional field is guaranteed to be *k*-covered with exactly k sensors, where r is the radius of the sensing range of the sensors [20]. Also, the regular triangle allows a perfect tiling of two-dimensional space. Based on this characterization, we designed an energy-efficient *k*-coverage configuration protocol for two-dimensional wireless sensor networks [16], [20].

Now, we provide some facts why the Reuleaux tetrahedron is not an appropriate solution to our *minimum connected k-coverage* problem. First of all, the Reuleaux tetrahedron does not have a constant breadth whose value is slightly larger than the radius r of the corresponding spheres [189]. In contrast to the regular triangle, the regular tetrahedron does not allow a perfect tiling of a three-dimensional space. Indeed, Conway and Torquato showed that the dihedral angle of a regular tetrahedron is equal to 70.53º, which is not sub-multiple of 360º [57]. They also gave two arrangements of regular tetrahedra such that five regular tetrahedra packed around a common edge would result in a small gap of 7.36° as shown in Figure 7.10a, and that twenty regular tetrahedra packed around a common vertex yield gaps that amount to a solid angle of 1.54 steradians as shown in Figure 7.10b [57]. This shows that some properties that hold for two-dimensional space are not valid for three-dimensional space. Thus, the extension of the analysis of *k*-coverage in two-dimensional space [20] to three-dimensional space is not straightforward, and hence another approach should be used. More precisely, we want to address the following question: *What is the "closest shape" to the Reuleaux tetrahedron that will guarantee energy-efficient k-coverage of a three-dimensional space?*

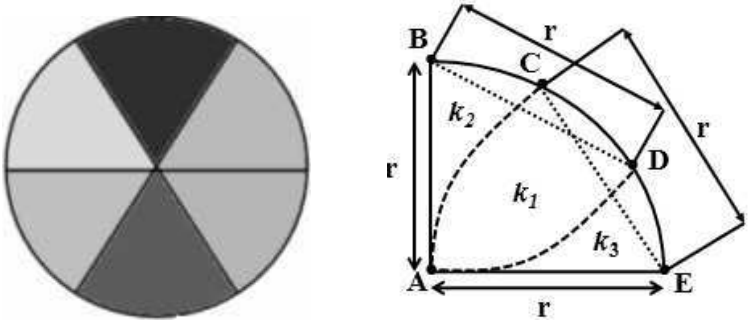

(a) (b)

Figure 7.11 Two-dimensional projection of (a) a half-sphere and its six slices, and (b) a slice.

To address this question efficiently, we consider two halves of the sensing sphere of the sensors, i.e., the top half and bottom half. Note that in two-dimensional wireless sensor networks, we divide the sensing disk of the sensors into six overlapping Reuleaux triangles [20]. By analogy with the two-dimensional analysis given in [20], we divide each of the halves of a sensing sphere into six congruent three-dimensional regions, called *slices*, each of which has three flat faces and one curved face representing an *equilateral spherical triangle* (Figure 7.11a). Unfortunately, the distance between the point B at the top of a slice and all the points E on the edge of any spherical triangle is larger than r. Thus, a sensor located at B cannot cover any point E and a sensor located at any point E cannot cover B. Any sensor located in the region $< A,C,D >$ is able to cover the whole slice as shown in Figure 7.11b,. However, sensors located in the regions $< A,B,C >$ and $< A,D,E >$ cannot cover the entire slice. Thus, if $k_1 = k,$ then $k_2 = k_3 = 0;$ otherwise, $k_2 = k_3 = k - k_1.$ In other words, to guarantee *k*-coverage of a slice and hence a sensing sphere with a minimum number of sensors, it is necessary that active sensors should be located in the region $< A,C,D >,$ thus efficiently solving the *minimum connected k-coverage* problem.

Theorem 7.2, which follows from the above analysis, states a *tight sufficient condition* for *k*-coverage of a three-dimensional field.

Theorem 7.2: Let $k > 1.$ A three-dimensional field is *k*-covered if any slice of the field contains at least k active sensors. □

Theorem 7.3, which follows from Theorem 7.2, computes the *minimum sensor spatial density necessary* to fully *k*-cover a three-dimensional field.

Theorem 7.3: Let r be the radius of the sensing spheres of sensors and $k > 1.$ The minimum sensor spatial density required to guarantee *k*-coverage of a three-dimensional field is computed as

$$\lambda(r,k) = \frac{9k}{\pi r^3}$$

Proof: The volume of a slice is $vol(slice) = \pi r^3/9.$ By Theorem 7.2, each slice should contain at least k sensors. Thus, *k*-covering a three-dimensional field with a minimum number of sensors requires that every slice in the three-dimensional field contain exactly k sensors. Thus, the minimum sensor density to *k*-cover a three-dimensional field is equal to $k/vol(slice).$ □

Using Theorem 7.2, Theorem 7.4 states a sufficient condition to maintain connectivity in three-dimensional *k*-covered wireless sensor networks.

Theorem 7.4: Let $k > 1$. A three-dimensional *k*-covered wireless sensor network is connected if $R \geq r$, where r and R stand for the radii of the sensing and communication spheres of sensors, respectively. □

Algorithm 1: k-Coverage-Candidacy
(* This code is run by each sensor *)
Begin
/* Sensing sphere slicing */
1. Randomly decompose a sensing sphere
   into twelve slices
/* Localized *k*-coverage candidacy checking */
2. For each slice Do
3. If it contains *k* awake sensors Then
4. Skip /* i.e., do nothing */
5. Else
6. Return ("candidate")
7. End
8. End
9. Return ("non-candidate")
End

Figure 7.12 *k*-Coverage-Candidacy algorithm.

7.2.1.2 Our Distributed *k*-Coverage Protocol

In this section, we describe our *distributed k-coverage protocol* (DCP_k) for three-dimensional field. First, we present our algorithm that enables a sensor to check its *candidacy* to become active.

k-Coverage-candidacy algorithm: A sensor turns active if its sensing sphere is not *k*-covered. Based on Lemma 5.2 (see Chapter 5), a sensor randomly decomposes its sensing sphere into twelve slices of side r and checks whether each one of them contains at least k sensors. Each sensor should know the status of its sensing neighbors only to decide whether it is candidate to turn active or not. If any of the twelve slices does not have k active sensors, a sensor is a candidate to become active. Else, it is not. Figure 7.12 shows the pseudo-code of our *k*-Coverage-Candidacy algorithm.

State Transition Diagram of DCP_k: We use the same state transition diagram described in Section 7.1.2.

7.2.2 Hybrid Geographic Forwarding

In this section, we propose a protocol, called *hybrid geographic forwarding on a duty-cycled three-dimensional k-covered wireless sensor network* (HYGF-DC$_k$). Sensors that can forward data are called *relays*.

In *deterministic forwarding*, a sensor chooses a next best forwarder based on some metric and forwards data to it, i.e., the next forwarder is determined *a priori*. In *opportunistic forwarding*, however, a next best forwarder is decided on-the-fly and after the data is transmitted. Because of duty-cycling, sensors holding data to be forwarded to the sink and using deterministic forwarding are not totally certain that their currently awake sensing neighbors would remain awake after data is being forwarded. Clearly, duty-cycling introduces *uncertainty* at the sender side when selecting a next best forwarder, thus making opportunistic forwarding a most suitable approach. However, with opportunistic forwarding, several active sensors may hear the transmitted data, thus creating high contention at the receiver side to select a next best forwarder. Thus, it is important to find a *trade-off* between *uncertainty* due to duty-cycling with deterministic forwarding, and *contention* due to opportunistic forwarding. Next, we describe our hybrid forwarding approach in details.

Our hybrid forwarding protocol HYGF-DC$_k$ takes advantages of both deterministic and opportunistic forwarding approaches in order to achieve good data forwarding performance in terms of data delivery ratio, delay, and control overhead. First, we define the notion of *potential energy* of a sensor.

As mentioned earlier, only sensors currently active to *k*-cover a three-dimensional field act as *relays*, i.e., can participate in data forwarding. Precisely, a sender s_i specifies in its data packet the id's of the next best p *candidate relays* with descending priorities (i.e., the first one has highest priority while the last one has the lowest priority) and broadcasts it using a transmission distance equal to r. Recall that the sensing sphere of a sensor has six slices, each of which has width equal to r. While the first sensor is the *primary relay*, the other $p-1$ sensors act as *backup relays*. The priorities assigned by s_i to sensors are based on the knowledge it has about their *activity time*, i.e., the time interval a sensor has been recently awake (or active), where high priority means high small *activity time*. If there is a tie, s_i would break it using the knowledge it has about their *potential energy*. Thus, s_i sorts its active sensing neighbors based

on their priority defined earlier and chooses the first p ones as candidate relays. The question we want to address now is: *which slice, c*all*ed target slice, the next best* p *candidate forwarders are selected from*? First, a sensor s_i randomly decomposes its sensing sphere into twelve slices (Figure 7.11b). The *target slice* is the one that is traversed by a segment line between the locations of s_i and the sink s_m. Given that all next best p candidate *relays* belong to the same slice, they are guaranteed to be connected to each other. Precisely, they are within sensing range of each other, and hence can be aware of the status of each other (i.e., awake vs. asleep). Thus, the problem of multiple transmissions does not arise in our approach. When a sensor forwards a data packet towards the sink, it would also send an ACK to the sender from which it has received the packet. This would allow all potential relays to know that the underlying data packet has been successfully forwarded to the sink, i.e., no more action is needed by all other candidate relays.

When a sensor that is not located in a target slice receives data, it would simply ignore it. Otherwise, it checks whether it is one of the next best p candidate relays. If so, it checks its priority and if it is the highest or the other next best $p-1$ candidate relays are not awake, it would forward the data packet towards the sink using the same approach as the original sender. However, when a sensor that is located in a target slice receives data and the next best p candidate forwarders are not awake, it is considered as a *potential relay*. It would run the *opportunistic component* of our hybrid forwarding protocol. First, we define the *competition function* $\varphi(l,m)$ of a potential relay s_l as the ratio of its potential energy $\pi(s_l)$ to the Euclidean distance $\delta(s_l,s_m)$ between it and the sink s_m, i.e.,

$$\varphi(l,m)=\frac{\pi(s_l)}{\delta^{\alpha}(s_l,s_m)}$$

Intuitively, preference is given to potential relays that have higher potential energy and are closer to the sink. The opportunistic component of our hybrid forwarding protocol is based on the following lemma [39] (page 64), which adds some randomness to the selection process of a potential relay:

Lemma 7.4 (Loaded Dice [39]): No matter what two loaded dices we have, it cannot happen that each of the sums 2, 3, …, 12 comes up with the same probability. □

ALGORITHM 2: HYGF-DC$_k$

Procedure Official_Relay_Declared
Begin
1. s_l forwards sensed data to the sink s_m
2. s_l sends an ACK to the sensed (i.e., previous relay)

End
Begin
/* This code section is run by a sender */
1. Sort all potential relays in a descending order of their most recent time activity and break their tie using their closeness to the sink s_m
2. Select the first p candidate relays as one *primary* and $p-1$ *back-up relays*, store them in a sensed data packet, and broadcast it using a transmission distance equal to r

/* This code section is run by a candidate relay s_l */
3. If s_l is active primary relay Then
4. s_l forwards sensed data to the sink s_m
5. Else
6. If s_l is highest-priority, active back-up relay Then
7. s_l forwards sensed data to the sink s_m
8. Else /* all other potential relays */
9. Generate two random numbers in [1..6] and compute their sum
10. Compute the competition function $\varphi(l,m)$
11. Broadcast $BID(s_l) =< id_1, val, \varphi(l,m), id_2 >$

/* Compare $BID(s_l)$ to all received $BID(s_j)$ broadcast by potential relays s_j */
12. If $val(s_l) > \max\{val(s_j))$ Then
13. Call Official_Relay_Declared
14. Else
15. If $val(s_l) = \max\{val(s_j)) \wedge \varphi(l,m) > \max\{\varphi(j,m)\}$
16. Then Call Official_Relay_Declared
17. Else
18. If $val(s_l) = \max\{val(s_j)) \wedge \varphi(l,m) = \max\{\varphi(j,m)\}$ and $id(l) > \max\{id(j)\}$ Then
19. Call Official_Relay_Declared
20. End
21. End
22. End
23. End
24. End
25. Return
End

Figure 7.13 Joint *k*-coverage and hybrid forwarding protocol.

Each potential relay s_l runs the following steps:

- Flips two loaded dices (i.e., randomly generates two numbers in [1..6]) and computes their sum *val*.
- Computes its competition function $\varphi(l,m)$.
- Builds a small packet $BID(s_l)$ containing the quadruplet $< id_1, val, \varphi(l,m), id_2 >$ and broadcasts it within its sensing range only, where id_1 is the id of a sender of a sensed data packet and id_2 is the id of s_l.

Any active sensor s_a that receives $BID(s_l)$ will have to run the following sequence of steps:

- Checks whether it is a *potential relay* for the underlying data packet by looking at the first field id_1 of $BID(s_l)$. If not, it just drops the packet. Else, it runs the next step.
- Compares its random value (generated by flipping two loaded dices) to the second field val of all $BID(s_l)$. If it is smaller, s_a cannot be a candidate relay. If both values are equal, it compares the value of its competition function with the third field $\varphi(l,m)$ of all $BID(s_l)$. If it is smaller, it does not consider itself as a candidate relay. If it is equal, it compares its id with the fourth field id_2 of all $BID(s_l)$. If it is smaller, s_a is not a candidate relay.

As can be seen, the official relay of a sensed data packet is the one with the highest value of the second field val. The values of the other two fields, namely the value of competition function and *id*, are used to break ties. At the end of this selection process, the potential relay that has been designated as an *official relay* would forward the data packet to the sink and send back an ACK to the sender of the data.

Note that the opportunistic component of our hybrid approach requires a *little coordination* between potential relays. The pseudo-code of HYGF-DC$_k$ is given in Figure 7.13.

7.2.3 Performance Evaluation

In this work, we propose the first analysis and solution to the problem of joint *k*-coverage and forwarding in duty-cycled three-dimensional wireless sensor networks. Thus, it is impossible to provide a fair quantitative comparison between our protocols and other existing ones, such as ExOR [38], CKN [133], and GeRaF [184], which were proposed for two-dimensional wireless sensor networks. Also, CKN [133] considered only 1-coverage while Kao *et al*. [99] did not consider duty-cycling. In this section, we

evaluate the performance of HYGF-DC$_k$ with a high-level simulator written in the C programming language.

We consider a cubic sensor field of side length $1000\,\mathrm{m}$ where all sensors are randomly and uniformly deployed. We use the energy model used in [171], where the sensor energy consumption in transmission, reception, idle, and sleep modes are 60 mW, 12 mW, 12 mW, and 0.03 mW, respectively. Following [176], *one unit of energy* is defined as the energy required for a sensor to stay idle for 1 second. We assume that the initial energy of each sensor is 60 Joules enabling a sensor to operate about 5000 seconds in reception/idle modes [171]. All simulations are repeated 20 times and the results are averaged.

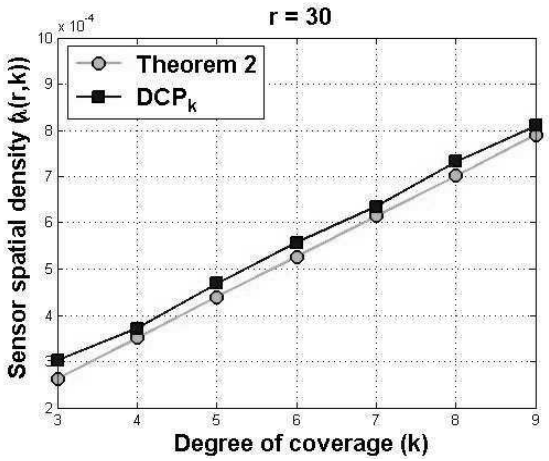

Figure 7.14 $\lambda(r,k)$ vs. *k*.

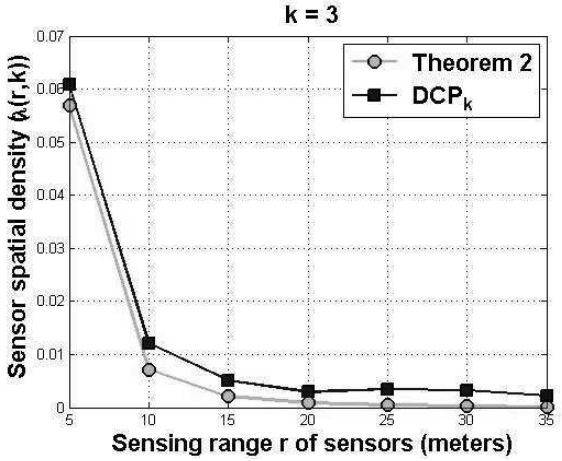

Figure 7.15 $\lambda(r,k)$ vs. *r*.

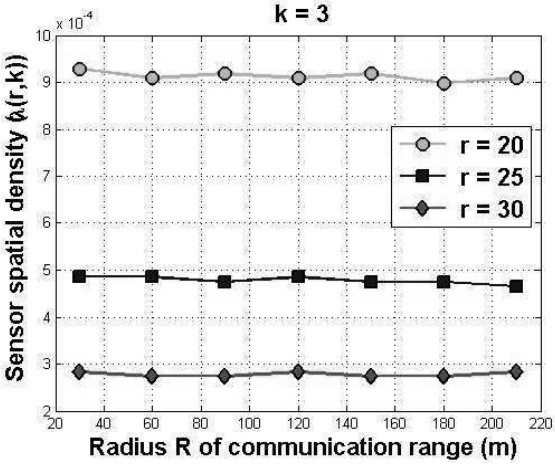

Figure 7.16 $\lambda(r,k)$ vs. *R*.

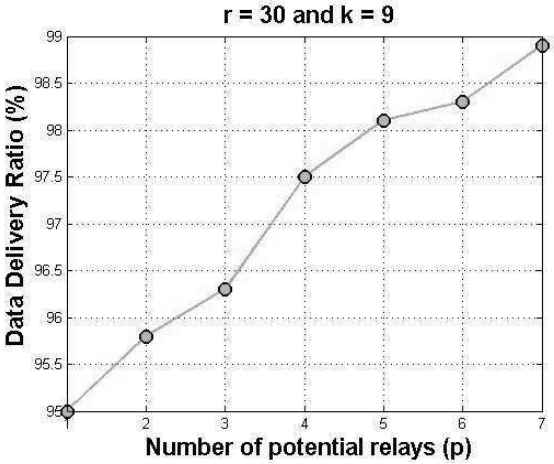

Figure 7.17: Data delivery vs. *p*.

Figure 7.14 plots the sensor spatial density $\lambda(r,k)$ versus the coverage degree k, where the radius r of the sensing range of sensors is equal to $30\,\mathrm{m}$. We observe a close to perfect match between our simulation and analytical results. Notice that $\lambda(r,k)$ increases with k for a fixed r. Indeed, higher coverage degree of a field would require more active sensors.

Figure 7.15 plots $\lambda(r,k)$ versus the radius r of the sensing range of sensors, where the degree of coverage k is equal to 3. We observe that $\lambda(r,k)$ decreases with r for a fixed k. In fact, sensors with larger sensing range would cover more areas and hence less number of active sensors is required to achieve a certain coverage degree k of a field.

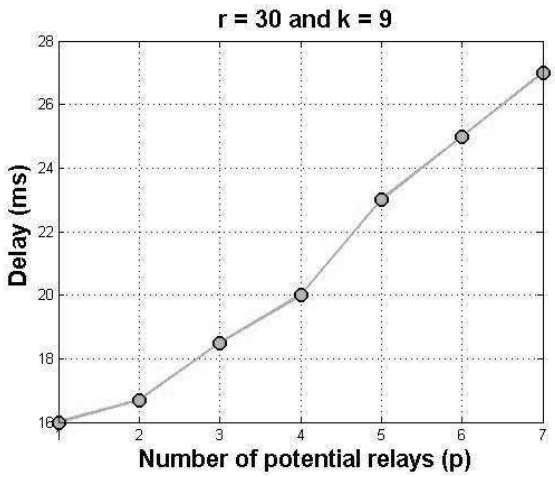

Figure 7.18 Delay vs. *p*.

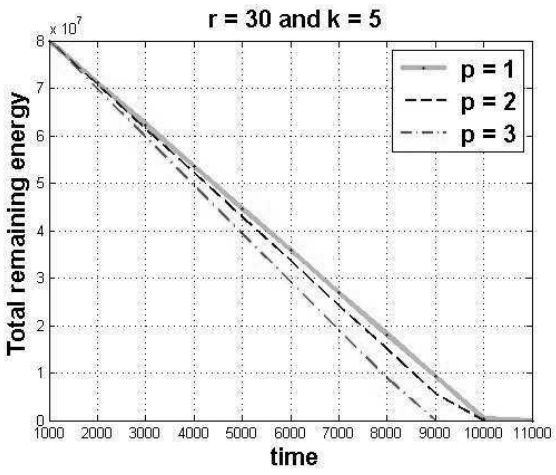

Figure 7.19 Remaining energy vs. *p*.

Figure 7.16 plots $\lambda(r,k)$ versus the radius R of the communication range of sensors for different values of the radius r of their sensing range, where the degree k of coverage is equal to 3. Notice that $\lambda(r,k)$ does not increase with R. Indeed, as we have found in Theorem 7.3, the sensor spatial density $\lambda(r,k)$ of active sensors to *k*-cover a field depends only on the radius r of the sensing range of sensors. Also, our *k*-coverage protocol DCP_k is based on the sensing range of sensors in the sense that each sensor guarantees that its sensing range only is *k*-covered.

Figures 7.17, 7.18, and 7.19 show the impact of the number of *candidate relays* on the performance of our *k*-coverage and hybrid forwarding protocol HYFGF-DC_k. As we increase the number p of *candidate relays*, the data delivery ratio (i.e., percentage of sensed data packets successfully received by the sink)

increases (Figure 7.17). Notice that the setting $p = 1$ corresponds to deterministic forwarding. When a single sensor is selected as a candidate relay $(p = 1),$ there is no guarantee that after data transmission this selected sensor would remain active. If it does not stay active, data packets destined to it would never reach the sink. Thus, the presence of multiple candidate relays increases the chance that sensed data would reach the sink. However, this improvement of data delivery ratio would lead to additional delay (Figure 7.18) and more energy consumption (Figure 7.19). Indeed, candidate relays need to exchange their local data to identify the best one of them as a relay. This process, however, needs more time and control overhead. These simulation results show that opportunistic forwarding helps improve data delivery ratio but requires more delay. However, deterministic forwarding yields better delay but does not guarantee high data delivery ratio. Our hybrid forwarding protocol on duty-cycled three-dimensional wireless sensor networks benefits from these nice features of opportunistic and deterministic schemes.

7.3 Summary

In this chapter, we have proposed a distributed approach to solve the scheduling problem in stochastic *k*-covered wireless sensor networks [23], where the sensing ability of the sensors is represented by a probability function. Indeed, stochastic sensing models are more realistic than the deterministic sensing model, which does not capture the probabilistic nature of the sensors' characteristics. Our methodology is based on a geometric analysis using the Reuleaux triangle model. For problem tractability, we have considered the deterministic sensing model and then extended the analysis to a stochastic sensing model. First, we have characterized *k*-coverage in wireless sensor networks and provided a necessary and sufficient condition to achieve *k*-coverage with a minimum number of sensors. Then, we presented our *k*-coverage-preserving scheduling protocol (SCP_k) based on this characterization. Precisely, sensors activate themselves by running a *k*-coverage candidacy algorithm to ensure that their sensing ranges are *k*-covered. We have found a good match between simulation and analytical results.

We have also investigated the problem of joint *k*-coverage and geographic forwarding in duty-cycled three-dimensional wireless sensor networks [19]. We have found that our model for *k*-coverage in wireless sensor networks does not generalize to three-dimensional wireless sensor networks due to the inherent characteristics of the Reuleaux tetrahedron that totally differ from those of its two-dimensional Reuleaux

triangle counterpart. Hence, we have proposed a new model and derived the minimum sensor spatial density to guarantee full *k*-coverage of a three-dimensional field. Furthermore, we have designed a hybrid geographic forwarding protocol for duty-cycled three-dimensional *k*-covered wireless sensor networks, thus combining both deterministic and opportunistic forwarding schemes. We have also relaxed some assumptions to promote the practicality of our joint protocol and evaluated its performance.

CHAPTER 8

INVESTIGATING THE ENERGY SINK-HOLE PROBLEM AND ITS SOLUTIONS

One way to extend the lifetime of a wireless sensor network is through load balancing so that all sensors deplete their energy slowly and uniformly during their monitoring activity. Particularly, the behavior of the sink has an impact on the network lifetime. Indeed, static always-on wireless sensor network (i.e., the radios of the sensors are turned on all the time) are much affected by the *energy sink-hole* problem, where sensors located around a sink suffer from severe battery power depletion problem. Indeed, the sensors close to the sink act as relays to the sink on behalf of *all* other sensors, and hence deplete their battery power more quickly, thus leading to possible disconnection of the network and disruption of the sensed data from reaching the sink. It was proved that it is impossible to guarantee uniform energy depletion of all the sensors in static, uniformly distributed, always-on wireless sensor network with constant data reporting to the sink when sensors use their maximum communication range to transmit sensed data to the sink [117], [120], [136], [162].

The deployment of static sink and sensors in real-world applications is very common, and hence efficient solutions should be provided to tackle the *energy sink-hole* problem, which is inherent to static wireless sensor networks. We believe that the network lifetime depends on three key design metrics, namely type of data forwarding (long range vs. short range), type of sensors (homogeneous vs. heterogeneous), and type of sink (static vs. mobile). This motivates us to account for these three design metrics in order to the energy sink-hole problem. First, we consider the *transmission distance* that distinguishes between short-range and long-range forwarding. Second, we consider *sensor heterogeneity* when deploying sensors for its ability to improve the reliability of the network and extend its lifetime [63], [169]. Third, when sensors have the same initial energy, we consider *sink mobility* for its ability to evenly distribute the data forwarding load among all the sensors to extend the network lifetime [158].

The remainder of this chapter is organized as follows: Section 8.1 analyzes the energy sink-hole problem and proposes a restricted solution [12]. Section 8.2 exploits energy heterogeneity to solve the

energy sink-hole problem [12]. Section 8.3 makes use of the sink mobility and our new proposed concept of energy aware Voronoi diagram [12] to solve the energy sink-hole problem for homogeneous wireless sensor networks. Section 8.4 concludes the chapter.

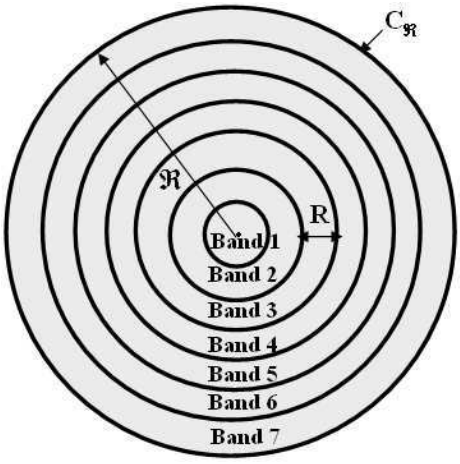

Figure 8.1 Slicing field into circular bands.

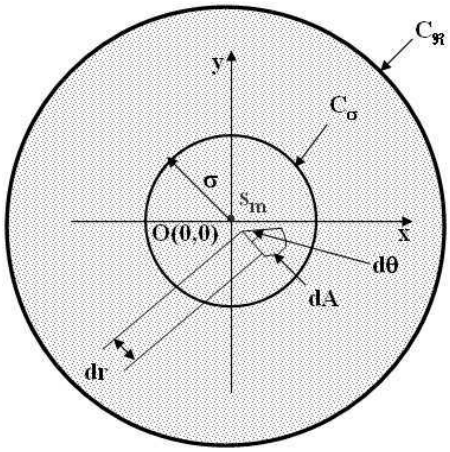

Figure 8.2 Circular field with a centered static sink.

8.1 Energy Sink-Hole Problem Analysis

We consider always-on wireless sensor networks, where the sensors constantly report their sensed data to a single static sink. Hence, the sensor cannot be turned off while monitoring a physical phenomenon. We assume that the sensors are static and uniformly distributed in a circular field of radius $\Re$ with sensor spatial density λ (Figure 8.1).

First, we discuss a *base protocol*, where the network has a static sink and uses a short-path routing protocol [75]. The static sink is supposed to be located at its optimum position in terms of energy efficient data gathering, which corresponds to the center of the field [125]. We will show that the sensors around the sink have higher energy consumption than all other sensors.

8.1.1 Base Protocol Average Energy Consumption

The model that we use to compute the maximum average energy consumption of sensors is similar to the model in [74]. The average energy consumption of a node located in an area of size A_2 that forwards traffic for other nodes located in another area of size A_1 is proportional to $A_1 + A_2 / A_2$. Our model focuses on the nodes within a distance $\ell \le \sigma \le R$ from the sink, where R is the radius of the nominal communication range of sensors and $\ell << R.$ Specifically, we consider a circle C_σ of radius σ

around the sink s_m which includes the most active forwarders to the sink, where $\ell \le \sigma \le R$ and ℓ is an infinitesimal value, as shown in Figure 8.2. The number of sensors inside and outside C_σ is $\lambda \pi \sigma^2$ and $\lambda \pi (\Re^2 - \sigma^2)$, respectively, where $\Re$ is the radius of the circular field $C_\Re$ and λ is the sensor spatial density. Let r be the radius of an infinitesimal circular region whose area is $dA = r\, dr\, d\theta$, where $0 \le r \le \sigma$ and $0 \le \theta \le 2\pi$. The average distance between a sensor in C_σ and the sink s_m is computed as

$$d_{\text{avg}} = \frac{1}{\pi \sigma^2} \int_{C_\sigma} r\, dA = \frac{2\sigma}{3}$$

The energy consumption rate per sensor in C_σ is given by

$$ER(C_\sigma) = ER(C_\sigma, s_m) + ER(\overline{C_\sigma}, s_m)$$

where $ER(C_\sigma, s_m)$ is the average energy consumption rate per sensor in C_σ to directly send its data to the sink, and $ER(\overline{C_\sigma}, s_m)$ is the average energy consumption rate per sensor in C_σ to forward a subset of sensed data packets originated from sensors in $\overline{C_\sigma} = C_\Re - C_\sigma$ to the sink. Using the energy model in Chapter 2 (see Section 2.4), we obtain

$$ER(C_\sigma, s_m) = \frac{1}{\lambda \pi \sigma^2} \times \int_{C_\sigma} ER_{tx}(r)\, \lambda\, dA = (E_{elec} + \frac{2\varepsilon}{\alpha + 2} \sigma^\alpha)\, b$$

$$ER(\overline{C_\sigma}, s_m) = \frac{\pi (\Re^2 - \sigma^2)}{\pi \sigma^2} \left(2\, E_{elec} + \varepsilon \left(\frac{2\sigma}{3} \right)^\alpha \right) b$$

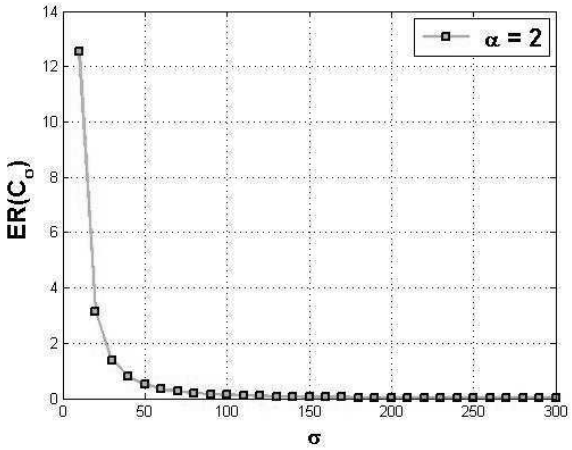

Figure 8.3 Plot of $ER(C_\sigma)$.

Thus, the energy consumption rate per sensor using the base protocol is given by

$$ER(C_\sigma) = b\,\varepsilon\left(\frac{2}{\alpha+2}+\left(\frac{2}{3}\right)^{\alpha}\right)\sigma^{\alpha}+\left(\frac{2\,\Re^2}{\sigma^2}-1\right)b\,E_{elec}$$

Figure 8.3 shows that $ER(C_\sigma)$ increases significantly as we approach the center of the field (i.e., location of the sink). It is clear that all sensed data will be forwarded by sensors whose distance from the sink is at most equal to $R = 300\,\text{m}.$ Hence, we slice the field $C_\Re$ into *concentric circular bands* (or simply *bands*) of width R (Figure 8.1) and assume that the field has $k > 1$ bands such that $\Re = k\,R.$

8.1.2 Nominal Communication Range–Based Data Forwarding

Under the above-mentioned field slicing method, the energy consumption rate of sensors depends on which band they belong to as well as the communication range used in reporting their data to the sink. We assume that sensors are homogeneous and use their nominal communication range.

Lemma 8.1 proves that sensors located in the k^{th} (i.e., outmost) band consume less energy than all other sensors.

Lemma 8.1: Assume a uniform sensor distribution with spatial density λ and sensors constantly transmit their data to the sink using their nominal communication range of radius $R.$ Sensors located in the k^{th} band have longer lifetime than all sensors in the network.

Proof: Any sensor located in the k^{th} band has only to report its own data to the sink. Indeed, given that the communication range of sensors coincides with the width of the bands, no one of the sensors in the k^{th} band can participate in forwarding data to the sink on behalf of others. Using the energy model in Section 2.4 of Chapter 2, the energy consumption rate per sensor in the k^{th} band is computed as

$$ER(k) = ER_{tx}(R) = (\varepsilon\,R^{\alpha} + E_{elec})\,b$$

Let E_{init} be the initial energy of a given sensor. The average lifetime of a given sensor in the k^{th} band is equal to $\frac{E_{init}}{ER(k)}$. To the contrary, all sensors located in any other band forward data on behalf of others. Precisely, a sensor in the i^{th} band forwards data originated from sensors in the j^{th} band, where $i < j \le k.$

The number of sensors in the i^{th} band is equal to

$$N(i) = \lambda \pi (i^2 - (i-1)^2) R^2 = \lambda \pi (2i-1) R^2$$

Let s_i be an arbitrary sensor located in the i^{th} band. Thus, under uniform sensor distribution and constant data reporting, the average number of messages forwarded by s_i per unit of time is given by

$$M(i) = \frac{\sum_{l=i}^{k} N(l)}{N(i)} = \frac{\lambda \pi R^2 (k^2 - (i-1)^2)}{\lambda \pi R^2 (2\,\mathrm{i} - 1)} = \frac{k^2 - (i-1)^2}{2\,\mathrm{i} - 1}$$

Hence, the average energy consumption rate of a sensor in the i^{th} band is given by

$$ER(i) = (M(i) - 1)(ER_{\mathrm{tx}}(R) + ER_{\mathrm{rx}}) + ER_{\mathrm{tx}}(R)$$

Using the energy model in Chapter 2 and the value of $M(i)$, the above equation leads to

$$ER(i) = \frac{k^2 - (i-1)^2}{2i-1} b\, \varepsilon\, R^{\alpha} + \left(\frac{2k^2 - 2i^2}{2i-1} + 1 \right) b\, E_{elec} \quad (1)$$

Hence, the average lifetime of the sensors in the i^{th} band is $\frac{E_{init}}{ER(i)}$, where $i < k$. It is easy to check that $\frac{E_{init}}{ER(i)} < \frac{E_{init}}{ER(k)}$, meaning that the lifetime of the sensors in the k^{th} band is longer than that of the sensors in all other bands. □

Lemma 8.2, which follows from Lemma 8.1, states that uniform energy depletion cannot be guaranteed under the assumption of constant data reporting by sensors using their nominal transmission range. Thus, all sensors do not have same lifetime.

Lemma 8.2: Assume a uniform sensor distribution with sensor spatial density λ. Also, suppose that sensors are always on and constantly report their sensed data to the sink using their nominal communication range of radius R. It is impossible for a given pair of sensors in two different bands to have the same energy consumption rate in their lifetime. □

Next, we investigate the case where sensors may use their *adjustable communication range* to transmit or forward data to the sink.

8.1.3 Adjustable Communication Range-Based Data Forwarding

Given that the sensor distribution is uniform and that sensors constantly report their data to the sink,

the transmission distance remains the key parameter to check whether it is possible to guarantee uniform energy depletion of sensors. We consider the following two problems.

8.1.3.1 Perfect Uniform Energy Depletion

In the case of *perfect uniform energy depletion*, sensors in *all* bands consume energy at the same rate. Precisely, we want to compute the number k of bands of a field such that the sensors located in the first and k^{th} bands have the same lifetime.

Let $\mathrm{N} = \lambda \pi \Re^2$ be the total number of sensors forming the network. Now, consider two arbitrary sensors s_1 and s_k that belong to the first and k^{th} bands, respectively. Given that sensors are uniformly distributed in the field, the average number of sensors in the first and the remaining $(k-1)$ bands, denoted by $N(1)$ and $N(2 \rightarrow k),$ respectively, are equal to

$$N(1) = \lambda \pi R^2$$

$$N(2 \rightarrow k) = \lambda \pi (\Re^2 - R^2) = \lambda \pi (k^2 - 1) R^2$$

Moreover, sensors in the *first band* and, in particular, sensor s_1 acts as forwarder of the data coming from *all other bands*. Thus, the average number of messages forwarded by s_1 (including its own message) per unit of time is

$$M(1) = \frac{\mathrm{N}}{N(1)} = \frac{\lambda \pi \Re^2}{\lambda \pi R^2} = k^2$$

Out of these k^2 messages, $(k^2 - 1)$ were sent by sensors located in the $(k-1)$ remaining bands. To simplify the analysis, we assume that the sensor s_1 uses the transmission distance d_1. Hence, the average rate of energy consumption of s_1 is given by

$$\begin{aligned} ER(d_1,1) &= \left(\sum_{l=1}^{k^2-1} ER_{tx}(d_1) + ER_{rx} \right) + ER_{tx}(d_1) \\ &= (k^2 \, \varepsilon \, {d_1}^{\alpha} + (2k^2 - 1) E_{elec}) \, b \end{aligned} \tag{2}$$

On the other hand, the average rate of energy consumption of the sensor s_k is computed as

$$ER(D_k, k) = ER_{tx}(D_k) = (\varepsilon \, {D_k}^{\alpha} + E_{elec}) \, b$$

where D_k is the transmission distance used by s_k. The metric of energy depletion uniformity requires that

the average rate of energy consumption of all sensors is the same. Hence, equating the above two equations, i.e., $ER(d_1,1) = ER(D_k,k),$ yield

$$D_k{}^{\alpha} - k^2\, d_1{}^{\alpha} - \frac{2E_{elec}}{\varepsilon}(k^2-1) = 0 \tag{3}$$

where $0 < D_k \le R, \quad 0 < d_1 \le R, \quad 2 \le \alpha \le 4,$ and $k > 1.$ Notice that under uniform sensor distribution and constant data reporting, it is possible to guarantee uniform energy consumption of sensors located in the first and k^{th} bands if the transmission distances d and D_k satisfy Equation (3). Thus, given that sensors in the k^{th} band do not forward data on behalf of others, their transmission distance D_k should be larger than that used by sensors in the lower $(k-1)$ bands. Achieving the goal of energy depletion uniformity requires that sensors in the lower $(k-1)$ bands adjust their transmission distances according to $D_k.$ Particularly, the transmission distance d_1 for sensors in the *first* band given by

$$d_1 = \frac{1}{k^{2/\alpha}}\left(D_k{}^{\alpha} - \frac{2E_{elec}}{\varepsilon}(k^2-1)\right)^{1/\alpha} \tag{4}$$

Lemma 8.3 [14], [30], [31] approximates the minimum transmission distance $d_{\min}$ a given sensor can use for transmitting its own data or forwarding data on behalf of others to the sink.

Lemma 8.3: The minimum transmission distance used by a sensor when it sends/forwards data to the sink, can be approximated by

$$d_{\min} = \left(\frac{E_{elec}}{\varepsilon}\right)^{1/\alpha}$$ □

From Lemma 8.3, it follows that a physical solution to Equation (3) exists if and only if

$$\frac{1}{k^{2/\alpha}}\left(D_k{}^{\alpha} - \frac{2E_{elec}}{\varepsilon}(k^2-1)\right)^{1/\alpha} \ge \left(\frac{E_{elec}}{\varepsilon}\right)^{1/\alpha}$$

The above inequality implies that guaranteeing uniform energy depletion of all sensors is possible if and only if the number k of bands of the field satisfies

$$k \le \sqrt{\frac{\varepsilon}{3\,E_{elec}} D_k{}^{\alpha} + \frac{2}{3}}$$

Theorem 8.1 generalizes equation (4) and states the conditions under which uniform energy

depletion of sensors is achieved.

Theorem 8.1: Assume that sensors can adjust their communication ranges when they transmit sensed data to the sink. Let D_k be the transmission distance used by sensors in the k^{th} band. Then, uniform energy depletion of sensors in the network can be guaranteed provided that

(Condition 1) sensors in the i^{th} band with $i < k$ use a transmission distance d_i given by

$$d_i = \left(\left({D_k}^{\alpha} - \frac{2E_{elec}}{\varepsilon} \frac{(k^2 - i^2)}{2i-1} \right) \times \frac{2i-1}{k^2 - (i-1)^2} \right)^{1/\alpha}$$

(Condition 2) the number of bands in a circular field is upper-bounded by

$$k_u = \sqrt{\frac{\varepsilon}{3E_{elec}} {D_k}^{\alpha} + \frac{2}{3}}$$

Table 8.1: Values of E_{elec} and ε depending on α.

	E_{elec}	ε
$\alpha = 2$	$50nJ/bit$	$10pJ/bit/m^2$
$2 < \alpha \leq 4$	$50nJ/bit$	$0.0013pJ/bit/m^2$

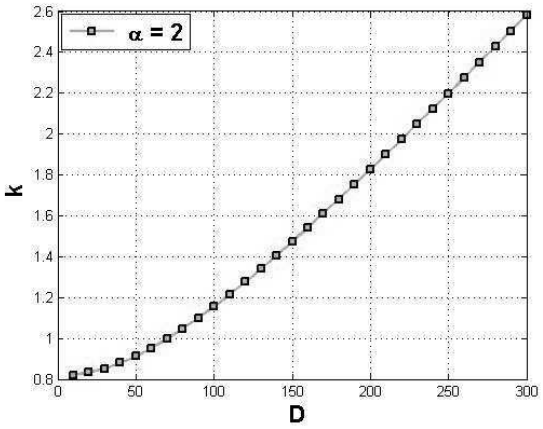

Figure 8.4: Plot of $k_u = \sqrt{0.000067\,{D_k}^2 + 2/3}$ for $\alpha = 2$.

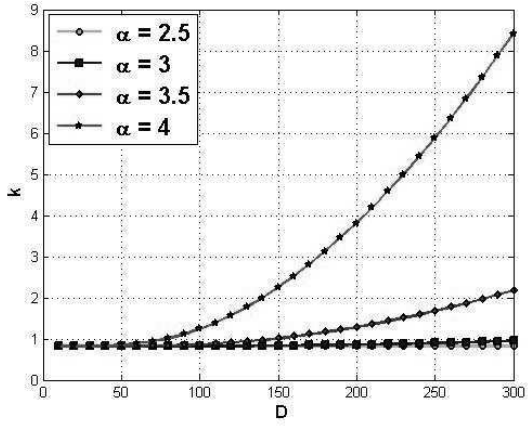

Figure 8.5: Plot of $k_u = \sqrt{87 \times 10^{-10} {D_k}^{\alpha} + 2/3}$ for $2 < \alpha \leq 4$.

Table 8.1 summarizes the values of the constants $\varepsilon \in \{\varepsilon_{fs}, \varepsilon_{mp}\}$ and E_{elec} [88], which depend on α. The upper bound on k depends on whether the free-space $(\alpha = 2)$ or multi-path $(2 < \alpha \leq 4)$ propagation

model is used, and is computed as

$$k_u = \begin{cases} \sqrt{0.000067\, {D_k}^2 + 2/3} & if\ \alpha = 2 \\ \sqrt{87 \times 10^{-10}\, {D_k}^{\alpha} + 2/3} & if\ 2 < \alpha \le 4 \end{cases}$$

Assume that the radius of the nominal communication range of sensors is equal to $R = 300\,\mathrm{m}.$ Figure 8.4 plots the function k_u for the free-space model, while Figure 8.5 plots k_u for the multi-path model for different values of $\alpha.$ As can be seen from Figure 8.4, the maximum number of bands for $\alpha = 2$ is $k_u = 2$ and can be obtained only when sensors located in the k^{th} band use a transmission distance equal to at least $D_k = 225\,\mathrm{m}.$ However, for $\alpha \in \{2.5, 3, 3.5\},$ as shown in Figure 8.5, there is no solution to the problem since $k_u = 1,$ i.e., uniform energy depletion cannot be guaranteed for those values of $\alpha.$ For $\alpha = 4,$ however, the number of bands can vary from 2 to 8. For instance, for $k_u = 8,$ the transmission distance used by sensors in the k^{th} band should be $D_k \ge 290\,\mathrm{m}.$ The corresponding value of the transmission distance d used by sensors in the lower $(k-1)$ bands can be computed based on Equation (4) for each pair of values $(k_u, D_k).$

Discussion: In [136], it was proved that that unbalanced energy depletion is unavoidable for $\alpha = 2.$ Using our analysis, however, we have proved that providing uniform energy consumption of sensors in all the bands (i.e., *perfect uniform energy depletion*) is possible although hard to achieve, especially for $\alpha = 2.$ Indeed, the number of bands cannot exceed 2, which imposes a severe restriction on the size of the field. This is due to the gap in the energy consumed by sensors in the first and k^{th} bands. Indeed, most of sensors in the k^{th} band never forward data on behalf of others regardless of their transmission distance $D.$ Thus, our result is in sharp contrast with the one reported in [136]. Also, while our analysis shows that the number of bands has a certain upper bound that does not depend on the size of the field but depends only on the transmission distance D and the propagation model considered, Olariu and Stojmenovic [136] found that the number of coronnas (or bands) is based on the size of the field.

Next, we consider the following relaxed version of the above-mentioned problem.

8.1.3.2 Partial Uniform Energy Depletion

Here, we investigate the value of i, where $1 < i < k$ and $\Re = k\,R$, such that a uniform energy depletion could be achieved among all sensors located in the lower i bands (1 to i). Hence, our objective is to compute the value of i such that sensors located in the first and i^{th} bands have the same energy consumption rate. Guaranteeing uniform energy depletion of sensors in the first and i^{th} bands will definitely yield uniform energy depletion of sensors located in the j^{th} and i^{th} bands, for any $j < i$. Thus, we focus only on the lower i bands instead of all bands in the field and investigate the achievement of *partial energy depletion uniformity*.

Let s_i be an arbitrary sensor located in the i^{th} band and $ER(D_i,i)$ the average energy consumption rate of s_i, where D_i is the transmission distance of s_i. If we replace R by D_i in Equation (1), we obtain

$$ER(D_i,i) = \frac{k^2-(i-1)^2}{2i-1} b\,\varepsilon\, D_i^{\alpha} + \left(\frac{2k^2-2i^2}{2i-1}+1\right) b\,E_{elec} \tag{5}$$

In order to achieve partial uniform energy depletion in the first and i^{th} bands, their corresponding sensors must have the same energy consumption rate, i.e., $ER(d_1,1) = ER(D_i,i)$. Hence, by equating equations (2) and (5), the transmission distance d_1 is computed as:

$$d_1 = \frac{1}{k^{2/\alpha}}\left(\frac{k^2-(i-1)^2}{2i-1} D_i^{\alpha} + \left(\frac{k^2-i^2}{2i-1} - k^2 + 1\right)\frac{2\,E_{elec}}{\varepsilon}\right)^{1/\alpha} \tag{6}$$

where $0 < D_i \le R$ and $0 < d_1 \le R$. The value of i should be chosen in a way such that the transmission distance d_1 is lower-bounded by $d_{\min}$. Hence, a value of d_1 in Equation (6) exists if and only if $d_1 \ge d_{\min}$. Hence, Equation (6) and Lemma 8.3 imply

$$\frac{k^2-(i-1)^2}{2i-1} D_i^{\alpha} + \left(\frac{2k^2-2i^2}{2i-1} - 3k^2 + 2\right)\frac{E_{elec}}{\varepsilon} \ge 0$$

Let $F(i,k)$ be a function defined as follows:

$$F(i,k) = \frac{k^2-(i-1)^2}{2i-1} D_i^{\alpha} + \left(\frac{2k^2-2\,i^2}{2i-1} - 3k^2 + 2\right)\frac{E_{elec}}{\varepsilon}$$

Let us evaluate the value of i such that the function $F(i,k)$ is positive. For this purpose, we solve the

following two equations:

$$\begin{cases} \dfrac{\partial F(i,k)}{\partial i} = \left(D_i^{\alpha} + \dfrac{2\,E_{elec}}{\varepsilon} \right)(k^2 + i^2 - i) = 0 & \textbf{(7)} \\ \dfrac{\partial F(i,k)}{\partial k} = k\left(D_i^{\alpha} + \dfrac{E_{elec}}{\varepsilon}(5 - 6\,i) \right) = 0 & \textbf{(8)} \end{cases}$$

Notice that the value of k is immaterial because we are only interested in achieving partial uniform energy depletion among the first i bands, where $i < k.$ Equation (8) provides a physical solution i_{opt} given by

$$i_{opt} = \frac{\varepsilon}{6\,E_{elec}} D_i^{\alpha} + \frac{5}{6}$$

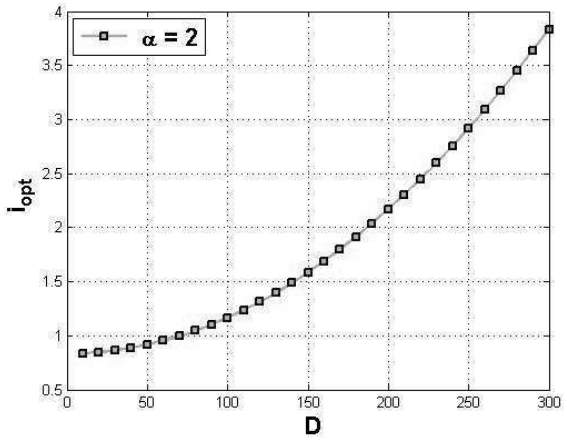

Figure 8.6 Plot of i_{opt} for $\alpha = 2.$

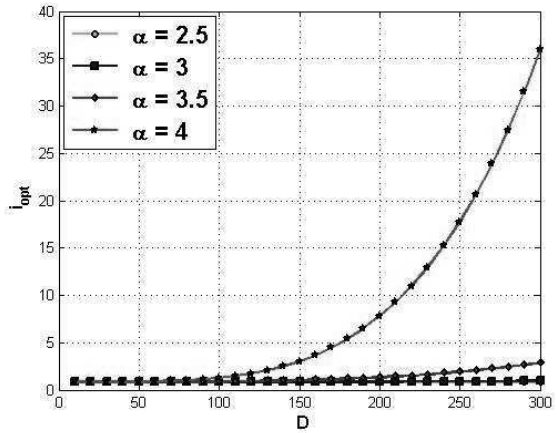

Figure 8.7 Plot of i_{opt} for $2 < \alpha \leq 4.$

Figure 8.6 shows that partial uniform energy depletion can be achieved with regard to the first and the 3^{rd} bands when $\alpha = 2,$ where the sensors in this band use their nominal communication range. Figure 8.7 shows that for $\alpha = 3.5,$ we get $i = 2;$ while for $\alpha = 4,$ its value varies between 2 and 35. The number of bands does not depend on the size of the field.

Therefore, the energy sink-hole problem can be solved provided that sensors adjust the radii of their communication ranges. However, this solution imposes a severe restriction on the size of the field in terms of the number of its bands especially for the free-space propagation model $(\alpha = 2).$ Next, we propose a scheme to overcome this shortcoming with the help of heterogeneous sensors, and evaluate its performance.

8.2 Using Heterogeneous Sensors

We consider heterogeneous sensors that are equipped with batteries with different initial energy. First, we describe our architecture for such a network with a goal to guarantee that all the sensors deplete their initial energy at the same time. Then, we evaluate its performance.

8.2.1 Multi-Tier Architecture

In this approach, heterogeneous sensors are assigned to the bands of the field in such a way that they all deplete their initial energy at the same time. In real-world scenarios, wireless sensor networks can have *heterogeneous* sensors with different capabilities, thus increasing the network reliability and lifetime. For tractability of the problem, we assume that *energy* is the only criterion that decides whether sensors are homogeneous or heterogeneous. Now, the bands do not contain the same type of sensors regarding their initial battery power. Precisely, each band has homogeneous sensors (i.e., sensors having the same amount of initial energy). But, any two bands have heterogeneous sensors (i.e., sensors with unequal amounts of initial energy). Sensors are supposed to use their nominal communication range when they forward data to the sink. Our goal is to guarantee uniform energy depletion of *all* sensors regardless of their bands.

Yarvis *et al.* [169] proposed a three-tier architecture for heterogeneous wireless sensor networks. The top layer contains only one sink that receives sensed data and analyzes them. The second layer includes sensors with no energy constraint. These sensors, called *line-powered* sensors, have unlimited energy resources by connecting them to a wall outlet. The third layer contains battery-powered sensors that are one-hop away from line-powered sensors. The rationale behind this architecture is that sensors closer to the sink in multi-hop sensor network with many-to-one delivery, consume more energy than all other sensors in the network. Thus, those sensors should be line-powered. As can be observed, this three-tier architecture forms a dominating tree where each battery-powered sensor communicates with the sink via only line-powered sensors to transmit its sensed data. There is no communication among battery-powered sensors in order to save their energy, and hence no battery-powered sensor can play the role of data forwarder on behalf of other sensors. Definitely, there should be a sufficient number of line-powered sensors.

Now, we propose a multi-tier wireless sensor network architecture, where each band represents a

tier and no sensor is supposed to be line-powered. The data forwarding algorithm used by sensors is called *next band-based data forwarding* (NEAR) and is mainly based on the following premise: each sensor selects a neighbor in its adjacent band as its next hop forwarder the one whose remaining energy is the highest among all sensors in that band. Also, their transmission distance R. We prove that with such a sensor distribution, *all* sensors in the network deplete their initial energy at the same time. Consider the k^{th} band. As discussed earlier, the average energy consumption rate per sensor in this band is $ER_{tx}(R) = (\varepsilon R^{\alpha} + E_{elec})\, b,$ where b (in bits/sec) is the sensor's data rate. According to [74], the average lifetime of sensors of the k^{th} band is given by

$$T(k) = \frac{e_0(j,k)}{ER_{tx}(R)} = \frac{e_0(k)}{ER_{tx}(R)}$$

where $e_0(j,k)$ is the *total initial energy* of the j^{th} sensor in the k^{th} band whose total number of sensors is $N(k).$ Since a given band is homogeneous in terms of initial energy,

$$e_0(1,k) = ... = e_0(N(k),k) = e_0(k)$$

Similarly, for the i^{th} band, the average energy consumption rate per sensor in this band is given by

$$ER_{tx}(R) + \frac{\sum_{j=i+1}^{k} N(j)}{N(i)} (ER_{tx}(R) + ER_{rx})$$

where the first term is due to a sensor transmitting its own data and the second term is due to data forwarding on behalf of sensors in the $(i+1)^{th},...,k^{th}$ bands. Similarly, the average lifetime of sensors of the i^{th} band is given by

$$T(i) = \frac{N(i)\, e_0(i)}{\left(\sum_{j=i+1}^{k} N(j)\, (ER_{tx}(R) + ER_{rx})\right) + N(i)\, ER_{tx}(R)}$$
$$= \frac{(2i-1)\, e_0(i)}{(k^2 - i^2)\, (ER_{tx}(R) + ER_{rx}) + (2i-1)\, ER_{tx}(R)}$$

Note that the above equation holds for all $1 \le i \le k.$ Sensors in all bands will deplete their initial energy at the same time if

$$T(1) = ... = T(i) = ... = T(k)$$

Thus, $T(i) = T(k),$ for all $1 \le i \le k-1,$ which implies the following relationship between the initial energy $e_0(i)$

and $e_0(k)$ of the i^{th} and k^{th} bands, respectively,

$$e(i) = g(i,k)\, e_0(k) \text{ for } 1 \le i \le k-1 \tag{9}$$

where their ratio $g(i,k)$ is given by

$$g(i,k) = \frac{(k^2 - i^2)(ER_{tx}(R) + ER_{rx}) + (2i-1)\, ER_{tx}(R)}{(2i-1)\, ER_{tx}(R)} \tag{10}$$

Theorem 8.2 states the condition under which uniform energy depletion of all sensors can be guaranteed.

Theorem 8.2: Consider a deployment strategy where a circular field is sliced into k concentric bands of constant width R (i.e., nominal communication range of sensors) and the sensor spatial density is constant. Uniform energy depletion of sensors is guaranteed if each band is homogeneous and all bands are mutually heterogeneous in such a way that the ratio of the initial energy $e_0(i)$ of a sensor in the i^{th} band to the initial energy $e_0(k)$ of a sensor in the k^{th} band satisfies

$$\frac{e_0(i)}{e_0(k)} = g(i,k) \text{ for } 1 \le i \le k-1$$

where

$$g(i,k) = \frac{(k^2 - i^2)(ER_{tx}(R) + ER_{rx}) + (2i-1)\, ER_{tx}(R)}{(2i-1)\, ER_{tx}(R)}$$ □

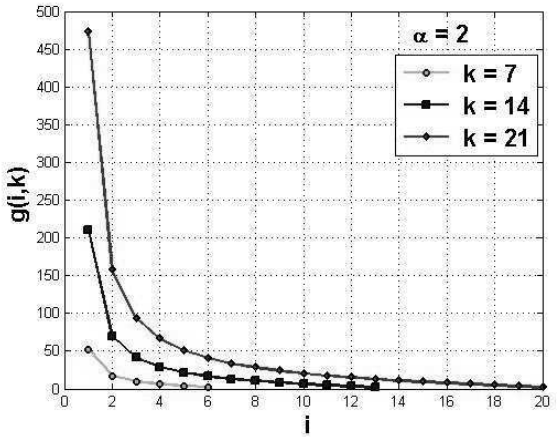

Figure 8.8 Plot of $g(i,k)$ for $\alpha = 2$.

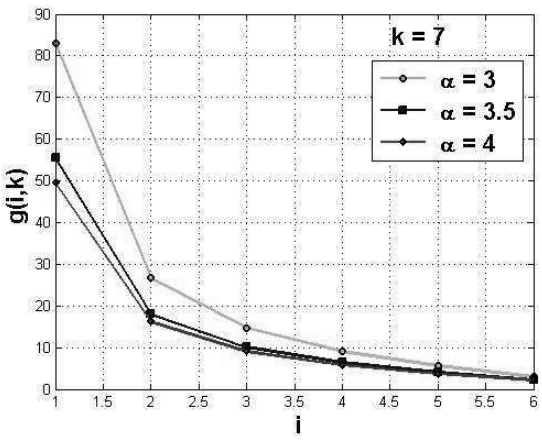

Figure 8.9 Plot of $g(i,k)$ for $2 < \alpha \le 4$.

Figures 8.8 and 8.9 plot the function $g(i,k)$ for different values of i, k, and α assuming a data rate

of 1024 bits/sec and $R = 300\,\text{m}.$ We use the same values of the other constants listed in Table 1. Both figures show that $g(i,k)$ is high for the first inner bands and decreases continuously for the outer bands that tend to have comparable data forwarding load.

8.2.2 NEAR Performance Evaluation

We assume that $R = 300\,\text{m},\ \alpha = 2,$ and $\Re = 1500\,\text{m},$ i.e., $k = 5$ (there are 5 concentric circular bands in the circular field). The corresponding values of the constants ε_{fs} and E_{elec} are given in Table 1. Moreover, we assume that every sensor continuously generates constant bit rate (CBR) data of 1024 bits/second, i.e., 4 data packets per second $(b = 1024\ \text{bits/sec}).$ Sensors are randomly deployed in the circular field and their initial energy is determined based on their bands following Equations (9) and (10). The simulation is run for multiple times and the simulated time for each run is equal to 1000 sec. Then, we average the results of all those runs.

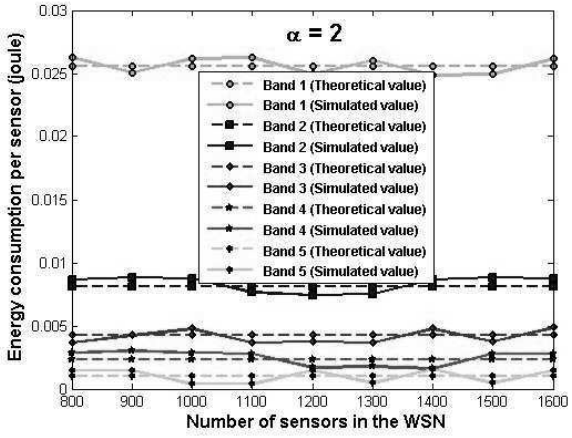

Figure 8.10 Average energy consumption of NEAR

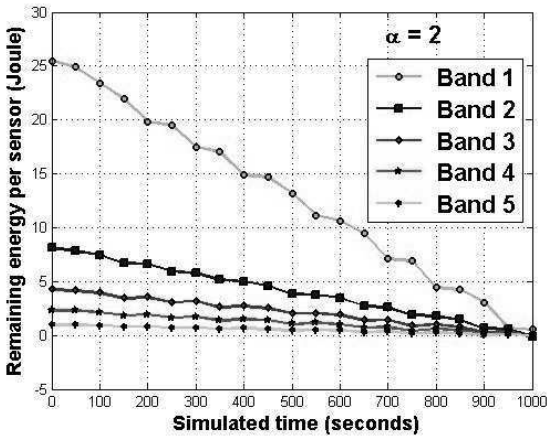

Figure 8.11 Uniform energy depletion of all sensors.

In the first simulation, the number of sensors varies from 800 to 1600 (i.e., we vary the sensor spatial density). Figure 8.10 shows that sensors in all bands do not consume the same amount of energy. This remains true given that sensors are randomly and uniformly deployed. Indeed, sensors located in the bands closer to the sink still consume more energy than those placed in higher bands. However, the average energy consumption of sensors in a given band stays almost constant as we vary the total number of sensors deployed in the field. This implies that the energy sink-hole problem cannot be solved by simply increasing the number of sensors.

In the second simulation, the number of sensors is fixed to 1600. Assume that the initial energy of sensors in the k^{th} band is $e_0(k) = 0.97$ joule. By Theorem 8.2, the initial energy of sensors in all other bands are computed based on $e_0(k)$. Figure 8.11 shows that the total remaining energy of sensors in all bands decreases as time advances since those sensors are continuously sending or forwarding sensed data to the sink. The simulation results almost totally agree with the theoretical results, which are omitted for the clarity of Figure 8.11. Notice that the curves related to those five bands do not have the same slope. This is due to the fact that sensors in those bands do not have the same load and hence the remaining energy of the inner bands depletes faster than that of the outer bands. More importantly, all sensors in all bands deplete their initial energy at the same time. This result confirms with the analysis of our sensor deployment strategy that assigns initial energy to sensors based on their load in data forwarding to the sink. Definitely, sensors closer to the sink have the highest initial amount of energy given that any sensed data should go through them before reaching the sink.

Next, we propose a data forwarding protocol for homogeneous wireless sensor networks, which uses sink mobility and a new variant of Voronoi diagram whose structure is time-varying.

8.3 Sink Mobility and Energy Aware Voronoi Diagram

Here, we assume that the sink is mobile so its neighbors change over time. Moreover, all sensors are homogeneous and randomly and uniformly distributed in a circular field of radius $\Re$ with sensor density λ. We also assume that the mobility trajectory of the sink follows the *random waypoint* (RWP) mobility model [98], thus covering the entire field (i.e., all locations in the field are equally likely to be visited). Initially, the sink randomly selects a waypoint and a speed between 0 and $v_{\max}$, and moves towards the selected waypoint at this constant speed. When it reaches a waypoint, the sink stays for a pause time and randomly selects new waypoint and speed. The sink repeats this process during the network lifetime. We assume that data collection continues via multi-hop forwarding wherever the sink stays. Thus, only the pause time has an impact on data dissemination.

To answer both questions raised in Chapter 1 (see Section 1.4), we propose a new concept, called *energy aware Voronoi diagram*, where all sensors in $SCN(s_i, s_m)$ act as candidate forwarders. When the sink arrives at a waypoint, it randomly selects its next waypoint and broadcasts it along with its current one

and pause time in a single *info* packet, i.e., $info = \{rwp_{cur}, rwp_{fut}, ptime\}$. Each sensor that receives this *info* packet decides whether it would transmit its data to either the current or future waypoint of the sink based on its location and the average transmission delay. For a field whose size is in the order of a few miles, the average propagation delay is negligible compared to the average transmission delay [101]. Next, we discuss the concept of energy aware Voronoi diagram and compare it to weighted Voronoi diagram.

8.3.1 Why Energy Aware Voronoi Diagram?

The newly proposed concept of *energy-aware Voronoi diagram* differs from *weighted Voronoi diagram* [33]. While the Voronoi edges of the latter are not straight segments, the ones generated by the former are, indeed, straight segments. Also, energy aware Voronoi diagram depends on both the locations of sensors and their remaining energy. Hence, the structure of energy aware Voronoi diagram is dynamic in nature. As will be seen later, energy aware Voronoi diagram is an appropriate structure for data forwarding in wireless sensor networks for the following three reasons: First, it helps us design a localized routing protocol for wireless sensor networks in the sense that each sensor builds its energy aware Voronoi diagram based on its neighbors' information. Second, most of the existing geographical routing protocols, except GeRaF [184], consider the closest sensor to destination as candidate forwarder. However, in GeRaF, a sensor may have the same subset of sensors alive as candidate forwarders. The concept of energy aware Voronoi diagram enables a sensor to have a subset of candidate forwarders from which it chooses the best one with respect to some metric. Third, it gives an equal chance to all sensors in the network to act as candidate forwarders on behalf of others to the sink. This is due to the randomness caused by the remaining energy metric to construct such a Voronoi diagram.

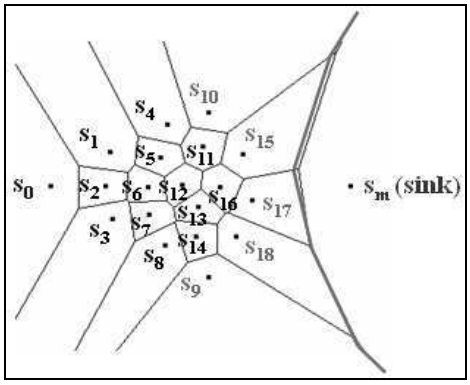

Figure 8.12 Candidate forwarders of s_0.

Protocol: EVEN
Begin
// Actions executed by a source sensor s_0
1: If sink $s_m \in CN(s_0)$ Then
2: Forward sensed data packet directly to s_m
3: Else
4: Identify a reference sensor s_{ref} such that
$E_{rem}(s_{ref}) = \max\{E_{rem}(s_j) : s_j \in SCN(s_0, s_m, \beta)\}$
5: Compute the relative positions of the neighbors
$s_j \in SCN(s_0, s_m)$
6: Compute the energy-aware Voronoi diagram:
$EAVor(\{s_0, s_{ref}, s_m\} \cup SCN(s_0, s_m))$
7: Identify a subset of candidate forwarders $CF(s_0, s_m)$
8: Select an appropriate forwarder s_{af} in $CF(s_0, s_m)$
such that $CE_r(s_{af}) = \max\{CE_r(s_k) : s_k \in CF(s_0, s_m)\}$
9: Forward the sensed data packet to s_{af}
// Actions executed by appropriate forwarders
10: While (sensed data packet has not reached s_m) Do
11: If sink $s_m \in CN(s_{af})$ Then
12: Forward sensed data packet directly to s_m
13: Break;
14: Else Repeat Steps 1-9 by replacing s_0 with s_{af}
15: EndIf
16: EndWhile
End

Figure 8.13 The EVEN Protocol.

Let $CN(s_i)$ be the *communication neighbor set* of a sensor s_i, which are located in its communication disk whose radius is equal to R_i. From $CN(s_i)$, the sensor s_i considers only a subset of sensors, denoted by $SCN(s_i, s_m)$, located between s_i and the sink s_m to act as data *forwarders* to the sink.

Definition 8.1 (Adjacent Voronoi region): Let $s_j \in SCN(s_i, s_m)$ and $Vor(\{s_i, s_m\} \cup SCN(s_i, s_m))$ be a localized Voronoi diagram computed by s_i. A Voronoi region $VR(s_m)$ of the sink s_m is said to be *adjacent* to the sensor s_j if $VR(s_m)$ and $VR(s_j)$ of s_m and s_j, respectively, have *at least one common* Voronoi edge. □

Definition 8.2 (Candidate forwarder): Let $s_j \in SCN(s_i, s_m)$. The sensor s_j is said to be a *candidate forwarder*

of s_i if $VR(s_m)$ is adjacent to s_j, where $VR(s_m) \in Vor(\{s_i, s_m\} \bigcup SCN(s_i, s_m))$. The set of candidate forwarders of s_i is denoted by $CF(s_i, s_m)$. □

Assume that a source s_0 wishes to disseminate its data to the sink s_m. Figure 8.12 shows the localized Voronoi diagram of s_0, where $SCN(s_0, s_m) = \{s_i \mid 1 \le i \le 18\}$. Notice that $CF(s_0, s_m) = \{s_9, s_{10}, s_{15}, s_{17}, s_{18}\}$, where the Voronoi region of each of those sensors shares one Voronoi edge with that of s_m. These shared edges are marked bold.

Definition 8.3 (Reference sensor): Let $s_{ref} \in SCN(s_i, s_m)$. *A sensor* s_{ref} *is said to be a* reference sensor *of* s_i *if* s_{ref} *has the highest remaining energy among all sensors in* $SCN(s_i, s_m)$. □

Next, we describe our protocol, evaluate its performance through simulations, and compare it with existing ones.

8.3.2 EVEN Detailed Description

Our proposed protocol (Figure 8.13), called *energy aware Voronoi diagram-based data forwarding* (EVEN), is composed of three phases, namely *computing relative positions*, *computing energy-aware Voronoi diagram*, and *selecting appropriate forwarder*.

Computing Relative Positions: First, a source s_0 identifies its reference sensor s_{ref}. All other neighbors will be positioned relatively to s_{ref} based on their remaining energy. If there are multiple reference sensors, EVEN selects s_{ref} with the smallest distance to the shortest path $[s_0, s_m]$. The relative (*x,y*)-coordinates of a neighbor s_j of s_0 are computed as follows:

$$\begin{cases} x_{rel}(s_j) = x(s_0) + x_{move}(s_j, s_0, s_{ref}) \\ y_{rel}(s_j) = y(s_0) + y_{move}(s_j, s_0, s_{ref}) \end{cases}$$

where

$$\begin{cases} x_{move}(s_j, s_0, s_{ref}) = [x(s_{ref}) - x(s_0)] \dfrac{E_{rem}(s_j)}{E_{rem}(s_{ref})} \\ y_{move}(s_j, s_0, s_{ref}) = [y(s_{ref}) - y(s_0)] \dfrac{E_{rem}(s_j)}{E_{rem}(s_{ref})} \end{cases}$$

The intuition behind this computation is to "virtually" move sensors with low remaining energy away from the sink. Thus, these sensors will not be considered as "good" candidate forwarders until their

available energy reaches a certain value. Notice that only s_{ref} has the same relative and physical positions with respect to s_i as the ratio is equal to 1.

Computing Energy-Aware Voronoi Diagram: A source s_0 computes its energy-aware Voronoi diagram, $EAVor(\{s_0, s_{ref}, s_m\} \cup SCN(s_0, s_m))$ with respect to its own actual location and that of the sink s_m as well as the relative positions of sensors in the subset $SCN(s_0, s_m)$. As the remaining energy of sensors varies with time, the obtained structure of energy aware Voronoi diagram computed by sources and all forwarding sensors is time-varying too.

Selecting Appropriate Forwarder: A source s_0 uses the *relative* $Closeness \times Energy$ metric defined by $CE_r(s_j) = w_r(s_j) \times \overline{w}(s_j)$ to choose its appropriate forwarder s_{af}, where $s_j \in CF(s_0, s_m)$, $w_r(s_j) = \frac{\delta(s_0, s_m)}{\delta_r(s_0, s_j) + \delta_r(s_j, s_m)}$ is the *relative closeness ratio*, $\overline{w}(s_j) = \frac{E_{rem}(s_j)}{\sum_{s_k \in CF(s_0, s_m, \beta)} E_{rem}(s_k)}$ is the *energy ratio* with $E_{rem}(s_j)$ being the remaining energy of sensor s_j, $\delta_r(s_0, s_j)$ is the relative Euclidean distance between s_0 and s_j, and $\delta_r(s_j, s_m)$ is the relative Euclidean distance between s_j and s_m. The source s_0 selects s_{af} such that $CE_r(s_{af}) = \max\{CE_r(s_k) : s_k \in CF(s_0, s_m)\}$. Then s_0 forwards its data to s_{af}. After receiving the data packet, s_{af} performs the same above phases to identify its appropriate forwarder. This process repeats until the sink receives the data.

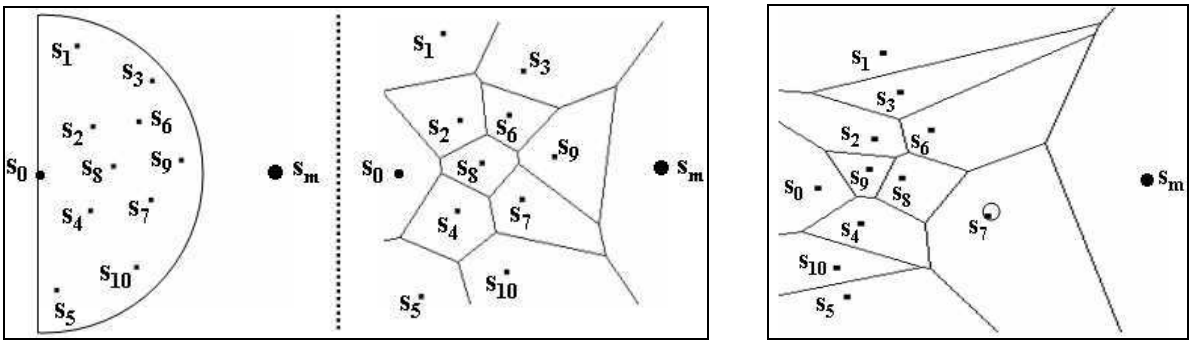

Figure 8.14 (a) Voronoi diagram $Vor(\{s_0, s_m\} \cup SNS(s_0, s_m))$ and (b) energy-aware Voronoi diagram $EAVor(\{s_0, s_{ref}, s_m\} \cup SNS(s_0, s_m))$.

Using the concept of Voronoi diagram, only s_3, s_7, s_9, and s_{10} can act as candidate forwarders for s_0 as shown in Figure 8.14a. However, the subset of candidate forwarders $CF(s_0, s_m)$ may vary depending on the remaining energy of the sensors when the concept of energy-aware Voronoi diagram is used. Figure 8.14b shows that s_1, s_3, s_6, and s_7 are candidate forwarders for s_0, which are computed based on the reference sensor s_7.

Lemma 8.4 states that all sensors in $SCN(s_i, s_m)$ are equally likely to be selected as appropriate forwarders for s_i.

Lemma 8.4: All sensors in $SCN(s_i, s_m)$ are equally likely to be selected as appropriate forwarders for s_i.

Proof: First, s_i will pick sensor s_{i1} having the maximum closeness ratio, i.e., $w(s_{i1}) = \max\{w(s_k) : s_k \in SCN(s_i, s_m)\}$, as a reference sensor and also as an appropriate forwarder. Obviously, s_i will not select s_{i1} as reference sensor in the next data dissemination as s_{i1} will have less remaining energy than other sensors in $SCN(s_i, s_m)$. Let s_{i2} be the second reference sensor, where $\overline{w}(s_{i2}) = \overline{w}(s_{i1}) + \overline{w}_2$ and $0 < \overline{w}_2 < 1$. However, s_{i1} could be selected as an appropriate forwarder only if $CE_r(s_{i1}) > CE_r(s_{i2})$ or $w(s_{i1}) > w(s_{i2}) \times \frac{\overline{w}(s_{i2})}{\overline{w}(s_{i2}) - \overline{w}_2}$. Otherwise, either s_{i2} or another sensor in $SCN(s_i, s_m)$ will be selected as an appropriate forwarder. As can be seen, any sensor could be successively selected as an appropriate forwarder a very few times. Because of the relative values of the metric $Closeness \times Energy$ and the notion of reference sensor, each sensor in $SCN(s_i, s_m)$ will be considered as an appropriate data forwarder for s_i. □

8.3.3 EVEN Performance Evaluation

In this section, we study the performance of EVEN based on simulation programs written in the C programming language. Our simulation set-ups consider 800 sensors randomly and uniformly distributed in a circular field of radius $\Re = 3000\,\text{m}$. The radius of the communication range of the sensors is $R = 300\,\text{m}$. Also, when mobility is considered, the maximum speed of a mobile sink is $v_{\max} = 5\,\text{m/s}$.

8.3.3.1 Impact of Sink Mobility

In this experiment, we consider a *Voronoi diagram-based greedy forwarding* (VGF) protocol. VGF is similar to a greedy geographic routing algorithm, called *Bounded Voronoi Greedy Forwarding* (BVGF)

[165]. On the one hand, BVGF chooses the sensor that has the shortest distance to the sink and does not consider energy as a selection metric. On the other hand, VGF considers both the closeness of sensors to the sink as well as their remaining energy to build localized Voronoi diagram and select the best candidate forwarders. Notice that VGF and EVEN are quite identical except that the former uses the actual locations of sensors while the latter uses the virtual locations of sensors (computed in Section 8.3.2). We evaluate the performance of VGF for both cases of networks using a static sink and a mobile sink, respectively. We compute the average energy consumption of sensors as a function of their distance from the center of the field. A static sink is positioned at the center of the field for energy-efficient data gathering [125]. As can be seen in Figure 8.15, VGF has better performance with a mobile sink than with a static sink. Indeed, sink mobility distributes the data forwarding load among all the sensors.

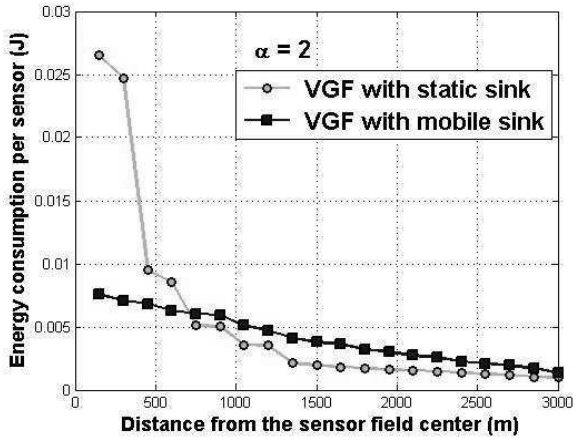

Figure 8.15 VGF – static sink vs. mobile sink.

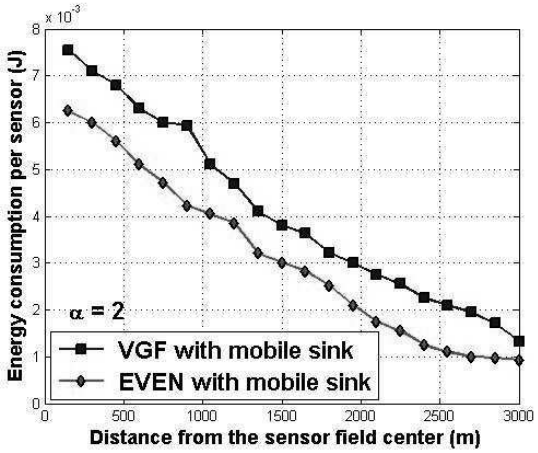

Figure 8.16 Comparing EVEN with VGF.

8.3.3.2 Comparing EVEN with VGF

In this experiment, we consider a mobile sink and compare the performance of EVEN with that of VGF. EVEN leads to better load balance than VGF as shown in Figure 8.16. While EVEN allows a sensor to select best forwarders among all of its neighbors, VGF considers only the closest sensors to the sink. As expected, EVEN distribute more evenly the data dissemination load among the neighbors of each sensor, and hence outperforms VGF. Figure 8.17 shows the impact of pause time of the mobile sink on the average energy consumption of sensors. As the pause time increases, more sensors will have the chance to transmit sensed data to the sink. Thus, sensors close to the sink become more active as they

receive more data from sources. When the pause time has large value, those heavily used sensors surrounding the sink deplete their energy more quickly than all other sensors. The performance of EVEN tends to that of VGF with a static sink. It is worth noting that no matter how energy-efficient a data forwarding protocol is, the use of static sink significantly degrades its performance.

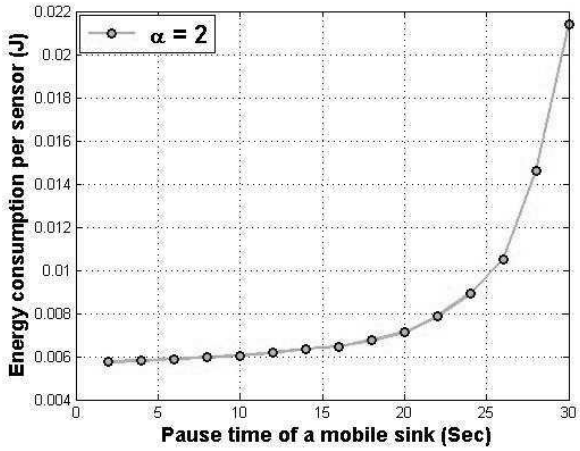

Figure 8.17 Impact of pause time on EVEN.

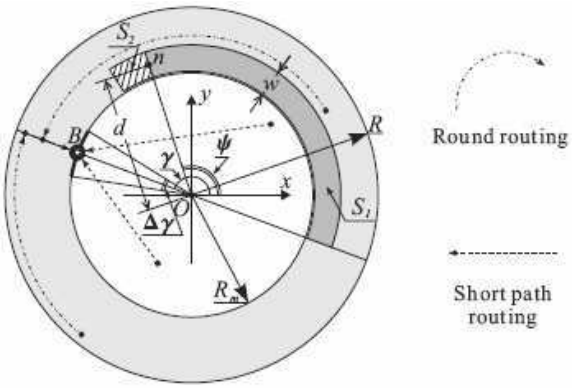

Figure 8.18 Joint mobility and routing strategy [125].

8.3.3.3 Comparing EVEN with Another Protocol

Luo and Hubaux [125] showed through simulations that under the short path routing strategy, a mobile sink reduces the average load of the sensors by about 75% compared to a static sink. This reduction implies approximately a 400% increase of the network lifetime. Luo and Hubaux [125] also showed by simulation that their joint mobility and routing strategy further reduces the network load by about 10% which corresponds to an overall improvement of the network lifetime of about 500% compared

with the case of static sink. Their joint mobility and routing strategy is elegant and efficient in that it exploits the available energy at the sensors close to the border of the network, which are almost not used in data forwarding. Moreover, the sink moving on a circle of radius $R_m < R$, where R stands for the radius of the field. Thus, the field is divided into two regions: the inner circle of radius R_m and the annulus between the periphery of the network and the trajectory of the sink as shown in Figure 8.18. The sensors within the inner circle use short path routing to transmit their sensed data to the sink whereas the sensors in the annulus send their data to the sink using two steps. First, a sensor uses *round routing* around the center of the network O until the segment OB is reached, where B is the current position of the mobile sink. Then, the data is sent to the sink using a short path.

EVEN does not necessarily choose a short path. Using the concept of energy-aware Voronoi diagram, *all* neighbors of each sensor have the chance to participate in data forwarding toward the sink. Thus, a mixture of short-range and long-range data forwarding patterns would take place. This helps the sensors deplete their energy slowly and uniformly. Also, as the sink is moving randomly, all areas in the field are equally likely to be visited, including those on its periphery. Thus, sensors close to the border of the network would be selected to act as forwarders towards the sink as their remaining energy permits. According to [125], the network lifetime is inversely proportional to the maximum average energy consumption of the sensors. Thus, as can be seen from Figure 8.16, EVEN improves the network lifetime by more than 430% compared with VGF that uses a static sink. Thus, EVEN has performance that is comparable to that of the joint mobility and routing strategy [125].

8.4 Summary

In this chapter, we have studied the energy sink-hole problem in static always-on wireless sensor networks, where sensors around a sink are heavily used in data forwarding, thus depleting their energy quickly [12]. We proved that uniform energy depletion of all sensors can be achieved in uniformly distributed wireless sensor networks provided that the sensors adjust their communication ranges when forwarding data to a static sink. We have also proposed a deployment strategy using heterogeneous sensors that guarantees uniform depletion of sensors' initial energy. Sensors are placed in their bands based on their data forwarding activity and initial energy. Precisely, the inner bands contain sensors with

large amount of energy as they are heavily loaded with data forwarding to the sink. We have found that our simulation results agree almost perfectly with our theoretical results. A critical factor for extending the lifetime of wireless sensor networks is load balancing in data dissemination, which depends on the nature of the sink and the selection scheme of appropriate forwarders. We have proposed a data dissemination protocol, called EVEN, which uses the concept of energy-aware Voronoi diagram to evenly distribute the load of data forwarding on all the neighbors of a given sensor, and exploits sink mobility to update the neighbors of the sink. The design goal of EVEN is to balance the load among the sensors so they deplete their energy as uniformly and slowly as possible, thus extending the network lifetime. Our results demonstrate that energy-aware Voronoi diagram and sink mobility lead to more than 430% improvement of the network lifetime compared to the case of static sink.

CHAPTER 9

FAULT-TOLERANCE MEASURES OF CONNECTED *k*-COVERAGE CONFIGURATIONS

Connectivity, primarily a graph-theoretic concept, helps define the *fault tolerance* of wireless sensor networks in the sense that it enables the sensors to communicate with each other so their sensed data can reach the sink. Indeed, a fundamental aspect in the design of wireless sensor networks is to keep them *functional* as long as possible. Because of scarce battery power (or *energy*), sensors may entirely deplete their energy or have low energy level that will not enable them to function properly. Those sensors are called *faulty* as they cannot perform their monitoring task properly. A wireless sensor network is said to be *fault tolerant* if it remains *functional* in spite of the occurrence of sensor failures. Precisely, a wireless sensor network is said to be *functional* if at any time there is at least one communication path between every pair of non-faulty sensors in the network, and, in particular, between any source and a sink. The existence of communication paths between pairs of sensors, however, is related to *vertex-connectivity* (or simply *connectivity*). Therefore, network functionality and hence network fault-tolerance strongly depends on connectivity [116]. On the other hand, *sensing coverage*, an intrinsic architectural feature of wireless sensor networks plays an important role in meeting application-specific requirements, for example, to reliably extract relevant data about a sensed field.

Sensing coverage and network connectivity are not quite orthogonal concepts. In fact, it has been proven that connectivity strongly depends on coverage and hence considerable attention has been paid to establish tighter connection between them although only loose lower bound on network connectivity of wireless sensor networks is known. Furthermore, for a wireless sensor network to function correctly, both sensing coverage and network connectivity should be maintained. Hence, we investigate network connectivity, and hence network fault-tolerance, based on the degree of sensing coverage k provided by *k*-covered wireless sensor networks, where the sensors are randomly and uniformly deployed with density λ in a square field of area size *A*.

Although network connectivity can be used to measure the fault tolerance of small-scale networks, it is not appropriate for highly dense deployed networks, such as *k*-covered wireless sensor networks. Traditional (or *unconditional*) connectivity has no restriction on the faulty sensor set and assumes that any subset of sensors can potentially fail at the same time, including all the communication neighbors of a given sensor. However, *k*-covered wireless sensor networks can consist of thousands of sensors for which it is highly unlikely in this type of network that all the communication neighbors of a given sensor fail simultaneously. This is due to the following two reasons, assuming a planar field:

- Assuming a uniform sensor distribution, the ratio of the size of the communication neighbor set of a given sensor to the total number of sensors in a planar field of area size A is given by $\pi R^2 / A,$ where R $(R << \sqrt{A})$ is the radius of the communication ranges of the sensors forming a homogeneous wireless sensor network. The probability of the failure of the entire neighbor set of a given sensor can be identified with this ratio and hence is very low.
- In real-world scenarios, wireless sensor networks can be *heterogeneous*, where sensors have different sensing, processing, and communication capabilities, thus increasing the network reliability and lifetime [63], [169]. Hence, the probability that an entire neighbor set of a given sensor fail simultaneously in this type of network is very low.

Thus, the *unconditional* connectivity may not reflect the actual fault tolerance of large-scale dense networks, such as *k*-covered wireless sensor networks, due to the above shortcomings. To alleviate this problem, we use the concept of restricted connectivity, which is based on the notion of forbidden faulty set

The remainder of this chapter is organized as follows. Section 9.1 derives fault-tolerance measures for two-dimensional *k*-covered wireless sensor networks while Section 9.2 computes their conditional fault-tolerance measures. Section 9.3 summarizes the chapter.

9.1 Unconditional Fault-Tolerance Measures

In this section, we compute connectivity and fault-tolerance measures for homogeneous and heterogeneous two-dimensional *k*-covered wireless sensor networks [26] while those for three-dimensional wireless sensor networks can be found in [15].

9.1.1 Homogeneous *k*-Covered Wireless Sensor Networks

We assume that the sink has the same communication range as the other sensors. In Chapter 5, we have computed the minimum sensor spatial density required to *k*-cover a two-dimensional field based on the *Reuleaux triangle* [188] model. We also have proved that when a two-dimensional wireless sensor network is configured to provide *k*-coverage of a two-dimensional field and the radius R of the communication disks of the sensors is at least equal to the radius r of their sensing disks, a two-dimensional wireless sensor network is guaranteed to be connected. For the sake of making this chapter self-contained, we recall Lemma 5.2 given in Chapter 5.

Lemma 5.2: Let r be the radius of the sensing disks of the sensors and $k \geq 3.$ A field is *k*-covered if any Reuleaux triangle region of width r in a field contains at least k active sensors. □

From Lemma 5.2, we deduce that the minimum sensor spatial density required to guarantee *k*-coverage of a field is given by

$$\lambda(r,k) = \frac{2k}{(\pi - \sqrt{3})\, r^2} \tag{9.1}$$

Indeed, since we are interested in the number of neighbors of a sensor, we need to consider this lemma instead of Theorems 5.2, which characterizes minimum *k*-coverage, and Theorem 5.3, which gives a tight bound on the sensor spatial density required for *k*-coverage.

Theorem 9.1 computes the connectivity of homogeneous *k*-covered wireless sensor networks and derives their fault tolerance. In sharp contrast with the work in [166], which computes connectivity based on boundary and interior sensors, our study considers the sink given its critical role in data collection. Precisely, we focus on the size of the connected component containing the sink. Indeed, it is more realistic to relate network connectivity measure to the sink. Indeed, we may have a giant connected component of sensors that does not include the sink, and hence their data cannot reach the sink.

Theorem 9.1: Let G be a communication graph of a homogeneous *k*-covered wireless sensor network deployed in a square field of area size A. The connectivity of G is given by

$$\frac{2\,\pi\,\alpha^2\,k}{(\pi - \sqrt{3})} \leq \kappa(G) \leq \frac{2\,R\,\sqrt{A}\,k}{(\pi - \sqrt{3})\, r^2} \tag{9.2}$$

where $\alpha = R/r$ and $k \geq 3.$ Its fault tolerance $\eta(G)$ is given by

$$\frac{2\pi\alpha^2 k}{(\pi-\sqrt{3})}-1 \le \eta(G) \le \frac{2R\sqrt{A}\,k}{(\pi-\sqrt{3})r^2}-1 \tag{9.3}$$

Proof: To compute the network connectivity of homogeneous *k*-covered wireless sensor networks, we need to consider the following three cases, which depend on the sink, denoted by s_0 and located at ξ_0. Since we assume that sensor failure is due to low battery power, we can use a powerful sink with infinite energy, thus eliminating the possibility of sink failure.

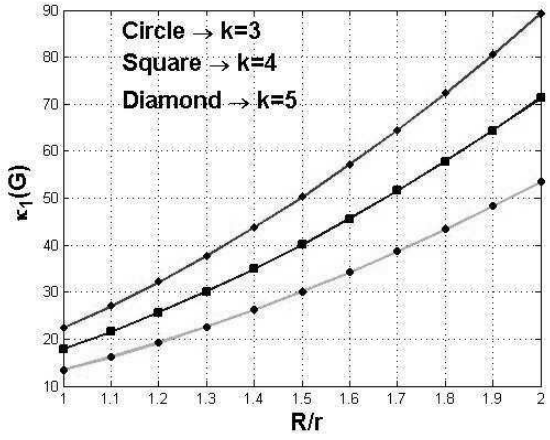

Figure 9.1 Plot of $\kappa_1(G)$ (fix k and vary α).

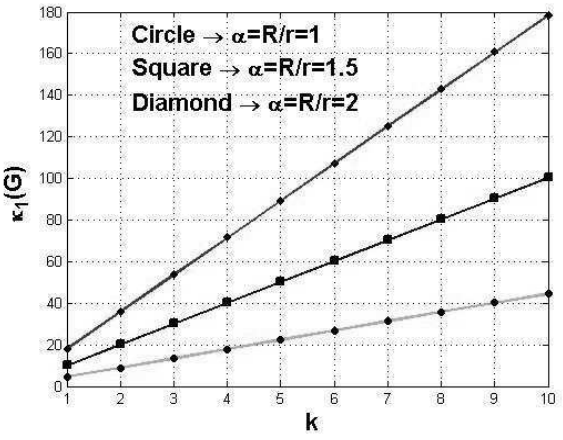

Figure 9.2 Plot of $\kappa_1(G)$ (fix α and vary k).

Case 1 - Isolated sink: This situation occurs when the disconnected network has at least two connected components, one of them is the trivial component containing the sink. Given the definition of network connectivity, the number of disconnected components should be equal to two. Notice that the optimum location of the sink in terms of energy-efficient data gathering from the available sensors is the center of the square field [125]. The sink can be isolated only when all its neighbors fail. Therefore, we compute the number of neighbors of the sink whose failure would disconnect the sink.

Let X be a random variable that counts the number of sensor failures to isolate the sink. The expected minimum number of sensor failures to isolate s_0 is given by

$$E[\mathrm{X}] = \lambda(r,k)\,|\,D(\xi_0,R)\,| \tag{9.4}$$

where $|\,D(\xi_0,R)\,| = \pi R^2$ is the measure of the area of the communication disk $D(\xi_0,R)$ of the sink s_0 located at ξ_0. Hence, the network connectivity in this case is given by

$$\kappa_1(G) = E[\mathrm{X}] = \lambda(r,k)\,\pi R^2 \tag{9.5}$$

Substituting Equation (9.1) in Equation (9.5) yields

$$\kappa_1(G) = \frac{2\pi\alpha^2 k}{(\pi - \sqrt{3})} \tag{9.6}$$

where $\alpha = R/r$ and $k \geq 3.$ Figures 9.1 and 9.2 plot the function $\kappa_1(G)$ given in Equation (9.6). Notice that connectivity increase with the ratio α and the sensing coverage $k.$ We observe that the network connectivity $\kappa_1(G)$ is also higher than the sensing coverage $k.$

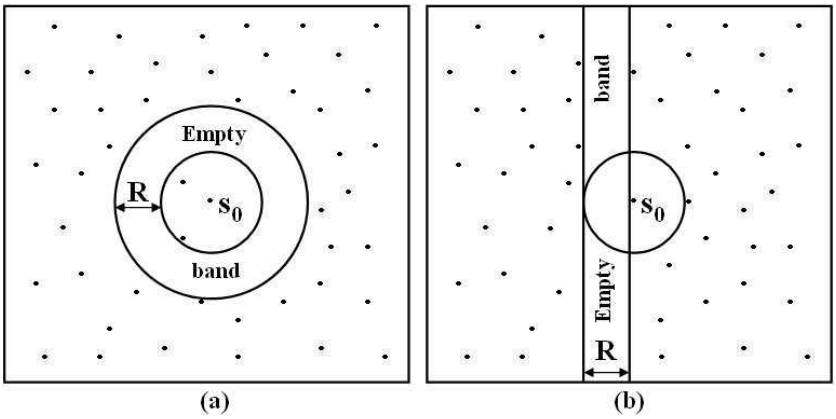

Figure 9.3 Non-trivial connected components of the disconnected network: (a) Connected component consists of all the neighboring sensors of the sink and (b) smallest connected component including the sink where the two connected components of the network do not surround each other.

Case 2 - Non-trivial connected components: Similarly, the disconnected network has two connected component. We distinguish two particular network configurations that are worth of study. In the first one (Figure 9.3a), the connected component including the sink corresponds to its communication disk (whose area is πR^2) and is surrounded by a circular band that contains no sensors. Furthermore, the distance between any pair of sensors from these two components is at least R in order to disable any communication between the two connected components. Thus, the width of this empty band should be at least $R.$ Hence, the area of the smallest empty circular band $\mathrm{B}(\xi_0, R)$ should be equal to

$$|\,B(\xi_0,R)\,| = \pi\,(2R)^2 - \pi R^2 = 3\pi R^2 \tag{9.7}$$

Thus, the expected minimum number of sensor failures to isolate the connected component of the sink is given by

$$E[\mathrm{X}] = \lambda(r,k) \mid B(\xi_0, R) \mid \tag{9.8}$$

Hence the network connectivity is equal to

$$\kappa_2(G) = E[\mathrm{X}] = 3\,\lambda(r,k)\,\pi\,R^2 \tag{9.9}$$

If we set $\alpha = R/r$ and substitute Equation (9.1) in equation (9.9), we obtain

$$\kappa_2(G) = \frac{6\,\pi\,\alpha^2\,k}{(\pi - \sqrt{3})} \tag{9.10}$$

The second configuration of the disconnected network (Figure 9.3b) corresponds to the smallest connected component containing the sink if the field has to be divided into two regions such that none of them surrounds the other. Hence, the width of the empty rectangular band, denoted by $\mathrm{B}(R,\sqrt{A})$, which splits the field vertically should be equal to R. The expected minimum number of sensor failures to isolate the sink is given by

$$E[\mathrm{X}] = \lambda(r,k)\,R\,\sqrt{A} \tag{9.11}$$

We find that the network connectivity is equal to

$$\kappa_3(G) = E[\mathrm{X}] = \lambda(\mathrm{r},\mathrm{k})\,R\,\sqrt{A} \tag{9.12}$$

Setting $\alpha = R/r$ and substituting Equation (9.1) in equation (9.12) yields

$$\kappa_3(G) = \frac{2\,R\,\sqrt{A}\,k}{(\pi - \sqrt{3})\,r^2} \tag{9.13}$$

Notice that $\kappa_3(G) > \kappa_2(G)$ given the hypothesis $R << \sqrt{A}.$

Case 3 – Largest connected component: One of the components of the disconnected network has only one sensor that is not the sink. This case is similar to the first case in that a single sensor becomes isolated when all of its neighbors fail. Applying the same reasoning leads to the same result found in Case 1. Thus, we have $\kappa_1(G) \le \kappa(G) \le \kappa_3(G)$ and hence the network fault tolerance $\eta(G)$ is given by $\kappa_1(G) - 1 \le \eta(G) \le \kappa_3(G) - 1.$ □

It is easy to check that $\kappa(G) > k.$ Indeed, the Hopital's theorem gives $\lim_{k\to\infty} k/\kappa(G) = 0.$ Our result of connectivity for two-dimensional *k*-covered wireless sensor networks is in sharp contrast with that reported in [166] stating that the network connectivity of a homogeneous *k*-covered wireless sensor network is

equal to k provided that the radius of the communication range of the sensors is at least double the radius of their sensing ranges, i.e., $R \geq 2r.$.

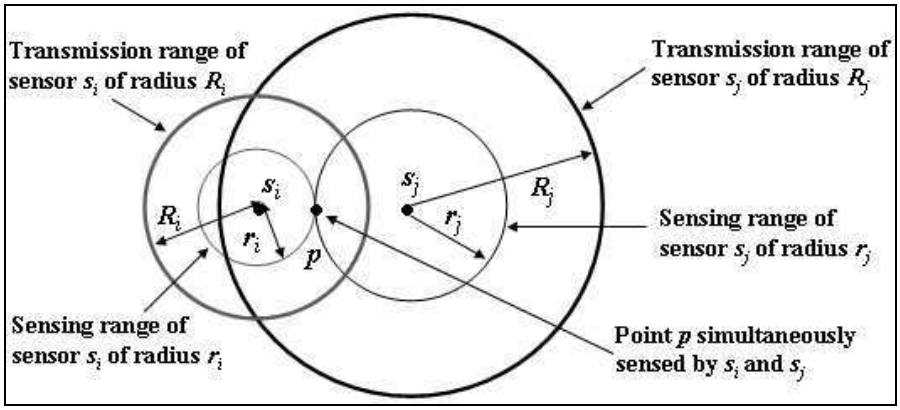

Figure 9.4 1-Coverage and $R_i \geq 2\, r_i$ do not imply connectivity.

9.1.2 Heterogeneous *k*-Covered Wireless Sensor Networks

In this section, we consider *k*-covered wireless sensor networks with heterogeneous sensors. In this case, it is easy to prove that the relationship $R \geq 2r$ cannot guarantee network connectivity even when the network is configured to provide sensing coverage. Figure 9.4 shows that s_j can connect to s_i but s_i cannot connect to s_j. Lemma 9.1 establishes a necessary and sufficient condition for connectivity of heterogeneous wireless sensor networks.

Lemma 9.1: A heterogeneous wireless sensor networks is connected if for any sensor, the radius of its communication disk is at least equal to the sum of the radii of its own sensing disk and that of the most powerful sensor in terms of sensing capability, i.e., for all $s_i \in S$, $R_i \geq r_i + r_{\max}$, where $r_{\max} = \max\{r_j : s_j \in S\}.$

Proof: Consider two sensors s_i and s_j whose sensing disks are tangential to each other at point p (Figure 9.6). Let $R_i = r_i + r_{\max}$ and $R_j = r_j + r_{\max}.$ Thus, $R_i \geq r_i + r_j$ and $R_j \geq r_i + r_j,$ thus implying $| \xi_i - \xi_j | \leq \min\{R_i, R_j\}.$ Hence, s_i and s_j are mutually connected. Thus, the underlying heterogeneous wireless sensor network is connected because it is *k*-covered. □

It is worth noting that achieving *k*-coverage depends on the least powerful sensors in terms of their sensing capability. Lemmas 9.2 and 9.3 for heterogeneous *k*-covered wireless sensor networks correspond to Lemmas 5.1 and 5.2 of Chapter 5, respectively.

Lemma 9.2: Let $k \geq 3.$ If the width of a closed convex area A, $\omega(\mathrm{A})$, satisfies $\omega(\mathrm{A}) \leq r_{\min}$, where $r_{\min} = \min\{r_j : s_j \in S\}$, then A is guaranteed to be *k*-covered by k heterogeneous sensors.

Proof: Our reasoning should be based on the least powerful sensors in terms of their sensing capability. In the worst case, when k least powerful sensors (all of them have the smallest radius of their sensing disks) are deployed in the Reuleaux triangle of constant (maximum) width equal to $r_{\min},$ denoted by $RT(r_{\min}),$ then $RT(r_{\min})$ is guaranteed to be *k*-covered, where $r_{\min} = \min\{r_j : s_j \in S\}$. □

Lemma 9.3: Let $r_{\min} = \min\{r_j : s_j \in S\}$ and $k \geq 3.$ The sensor spatial density necessary to guarantee *k*-coverage of a field sensed by spatially distributed heterogeneous sensors is given by

$$\lambda(r_{\min}, k) = \frac{2k}{(\pi - \sqrt{3})\, {r_{\min}}^2} \tag{9.14}$$

Proof: The proof is verbatim and stems from the fact that if k least powerful sensors (in terms of their sensing ranges) are able to *k*-cover a region A, then any subset of k sensors deployed in A will be able to do so. Using the Reuleaux triangle model, we can easily prove that the maximum size of A is $\mathrm{A}_{\max}(r_{\min}) = (\pi - \sqrt{3})\frac{{r_{\min}}^2}{2}$. Thus, the required sensor spatial density is $\lambda(r_{\min}, k) = \frac{k}{\mathrm{A}_{\max}(r_{\min})} = \frac{2k}{(\pi - \sqrt{3})\ {r_{\min}}^2}$, where $r_{\min} = \min\{r_j : s_j \in S\}$. □

Lemma 9.4 computes connectivity of heterogeneous *k*-covered wireless sensor networks and their fault tolerance.

Lemma 9.4: Let G be a communication graph of a heterogeneous *k*-covered wireless sensor networks with $k \geq 3$. The connectivity of heterogeneous *k*-covered wireless sensor networks is given by

$$K_1 \leq \kappa(G) \leq K_2 \tag{9.15}$$

where

$$K_1 = \frac{2\pi {R_{\min}}^2 k}{(\pi - \sqrt{3})\, {r_{\min}}^2}$$

$$K_2 = \frac{2 R_{\max} \sqrt{A}\, k}{(\pi - \sqrt{3})\, {r_{\min}}^2}$$

$r_{\min} = \min\{r_j : s_j \in S\}$ and $R_{\max} = \max\{R_j : s_j \in S\}.$ The fault tolerance, $\eta(G),$ is given by

$$K_1 - 1 \leq \eta(G) \leq K_2 - 1 \tag{9.16}$$

Proof: Similarly, we consider three cases depending on the types of components of the disconnected network that contain the sink.

Case 1 - Isolated sink: The sink is supposed to be the most powerful node in the network and hence the radius of its communication disk is equal to $R_{\max}$. Thus, the expected minimum number of sensor failures to isolate the sink is given by

$$E[\mathrm{X}] = \lambda(r_{\min}, k) \mid D(\xi_0, R_{\max}) \mid \tag{9.17}$$

Substituting Equation (9.14) in equation (9.17), we find that the network connectivity of heterogeneous *k*-covered wireless sensor networks is computed as

$$\kappa_1(G) = E[\mathrm{X}] = \frac{2\pi {R_{\max}}^2 k}{(\pi - \sqrt{3}) {r_{\min}}^2} \tag{9.18}$$

where $r_{\min} = \min\{r_j : s_j \in S\}, \quad R_{\max} = \max\{R_j : s_j \in S\},$ and $k \geq 3.$

Case 2 - Non-trivial connected components: We consider the same two network configurations, which were studied in the case of homogeneous *k*-covered wireless sensor networks. Notice that the sensors located around the sink are heavily used in data forwarding and hence should be the most powerful ones in terms of sensing and communication capabilities. Otherwise, they will suffer severe energy depletion and die very quickly. Thus, the communication disk of the sink contains only powerful sensors. Hence, the width of the circular empty band surrounding the connected component containing the sink should be equal to $R_{\max}$. Thus, the area of this empty band $B(\xi_0, R_{\max})$ should be equal to

$$\mid B(\xi_0, R_{\max}) \mid = \pi (2R_{\max})^2 - \pi {R_{\max}}^2 = 3\pi {R_{\max}}^2 \tag{9.19}$$

The expected minimum number of sensor failures to isolate the sink is given by

$$E[\mathrm{X}] = \lambda(r_{\min}, k) \mid B(\xi_0, R_{\max}) \mid \tag{9.20}$$

If we substitute Equation (9.14) in Equation (9.20), we find that connectivity is equal to

$$\kappa_2(G) = E[\mathrm{X}] = \frac{6\pi {R_{\max}}^2 k}{(\pi - \sqrt{3}) {r_{\min}}^2} \tag{9.21}$$

Likewise, for the second configuration of the disconnected network, the width of the empty rectangular band $\mathrm{B}(R, \sqrt{A})$ should be equal to $R_{\max}$ and hence its area is equal to $\mid \mathrm{B}(R, \sqrt{A}) \mid = R_{\max}\sqrt{A}$. Therefore, the expected minimum number of sensor failures to isolate the sink is given by

$$E[\mathrm{X}] = \lambda(r_{\min}, k) \mid \mathrm{B}(R, \sqrt{A}) \mid \tag{9.22}$$

Thus, the network connectivity is given by

$$\kappa_3(G) = E[\mathrm{X}] = \frac{2\, R_{\max} \sqrt{A}\, k}{(\pi - \sqrt{3})\, r_{\min}{}^2} \tag{9.23}$$

Case 3 – Largest connected component: In this case, the single-node component may include the least powerful or the most power sensor in terms of its communication capability. Hence, the network connectivity will have lower and upper bounds depending on whether the isolated sensor is the least or most powerful sensor, respectively. The expected minimum number of sensor failures to isolate a least powerful sensor is given by

$$E_{lb}[\mathrm{X}] = \lambda(r_{\min}, k) \mid D(\xi_0, R_{\min}) \mid \tag{9.24}$$

while the expected minimum number of sensor failures to isolate a most powerful sensor is given by

$$E_{ub}[\mathrm{X}] = \lambda(r_{\min}, k) \mid D(\xi_0, R_{\max}) \mid \tag{9.25}$$

Let K_{lb} and K_{ub} be lower and upper bounds, respectively, on connectivity $\kappa_4(G)$ of heterogeneous *k*-covered wireless sensor networks. In this case, it is easy to establish that $\kappa_4(G)$ satisfies

$$K_{lb}(G) \le \kappa_4(G) \le K_{ub}(G) \tag{9.26}$$

where

$$K_{lb}(G) = E_{lb}[\mathrm{X}] = \frac{2\,\pi\, R_{\min}{}^2\, k}{(\pi - \sqrt{3})\, r_{\min}{}^2}$$

$$K_{ub}(G) = E_{ub}[\mathrm{X}] = \frac{2\,\pi\, R_{\max}{}^2\, k}{(\pi - \sqrt{3})\, r_{\min}{}^2}$$

Using the results of the above three cases, we find that connectivity of heterogeneous *k*-covered wireless sensor networks satisfies

$$K_1 \le \kappa(G) \le K_2$$

and their fault tolerance is given by

$$K_1 - 1 \le \eta(G) \le K_2 - 1$$

where

$$K_1 = K_{lb}(G) = \frac{2\,\pi\, R_{\min}{}^2\, k}{(\pi - \sqrt{3})\, r_{\min}{}^2}$$

$$K_2 = \kappa_3(G)\frac{2\,R_{\max}\sqrt{A}\,k}{(\pi-\sqrt{3})\,r_{\min}{}^2}$$

$r_{\min} = \min\{r_j : s_j \in S\}$, $R_{\min} = \min\{R_j : s_j \in S\}$, and $R_{\max} = \max\{R_j : s_j \in S\}$. Using Hopital's theorem, it is easy to prove that $\kappa(G) > k$. □

9.2 Conditional Fault-Tolerance Measures

Motivated by the above-mentioned shortcomings of classical connectivity, we propose a new measure of fault tolerance for *k*-covered wireless sensor networks, called *conditional fault-tolerance*, using the concepts of *conditional connectivity* and *forbidden faulty sensor set*. In this section, we use the concepts of *conditional connectivity* [87] and *forbidden faulty set* [67], [68], as a remedy to the above shortcomings of the traditional (unconditional) connectivity metric. Our approach [17], [26] is based on forbidden faulty sensor sets.

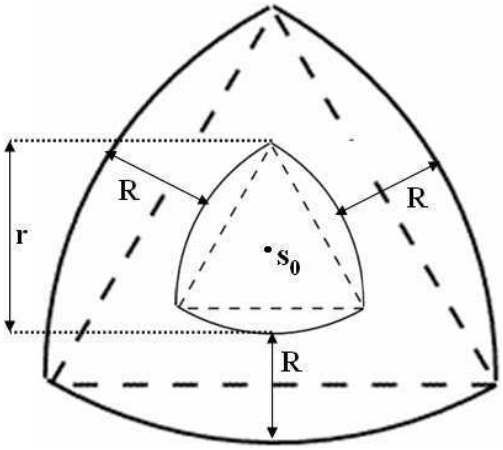

Figure 9.5 $RT(\xi_0, r)$ and $A(\xi_0, R)$ regions.

Let $G = (S, E)$ be a communication graph representing a *k*-covered wireless sensor network and $CN(s_i)$ the communication neighbor set of sensor s_i. Define a *forbidden faulty sensor set* of G as a set of faulty sensors that includes the entire neighbor set of a given sensor. Consider the property P: "A faulty sensor set cannot include the entire neighbor set of a given sensor". A faulty sensor set satisfying property P is denoted by F_{P}, where $F_{\mathrm{P}} \subset S$, and defined by

$$F_{\mathrm{P}} = \{U \subset S \mid \forall s_i \in S : CN(s_i) \not\subset U\}$$

The *conditional connectivity* of G with respect to P, denoted by $\kappa(G : \mathrm{P})$, is the minimum size of F_{P}

such that the graph $G_d = (S - F_P, E_{S-F_P})$ is disconnected, where E_{S-F_P} is a set of remaining communication edges between the non-faulty sensors.

9.2.1 Homogeneous *k*-Covered Wireless Sensor Networks

In this section, we consider homogeneous sensors that possess the same sensing range and the same communication range. Our results prove that *k*-covered wireless sensor networks can sustain a larger number of sensor failures under the restriction imposed on a faulty sensor set. Theorem 9.4 computes the conditional connectivity and conditional fault-tolerance of homogeneous *k*-covered wireless sensor networks.

Theorem 9.4: The conditional connectivity of homogeneous *k*-covered wireless sensor networks is given by

$$\kappa(G:P) = \frac{4R(R+r)k}{r^2} \tag{9.27}$$

where $\alpha = R/r$ and $k \geq 3.$ The conditional fault-tolerance of G, is given by $\eta(G:P) = \kappa(G:P) - 1.$

Proof: We consider two cases based on the type of component to which the sink belongs.

Case 1 - Smallest-size component including the sink: Under the assumption of forbidden faulty set, we assume the sink belongs to the smallest connected component that is disconnected from the rest of the network. Let ξ_0 be the location of the sink s_0. By hypothesis, any location in the field is *k*-covered with $k \geq 3$, and in particular the location ξ_0. Therefore, there must be a subset of sensors located at distance at most equal to r from ξ_0. Using the *Reuleaux Triangle* model, the Reuleaux triangle of width $r + \varepsilon_1$ and centered at ξ_0, denoted by $RT(\xi_0, r + \varepsilon_1)$, where ε_1 is an infinitesimal value, must be not empty; otherwise, the *k*-coverage property at ξ_0 is not satisfied, and particularly the forbidden faulty set constraint is not met. Our goal is to compute the minimum number of sensors to fail in order to disconnect the sink under the forbidden set constraint. Notice that the smallest connected component including the sink requires $\varepsilon_1 = 0.$ The region $RT(\xi_0, r)$ is a guarantee that the sink will not be isolated by itself and hence the forbidden faulty sensor set constraint with respect to the sink is not violated. Indeed, only a subset of its neighbors fails and not all of them as in the case of classical connectivity (see previous section). In this configuration, the majority of the sensors are not connected to the sink, and hence the network is dead. Now, to disconnect

the sink together with its neighbors located in $RT(\xi_0, r),$ the annulus surrounding the region $RT(\xi_0, r)$ and centered at ξ_0 should be empty and have a width equal to $R + \varepsilon_2$; otherwise the network remains connected. Notice that the minimum number of sensor failure requires $\varepsilon_2 = 0$. Thus, this empty annulus, denoted by $A(\xi_0, R)$ (Figure 9.5), will guarantee that the connected component in $RT(\xi_0, r)$ is disconnected. Notice that the width of the outmost Reuleaux triangle centered at ξ_0 is equal to $2R + r$. Hence, the area of the annulus $A(\xi_0, R)$ is given by

$$| A(\xi_0, R) | = | RT(\xi_0, 2R + r) | - | RT(\xi_0, r) | = 2(\pi - \sqrt{3}) R(R + r) \tag{9.27a}$$

Thus, the conditional expected minimum number of sensor failures to disconnect the smallest component including the sink is computed as

$$E[X : P] = \lambda(r, k) | A(\xi_0, R) |] \tag{9.27b}$$

where Substituting Equation (9.1) and Equation (9.26a) in Equation (9.26b), we find that the conditional connectivity is computed as

$$\kappa_1(G : P) = E[X : P] = \frac{4R(R + r)k}{r^2} \tag{9.27c}$$

where r and R are the radii of the sensing and communication disks of the sensors, respectively, and k is the degree of coverage of the field. It is easy to prove that the forbidden faulty sensor set constraint is satisfied for both the faulty and non-faulty sensors. Any sensor inside the region $RT(\xi_0, r)$ still has non-faulty neighbors located in $RT(\xi_0, r).$ Also, any sensor outside the region $RT(\xi_0, R + r)$ has non-faulty neighbors within $RT(\xi_0, R + r).$ Similarly, any faulty sensor within the annulus $A(\xi_0, R)$ has non-faulty neighbors located in $RT(\xi_0, r)$ and outside $RT(\xi_0, R + r).$

Case 2 – Largest connected component: We assume that the sensors located in the annulus $A(\xi_i, R)$ as defined earlier fail. This case is similar to the previous one except that the sink belongs to the largest connected component of the disconnected network. Using the same reasoning as in Case 1, we obtain the same conditional network connectivity. Here again, to consider whether or not the resulting network is connected or not depends on the type of coverage (full coverage or partial coverage) required by the sensing application. Thus, we have $\kappa_2(G : P) = \kappa_1(G : P).$

From both cases 1 and 2, it follows that the conditional network connectivity is $\kappa(G:P) = \kappa_1(G:P)$, and hence the conditional network fault-tolerance is given by $\eta(G:P) = \kappa(G:P) - 1$. It is easy to check that $\kappa(G:P) > \kappa(G)$ and hence $\kappa(G:P) > k$. Indeed, the Hopital's theorem gives $\lim_{k\to\infty} k / \kappa(G:P) = 0$. By definition, the conditional network fault tolerance is given by $\eta(G:P) = \kappa(G:P) - 1$. □

This new measure shows that the classical connectivity used to capture network fault tolerance underestimates the resilience of large-scale dense wireless sensor networks, such as *k*-covered wireless sensor networks.

9.2.2 Heterogeneous *k*-Covered Wireless Sensor Networks

Because heterogeneous sensors are deployed randomly, they can be located anywhere in the square field. In this case, computing the conditional connectivity of heterogeneous *k*-covered wireless sensor networks is not a straightforward generalization of the process used previously for homogeneous *k*-covered wireless sensor networks. We found that disconnecting the network while satisfying the forbidden faulty set constraint is a challenging problem. If, on the one hand, we choose the width of the annulus to be $R_{\max}$, then the sensors with communication range less than or equal to half of $R_{\max}$ may be located in the annulus. Thus, the property P will be violated (Figure 9.6a) as the entire neighbor set of some sensors located within the annulus would fail at the same time. If, on the other hand, the width of the annulus is less than $R_{\max}$, then the non-faulty sensors of one connected component might be able to connect to the non-faulty sensors of the other connected component of the disconnected network. Hence, the obtained network is not disconnected (Figure 9.6b). As can be seen, we cannot find an exact value of the conditional connectivity of heterogeneous *k*-covered wireless sensor networks in the absence of any deterministic sensor deployment strategy. Hence, we propose to compute lower and upper bounds on conditional connectivity based on particular sensor configurations in the annulus and around the annulus. While in the first scenario we assume that the annulus contains only least powerful sensors, the second scenario supposes that the annulus consists of most powerful sensors.

Lemma 9.5 computes the conditional connectivity and conditional fault-tolerance of heterogeneous *k*-covered wireless sensor networks.

Lemma 9.5: The conditional connectivity of heterogeneous *k*-covered wireless sensor networks is given by

$$\kappa_1(G:P) \le \kappa(G:P) \le \kappa_2(G:P) \tag{9.28}$$

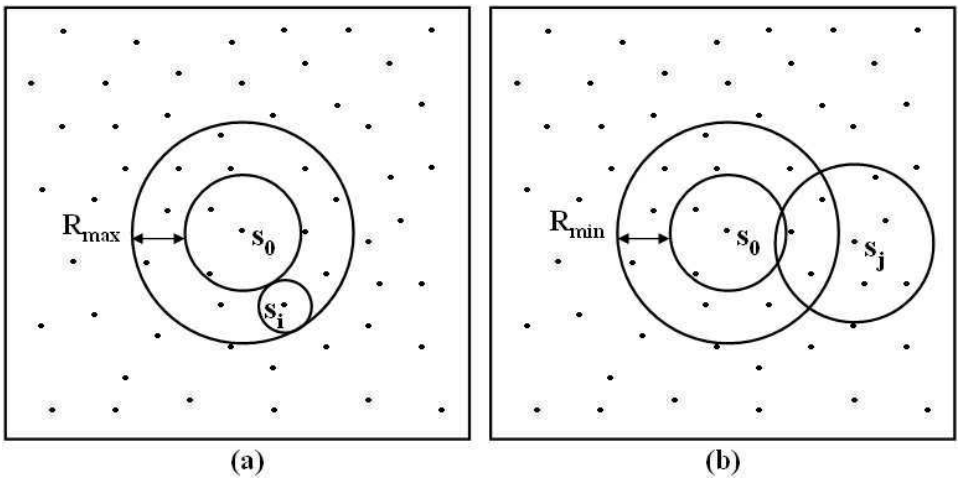

Figure 9.6 (a) The forbidden fault set constraint is violated (neighbor set of s_i is within the circular band of width $R_{\max}$) and (b) connectivity is maintained (the radius of s_j's communication disk is larger than $R_{\min}$).

where

$$\kappa_1(G:P) = \frac{4\,R_{\min}\,(R_{\min} + r_{\min})\,k}{{r_{\min}}^2}$$

$$\kappa_2(G:P) = \frac{4\,R_{\max}\,(R_{\max} + r_{\max})\,k}{{r_{\min}}^2}$$

$k \ge 3$, $r_{\min} = \min\{r_j : s_j \in S\}$, $r_{\max} = \max\{r_j : s_j \in S\}$, $R_{\min} = \min\{R_j : s_j \in S\}$, and $R_{\max} = \max\{R_j : s_j \in S\}$. The conditional fault tolerance of the network is given by

$$\kappa_1(G:P) - 1 \le \eta(G:P) \le \kappa_2(G:P) - 1 \tag{9.29}$$

Proof: First assume that the annulus as well as the area surrounding it contains only least powerful sensors, and hence its width is equal to $R_{\min}$. Furthermore, in order to guarantee that the sink will not be isolated, which would violate the forbidden faulty sensor set constraint, the width of the Reuleaux triangle centered at the location ξ_0 of the sink s_0 should be equal to $r_{\min}$. These two conditions yield a disconnected network that satisfies the forbidden faulty sensor set constraint. First assume that the annulus as well as the area surrounding it contains only least powerful sensors, and hence its width is equal to $R_{\min}$. The area of the annulus $A(\xi_0, R_{\min})$ is given by

$$\begin{aligned} |\,A(\xi_0, R_{\min})\,| &= |\,RT(\xi_0, 2\,R_{\min} + r_{\min})\,| - |\,RT(\xi_0, r_{\min})\,| \\ &= 2\,(\pi - \sqrt{3})\,R_{\min}\,(R_{\min} + r_{\min}) \end{aligned}$$

Hence, the conditional expected minimum number of sensor failures to disconnect the connected component including the sink from the rest of the network is computed as

$$E[\mathrm{X} : P] = \lambda(r_{\min}, k) \mid A(\xi_0, R_{\min}) \mid$$

Thus, the lower bound on conditional connectivity is computed as

$$\kappa_1(G : P) = E[\mathrm{X} : P] = \frac{4\, R_{\min}\,(R_{\min} + r_{\min})\, k}{{r_{\min}}^2} \tag{9.30}$$

where $r_{\min} = \min\{r_j : s_j \in S\}$ *and* $R_{\min} = \min\{R_j : s_j \in S\}$. To compute the upper bound on network connectivity, we assume that the sensors inside the annulus and around it are the most powerful ones. The analysis is similar to the previous one except that we just replace $r_{\min}$ by $r_{\max}$ and $R_{\min}$ by $R_{\max}$ in the denominator of the first part of Equation (9.7) in order to disconnect the network while meeting the forbidden faulty set constraint. We found that the network connectivity is given by

$$\kappa_2(G : P) = \frac{4\, R_{\max}\,(R_{\max} + r_{\max})\, k}{{r_{\min}}^2} \tag{9.31}$$

where $r_{\max} = \max\{r_j : s_j \in S\}$, $R_{\min} = \min\{R_j : s_j \in S\}$, *and* $R_{\max} = \max\{R_j : s_j \in S\}$. Thus, the conditional network connectivity of heterogeneous *k*-covered wireless sensor networks with respect to the forbidden faulty set constraint P satisfies

$$\kappa_1(G : P) \le \kappa(G : P) \le \kappa_2(G : P)$$

and their conditional network fault-tolerance is given by

$$\kappa_1(G : P) - 1 \le \eta(G : P) \le \kappa_2(G : P) - 1$$ □

It is worth noting that there is neither a polynomial-time algorithm for computing $\kappa(G : \mathrm{P})$ for a general graph nor any tight upper bound for $\kappa(G : \mathrm{P})$. However, our characterization *of k*-coverage based on the intersection of k sensing disks and the Reuleaux triangle make it possible to compute the corresponding minimum sensor spatial density. This helps us derive conditional connectivity and conditional fault-tolerance of *k*-covered wireless sensor networks.

9.3 Summary

In this chapter, we have computed the connectivity of two-dimensional *k*-covered wireless sensor networks, where the sensors can be homogeneous or heterogeneous [17], [26], [27]. Network fault-

tolerance and sensed data accuracy are highly desirable characteristics for wireless sensor networks that can be met through connected *k*-coverage. Our results on connectivity take into consideration an inherent characteristic of wireless sensor networks in that the sink has a critical role in terms of data processing and decision making, compared to the rest of the network. Therefore, we have computed the connectivity of two-dimensional *k*-covered wireless sensor networks based on the size of the connected component that includes the sink. We found that the connectivity of two-dimensional *k*-covered wireless sensor networks is much higher than the degree of sensing coverage *k* provided by the network. The traditional connectivity metric, however, is defined in an abstract way and does not consider the inherent properties of wireless sensor networks because it assumes that any subset of nodes can fail at the same time. This assumption is not valid for heterogeneous *k*-covered wireless sensor networks. To compensate for these shortcomings, we have used proposed more realistic measures of connectivity based on the concept of forbidden faulty set. We found that *k*-covered wireless sensor networks can sustain a large number of sensor failures if the neighbor set of a given sensor cannot fail simultaneously.

CHAPTER 10

CONCLUSION AND FUTURE WORK

The main challenge in the design of wireless sensor networks is the limited energy of the sensors and the difficulty of replacing and/or recharging their batteries due to the inherent characteristics of a field (hostile environments, for instance) and cost. To alleviate this problem, it is necessary that the sensors be densely deployed (i.e., *redundant sensor deployment*) and appropriate protocols be designed in order to exploit this redundancy while maximizing the operational lifetime of the network. Several network configuration protocols for connected *k*-coverage have been proposed in the literature with a goal to save the sensors' energy while meeting the specific, critical application requirements in terms of coverage and connectivity. All those proposed protocols helped us design energy-efficient, centralized and distributed protocols for network configuration. Furthermore, this dissertation addressed the design issues of joint coverage, connectivity, duty-cycling, and data forwarding protocols for wireless sensor networks while considering energy efficiency in order to maximize the energy conservation, thus extending the operational network lifetime as much as possible. Our study has considered a *many-to-one* wireless sensor network architecture, where *all* sources sensors report their sensed data to a *single* sink.

In this chapter we summarize the contributions that we have made in data forwarding, coverage, and connectivity in wireless sensor networks. Then, we present our future research work.

10.1 Summary of Contributions

We have studied coverage and connectivity in wireless sensor networks using percolation theory. Precisely, we have computed a non-trivial value of the *covered area fraction* at critical percolation, called *critical covered area fraction*, and derived the critical sensor spatial density above which a field is almost surely covered. Furthermore, we proposed a model for percolation in wireless sensor networks, called *correlated disk model*, to study both coverage and connectivity in an integrated manner based on the relationship between the communication and sensing ranges of the sensors. We have found that the value of the critical sensor spatial density depends on the ratio of the radius of the communication disks of the

sensors to the radius of their sensing disks. This study helps network designer fully cover a field with a minimum number of sensors while maintaining connectivity between them.

Motivated by the existence of different applications and environments with diverse requirements in terms of degrees of coverage and connectivity, we extended our above analysis for 1-coverage to redundant coverage (or *k*-coverage) so the network can be self-configured in order to support these applications. Precisely, we considered a deterministic approach to analyze and characterize *k*-coverage of a field, and compute the minimum active sensor spatial density required to full *k*-cover a field. Our analysis is based on a fundamental theorem, namely Helly's Theorem, which characterizes the intersection of convex sets, as well as the geometric properties of the Reuleaux triangle. We found that this density depends only on the degree of coverage *k* requested by a sensing application and the radius of the sensing disks of the sensors, thus reflecting the expected behavior of the sensors. Moreover, our analysis requires that the communication range of the sensors be at least equal to their sensing range so all active sensors in a *k*-covered wireless sensor network are guaranteed to be connected. Based on this analysis, we computed the unconditional and conditional connectivity of *k*-covered wireless sensor networks and proved that is higher than the degree of coverage *k*. Furthermore, we proposed four configuration protocols to achieve connected *k*-coverage in wireless sensor networks. In the first one, called *centralized randomized connected k-coverage*, the sink is responsible for selecting a minimum number of sensors to guarantee *k*-coverage of a field while maintaining connectivity between active selected sensors. Each of the second and third protocols, called *Reuleaux triangle-based clustered randomized connected k-coverage* and *disk-based clustered randomized connected k-coverage*, is run under the control of the sink and a subset of sensors. Precisely, in each round, the sink selects a subset of sensors, called *cluster-heads*, each of which is responsible for selecting a subset of neighboring sensors to *k*-cover its underlying cluster while remaining connected to each other. Both protocols consider different degree of network clustering. In the fourth protocol, called *distributed randomized connected k-coverage*, all the sensors are required to coordinate among themselves to *k*-cover a field in each round while being mutually connected. For our distributed connected *k*-coverage protocol, we designed two sensor scheduling schemes to guarantee full *k*-coverage of a field. In the first scheme, called *Self-Scheduling driven k-Coverage*, each

sensor turns itself *on* based on the local information it has about its sensing neighbors in order to *k*-cover sensing range. In the second scheme, called *Triggered-Scheduling driven k-Coverage*, each sensor is allowed to trigger a necessary number of its sensing neighbors to become active in order to achieve *k*-coverage of its sensing range. We found that the latter outperforms the former in terms of the number of active sensors needed for *k*-coverage and network lifetime. Furthermore, we relaxed some commonly used assumptions for coverage configuration in wireless sensor networks, namely the sensing and communication disk model and sensor homogeneity model, in order to enhance the applicability of our connected *k*-coverage protocols in real-world sensing applications. Based on these connected *k*-coverage protocols, we designed an energy-efficient, unified framework, called Cover-Sense-Inform (CSI), where connected *k*-coverage, duty-cycling, and geographic forwarding are jointly considered. More specifically, on top of the connected *k*-coverage configuration protocols, we proposed several potential fields-based geographic forwarding protocols on duty-cycled sensors depending on whether data aggregation is considered. This effort constitutes the first design of geographic forwarding protocols for duty-cycled *k*-covered wireless sensor networks with and without data aggregation.

In order to account for the stochastic nature of the sensors, we adapted the analysis of the connected *k*-coverage problem in two-dimensional wireless sensor networks under a deterministic sensing model to solve the stochastic connected *k*-coverage problem under a stochastic sensing model. This helps us develop a global framework for connected *k*-coverage in wireless sensor networks that considers both deterministic and stochastic sensing models. Our stochastic sensing model takes into account not only the distance between the sensors and the target locations but also the type of propagation model, i.e. free-space model or multi-path model. In addition, we have focused on the problem of forwarding in duty-cycled three-dimensional *k*-covered wireless sensor networks, where *k*-coverage, duty-cycling, and data forwarding are discussed and addressed in a novel joint framework. Using *Helly's Theorem* [6], we find that the extension of the analysis of *k*-coverage in two-dimensional to three-dimensional wireless sensor networks is not straightforward. This is due to the fact that some properties that hold for two-dimensional space cannot generalize to three-dimensional space. Moreover, we have proposed a hybrid forwarding protocol in duty-cycled three-dimensional *k*-covered wireless

sensor networks, where both *deterministic* and *opportunistic forwarding* approaches are considered. Our hybrid forwarding approach provides a trade-off between uncertainty and contention, thus helping achieve good data forwarding performance in terms of delay and control overhead.

Our CSI framework considers static wireless sensor networks, where all the sensors and the sink do not move. This type of architecture, however, suffers from a severe problem, called *energy sink-hole*, where the sensors nearer the sink suffer from severe battery power depletion problem. Indeed, the sensors close to the sink act as relays to the sink on behalf of *all* other sensors, and hence deplete their battery power more quickly, thus disconnecting the network. We have proposed solutions that exploit heterogeneity, mobility, and our new concept of energy-aware Voronoi diagram. However, these solutions do not take coverage into consideration as the *energy sink-hole* is coverage-independent, but assume that the network is connected for data forwarding to take place. For homogeneous sensors in terms of their initial energy, we proposed EVEN, an *energy aware Voronoi diagram-based data forwarding* protocol. EVEN is a greedy, localized protocol that combines sink mobility with a new concept, called *energy aware Voronoi diagram* whose sites (i.e., sensors' locations) are time-varying as they depend on the remaining energy of the sensors. We find that EVEN yields a significant improvement in terms of network lifetime.

10.2 Future Work

As future work, we plan to extend our results described earlier as follows:

The analysis of phase transitions in coverage and connectivity in wireless sensor networks considers homogeneous, two-dimensional wireless sensor networks. We plan to extend this analysis by considering heterogeneous sensors with different sensing and communication ranges capabilities. Real-world sensing applications may require heterogeneous sensors in order to enhance the reliability of the network and extend its lifetime. Moreover, even sensors equipped with identical hardware may not always have the same sensing model. We also plan to extend our work to irregular sensing and communication ranges of the sensors whose shape is not necessarily circular. In addition, we plan to study coverage and connectivity in three-dimensional wireless sensor networks from a percolation theory perspective.

Our CSI framework considers static, connected *k*-covered wireless sensor networks, which still suffer from the energy-sink problem although it uses sensor duty-cycling. Indeed, this problem is inherent

to static wireless sensor networks. We plan to benefit from the mobility that EVEN uses to solve the energy-sink problem. Precisely, we intend to study joint connected *k*-coverage and geographic forwarding in mission-oriented wireless sensor networks, where sensors are mobile to accomplish a specific mission at some time that is requested by the sink. In particular, we will exploit our previous results for static, connected *k*-covered wireless sensor networks in order to investigate the problem of guaranteeing mobile *k*-coverage while maintaining network connectivity in mission-oriented wireless sensor networks [24], [25].

We are also interested in solving the following problem: given that the sensors may die or fail anytime due to their low battery power, it is necessary to determine the necessary minimum number of sensors that need to join the network to guarantee certain requirements in terms of coverage and connectivity that should be satisfied for a sensing application. It is worth mentioning that heterogeneous wireless sensor networks require an adaptive approach in the sense that the sensor density should be defined based on the type of sensors deployed in a given area so as to achieve a certain degree of coverage of a field using as minimum number of sensors as possible.

We believe that the problems of connected *k*-coverage and geographic forwarding in three-dimensional, static wireless sensor networks deserve deep investigation. Particularly, the problem of ensuring *k*-coverage of a three-dimensional field needs to be addressed using different tiling strategies of a sphere, assuming that the sensing range of the sensors is represented by a sphere. Indeed, the problems of *k*-coverage and tiling in three-dimensional space seem to be very inter-related. Different models of titling of a sphere could be adapted to solve the problem of *k*-coverage in three-dimensional wireless sensor networks with better bounds on the required sensor spatial density. We also plan to compute tight bounds on their unconditional and conditional connectivity and fault-tolerance. Furthermore, we plan to extend the analysis our previous results to investigate the problem of stochastic *k*-coverage in three-dimensional wireless sensor networks using our stochastic sensing model.

We also plan to extend our work [8], [9], [10] in order to build a hybrid network through the integration of wireless sensor networks, mobile ad hoc networks, and the global IP Internet. The hybrid network would benefit from the advantages of each of these three networks, namely mobility of mobile ad hoc networks, high density of wireless sensor network, and continuous connectivity of the IP Internet.

Finally, the implementation of our CSI on a real sensor testbed is our ultimate goal.

REFERENCES

[1] Z. Abrams, A. Goel, and S. Plotkin, "Set *k*-cover algorithms for energy efficient monitoring in wireless sensor networks," *Proc. IPSN*, Berkeley, California, USA, pp. 424-432, Apr. 2004.

[2] S. Adlakha and M. Srivastava, "Critical density threshold for coverage in wireless sensor networks," *Proc. IEEE WCNC*, pp. 1615-1620, 2003.

[3] J. Ai and A. Abouzeid, "Coverage by directional sensors in randomly deployed wireless sensor networks," *Journal of Combinatorial Optimization*, 11(1), pp. 21-41, Feb. 2006.

[4] I. F. Akyildiz, D. Pompili, and T. Melodia, "Underwater acoustic sensor networks: research challenges," *Ad Hoc Networks*, 3, pp. 257-279, Mar. 2005.

[5] I. Akyildiz, D. Pompili, and T. Melodia, "Challenges for efficient communications in underwater acoustic sensor networks," *ACM SIGBED Review,* 1(2), pp. 3-8, Jul. 2004.

[6] I. F. Akyildiz, W. Su, Y. Sankarasubramaniam, and E. Cayirci, "Wireless sensor networks: A survey," *Computer Networks*, (38), pp. 393-422, Mar. 2002.

[7] S. Alam and Z. Haas, "Coverage and connectivity in three-dimensional networks," *Proc. ACM MobiCom*, pp. 346-357, 2006.

[8] H. M. Ammari, "A survey of current architectures for connecting wireless mobile ad hoc networks to the Internet," *International Journal of Communication Systems* (IJCS), 20(8), pp. 943-968, Aug. 2007.

[9] H. M. Ammari, "Lessons learned from the simulation experience of a three-tier multi-hop wireless Internet architecture," *Information Sciences*, 177(8), pp. 1806-1833, Apr. 2007.

[10] H. M. Ammari, "Using group mobility and multihomed mobile gateways to connect mobile ad hoc networks to the global IP Internet," *International Journal of Communication Systems* (IJCS), 19(10), pp. 1137-1165, Dec. 2006.

[11] H. M. Ammari and S. K. Das, "Integrated coverage and connectivity in wireless sensor networks: A two-dimensional percolation problem," *IEEE Transactions on Computers* (IEEE TC), to appear

in 2008.

[12] H. M. Ammari and S. K. Das, “Promoting heterogeneity, mobility and energy-aware Voronoi diagram in wireless sensor networks,” *IEEE Transactions on Parallel and Distributed Systems* (IEEE TPDS), To appear in 2008.

[13] H. M. Ammari and S. K. Das, “Coverage and connectivity in three-dimensional wireless sensor networks using percolation theory,” *IEEE Transactions on Parallel and Distributed Systems* (IEEE TPDS), To appear in 2008.

[14] H. M. Ammari and S. K. Das, ““A trade-off between energy and delay in data dissemination for wireless sensor networks using transmission range slicing,” *Computer Communications*, to appear in 2008.

[15] H. M. Ammari and S. K. Das, “*k*-Coverage and connectivity in three-dimensional wireless sensor networks,” *IEEE Transactions on Mobile Computing* (IEEE TMC), Under second review, Dec. 2007.

[16] H. M. Ammari and S. K. Das, “Randomized *k*-coverage protocols for wireless sensor networks,” *IEEE Transactions on Computers* (IEEE TC), Under review, May 2008.

[17] H. M. Ammari and S. K. Das, “Fault tolerance measures for large wireless sensor networks,” *ACM Transactions on Autonomous and Adaptive Systems* (ACM TAAS), Under review, Mar. 2007.

[18] H. M. Ammari and S. K. Das, “Energy-delay trade-off for forwarding in wireless sensor networks: A multi-objective optimization problem,” *Wireless Networks* (WiNet), Under review, Feb. 2008.

[19] H. M. Ammari and S. K. Das, “Joint *k*-Coverage and Hybrid Forwarding in Duty-Cycled Three-Dimensional Wireless Sensor Networks,” *Proc. IEEE SECON*, 2008.

[20] H. M. Ammari and S. K. Das, “Clustering-based minimum energy *m*-connected *k*-covered wireless sensor networks,” *Proc. EWSN’08*, TPC Best Paper Award, *Lecture Notes in Computer Science (LNCS) 4913*, pp. 1-16, 2008.

[21] H. M. Ammari and S. K. Das, “Geographic forwarding in duty-cycled connected k-covered wireless sensor networks,” *Proc. IEEE PerCom’08: Google Ph.D. Forum - A Ph.D. Forum on Pervasive Computing and Communications*, 2008.

[22] H. M. Ammari and S. K. Das, "A unified framework for *k*-coverage, duty-cycling, and geographic forwarding in wireless sensor networks," Submitted to a conference, Mar. 2008.

[23] H. M. Ammari and S. K. Das, "Joint stochastic *k*-coverage and scheduling in densely deployed wireless sensor networks," Submitted to a conference, May 2008.

[24] H. M. Ammari and S. K. Das, "Distributed *k*-coverage protocols for wireless sensor networks," Submitted to a workshop, May 2008.

[25] H. M. Ammari and S. K. Das, "Achieving mobile *k*-coverage in mission-oriented wireless sensor networks," To be submitted to a conference, May 2008.

[26] H. M. Ammari and S. K. Das, "On computing conditional fault-tolerance measures for *k*-covered wireless sensor networks," *Proc. ACM/IEEE MSWiM*, pp. 309-316, 2006.

[27] H. M. Ammari and S. K. Das, "Coverage, connectivity, and fault tolerance measures of wireless sensor networks," *Proc. SSS*, A. K. Datta and M. Gradinariu (Eds.), LNCS 4280, pp. 35-49, 2006.

[28] H. M. Ammari and S. K. Das, "An energy-efficient data dissemination protocol for wireless sensor networks," *Proc. IEEE PerSenS*, in conjunction with *PerCom*, pp. 357-361, 2006.

[29] H. M. Ammari and S. K. Das, "Data dissemination to mobile sinks in wireless sensor networks: An information theoretic approach", *Proc. IEEE MASS*, pp. 1-10, 2005.

[30] H. M. Ammari and S. K. Das, "Trade-off between energy savings and source-to-sink delay in data dissemination for wireless sensor networks," *Proc. ACM/IEEE MSWiM*, pp. 126-133, 2005.

[31] H. M. Ammari and S. K. Das, "Data dissemination in sensor networks: Trading off energy savings and source-to-sink delay," Poster, *ACM Student Research Competition (ACM SRC), ACM MobiCom*, 2005.

[32] T. Antoniou, I. Chatzigiannakis, G. Mylonas, S. Nikoletseas, and A. Boukerche, "A new energy efficient and fault-tolerant protocol for data propagation in smart dust networks using varying transmission range," *Proc. ANSS*, pp. 43-52, 2004.

[33] F. Aurenhammer, "Voronoi diagrams – A survey of a fundamental data structure," *ACM Computing Surveys,* 23 (3), pp. 345-405, Sept. 1991.

[34] X. Bai, S. Kumar, D. Xuan, Z. Yun, and T. H. Lai, "Deploying wireless sensors to achieve both

coverage and connectivity," *Proc. ACM MobiHoc*, pp. 131-142, 2006.

[35] P. Balister, B. Bollobas, A. Sarkar, and S. Kumar, "Reliable density estimates for achieving coverage and connectivity in thin strips of finite length," *Proc. ACM MobiCom*, pp. 75-86, 2007.

[36] S. Bandyppadhyay and E. Coyle, "Spatio-temporal sampling rates and energy efficiency in wireless sensor networks," *Proc. IEEE INFOCOM,* pp. 1729-1740, 2004.

[37] E. Bertin, J.-M., Billot, and R. Drouilhet, "Continuum percolation in the Gabriel graph," *Advances in Applied Probability*, 34(4), pp. 689–701, 2002.

[38] S. Biswas and R. Morris, "ExOR: Opportunistic multi-hop routing for wireless networks," *Proc. ACM SIGCOMM 2005 Conf. on Applications, Technologies, Architectures, and Protocols for Computer Communication*, pp. 133-143, 2005.

[39] B. Bollobás, *The Art of Mathematics: Coffee Time in Memphis*, Cambridge University Press, 2006.

[40] L. Booth, J. Bruck, M. Franceschetti, and R. Meester, "Covering algorithms, continuum percolation and the geometry of wireless networks," *The Annals of Applied Probability*, vol. 13, no. 2, pp. 722-741, 2003.

[41] P. Bose and P. Morin, "Online Routing in Triangulations," *SIAM Journal on Computing*, 33(4), pp. 937-951, 2004.

[42] P. Bose, P. Morin, I. Stojmenovic, and J. Urrutia, "Routing with guaranteed delivery in ad hoc wireless networks," *ACM/Kluwer Wireless Networks*, 7(6), pp. 609-616, 2001.

[43] A. Boukerche, I. Chatzigiannakis, and S. Nikoletseas, "A new energy efficient and fault-tolerant protocol for data propagation in smart dust networks using varying transmission range," *Computer Communications*, 4(29), pp. 477-489, Feb. 2006.

[44] A. Boukerche, I. Chatzigiannakis, and S. Nikoletseas, "Power-efficient data propagation protocols for wireless sensor networks," *Simulation*, 81(6), pp. 399-411, 2005.

[45] A. Boukerche, X. Cheng, and J. Linus, "Energy-aware data-centric routing in microsensor networks," *Proc. ACM MSWiM*, in conjunction with *ACM MobiCom*, pp. 42-49, 2003.

[46] S. R. Broadbent and J. M. Hammersley, "Percolation processes, I. Crystals and mazes," *Proc. Cambridge Philosophical Society*, 53, pp. 629-641, 1957.

[47] N. Bulusu, J. Heidemann, and D. Estrin, “GPS-less low cost outdoor localization for very small devices,” *IEEE Personal Communications Magazine,* 7(5), pp. 28-34, Oct. 2000.

[48] Q. Cao, T. Yan, J. Stankovic, and T. Abdelzaher, “Analysis of target detection performance for wireless sensor network,” in *Proc. DCOSS*, 2005, LNCS 3560, V. Prasanna et al. (Eds.), pp. 276-292.

[49] M. Cardei and J. Wu, “Energy-efficient coverage problems in wireless ad-hoc sensor networks,” *Computer Communications*, 29(4), pp. 413-420, Feb. 2006.

[50] P. Casari, A. Maruccci, M. Nati, C. Petrioli, and M. Zorzi, “A detailed simulation study of geographic random forwarding (GeRaF) in wireless sensor networks,” *Proc. IEEE VTC*, pp. 59-68, 2004.

[51] J.-H Chang and L. Tassiulas, “Energy conserving routing in wireless ad-hoc networks,” *Proc. IEEE INFOCOM,* pp. 22-31, 2000.

[52] B. Chen, K. Jameson, H. Balakrishnan, and R. Morris, “Span: An energy-efficient coordination algorithm for topology maintenance in ad hoc wireless networks,” *ACM Wireless Networks* 8(5), 481-494.

[53] J. Chen, I. Kanj, and G. Wang, “Hypercube network fault tolerance: A probabilistic approach,” *Proc. Int. Conf. on Parallel Processing (ICPP)*, pp. 65-72, Aug. 2002.

[54] A. Chen, S. Kumar, and T. H. Lai, “Designing localized algorithms for barrier coverage.” *Proc. ACM MobiCom*, Montreal, Quebec, Canada, pp. 75-86, Sep. 2007.

[55] W. Choi and S. Das, “Design and performance analysis of a proxy-based indirect routing scheme in ad hoc wireless networks,” *Mobile Networks and Applications*, 8(5), pp. 499-515, Oct. 2003.

[56] W. Choi and S. Das, “A novel framework for energy-conserving data gathering in wireless sensor networks,” *Proc. IEEE INFOCOM*, pp. 1985-1996, 2005.

[57] J. Conway and S. Torquato, “Tiling, packing, and covering with tetrahedra,” *Proc. National Academy of Sciences of the United States of America* (*PNAS*), 103(28), pp. 10612-10617, Jul. 2006.

[58] J. Cortes, S. Martinez, T. Karatas, and F. Bullo, “Coverage control for mobile sensing networks,” *IEEE Transactions on Robotics and Automation*, 20(2), 243-255, Apr. 2004.

[59] N. Cressie, *Statistics for spatial data*, John Wiley & Sons, Inc., 1991.

[60] S. K. Das and H. M. Ammari, "Routing and data dissemination in wireless sensor networks," Book chapter, *Wireless Sensor Networks: A Networking Perspective* (J. Zheng and A. Jamalipour, Eds.), Wiley-IEEE Press, To appear in 2008.

[61] A. K. Datta, M. Gradinariu, P. Linga, and P. Raipin-Parvedy, "Self-* distributed query region covering in sensor networks," *Proc. IEEE SRDS*, 2005.

[62] X. Du and F. Lin, "Maintaining differentiated coverage in heterogeneous sensor networks," *EURASIP Journal on Wireless Comm. and Networking*, 5(4), pp. 565-572, 2005.

[63] X. Du and F. Lin, "Improving routing in sensor networks with heterogeneous sensors", *Proc. IEEE VTC*, pp. 2528-2532, 2005.

[64] M. Duarte and Y. Hu, "Distance based decision fusion in a distributed wireless sensor network," in *Proc. IPSN*, 2003, pp. 392-404.

[65] E. Efthymiou, S. Nikoletseas, and J. Rolim, "Energy balanced data propagation in wireless sensor networks," *WINET*, 12, pp. 691-707, Dec. 2006.

[66] A. Elfes, "Using Occupancy Grids for Mobile Robot Perception and Navigation," *IEEE Computer*, vol. 22, no. 6, pp. 46-57, 1989.

[67] A. Esfahanian, "Generalized measures of fault tolerance with application to n-cube networks," *IEEE TC*, 38(11), pp. 1586-1591, Nov. 1989.

[68] A. Esfahanian and S. Hakimi, "On computing a conditional edge-connectivity of a graph," *IPL*, (27), pp. 195-199, 1988.

[69] J. W. Essam, "Percolation theory," *Reports on Progress in Physics*, (43), pp. 833-912, 1980.

[70] C. Fonesca and P. Fleming, "Genetic algorithms for multiobjective optimization: Formulation, discussion and generalization," *Proc. Int. Conf. on Genetic Algorithms,* Stephanie Forrest (Ed.), pp. 416-423, 1993.

[71] M. Franceschetti, M. cook, and J. Bruck, "A geometric theorem for wireless network design optimization," *Tech. Report*, http://paradise.caltech.edu/papers/, 2002.

[72] D. H. Fremlin, "The clustering problem: some Monte-Carlo results," *Journal de Physique*, (37), pp.

813-817, 1976.

[73] K. R. Gabriel and R. R. Sokal, "A new statistical approach to geographic variation analysis," *Systematic Zoology*, 18(3), pp. 259-278, Sep. 1969.

[74] Y. Ganjali and A. Keshavarzian, "Load balancing in ad hoc networks: Single-path routing vs. multi-path routing," *Proc. IEEE INFOCOM,* pp. 1120-1125, 2004.

[75] J. Gao and L. Zhang, "Load balanced short path routing in wireless networks," *Proc. IEEE INFOCOM,* pp. 1099-1108, 2004.

[76] A. Ghosh and S. K. Das, "Coverage and connectivity issues in wireless sensor networks," Book chapter, *Mobile, Wireless and Sensor Networks: Technology, Applications and Future Directions*, (Eds. R. Shorey *et al.*), Wiley-IEEE Press, pp. 221-256, 2006.

[77] E. N. Gilbert, "Random plane networks," *Journal of SIAM*, 9(4), pp. 533-543, Dec. 1961

[78] I. Glauche, W. Krause, R. Sollacher, and M. Greiner, "Continuum percolation of wireless ad hoc communication networks," *Physica A*, 325, pp. 577-600, 2003.

[79] I. Gradshteyn and I. Ryzhik, *Tables of Integrals, Series, and Product,* 6th Edition, San Diego, CA: Academic Press, 2000.

[80] R. L. Graham, D. E. Knuth, and O. Patashnik, *Concrete Mathematics: A Foundation for Computer Science*, Addison-Wesley, 1994.

[81] G. Grimmett, *Percolation*, Springer Verlag, 1989.

[82] W. Guo, Z. Liu, and G. Wu, "An energy-balanced transmission scheme for sensor networks," Poster, *Proc. ACM SenSys*, pp. 300-301, 2003.

[83] H. Gupta, Z. Zhou, S. R. Das, and Q. Gu, "Connected sensor cover: Self-organization of sensor networks for efficient query execution," *IEEE/ACM TON*, 14(1), pp. 55-67, Feb. 2006.

[84] M. Haenggi, "Twelve reasons not to route over many short hops," *IEEE VTC*, pp. 3130–34, 2004.

[85] M. Haenggi and D. Puccinielli, "Routing in ad hoc networks: A case for long hops", *IEEE Communication Magazine*, 43(10), pp. 93-101, Oct. 2005.

[86] P. Hall, *Introduction to the theory of coverage processes*, John Wiley & Sons Inc., New York, 1988.

[87] F. Harary, "Conditional connectivity," *Networks*, 13, pp. 347-357, 1983.

[88] W. Heinzelman, A. Chandrakasan, and H. Balakrishnan, “An application-specific protocol architecture for wireless microsensor networks,” *IEEE TWC*, 1(4), pp. 660-670, Oct. 2002.

[89] L. L. V. Helms, *Introduction to Potential Theory*, New York, Wiley-Interscience, 1969.

[90] M. Horton, D. Culler, K. Pister, J. Hill, R. Szewczyk, and A. Woo, “MICA: The commercialization of microsensor motes,” *Sensors Magazine*, pp. 40-48, Apr. 2002.

[91] C. Huang, and Y. Tseng, “The coverage problem in a wireless sensor network,” *Proc. ACM WSNA*, pp. 115-121, 2003.

[92] C. Huang, Y. Tseng, and L. Lo, “The coverage problem in three-dimensional wireless sensor networks,” *Proc. IEEE Globecom*, pp. 115-121, 2004.

[93] C. Huang, Y. Tseng, and H. Wu, “Distributed protocols for ensuring both coverage and connectivity of a wireless sensor network,” *ACM TOSN*, 3(1), pp. 1-24, Mar. 2007.

[94] C. Intanagonwiwat, R. Govindan, and D. Estrin, “Directed diffusion: A scalable and robust communication paradigm for sensor networks,” *Proc. ACM MobiCom*, pp. 56-67, 2000.

[95] A. Jarry, P. Leone, O. Powell, and J. Rolim, “An optimal data propagation algorithm for maximizing the lifespan of sensor networks,” *Proc. DCOSS*, LNCS 4026, P. Gibbons *et al*. (Eds.), pp. 405-421, 2006.

[96] X. Ji and H. Zha, “Sensor Positioning in Wireless Ad-hoc Sensor Networks Using Multidimensional Scaling,” *Proc. IEEE INFOCOM*, pp. 2652-2661, 2004.

[97] A. Jiang and J. Bruck, “Monotone percolation and the topology control of wireless networks,” *Proc. IEEE INFOCOM*, pp. 327-338, 2005.

[98] D. Johnson and D. Maltz, “Dynamic source routing in ad hoc wireless networks,” Book chapter, *Mobile Computing*, Kluwer Academic Publishers, 1996.

[99] G. Kao, T. Fevens, and J. Opatrny, “Position-based routing on 3-D geometric graphs in mobile ad hoc networks,” *Proc. CCCG*, pp. 1-4, 2005.

[100] B. Karp and H. Kung, “GPSR: Greedy perimeter stateless routing for wireless networks,” *Proc. ACM/IEEE MobiCom*, pp. 243-254, 2000.

[101] H. Kim, T. Abdelzaher, and W. Kwon, “Minimum-energy asynchronous dissemination to mobile

sinks in wireless sensor networks," *Proc. ACM SenSys*, pp. 193-204, 2003.

[102] Klein, L, "A boolean algebra approach to multiple sensor voting fusion," *IEEE Trans. Aerospace and Electronic Systems* 29(2), pp. 317–327, Apr. 1993.

[103] F. Koushanfar, S. Meguerdichian, M. Potkonjak, and M. Srivastava, "Coverage problems in wireless ad-hoc sensor networks," in *IEEE Proc. INFOCOM*, 2001, pp. 1380-1387.

[104] E. Kranakis, H. Singh, and J. Urrutia, "Compass routing on geometric networks," *Proc. Canadian Conf. on Computational Geometry (CCCG)*, pp. 51-54, 1999.

[105] B. Krishnamachari, Y. Mourtada, and S. Wicker, "The energy-robustness tradeoff for routing in wireless sensor networks," *Proc. IEEE ICC*, pp. 1833-1837, 2003.

[106] J. Kruskal, "On the shortest spanning subtree of a graph and the traveling salesman problem," *Proc. American Mathematical Society*, 7, pp. 48-50, 1956.

[107] S. Kumar, T. H. Lai, and A. Arora, "Barrier coverage with wireless sensors," *Proc. ACM MobiCom*, pp. 284-298, 2005.

[108] S. Kumar, T. H. Lai, and J. Balogh, "On *k*-coverage in a mostly sleeping sensor network," *Proc. ACM MobiCom*, pp. 144-158, 2004.

[109] S. Kumar, T. H. Lai, M. E. Posner, and P. Sinha, "Optimal sleep-wakeup algorithms for barriers of wireless sensors," Proc. *IEEE BROADNETS,* Raleigh, North Carolina, USA, Sep. 2007.

[110] R. Kumar, V. Tsiatsis, and M. B. Srivastava, "Computation hierarchy for in-network processing," *Proc. ACM WSNA*, pp. 68-77, 2003.

[111] S. Latifi, M. Hegde, and M. Naraghi-Pour, "Conditional connectivity measures for large multiprocessor systems," *IEEE Transactions on Computers*, 43(2), pp. 218-222, Feb. 1994.

[112] L. Lazos and R. Poovendran, "Coverage in heterogeneous sensor networks," *Proc. WiOpt*, 2006.

[113] L. Lazos and R. Poovendran, "Stochastic coverage in heterogeneous sensor networks," *ACM TOSN*, 2(3), pp. 325-358, Aug. 2006.

[114] P. Leone, S. Nikoletseas, and J. Rolim, "An adaptive blind algorithm for energy balanced data propagation in wireless networks, *Proc. DCOSS*, LNCS 3560, V. Prasanna *et al*. (Eds.), pp. 35-48, 2005.

[115] X. Li, G. Calinescu, P. Wan, and Y. Wang, “Localized Delaunay triangulation with application in ad hoc wireless networks,” *IEEE TPDS*, 14(10), pp. 1035-1047, Oct. 2003.

[116] N. Li and J. Hou, “FLSS: A fault-tolerant topology control algorithm for wireless networks,” *Proc. ACM MobiCom*, pp. 275-286, 2004.

[117] J. Li and P. Mohapatra, “Analytical modeling and mitigation techniques for the energy hole problem in sensor networks,” *Elsevier PMC*, 3, pp. 233-254, Mar. 2007.

[118] J. Li and P. Mohapatra, “An analytical model for the energy hole problem in many-to-one sensor networks,” *Proc. IEEE VTC*, pp. 2721-2725, 2005.

[119] X.-Y. Li, P.-J. Wan, and O. Frieder, “Coverage in wireless ad-hoc sensor networks,” *IEEE TC*, 52, pp. 753-763, Jun. 2003.

[120] J. Lian, K. Naik, and G. Agnew, “Data capacity improvement of wireless sensor networks using non-uniform sensor distribution,” *Intl. Journal of Distributed Sensor Networks*, 2(2), pp. 121-145, Apr.–Jun. 2006.

[121] S. Lindsey, C. Raghavendra, and K. Sivalingam, “Data gathering algorithms in sensor networks using energy metrics,” *IEEE TPDS*, 13(9), pp. 924-935, Sep. 2002.

[122] B. Liu, P. Brass, and O. Dousse, “Mobility improves coverage of sensor networks,” Proc. *ACM MobiHoc,* Urbana-Champaign, Illinois, USA, pp. 300-308, May 2005.

[123] B. Liu and D. Towsley, “A study of the coverage of large-scale sensor networks,” *Proc. IEEE MASS*, pp. 475-483, 2004.

[124] C. Liu, K. Wu, Y. Xiao, and B. Sun, “Random coverage with guaranteed connectivity: Joint scheduling for wireless sensor networks,” *IEEE TPDS,* 17(6), pp. 562-575, 2006.

[125] J. Luo and J.-P. Hubaux, “Joint mobility and routing for lifetime elongation in wireless sensor networks,” *Proc. IEEE INFOCOM,* pp. 1735-1746, 2005.

[126] H. Luo, F. Ye, J. Cheng, S. Lu, and L. Zhang, “TTDD: Two-tier data dissemination in large-scale wireless sensor networks,” *Wireless Networks*, 11(1-2), pp. 165-175, Jan. 2005.

[127] P. Malde and O. Oellermann, “The F-connectivity of a graph,” *Scientia, Series A: Mathematical Sciences*, (1), pp. 65-71, 1988.

[128] R. Meester and R. Roy, *Continuum percolation*, Cambridge University Press, 1996.

[129] S. Megerian, F. Koushanfar, M. Potkonjak, and M. Srivastava, “Worst and best-case coverage in sensor networks,” *IEEE TMC*, 4(1), pp. 84-92, Jan.-Feb. 2005.

[130] S. Megerian, F. Koushanfar, M. Potkonjak, and M. Srivastava, “Exposure in wireless ad-hoc sensor networks,” in *ACM MobiCom*, 2001, pp. 139-150.

[131] S. Megerian, F. Koushanfar, M. Potkonjak, and M. Srivastava, “Coverage problems in wireless ad-hoc sensor networks,” *Proc. IEEE INFOCOM,* pp. 1380-1387, 2001.

[132] M. Miller, C. Sengul, and I. Gupta, “Exploring the energy-latency trade-off for broadcasts in energy-saving sensor networks,” *Proc. IEEE ICDCS*, pp. 17-26, 2005.

[133] S. Nath and P. B. Gibbons, “Communicating via fireflies: Geographic routing on duty-cycled sensors,” *Proc. IPSN*, pp. 440-449, 2007.

[134] Nicules, D. and Nath, B. Ad-hoc positioning system (APS) using AoA. *Proc. IEEE INFOCOM*, pp. 1734–1743, 2003.

[135] O. Oellermann, “Conditional graph connectivity relative to hereditary properties,” *Networks*, (21), pp. 245-255, 1991.

[136] S. Olariu and I. Stojmenovic, “Design guidelines for maximizing lifetime and avoiding energy holes in sensor networks with uniform distribution and uniform reporting,” *Proc. IEEE INFOCOM*, pp. 1-12, 2006.

[137] G. E. Pike and C. H. Seager, “Percolation and. conductivity: A computer study,” *Physical Review B*, 10, pp. 1421-1434, 1974.

[138] S. Poduri, S. Pattem, B. Krishnamachari, and G. S. Sukhatme, “Sensor network configuration and the curse of dimensionality,” *Proc. IEEE EmNets*, 2006.

[139] D. Pompili, T. Melodia, and I. F. Akyildiz, “Routing algorithms for delay-insensitive and delay-sensitive applications in underwater sensor networks,” *Proc. ACM MobiCom*, pp. 298-309, 2006.

[140] D. Pompili, T. Melodia, and I. F. Akyildiz, “Deployment analysis in underwater acoustic wireless sensor networks,” *Proc. ACM WUWNet*, pp. 48-55, 2006.

[141] O. Powell, P. Leone, and J. Rolim, “Energy optimal data propagation in wireless sensor networks,”

Journal of Parallel and Distributed Computing, 3(67), pp. 302-317, Mar. 2007.

[142] V. Ravelomanana, "Extremal properties of three-dimensional sensor networks with applications," *IEEE TMC*, 3(3), pp. 246-257, Jul.-Sep. 2004.

[143] F. D. K. Roberts, "A Monte Carlo solution of a two-dimensional unstructured cluster problem," *Biometrika*, 54(3/4), pp. 625-628, Dec. 1967.

[144] A. Sankar and Z. Liu, "Maximum lifetime routing in wireless ad-hoc networks," *Proc. IEEE INFOCOM,* pp. 1090-1098, 2004.

[145] R. Shah, R. Roy, S. Jain, and W. Brunette, "Data mules: Modeling a three-tier architecture for sparse sensor networks," *Proc. IEEE SNPA*, pp. 1058-1068, 2003.

[146] S. Shakkottai, R. Srikant, and N. Shroff, "Unreliable sensor grids: Coverage, connectivity and diameter," *Ad Hoc Networks* 3(6)*,* pp. 702-716, 2005.

[147] S. Shakkottai, R. Srikant, and N. Shroff, "Unreliable sensor grids: coverage, connectivity and diameter," *Proc. IEEE INFOCOM,* pp. 1073-1083, 2003.

[148] E. Shih, S. Cho, N. Ickes, R. Min, A. Sinha, A. Wang, and A. Chandrakasan, "Physical layer driven protocol and algorithm design for energy-efficient wireless Sensor Networks," *Proc. ACM MobiCom*, pp. 272-287, 2001.

[149] K. Sohrabi, J. Gao, V. Ailawadhi, and G. Pottie, "Protocols for self-organization of a wireless sensor network," *IEEE Personal Communications*, 7(5), pp. 16-27, Oct. 2000.

[150] I. Stojmenovic and X. Lin, "Loop-free hybrid single-path/flooding routing algorithms with guaranteed delivery for wireless networks, *IEEE TPDS*, 12(10), pp. 1023-1032, Oct. 2001.

[151] T. Sun, L. Chen, C. Han, and M. Gerla, "Reliable sensor networks for planet exploration," *Proc. IEEE Int'l Conf. Networking, Sensing and Control*, pp. 816–821, 2005.

[152] D. Tian and N. Georganas, "Connectivity maintenance and coverage preservation in wireless sensor networks," *Ad Hoc Networks*, 3(6), pp. 744-761, Nov. 2005.

[153] P. Tipler, *Physics for Scientists and Engineers: Electricity, Magnetism, Light, and Elementary Modern Physics*, 5th Edition, W. H. Freeman, 2004.

[154] T. Vicsek and J. Kertesz, "Monte Carlo renormalization-group approach to percolation on a

continuum: test of universality," *Journal of Physics A: Mathematical and General*, 14, pp. L31-L37, 1981.

[155] P.-J. Wan and C.-W. Yi, "Coverage by randomly deployed wireless sensor networks," *IEEE TIT*, 52(6), pp. 2658- 2669, Jun. 2006.

[156] G. Wang, G. Cao, and T. La Porta, "Movement-assisted sensor deployment," *Proc. IEEE INFOCOM,* pp. 2469-2479, 2004.

[157] G. Wang, G. Cao, and T. La Porta, "Proxy-based sensor deployment for mobile sensor networks," *Proc. IEEE MASS*, pp. 493-502, 2004.

[158] W. Wang, V. Srinivasan, and K.-C. Chua, "Using mobile relays to prolong the lifetime of wireless sensor networks," *Proc. ACM MobiCom*, pp. 270-283, 2005.

[159] Y.-C. Wang and Y.-C. Tseng, "Distributed deployment schemes for mobile wireless sensor networks to ensure multi-level coverage," *IEEE TPDS*, To appear (2008).

[160] X. Wang, G. Xing, Y. Zhang, C. Lu, R. Pless, and C. Gill, "Integrated coverage and connectivity configuration in wireless sensor networks," *Proc. ACM SenSys*, pp. 28-39, 2003.

[161] A. Woo, T. Tony, and D. Culler, "Taming the underlying challenges of reliable multihop routing in sensor networks," *Proc. ACM SenSys*, pp. 14-27, 2003.

[162] X. Wu, G. Chen, and S. K. Das, "Avoiding Energy Holes in Wireless Sensor Networks with Nonuniform Node Distribution," *IEEE TPDS* 19(5), pp. 710-720, May 2008.

[163] X. Wu, G. Chen, and S. K. Das, "On the energy hole problem of nonuniform node distribution in wireless sensor networks," *Proc. IEEE MASS*, pp. 180-187, 2006.

[164] J. Wu and G. Guo, "Fault tolerance measures for m-ary n-dimensional hypercubes based on forbidden faulty sets," *IEEE TC*, 47(8), pp. 888-893, Aug. 1998.

[165] G. Xing, C. Lu, R. Pless, and Q. Huang, "On greedy geographic routing algorithms in sensing-covered networks," *Proc. ACM MobiHoc*, pp. 31-42, 2004.

[166] G. Xing, X. Wang, Y. Zhang, C. Lu, R. Pless, and C. Gill, "Integrated coverage and connectivity configuration for energy conservation in sensor networks," *ACM TOSN*, 1(1), pp. 36-72, Aug. 2005.

[167] S. Yang, F. Dai, M. Cardei, and J. Wu, "On connected multiple point coverage in wireless sensor

networks," *Int. Journal of Wireless Information Networks*, 13(4), pp. 289-301, Oct. 2006.

[168] X. Yang and N. Vaidya, "A wakeup scheme for sensor networks: Achieving balance between energy saving and end-to-end delay," *Proc. IEEE RTAS*, pp. 19-26, 2004.

[169] M. Yarvis, N. Kushalnagar, H. Singh, A. Rangarajan, Y. Liu, and S. Singh, "Exploiting heterogeneity in sensor networks," *Proc. IEEE INFOCOM*, pp. 878-890, 2005.

[170] F. Ye, H. Luo, J. Cheng, S. Lu, and L. Zhang, "A two-tier data dissemination model for large-scale wireless sensor networks," *Proc. ACM MobiCom*, pp. 148-159, 2002.

[171] F. Ye, G. Zhong, J. Cheng, S. Lu, and L. Zhang, "PEAS: A robust energy conserving protocol for long-lived sensor networks," *Proc. ICDCS*, pp. 1-10, 2003.

[172] B. Yener, M. Magdon-Ismail, and F. Sivrikaya, "Joint problem of power optimal connectivity and coverage in wireless sensor networks," *ACM Wireless Networks* 13, pp. 537-550, 2007.

[173] W. Zhang, G. Cao, and T. La Porta, "Dynamic proxy tree-based data dissemination schemes for wireless sensor networks," *Proc. IEEE MASS*, pp. 21-30, 2004.

[174] H. Zhang and J. Hou, "Is deterministic deployment worse than random deployment for wireless sensor networks?," *Proc. IEEE INFOCOM*, pp. 1-13, 2006.

[175] H. Zhang and J. Hou, "On the upper bound of α-lifetime for large sensor networks," *ACM TOSN*, 1(2), pp. 272-300, Nov. 2005.

[176] H. Zhang and J. Hou, "Maintaining sensing coverage and connectivity in large sensor networks," *Ad Hoc & Sensor Wireless Networks*, 1(1-2), pp. 89-124, Mar. 2005.

[177] H. Zhang and J. Hou, "On Deriving the Upper Bound of α-Lifetime for Large Sensor Networks," *Proc. ACM MobiHoc*, pp. 121-132, 2004.

[178] H. Zhang, H. Shen, and Y. Tan, "Optimal energy balanced data gathering in wireless sensor networks," *Proc. IEEE IPDPS*, pp. 1-10, 2007.

[179] J. Zhao and R. Govindan, "Understanding packet delivery performance in dense wireless sensor networks," *Proc. ACM SenSys*, pp. 1-13, 2003.

[180] Z. Zhou, S. Das, and H. Gupta, "Fault tolerant connected sensor cover with variable sensing and transmission ranges," *Proc. IEEE SECON*, pp. 594-604, 2005.

[181] Z. Zhou, S. Das, and H. Gupta, “Connected *k*-coverage problem in sensor networks,” *Proc. ICCCN*, pp. 373-378, 2004.

[182] G. Zhou, T. He, S. Krishnamurthy, and J. Stankovic, “Impact of radio irregularity on wireless sensor networks,” *Proc. MobiSys*, pp. 125-138, 2004.

[183] Y. Zhou, M. R. Lyu, and J. Liu, “On setting up energy-efficient paths with transmitter power control in wireless sensor networks,” *Proc. MASS*, pp. 1-9, 2005.

[184] M. Zorzi and R. Rao, “Geographic random forwarding (GeRaF) for ad hoc and sensor networks: Multihop performance,” *IEEE TMC,* 2(4), pp. 337-348, Oct.-Dec. 2003.

[185] M. Zorzi and R. Rao, “Geographic random forwarding (GeRaF) for ad hoc and sensor networks: Energy and latency performance,” *IEEE TMC,* 2(4), pp. 349-365, Oct.-Dec. 2003.

[186] Y. Zou, and K. Chakrabarty, “A distributed coverage- and connectivity-centric technique for selecting active nodes in wireless sensor networks,” *IEEE TC*, 54(8), 978-991, 2005.

[187] Y. Zou and K. Chakrabarty, “Sensor deployment and target localization in distributed sensor networks,” *ACM TOSN*, vol. 3, no. 2, pp. 61-91, 2004.

[188] http://mathworld.wolfram.com/ReuleauxTriangle.html.

[189] http://mathworld.wolfram.com/ReuleauxTetrahedron.html

[190] http://mathworld.wolfram.com/BetaFunction.html.

[191] http://mathworld.wolfram.com/Erf.html.

BIOGRAPHICAL INFORMATION

Habib M. Ammari received the Diploma of Engineering in computer science and the Doctorat de Spécialité in computer science from the Faculty of Sciences of Tunis, Tunisia, in 1992 and 1996, respectively. He received the PhD in computer science and engineering from the University of Texas at Arlington (UTA) in May 2008. He was on the faculty of the Superior School of Communications of Tunis (Sup'Com) from 1992 to 2005 (Engineer, 1992-1993; Lecturer, 1993-1997; Assistant Professor, 1997-2005 and got tenure in 1999). He is on sabbatical leave for study and research at UTA. He joined the Center for Research in Wireless Mobility and Networking (CReWMaN) at UTA in January 2005. His main research interests lay in the areas of wireless sensor and mobile ad hoc networking and multihop mobile wireless Internet architectures and protocols. In particular, he is interested in coverage, connectivity, energy-efficient data routing and information dissemination, and fault tolerance in wireless sensor networks, and the interconnection between wireless sensor networks, mobile ad hoc networks, and the global IP Internet. He received the Computer Science and Engineering Outstanding PhD Student Award at UTA in 2008. He is a recipient of the TPC Best Paper Award at EWSN '08 and the Best Contribution Paper Award at IEEE PerCom '08–Google PhD forum. He was also an ACM Student Research Competition (ACM SRC) Nominee at ACM MobiCom '05. He received Travel Award Grants from NSF and SAP to attend IPSN '07 and IPSN '08. He was the Laureate in Physics and Chemistry at the Faculty of Sciences of Tunis in 1987 and 1988 (ranked the 1st among about 400 undergraduate students). He has been selected for inclusion in the 2006 edition of Who's Who in America. He has served as a reviewer of several international journals (IEEE Transactions on Mobile Computing, IEEE Transactions on Parallel and Distributed Systems, Ad Hoc & Sensor Wireless Networks, International Journal of Sensor Networks, Computer Communications, Journal of Parallel and Distributed Computing, Information Sciences, International Journal of Computer and Applications, and Data & Knowledge Engineering) and conferences and symposia (ACM MobiCom, IEEE INFOCOM, IEEE ICDCS, IEEE SECON, IEEE MASS, IEEE GlobeCom, IEEE ICC, HiPC, ACM MSWiM, DISC, IEEE VTC, and IEEE ISCC).